Horbachevskyi National Medical University, Ternopil, Ukraine
National Medical University, Ivano-Frankivsk, Ukraine
Kozyavkin International Rehabilitation Clinic, Truskavets, Ukraine
Nicolaus Copernicus University, Torun, Poland
Bohomolets Institute of Physiology National Academy of Sciences, Kyïv, Ukraine

Nataliya V. Kozyavkina
Yuliya V. Vovchyna
Nataliya M. Voronych-Semchenko
Walery Zukow
Igor L. Popovych

TENSIOREGULOME CONCEPT.
Quantitative-qualitative blood pressure clusters of patients at the Truskavets' spa and their accompaniments

TERNOPIL
TNMU
UKRMEDKNYHA
2024

Authors
Nataliya V. Kozyavkina, MD, PhD; Horbachevskyi National Medical University, Ternopil; Kozyavkin International Rehabilitation Clinic
nataliakozyavkina72@gmail.com; clinic@kozyavkin.com
Yuliya V. Vovchyna, MD; Ivano-Frankivsk National Medical University
Nataliya M. Voronych-Semchenko, MD, DS, Prof.; Ivano-Frankivsk National Medical University
Walery Zukow, MD, DS; Nicolaus Copernicus University, Torun, Poland
w.zukow@wp.pl
Igor L. Popovych, MD, PhD, senior res. fel.; Bohomolets Institute of Physiology; Kozyavkin International Rehabilitation Clinic; i.popovych@biph.kiev.ua; i.l.popovych@gmail.com

We dedicate this monograph to the memory of Volodymyr Illich Kozyavkin (1947-2022)
with gratitude for his support of
the Truskavetsian Scientific School of Balneology

Recommended for publication by the Academic Council
of Horbachevs'kyi National Medical University
(protocol No. 9 dated 25/06/2024)

Reviewers:

Vastyanov Ruslan S., MD, DS, Prof, Head of the Department of General and Clinical Pathophysiology named after VV Podvysotskyi at the National Medical University, Odesa, Ukraine

Regeda Mykhaylo S., MD, DS, Prof, Head of the Department of Pathophysiology at the Danylo Halytskyi National Medical University, Lviv, Ukraine

Kozyavkina NV, Vovchyna YV, Voronych-Semchenko NM, Zukow W, & Popovych IL. Tensioregulome Concept. Quantitative-qualitative Blood Pressure Clusters of Patients at Truskavets' Spa and Their Accompaniments. Ternopil: Ukrmedknyha; 2024: 194.
ISBN 978-1-4452-7212-2 DOI http://dx.doi.org/10.5281/zenodo.12664757

The monograph highlights the results of priority clinical-physiological studies of the state of blood pressure in patients at Truskavets' spa and its hemodynamics, neuro-endocrine, immune, metabolic, and biophysics accompaniments. The authors put forward the concept of ***Tensioregulome*** as a constellation of neural, endocrine, immune and metabolic factors that determines the level of blood pressure and its changes under the influence of balneotherapy. Is it intended for physiologists, cardiologists, endocrinologists, immunologists, biophysicists, medical rehabilitation specialists.

ISBN 978-1-4452-7212-2

DOI http://dx.doi.org/10.5281/zenodo.12664757

© Horbachevskyi National Medical University, Ternopil, 2024
© Ivano-Frankivsk National Medical University, 2024
© Kozyavkin International Rehabilitation Clinic, Truskavets', 2024
© Nicolaus Copernicus University, Torun, 2024
© Bohomolets Institute of Physiology, Kyïv, 2024
© Authors

ISBN 978-1-4452-7212-2
DOI http://dx.doi.org/10.5281/zenodo.12664757

CONTENT

INTRODUCTION 6

BACKGROUND 6

OWN PILOT STUDIES 11

Chapter 1 .....

...QUANTITATIVE-QUALITATIVE BLOOD PRESSURE CLUSTERS OF PATIENTS OF TRUSKAVETS' SPA AND THEIR HEMODYNAMIC ACCOMPANIMENT 38

Chapter 2 .....

AUTONOMIC AND ENDOCRINE ACCOMPANIMENTS OF QUANTITATIVE-QUALITATIVE BLOOD PRESSURE CLUSTERS 47

Chapter 3 .....

ELECTROENCEPHALOGRAPHIC ACCOMPANIMENT OF QUANTITATIVE-QUALITATIVE BLOOD PRESSURE CLUSTERS 60

Chapter 4 .....

IMMUNE ACCOMPANIMENT OF QUANTITATIVE-QUALITATIVE BLOOD PRESSURE CLUSTERS 73

Chapter 5 .....

METABOLIC ACCOMPANIMENT OF QUANTITATIVE-QUALITATIVE BLOOD PRESSURE CLUSTERS 82

Chapter 6 .....

TENSIOREGULOME AS AN ACCOMPANIMENT OF QUANTITATIVE-QUALITATIVE BLOOD PRESSURE CLUSTERS 92

Chapter 7 .....

EVALUATION OF QUANTITATIVE-QUALITATIVE LEVELS OF BLOOD PRESSURE BY TENSIOREGULOME 107

DISCUSSION 156

CONCLUSION 170

REFERENCES 174

INTRODUCTION

BACKGROUND

Despite the fact that Truskavets' Spa, officially opened in 1827, has long had a cardiological profile, the effect of balneotherapy on hemodynamics began to be fundamentally studied only in 1998, and blood pressure is still not in the focus of researchers, giving way to the urinary and digestive systems as the object of study, and then to the neuroendocrine-immune complex.

In the seminal monograph “Physiological effect of Naftusya mineral water” [Yessypenko BY, 1981] collected scant information on the effect of treatment at the Truskavets’ Spa on blood pressure.

It was reported that out of 100 patients who arrived at the Spa with blood pressure of 150-200 mmHg, in 21 patients it decreased by 10-20 mmHg, in 51 - by 40-50 mmHg, in 26 patients blood pressure did not change, and in 2 patients it increased [Bajkalov LK, 1966].

According to Fedyushko MM [1967], nephrogenic hypertension decreased in the vast majority of patients 14-18 days after treatment, and at the end of treatment, blood pressure normalized in many patients. In patients with urolithiasis with concomitant hypertension, blood pressure normalized at the end of treatment in 54% of cases, decreased in 35,5%, and remained unchanged in 10,5%. In patients with cholelithiasis, the corresponding figures were 48,5%, 39,3%, and 12,1%.

Of particular interest to us are the data of Khokhlov BA & Yessypenko BY [1975] on the normalizing effect of treatment on blood pressure in patients with chronic pyelonephritis: initial systolic blood pressure in the range of 125÷220 mmHg decreased, but in the range of 125÷100 mmHg increased, as documented by the regression equation:

Change in BPs = -0,56•BPs initial +72,6.

In the fundamental monograph “BALNEOCARDIOANGIOLOGY. Effect of balneotherapy in the Truskavets’ spa on the cardiovascular system and physical performance” [Popovych IL et al., 2005], the main subject of the study was inotropism, more precisely, cardioinotropic effects of balneotherapy, while blood pressure and its response to balneotherapy were considered as a concomitant parameter, along with other parameters of central and peripheral hemodynamics, autonomic nervous system, electrolyte, uric acid and lipid metabolism, and bicycle ergometry.

Using the example of a sample of 66 women aged 40-54 and 18 men aged 54-61 who underwent balneotherapy for chronic digestive diseases relevant to the resort, the authors analyzed the state of the cardiovascular system of this patient population.

At the first stage, the authors used the histogram analysis method [Majdannyk VH, 1994]. Parameters that deviate from the mean norm within ±7% were considered average; deviations within ±8÷20% were assessed as higher or lower than average, and more than 20% were considered high or low values, respectively. These percentage intervals correspond to sigmoidal intervals of ±σ, ±1σ÷2σ, and more than 2σ, respectively, as well as centile intervals 25÷75; 75÷90 and 25÷10; 90÷97 and 10÷3, respectively.

It should be noted that in the cited study, following the recommendations [Vinogradova TS, 1986], the normal values of blood pressure were calculated by the age (A) of the patients:

Ps = 109 + 0,4•A; Pd = 67 + 0,3•A; Pm = 81 + 0,333•A,

which is now considered an outdated approach.

According to this approach, the histogram of systolic blood pressure has a two-humped appearance: the maximum proportion is found for the range of values both above average (42,9%) and below average (26,2%), while the narrowed norm is found in only 21,4% of patients. High and low levels of systolic blood pressure occurred in 4,8% of the subjects. Instead, diastolic blood pressure within the narrowed range was found in 61,9%; above-

average values were detected in 16,7%, and below-average in 19,0%. The distribution of mean dynamic blood pressure largely coincides with that of diastolic blood pressure: the narrowed norm was found in 52,4%; above average values in 28,6%, and below average in 16,7%.

Using the method of cluster analysis, which allows for a natural classification of the sample by ***simultaneously taking into account all the features*** [Aldenderfer MS & Blashfield RK, 1985], Popovych IL et al. [2005] identified three groups whose members differ minimally from each other within each group, while differing as much as possible from the members of the other two groups of patients.

It was found that the maximum contribution to the division of the sample into clusters was made by the general peripheral vascular resistance (GPVR). In the members of the major cluster (78% of patients), it was 14,6±0,4 kPa•sec/m^3, i.e. 94,9±3,8% of the average age norm (AAN). This was accompanied by systolic blood pressure of 123,0±2,5 mmHg, i.e. 96,2±1,8% of AAN, diastolic blood pressure of 80,2±1,3 mmHg, i.e. 98,4±1,4% of AAN and mean BP of 94,5±1,6 mmHg, i.e. 99,4±1,5% of AAN. The members of the second cluster (12% of patients) had a GPVR of 30,2±2,8 kPa•sec/m3, i.e. 180,0±23,5% of AAN, systolic BP of 120,0±6,5 mmHg (95,7±4,5% of AAN), diastolic BP of 76,0±4,0 mmHg (95,9±4,9% of AAN) and mean BP of 90,4±4,8 mmHg (97,6±4,7% of AAN). On the opposite pole, members of the third cluster (10% of patients) had a GPVR of 10,9±1,35 kPa•sec/m3 (77,8±5,7% AAN), systolic BP of 150,0±5,8 mmHg (113,0±5,3% AAN), diastolic BP of 91,3±1,2 mmHg (107,0±1,0% AAN) and mean BP of 111,0±1,1 mmHg (112,0±2,4% AAN).

After a two-week course of balneotherapy in members of the major cluster, GPVR increased by 18,1±6,5% in combination with a decrease in cardiac output (CO) by 9,1±4,5%. In the members of the second cluster, changes in these main hemodynamic parameters were more pronounced, amounting to +31,0±14,1% and -26,7±9,0%, respectively, while in the members of the third cluster they were oppositely directed: -34,3±5,9% and +63,6±16,5%, respectively. In contrast, no significant changes in either systolic or diastolic blood pressure were found in any cluster.

However, the authors' observation of another sample of 55 patients of both sexes yielded different results. After dividing patients into 5 clusters according to changes in cardiac hemodynamic parameters (the contractile activity index of the left ventricle, first proposed by Ruzhylo and Popovych, RPCAI; mean BP; heart rate, HR; stroke volume of the left ventricle, SV), the following patterns were found. In 16,4% of patients, BP did not change significantly; in 29,1%, there was a tendency to increase both diastolic BP (by 4,0±1,9%) and systolic BP (by 3,7±2,8%) in combination with an increase in GPVR and a decrease in SV, but not HR; in 20,0%, diastolic BP slightly increased (by 6,0±3,0%), but not systolic BP, in combination with an increase in SV and HR and a decrease in GPVR; 16,4% had a decrease in both diastolic BP (by 9,6±2,0%) and systolic BP (by 6,5±2,2%), combined with a decrease in GPVR and SV, but an increase in HR; the remaining 18,2% also had a decrease in both diastolic BP (by 13,1±3,1%) and systolic BP (by 9,9±3,0%), but in combination with a decrease in SV and HR and a tendency to increase in GPVR.

Cluster analysis was also used by Popovych IL et al. [2005] to naturally classify the variety of immediate (after 30 minutes) hemodynamic responses to the use of Naftussya bioactive water, which is the main component of the resort's balneotherapy complex. The maximum contribution to the division of the sample (21 women aged 35-45 and 38 men aged 38-52 years) into clusters was again found from GPVR, with significant contributions also from SV and end-diastolic (EDV) volume, HR, and RPCAI, but neither ejection time nor blood pressure. It was found that in 24 patients (41,4% of the sample), hemodynamic parameters remained without significant changes. In the other 23 patients (39,6% of the sample), a decrease in GPVR by 14,9±0,7% was noted, combined with an increase in SV by

11,2±1,3%, HR by 7,3±1,7%, EDV by 5,8±0,9%, and RPCAI by 4,4±1,9% in the absence of changes in blood pressure. In 4 patients (6,9% of the sample), the hemodynamic response was much more pronounced: a decrease in GPVR by 40,5±1,3% combined with an increase in SV by 46,5±7,8%, HR by 18,9±3,4%, EDV by 32,4±14,6%, RPCAI by 16,7±7,9%, as well as in systolic BP by 5,1±1,9%, but not in diastolic BP (1,4±3,0%). In 7 patients (12,1% of the sample), the opposite changes were found: an increase in GPVR by 13,2±5,1% combined with a decrease in SV by 17,6±2,7%, EDV by 8,0±5,1%, and RPCAI by 8,9±4,2%, but an increase in HR by 7,4±2,4% again in the absence of changes in blood pressure.

Interestingly, other components of the resort's balneotherapeutic complex, such as ozokerite application and mineral bath, also caused opposite types of urgent hemodynamic reactions [Popovych IL et al., 2005].

In the same year, Shakhbazova LV et al. [2005] for the first time in the Truskavets' spa recorded a daily blood pressure profile in 105 patients (63 men and 42 women aged 31-62 years). The level of office systolic blood pressure was in the range of 145÷178 mmHg (mean 154,6±4,2 mmHg), diastolic blood pressure 90÷107 mmHg (mean 96,3±3,2 mmHg).

As a result of a three-week complex treatment (Naftussya bioactive water, dry carbon dioxide baths, supravenous laser therapy, singlet oxygen therapy), daily systolic blood pressure (mmHg) decreased from 151,4±5,2 to 131,2±3,4; daytime - from 156,8±3,5 to 139,5±2,7; nighttime - from 142,6±4,1 to 126,7±4,5. Daily diastolic blood pressure decreased from 90,9±2,9 to 81,9±2,6; daytime - from 93,7±2,7 to 84,7±2,8; nighttime - from 87,8±2,5 to 74,9±2,1 mmHg. Regarding the variability of blood pressure, a significant decrease was noted only for daytime systolic blood pressure: from 19,2±2,0 to 14,1±1,4 mmHg. The pressure load, estimated by the hypertension time index (over 140/90 mmHg during the day and over 120/80 mmHg at night), decreased in relation to systolic blood pressure during the day from 68,7±5,8% to 41,6±5,2%; at night from 72,4±5,6% to 47,6±4,4%; in relation to diastolic blood pressure during the day from 46,8±4,7% to 28,0±3,6%; at night from 56,4±4,0% to 33,5±4,1%. The magnitude of the morning rise in systolic blood pressure decreased from 54,4±5,3 to 37,2±3,4 mmHg, and diastolic blood pressure from 38,7±4,8 to 29,0±3,4 mmHg. Target blood pressure (below 140/90 mmHg) was achieved in 70,3% of patients.

The described favorable changes in the parameters of the daily blood pressure profile were accompanied by favorable changes in the morning HRV parameters. In particular, the reduced levels of markers of vagal tone increased: SDNN from 58,4±4,2 to 74,2±5,5 msec; RMSSD from 34,7±1,9 to 45,2±2,1 msec; pNN_{50} from 5,8±0,8 to 11,1±0,8%; triangular index from 16,3±0,8 to 19,6±1,1 units; HF from 623±55 to 753±52 $msec^2$. At the same time, increased levels of sympathetic tone markers decreased: LF/HF from 2,43±0,12 to 1,64±0,11 and LFnu (calculated by us according to the available data) from 71,0% to 62,1%.

The next study of this group [Shakhbazova LV et al., 2006] showed that after a month of treatment of 35 patients of both sexes with office blood pressure 167±9,9/101±5,4 mmHg with enalapril in combination with Naftussya bioactive water, 62,8% achieved the target blood pressure level, while in the control group (n=20; BP 158±7,2/99±3,7 mmHg) monotherapy with enalapril was less effective (55,0%). In the other group (n=35; BP 164±6,3/101±3,6 mmHg), corvazan in combination with Naftussya bioactive water helped to achieve the target blood pressure level in 74,3% of patients versus 70,0% in the control group (n=20; BP 163±6,6/101±3,6 mmHg). The authors concluded that Naftussya bioactive water has additive activity in antihypertensive treatment.

Lukovych YuR et al. [2012] in their study of 30 women aged 30-60 years, whose systolic BP was in the range of 90÷160 mmHg and diastolic BP in the range of 60÷100 mmHg, found that its response to complex two-week balneotherapy (drinking Naftussya water and water from source #1 or #2, ozokerite applications, mineral baths) follows the law of initial level. In particular, the regression equation for systolic blood pressure is as follows:

Change in BPs = -0,6663•BPs initial +79,9; r=-0,746,

which is very similar to the one derived by Khokhlov BA & Yessypenko BY [1975].

The authors went further and documented the response of diastolic blood pressure:

Change in BPd = -0,7925•BPd initial +62,6; r=-0,592.

The points of change in the direction of the BP response were 120 and 79 mmHg, respectively.

In addition, this study analyzed the correlations between BP and HRV parameters before and after balneotherapy. It was found that balneotherapy initiates or strengthens the already existing positive correlations of diastolic BP with markers of sympathetic tone (LF relative: r=0,32 vs 0,04; AMo: r=0,54 vs 0,31; Stress Index: r=0,50 vs 0,29) and negative correlations with markers of vagal tone (HF relative: r=-0,40 vs -0,11; RMSSD: r=-0,43 vs -0,26; MxDMn: r=-0,53 vs -0,36; Triangular Index: r=-0,58 vs -0,38).

In relation to systolic blood pressure, the relationships were somewhat weaker (LF relative: r=0,32 vs -0,11; AMo: r=0,39 vs 0,24; Stress Index: r=0,43 vs 0,21; HF relative: r=-0,39 vs -0,04; RMSSD: r=-0,35 vs -0,15; MxDMn: r=-0,36 vs -0,19; Triangular Index: r=-0,41 vs -0,25). At the same time, balneotherapy negated the association of systolic blood pressure with ULF relative: r=-0,06 vs 0,38.

In the same population, other members of the same research group [Kozyavkina OV et al., 2013] found a negative relationship between *changes* in diastolic BP and Triangular Index (r=-0,65) as well as in systolic BP and MxDMn (r=-0,44).

Thus, as of 2013, a certain set of facts about the effect of balneotherapy on blood pressure, as well as some mechanisms of such an effect, had been accumulated. However, these findings were fragmentary and unsystematic. Moreover, in some observations, hypotensive factors were used for treatment, which are known to be much stronger than the balneofactors of the resort.

Therefore, we initiated the project ***"Neuro-endocrine-immune and metabolic mechanisms of the effects of balneotherapy on blood pressure".***

The materials from the monograph have been presented in the following publications:

1. Vovchyna YuV, Zukow W. The influence of balneotherapy on spa Truskavets' on arterial pressure and its regulation at children. Journal of Health Sciences. 2014;4(10):151-160.
2. Vovchyna JV, Voronych NM, Zukow W, Popovych IL. Relationships between normal or borderline blood pressure and some neural, endocrine, metabolic and biophysic parameters in women and men. Journal of Education, Health and Sport. 2016;6(2):163-182.
3. Kozyavkina NV, Kozyavkina OV, Vovchyna YB, Popovych IL. Neurogenic mechanism of the influence of balneotherapy on arterial pressure. Fiziol Zhurn. 2019;65(3,Sup):54-54.
4. Kozyavkina NV, Kozyavkina OV, Vovchyna YV. Balneotherapy influences on arterial pressure by neurogenic mechanism. In: Rehabilitation Medicine and Health-Resort Institutions Development. Proceedings of the 19th International Applied Research Conference (Kyïv, 11-12 December 2019). Edited by O. Gozhenko, W. Zukow. Toruń, Kyiv. 2019:41-42.
5. Kozyavkina NV, Voronych-Semchenko NM, Vovchyna YV, Zukow W, Popovych IL. Quantitative and qualitative blood pressure clusters in patients of Truskavets' spa and their hemodynamic accompaniment. Journal of Education, Health and Sport. 2020;10(6):445-454.
6. Kozyavkina NV, Voronych-Semchenko NM, Vovchyna YV, Zukow W, Popovych IL. Autonomic and endocrine accompaniments of quantitative-qualitative blood pressure

clusters in patients of Truskavets' spa. Journal of Education, Health and Sport. 2020;10(7):465-477.
7. Kozyavkina NV, Popovych IL, Popovych DV, Zukow W, Bombushkar IS. Sexual dimorphism in some psycho-neuro-endocrine parameters at human. Journal of Education, Health and Sport. 2021;11(5):370-391.
8. Kozyavkina NV, Voronych-Semchenko NM, Vovchyna YuV, Zukow W, Gozhenko OA, Popovych IL. Variety of blood pressure reactions in patients of Truskavets' spa and their hemodynamic, autonomic and hormonal accompaniments. Balneo and PRM Research Journal. 2021;12(3):A17.
9. Kozyavkina NV, Vovchyna YV, Voronych-Semchenko NM, Zukow W, Popovych IL. Electroencephalographic accompaniment of quantitative-qualitative blood pressure clusters in patients of Truskavets' spa. Journal of Education, Health and Sport. 2021;11(10):435-444.
10. Kozyavkina NV, Vovchyna YV, Voronych-Semchenko NM, Zukow W, Popovych IL. Metabolic accompaniment of quantitative-qualitative blood pressure clusters in patients of Truskavets' spa. Journal of Education, Health and Sport. 2022;12(2):377-386.
11. Kozyavkina NV, Vovchyna YV, Voronych-Semchenko NM, Zukow W, Popovych DV, Popovych IL. Immune accompaniment of quantitative-qualitative blood pressure clusters in patients of Truskavets' spa. Journal of Education, Health and Sport. 2022;12(3):320-329.
12. Popovych IL, Kozyavkina NV, Barylyak LG, Vovchyna YV, Voronych-Semchenko NM, Zukow W, Tsymbryla VV. Variants of changes in blood pressure during its three consecutive registrations. Journal of Education, Health and Sport. 2022;12(4):365-375.
13. Popovych IL, Kozyavkina NV, Vovchyna YV, Voronych-Semchenko NM, Zukow W, Popovych DV. Tensioregulome as an accompaniment of quantitative-qualitative blood pressure clusters. Journal of Education, Health and Sport. 2022;12(6):418-436.
14. Kozyavkina NV, Popovych IL, Vovchyna YV, Voronych-Semchenko NM, Zukow W, Popovych DV. Evaluation of quantitative-qualitative levels of blood pressure by Tensioregulome. Journal of Education, Health and Sport. 2022;12(8):1216-1236.

OWN PILOT STUDIES

The object of the first pilot study [Vovchyna YuV & Zukow W, 2014] were 25 girls and 22 boys 10-16 years old, arrived at the rehabilitation on the spa Truskavets' from the territories of Ukraine that are contaminated with radionuclides.

At admission and after two weeks of balneotherapy (drinking of Naftussya bioactive water, application of ozokerite, mineral bathes) recorded systolic and diastolic blood pressure ("Omron M4-I", Netherland), heart rate variability (HRV) [Baevskiy RM & Ivanov GG, 2001] (device "Cardio", Kyïv), duration of delay of breathing after inspiration (Stange's test) and expiration (Henchy's test), Teslenko's orthostatic test [Druz' VA, 1980], Anfimov's proof test [Vadzyuk SN & Shuhan TB, 2000], clinical blood analysis as well as leukocytogram (LCG) of peripheral blood, on basis of which calculated Popovych's strain index and adaptation index [Popovych IL et al., 2000; Barylyak LG et al., 2013].

The following research problems and corresponding hypotheses can be identified.

1. Research problem. How does blood pressure vary among patients at Truskavets' spa? Hypothesis. There is significant diversity in blood pressure levels among patients at Truskavets' spa.

2. Research problem. What are the relationships between blood pressure and hemodynamic parameters? Hypothesis. There are significant correlations between blood pressure and various hemodynamic parameters.

3. Research problem. Can natural clusters of patients be identified based on blood pressure and hemodynamic parameters? Hypothesis. Distinct clusters of patients characterized by different blood pressure and hemodynamic profiles can be identified.

4. Research problem. Which parameters best differentiate the identified patient clusters? Hypothesis. There is a set of hemodynamic parameters that significantly differentiate clusters of patients with different blood pressure profiles.

5. Research problem. How does balneotherapy affect blood pressure and hemodynamic parameters? Hypothesis. Balneotherapy exerts varied effects on blood pressure and hemodynamic parameters in different groups of patients.

6. Research problem. Are there associations between blood pressure variability and autonomic nervous system parameters? Hypothesis. Blood pressure variability is linked to markers of sympathetic and parasympathetic activity.

7. Research problem. What are the relationships between blood pressure and hormonal parameters? Hypothesis. There are significant correlations between blood pressure levels and concentrations of certain adaptive hormones.

8. Research problem. Can the blood pressure response to balneotherapy be predicted based on a patient's initial parameters? Hypothesis. A patient's initial physiological parameters allow prediction of the nature and magnitude of blood pressure change in response to balneotherapy.

Statistical processing was carried out with the help of the software package "Statistica 5.5" and "Microsoft Excel". A significance level of $p<0.05$ was used throughout. The methods employed represent a comprehensive multivariate approach to analyzing the complex relationships between blood pressure and various physiological parameters.

The following statistical methods were used.

1. Descriptive statistics. Calculation of means and standard errors for various parameters. Calculation of percentages/proportions for categorical variables.

2. Correlation analysis. Pearson's correlation coefficients calculated between various parameters. Strength of correlations is interpreted as weak, moderate, or strong.

3. Regression analysis. Simple linear regression used to model relationships between variables. Multiple linear regression used to assess combined effects of multiple predictors. R, R^2, adjusted R^2, F-statistic, p-values, and standard errors reported.

4. Discriminant analysis. Stepwise forward discriminant analysis used to identify parameters that best distinguish between blood pressure clusters. Wilks' Lambda, F-to-enter, p-values reported for variable selection. Standardized and raw canonical coefficients calculated. Mahalanobis distances between clusters computed. Classification functions derived for predicting group membership. Classification accuracy assessed via classification matrices.

5. Canonical Correlation Analysis. Used to examine relationships between sets of variables. Canonical R, R^2, Chi-square, p-values reported. Factor loadings for canonical variables are presented.

6. Z-score calculation. Used to standardize variables for comparison.

7. Calculation of derived indices. Various physiological indices calculated from raw measurements.

8. Visualization. Scatterplots of canonical variables. 3D Surface Plots of relationships between variables.

Ascertained (Table 1) that after completion of balneotherapy mean pressure in 51% of children has not changed, however, in 23% of children had declined by 8% ($p<0,001$), and in 26% increased by 6% ($p<0.001$). Thus diastolic pressure reduced to a greater extent than

the systolic pressure: -10% vs -5%, whereas higher mean pressure accompanied nearly identical component changes both (+5,5% vs +7%).

When recalculations individual due to pressure on hender and age was found that changes in systolic pressure are normalizing character. Clearly reduced diastolic pressure was increased to the level of moderately reduced, however, initially declined moderately reduced even more. Interestingly, the heart rate significantly decreased in children with stable mean pressure, whereas the two other groups of children reduction heart rate had a tendency character. As a result, contrary to expectations, pattern changes Kerdö's vegetative index, calculated for values heart rate and diastolic pressure, not corresponds pattern changes mean blood pressure.

Table 1. Clusters of changes in parameters of Blood Pressure and Heart Rate at children caused by balneotherapy on Truskavets' spa

Parameters	Term	Clusters of Changes in Mean Blood Pressure		
		Decrease (n=11)	Not significant (n=24)	Increase (n=12)
Mean Blood Pressure, mmHg	Before After Change	82,4±2,6 76,2±2,0 -6,2±1,1*	72,9±1,2 72,9±1,2 0,0±0,5	71,9±1,8 76,4±2,1 +4,4±0,8*
Blood Pressure Systolic, mmHg	Before After Change	116,4±4,6 110,5±3,8 -5,9±2,0*	101,7±2,1 101,7±2,1 0,0±0,9	97,5±2,8 104,2±3,1 +6,7±2,2*
Blood Pressure Diastolic, mmHg	Before After Change	65,5±2,0 59,1±1,6 -6,4±1,5*	58,5±0,9 58,5±0,9 0±0,5	59,2±1,5 62,5±1,9 +3,3±0,9*
Blood Pressure Systolic, % of norm	Before After Change	108±4 102±3 -6±2*	95±2 95±2 0±1	91±3 97±3 +6±2*
Blood Pressure Diastolic, % of norm	Before After Change	91±2 81±2 -10±2*	82±1 82±1 0±1	82±2 87±3 +5±1*
Heart Rate, beat/min	Before After Change	76,5±0,9 72,9±1,7 -3,6±2,0	79,6±1,3 73,4±2,2 -6,2±1,5*	77,0±0,5 72,9±2,0 -4,1±2,2
Kerdö's Vegetative Index (1-BPd/HR)•100	Before After Change	14,6±2,1 19,8±2,4 +5,3±2,5*	26,2±1,3 19,0±2,0 -7,2±1,7*	23,0±2,3 13,8±2,9 -9,2±2,9*

And it is quite unexpected, contrary to previous studies, it turned out, that pattern of changes in Baevskiy's stress index as integral marker of autonomic regulation is **inverted** to pattern of changes in mean blood pressure (Table 2).

On the other hand, a surprise at first glance, were significant relationships between change in mean pressure and Henchy's expiration test (Table 2) as well as thrombocytes blood level (Table 3). However, on further consideration of such ties seem to be quite natural. Thus, there is a perception [Berezovsky VA, 2012], that Henchy's test reflexes not so much resistance to hypoxia as the severity of inhibitory processes in CNS, or rather, inhibition of inspiratory neurons. From these positions implies that changes in mean pressure are caused by changes in inhibitory activity of reticular formation neurons. It is known about relationships between EEG and HRV parameters reflexes activity of cortical, brainstem and autonomic neural structures respectively [Popovych IL et al., 2013; Popovych IL et al., 2014].

Next, have long known that thrombocytes (plateles) are the source of vasoconstrictor factors (serotonin, thromboxane etc), so it is likely that changes in thrombocytes blood level are accompanied by changes in plasma levels of vasoconstrictor factors.

Relationship between change in mean blood pressure (Y, mmHg) and thrombocytosis (X, G/L) is positive and approximated by the equation:

$y = -0{,}001x^2 + 0{,}155x - 2{,}5$

$R = 0{,}408$.

Instead, the relationship between change in mean blood pressure (Y, mmHg) and Henchy's Test (X, sec) is negative and is approximated by the equation:

$y = -0{,}004x^2 - 0{,}122x + 1{,}1$

$R = 0{,}226$.

Table 2. Accompanying changes in parameters of HRV and some other tests at children with various changes in mean blood pressure

Parameters	Term	Clusters of Changes in Mean Blood Pressure		
		Decrease (n=11)	Not significant (n=24)	Increase (n=12)
Baevskiy's Stress Index (AMo/2Mo•ΔX)	Before After Change	58±15 92±29 +34±31	128±20 141±17 +13±26	128±43 94±19 -34±47
Mode HRV (Mo), sec	Before After Change	0,92±0,05 0,91±0,04 -0,01±0,03	0,80±0,03 0,82±0,02 +0,02±0,03	0,84±0,03 0,83±0,04 -0,01±0,05
Sympathetic Tone (AMo), %	Before After Change	31±3 33±4 +2±4	39±3 40±2 +1±3	37±4 36±3 -1±4
Vagal Tone (MxDMin), sec	Before After Change	0,37±0,03 0,34±0,05 -0,03±0,04	0,28±0,03 0,24±0,02 -0,04±0,03	0,25±0,03 0,29±0,03 +0,04±0,03
Henchy's Expiration Test, sec	Before After Change	26±3 41±5 +15±4*	28±2 33±2 +5±2*	36±5 33±4 -3±5
Stange's Inspiration Test, sec	Before After Change	44±4 47±6 +3±4	42±3 48±4 +6±3*	48±6 52±6 +4±4
Teslenko's Orthostatic Test, points	Before After Change	5,2±0,5 4,8±0,4 -0,4±0,6	3,3±0,4 2,9±0,2 -0,4±0,3	4,7±0,4 3,6±0,6 -1,1±0,7
Anfimov's Proof Test, signes/2 min	Before After Change	280±26 315±30 +35±13*	275±17 326±16 +51±7*	314±27 352±33 +38±10*
Anfimov's Proof Test, mistakes/2 min	Before After Change	2,8±1,1 3,1±0,6 +0,3±0,4	3,5±0,7 2,4±0,4 -1,1±0,7	3,2±0,7 1,3±0,5 -1,9±0,7*

Table 3. Accompanying changes in parameters of Hemogram and Leukocytogram at children with various changes in Mean Blood Pressure

Parameters	Term	Clusters of Changes in Mean Blood Pressure		
		Decrease (n=11)	Not significant (n=24)	Increase (n=12)
Thrombocytes level,	Before After Change	256±14 253±14	239±7 265±8	237±13 276±12

G/l		-3±5	+26±5*	+39±8*
Hemoglobin level, g/l	Before After Change	128,9±1,9 128,9±1,4 0,0±0,7	129,0±0,9 129,6±0,7 +0,6±0,4	130,8±1,0 130,7±0,9 -0,1±0,4
Leukocytes level, G/l	Before After Change	5,48±0,34 5,49±0,33 +0,01±0,15	5,86±0,24 5,89±0,16 +0,03±0,18	5,72±0,23 5,99±0,22 +0,27±0,20
Eosinophils[1], %	Before After Change	2,1±0,4 2,8±0,7 +0,7±0,7	3,6±0,4 3,1±0,4 -0,5±0,5	2,8±0,6 3,4±0,5 +0,6±0,4
Stab Neutrophils[2], %	Before After Change	3,4±0,3 2,5±0,9 -0,9±0,4*	3,5±0,3 2,9±0,3 -0,6±0,4	3,3±0,4 3,6±0,8 +0,3±0,7
Segmented Neutrophils[3], %	Before After Change	55,8±3,1 53,9±2,3 -1,9±2,5	54,0±1,5 54,3±1,2 +0,3±1,8	49,3±2,4 50,1±2,3 +0,8±2,5
Lymphocytes[4], %	Before After Change	34,1±3,0 38,1±1,9 +4,0±1,3*	35,1±1,2 35,6±0,8 +0,5±1,2	41,6±2,1 39,1±2,1 -2,5±1,9
Monocytes[5], %	Before After Change	3,6±0,4 3,0±0,6 -0,6±0,5	3,8±0,4 4,0±0,4 +0,2±0,5	3,5±0,5 4,2±0,8 +0,7±0,9
Entropy of Leukocytogram n $H=-\Sigma p_i \bullet \log_2 p_i$ (i=5)	Before After Change	0,61±0,01 0,61±0,02 0,00±0,02	0,65±0,01 0,64±0,01 -0,01±0,01	0,63±0,01 0,65±0,02 +0,02±0,02
Number of Elements of Strain in Leukocytogram	Before After Change	1,2±0,2 1,8±0,2 +0,6±0,2*	1,7±0,2 2,0±0,2 +0,3±0,3	1,6±0,2 2,4±0,1 +0,8±0,2*
Popovych's Strain Index of Leukocytogram	Before After Change	0,15±0,02 0,27±0,06 +0,12±0,06*	0,25±0,05 0,27±0,05 +0,02±0,08	0,23±0,03 0,32±0,03 +0,09±0,04*
Popovych's Adaptation Index of Leukocytogram	Before After Change	0,63±0,09 0,72±0,11 +0,09±0,07	0,85±0,07 0,75±0,05 --0,10±0,08	0,67±0,06 0,53±0,04 -0,14±0,06*

Joint dynamics of humoral and neural factors represented by thrombocytes level and Henchy's test respectively determinates changes in mean blood pressure on 44,2% (Fig. 1).

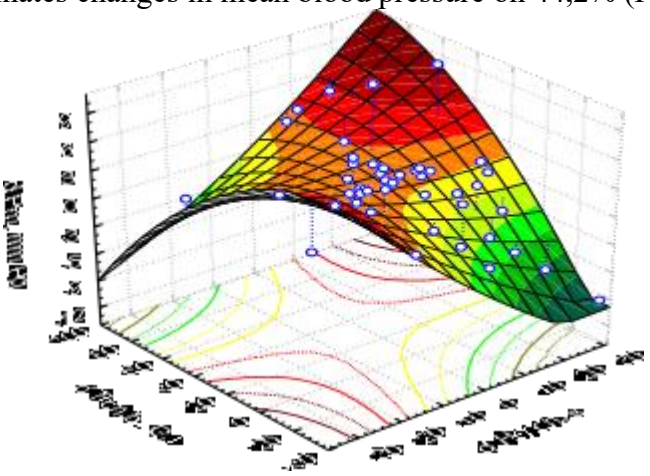

$R=0,665$; $R^2=0,442$; Adjusted $R^2=0,417$; $F_{(2,4)}=17,4$; $p<10^{-5}$; SE = 3,3 mmHg

Fig. 1. Relationship between changes in Henchy's test (X axis), thrombocytosis (Y axis) and mean blood pressure (Z axis) at children caused by balneotherapy on the Truskavets' spa

In order to identify yet other parameters which changes specific to different effects of balneotherapy on mean blood pressure, was conducted discriminant analysis (method forward stepwise). The program included in the model 12 discriminant variables (Table 4).

Table 4. Discriminant function analysis summary of changes in parameters specific to different effects of balneotherapy on mean blood pressure at children

Step 12, N of vars in model: 12; Grouping: 3 grs; Wilks' Λ: 0,218; approx. $F_{(24,4)}$=3,14; $p<10^{-4}$

Variables in the model (their changes)	Wilks' Lambda	Partial Lambda	F-remove (2,33)	p-level	Tole-rancy
Thrombocytes level	0,326	0,669	8,17	0,001	0,789
Henchy's Test	0,367	0,593	11,33	0,0002	0,535
Vagal Tone (MxDMn)	0,338	0,644	9,12	0,0007	0,238
Stab Neutrophils level	0,277	0,786	4,49	0,019	0,229
Lymphocytes level	0,231	0,943	1,00	0,377	0,580
Mode HRV	0,258	0,844	3,05	0,061	0,634
Heart Rate	0,241	0,904	1,76	0,188	0,707
Stange's Test	0,265	0,822	3,57	0,040	0,502
Elements of Strain LCG	0,262	0,830	3,37	0,047	0,390
Popovych's Strain Index	0,249	0,873	2,40	0,107	0,186
Signes in Proof Test	0,234	0,930	1,24	0,302	0,870
Sympathetic Tone (AMo)	0,234	0,932	1,20	0,315	0,327

The discriminant information is condensed in two canonical roots (Table 5). The major root contains 76% discriminant properties and, as evidenced by the structural coefficients for canonical variables (correlations variables - canonical roots), as expected, straight represents changes in duration of delay of breathing after expiration and inversely represents changes in blood level of thrombocytes. However, here also included patterns of changes in sympathetic tone and stab neutrophils level.

Table 5. Results of discriminant analysis of changes in parameters specific to different effects of balneotherapy on mean blood pressure (MP) in children

Changes in discriminant variables currently in the model	Parameters of Wilks' statistics			Coefficients for canonical variables				Changes in parameters specific to different changes in MP		
	Λ	F	p<	Raw		Structural		MP - (11)	MP ± (24)	MP + (12)
				R1	R2	R1	R2			
Henchy's Test, sec	0,520	8,3	10^{-4}	0,086	-0,021	**0,36**	-0,22	+15±4	+5±2	-3±5
AMo,%	0,234	3,3	10^{-3}	0,005	0,014	**0,03**	0,23	+2±4	+1±3	-1±4
Thrombocytes, G/l	0,702	9,3	10^{-3}	-0,026	0,029	**-0,41**	0,43	-3±5	+26±5	+39±8
Stab Neutrophils, %	0,421	5,6	10^{-4}	-0,293	-0,637	**-0,05**	-0,27	-0,9±0,4	-0,6±0,4	+0,3±0,7
MxDMn, sec	0,467	6,5	10^{-4}	-9,940	-6,603	**-0,16**	-0,17	-0,03±0,04	-0,04±0,03	+0,04±0,03
Stange's Test, sec	0,315	4,2	10^{-4}	-0,055	-0,039	-0,02	**-0,20**	+3±4	+6±3	+4±4
Signes in Proof Test	0,248	3,5	10^{-4}	2,896	3,049	-0,01	**-0,16**	+35±13	+51±7	+38±10
Mode HRV, sec	0,380	5,0	10^{-4}	0,037	0,082	0,23	**-0,09**	-0,01±0,03	+0,02±0,03	-0,01±0,05
Popovych's Strain Index	0,268	3,7	10^{-4}	-0,689	-0,575	-0,08	**-0,16**	+0,12±0,06	+0,02±0,08	+0,09±0,04
Elements of Strain	0,285	4,0	10^{-4}	-0,063	-0,000	-0,03	**0,08**	+0,6±0,2	+0,3±0,3	+0,8±0,2
Heart Rate, beat/min	0,344	4,6	10^{-4}	3,581	3,026	0,03	**0,10**	-3,6±2,0	-6,2±1,5	-4,1±2,2
	Constants			-0,066	-1,386					

Chi-square tests with successive roots removed	r_1^*=0,81; Wilks' Λ=0,22; $\chi^2_{(24)}$=59; $p<10^{-4}$	Means of Roots of canonical variables	**Root 1** 76%	+1,50	+0,37	-2,12
	r_2^*=0,61; Wilks' Λ=0,62; $\chi^2_{(11)}$=18; p=0,079		**Root 2** 24%	-1,06	+0,70	-0,44

The calculation of values of individual unstandardized canonical scores of roots by summation the multiplications of individual variables on the raw coefficients for canonical variables plus constants (see Table 5) allows the visualization all the children on the plane of the two roots (Fig. 2).

It is seen that children, liable to increase in mean blood pressure, localized in the negative zone (centroid: -2,12) of Root 1 axis. This reflects increasing in thrombocytosis and tendency to reduction in Henchy's test. Opposite effect accompanied with increasing in Henchy's test and tendency to reduction in thrombocytosis illustrated the placement in the positive zone (centroid: +1,50) of major root axis. Neutral effect on mean blood pressure (P±) corresponds to intermediate localization (centroid: +0,37). Downward pattern follows the dynamics of sympathetic tone, and the rising pattern follows the dynamics of stab neutrophils level. In general, exist two opposite pattern of changes (d):

dMP->dMP±>dMP+ and dMP-<dMP±<dMP+.

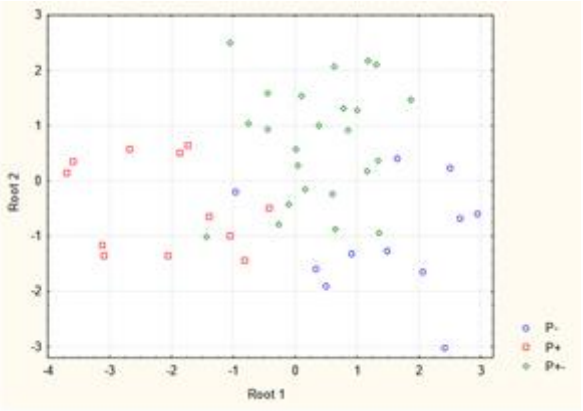

Fig. 2. Unstandardized canonical scores of roots of changes in parameters characterized various effects of balneotherapy on mean blood pressure (P) at children

However, along the axis of minor Root 2 (that contains 24% discriminant properties and is weakly structured) effects of alternative habitats overlap, whereas neutral effect is illustrated highest placing (centroid: +0,70), reflecting a both maximal increase in duration of delay of breathing after inspiration and in quantity registered signs in proof test and decrease in heart rate as well a minimal change in quantity elements of strain and Popovych's strain index of LCG. Changes in these parameters were approximately the same as with a decrease and an increase in MP and different from those in a stable MP. Two opposite pattern of changes looks as: dMP-≈dMP+<dMP± and dMP-≈dMP+>dMP±.

It is known that Stange's test reflexes resistance to hypoxia [Barylyak LG et al., 2011; Berezovskyi VY, 2012] and elements of strain in leukocytogram reflexes disturbances in relationships (disharmony) between major hormones of adaptation (adrenals, gonads and thyroid gland) [Popovych IL et al., 2000; Kostyuk PG et al., 2006; Barylyak LG et al., 2013]. It is shown that balneotherapy on Truskavets' spa causes various effects on resistance to hypoxia [Barylyak LG et al., 2011], leukocytogram and immunogram [Kostyuk PG et al., 2006; Popovych IL, 2011; Kozyavkina OV, 2011; Vis'tak HI & Popovych IL, 2011; Vis'tak HI et al., 2013; Chebanenko OI et al., 2013]. One must therefore assume that Anfimov's proof test affect cytokines released from immunocytes, since the psychotropic effects of cytokines are well known [Sheiko VI et al., 2007; Uchakin PN et al., 2007]. When account is taken of

these provisions it seems that when balneotherapy causes maximal release of nootropic cytokines in combination with the absence of significant changes in the relationships between hormones of adaptation, mean blood pressure remained stable, whereas disharmonizing effects of balneotherapy in conjunction with insufficiently pronounced stimulation of release of nootropic cytokines accompanied with those or other changes in mean blood pressure.

In general, all three clusters are mutually separated. Squared Mahalanobis distances (D^2_M) between clusters P- and P+ average 14,4 ($F=4,7$; $p<10^{-3}$), P- and P±: 4,7 ($F=2,03$; $p=0,053$), P+ and P±: 8,0 ($F=3,7$; $p=0,001$).

The calculation of classification functions (Table 6) makes it possible to aggregate changes in discriminant parameters retrospectively identify children with an increase in MP with an accuracy of 92% (one error per 12 persons), with a decrease in MP with an accuracy of 82% (two errors on 11 persons), and with stable MP to within 88% (three errors on 24 children). Overall classification accuracy is 87%.

Table 6. Classification functions for accompaniments of various effects of balneotherapy on mean blood pressure

Change in Variables	MP-	MP+	MP±
Thrombocytes	-0,023	0,088	0,057
Henchy's Test	0,166	-0,159	0,032
Vagal Tone	-14,49	17,45	-14,89
Stab Neutrophils LCG	-0,432	0,236	-1,221
Lymphocytes LCG	0,103	0,018	0,205
Mode HRV	6,69	-4,41	7,98
Heart Rate	-0,131	0,043	-0,137
Stange's Test	-0,076	0,151	-0,006
Elements of Strain LCG	-0,513	1,628	-0,746
Popovych's Strain Index	3,07	-5,54	5,17
Signes in Proof Test	0,042	0,032	0,061
Sympathetic Tone	-0,040	0,079	-0,028
Constants	-3,81	-5,01	-4,03

The question arises why the same treatment causes various changes in blood pressure? Obviously because children are different, but rather varies with respect their reactivity to balneotherapy. Using the same discriminant analysis, we identified 19 initial parameters conditionizing different effects of balneotherapy on blood pressure.

Results, reflected on Table 7 and Fig. 3, show that the mean blood pressure decreased in those children whose initial levels of it as well as normalized systolic and diastolic blood pressure, Teslenko's orthostatic index, vagal tone, actual and normalized body weight as well as thrombocytes level were to fetch maximum, whereas initial levels of Kerdö's vegetative index, sympathetic tone, entropy of leukocytogram, Popovych's adaptation index and body temperature were minimal. Was minimal also hender index, calculated for the algorithm: boys=0, girls=1, reflecting the predominance of boys. Children whose MP was increased or remained stable, characterized by smaller or larger values of the discriminant variables, information on which is condensed to the major root, not differing significantly among themselves (patterns: MAP->MAP+≈MAP± and MAP-<MAP+≈MAP±). But the differences between the groups were found on the variables, associated with minor root. As you can see, MP was increased in children with a maximum for the sample values in blood lymphocytes and hemoglobin as well as Henchy's and proof tests, whereas at the children of the other two groups the rates were about the same (pattern: MAP+>MAP-≈MAP±).

Table 7. Results of discriminant analysis of parameters conditionizing the various effects of balneotherapy on mean blood pressure

N of vars in model: 19; Grouping: 3 groups; Wilks' Λ: 0,035; approx. $F_{(38,5)}$=5,99; $p<10^{-4}$

Discriminant variables-predictors currently in the model	Parameters of Wilks' statistics			Coefficients for canonical variables				Means of parameters conditionizing different changes in Mean Pressure		
	Λ	F	p<	Raw		Structural		MP- n=11	MP+ n=12	MP± n=24
				R1	R2	R1	R2			
Mean Pressure, mm Hg	0,352	7,0	10^{-6}	0,782	-0,448	**-0,16**	0,26	82,4±2,6	71,9±1,8	72,9±1,2
BP systolic, % of norm	0,037	6,3	10^{-6}	-0,252	0,210	**-0,14**	0,34	108±4	91±3	95±2
BP diastolic, % of norm	0,080	6,3	10^{-6}	0,482	0,230	**-0,13**	0,14	91±2	83±2	82±1
Teslenko Orthostatic Ind.	0,191	7,0	10^{-6}	-0,056	-0,102	**-0,11**	-0,23	5,2±0,5	4,7±0,5	3,3±0,4
Vagal Tone (ΔX), sec	0,538	7,8	10^{-4}	-14,27	6,293	**-0,09**	0,22	0,37±0,03	0,25±0,03	0,28±0,03
Body Weight, kg	0,035	6,0	10^{-6}	-0,069	0,188	**-0,07**	0,02	50,8±3,5	45,5±2,3	44,0±2,1
Body Weight, % of norm	0,071	6,1	10^{-6}	-0,041	-0,088	**-0,06**	-0,02	109±6	103±3	100±3
Thrombocytes level, G/l	0,062	6,0	10^{-6}	-0,035	-0,012	**-0,05**	0,08	256±14	237±13	239±7
Kerdö's Vegetative Index	0,667	11	10^{-4}	1,340	0,060	**0,19**	-0,01	15±2	23±2	26±1
Sympathotone (AMo), %	0,052	6,2	10^{-6}	0,073	0,056	**0,07**	0,01	31±3	37±4	39±3
Entropy of Leukogram	0,154	6,2	10^{-6}	2,853	-1,416	**0,07**	0,04	0,61±0,01	0,63±0,01	0,65±0,01
Popovych's Adaptat. Ind.	0,298	6,7	10^{-6}	3,692	-0,688	**0,07**	0,15	0,63±0,09	0,67±0,06	0,85±0,07
Hender Index	0,042	6,4	10^{-6}	-1,317	0,273	**0,05**	-0,06	0,36±0,15	0,58±0,15	0,58±0,10
Body Temperature, ^{0}C	0,420	7,6	10^{-5}	8,084	1,829	**0,07**	0,07	36,2±0,07	36,3±0,08	36,4±0,05
Heart Rate, beats/min	0,108	5,6	10^{-6}	-1,150	-0,006	**0,07**	0,17	77±1	77±1	80±1
Lymphocytes level, %	0,224	7,2	10^{-6}	0,072	-0,099	0,02	**-0,41**	34±3	42±2	35±1
Henchy's Expirat. Test, s	0,170	6,6	10^{-6}	-0,051	-0,034	0,01	**-0,31**	26±3	36±5	28±2
Proof Test, signes/2 min	0,118	5,9	10^{-6}	-0,005	-0,010	-0,00	**-0,20**	280±26	314±27	275±17
Hemoglobin level, g/l	0,130	6,2	10^{-6}	-0,085	0,052	0,02	**-0,05**	128,9±1,9	130,8±1,0	129,0±0,9
	Constants			-295	-65,2					
Chi-square tests with successive roots removed	r_1^*=0,966; Wilks' Λ=0,035; $\chi^2_{(38)}$=118; $p<10^{-6}$			Root Mean		**Root 1** 94%		-6,25	+0,24	+2,75
	r_2^*=0,696; Wilks' Λ=0,516; $\chi^2_{(18)}$=23; p=0,183					**Root 2** 6%		+0,49	-1,60	+0,58

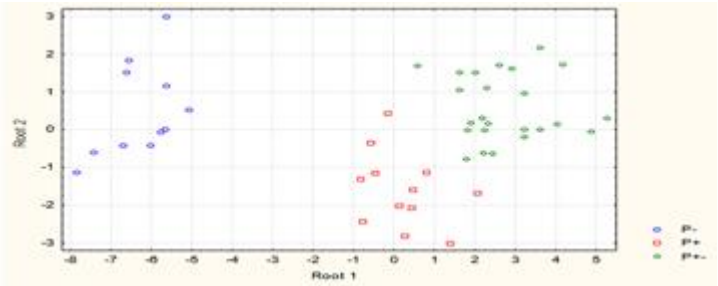

Fig. 3. Unstandardized canonical scores of roots of initial parameters as predictors of various effects of balneotherapy on mean blood pressure at children

In general, all three clusters are clearly mutually separated. D^2_M between clusters MAP- and MP+ average 49,6 (F=8,1; $p=10^{-6}$), MAP- and MAP±: 86,5 (F=18,7; p<10-6), MAP+ and MAP±: 11,8 (F=2,7; p=0,009).

Calculation of classification functions (Table 8) allows forecast the character of effect of balneotherapy on mean blood pressure with accuracy of 100%!

Table 8. Classification functions for forecast of various effects of balneotherapy on mean blood pressure at children

Variables-predictors	**MP-**	**MP+**	**MP±**
Kerdö's Vegetative Index, units	420,4	429,0	432,5
Vagal Tone (ΔX), sec	-3533	-3639	-3661
Body Morning Temperature, ^{0}C	3034	3083	3107
Mean Blood Pressure, mmHg	254,6	260,6	261,6
Popovych's Adaptation Index, units	853,9	879,3	887,0

Lymphocytes level of LCG, %	13,7	14,4	14,4
Teslenko's Orthostatic Index, units	16,3	16,1	15,8
Henchy's Expiration Test, sec	-16,2	-16,5	-16,7
Entropy of Leukocytogram (LCG)	562,1	583,6	587,6
Hemoglobin level, g/l	-23,8	-24,4	-24,5
Anfimov's Proof Test, signes/2 min	-2,0	-2,0	-2,0
Heart Rate, beats/min	-351,8	-359,3	-362,1
BP systolic, % of norm	-76,2	-78,3	-78,4
BP diastolic, % of norm	151,3	153,9	155,6
Body Weight, kg	-21,0	-21,9	-21,6
Body Weight, % of norm	-11,4	-11,5	-11,8
Thrombocytes level, G/l	-10,9	-11,1	-11,3
Sympathotone (AMo), %	27,8	28,1	28,4
Hender Index (boys=0; girls=1)	-361,4	-370,5	-373,2
Constants	-55227	-56987	-57871

It turns out that it is possible to predict not only the character, but also the value of the individual reaction of mean blood pressure to balneotherapy. Initial level of mean blood pressure determinates its change on 29-35% (Fig. 4).

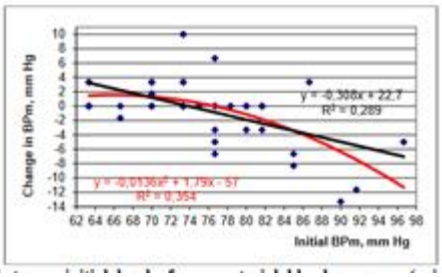

Fig. 4. Correlation between initial level of mean blood pressure (axis X) and changes in mean blood pressure caused by balneotherapy (axis Y)

Given the weak relationships between changes in mean blood pressure and initial levels both vagal tone (r = -0,24) and blood lymphocytes (r = 0,19) measure of determination increases to 38% (Fig. 5).

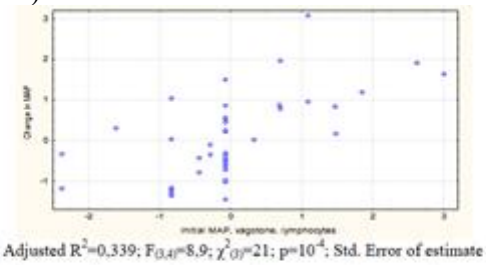

R=0,618; R^2=0,382; Adjusted R^2=0,339; $F_{(3,4)}$=8,9; $\chi^2_{(3)}$=21; p=10^{-4}; Std. Error of estimate dMAP: 3,6 mm Hg

Interception	β	SE of β	B	SE of B	$t_{(43)}$	p-level	r dMAP/ Initial levels
Initial levels of			22,73	6,13	3,71	0,0006	
MAP, mm Hg	-0,542	0,120	-0,311	0,069	-4,51	0,00005	-0,54
Vagal Tone (ΔX), s	-0,261	0,120	-9,620	4,433	-2,17	0,035	-0,24
Lymphocytes, %	0,147	0,120	0,086	0,070	1,22	0,228	0,19

Fig. 5. Canonical correlation between initial levels of mean blood pressure, vagal tone and
lymphocytes blood level (axis X) and changes in mean blood pressure caused by balneotherapy (axis Y)

Thus, in first pilot study we have shown that at children reaction of blood pressure to course of balneotherapy on spa Truskavets' is ambiguous. However, this naturally polyalternativeness conditionized by constellation initial parameters of hemodynamics,

autonomous regulation, hemogram, leukocytogram etc, as well as by hender. This is fully consistent with the concept of Truskavetsian Scientic School of Balneology about polyvariety effects on the body of factors of Truskavets' spa [Popovych IL et al., 2005; Barylyak LG et al., 2011; Chebanenko OI et al., 2011; Vis'tak HI et al., 2013].

The second pilot study [Vovchyna YuV et al., 2016] involved twenty volunteers – ten women and ten men aged 33-76 years without clinical diagnose. In the morning on an empty stomach recorded thrice running Blood Pressure and Heart Rate ("Omron M2 Compact", Netherland). Then ECG in standard lead II recorded hardware-software complex "Cardiolab+VSR" (KhAI Medica, Kharkiv, Ukraine). For further analyses the following HRV parameters were selected. Temporal parameters (Time Domain Methods): the standard deviation of all NN intervals (SDNN), the square root of the mean of the sum of the squares of differences between adjacent NN intervals (RMSSD), the percent of interval differences of successive NN intervals greater than 50 ms (pNN_{50}), Triangulary Index (TI); heart rate (HR), mode (Mo), amplitude of mode (AMo), variation scope (MxDMn). Spectral parameters (Frequency Domain Methods): power spectral density (PSD) components of HRV - high-frequency (HF, range 0,4÷0,15 Hz), low-frequency (LF, range 0,15÷0,04 Hz), very low-frequency (VLF, range 0,04÷0,015 Hz) and ultralow-frequency (ULF, range 0,015÷0,003 Hz). We calculated classical indexes: LF/HF, LFnu=100%•LF/(LF+HF), Baevskiy's Stress Index (BSI=AMo/2•Mo•MxDMn) as well as Baevskiy's Activity of Regulatory Systems Index (BARSI) [Baevskiy RM et al., 1984; HRV, 1996; Berntson GG et al., 1997; Baevskiy RM & Ivanov GG, 2001].

Simultaneosly electroencephalogram (EEG) recorded a hardware-software complex "NeuroCom Standard" (KhAI Medica, Kharkiv, Ukraine) monopolar in 16 loci (Fp1, Fp2, F3, F4, F7, F8, C3, C4, T3, T4, P3, P4, T5, T6, O1, O2) by 10-20 international system, with the reference electrodes A and Ref on the tassels of ears. Among the options considered the average EEG amplitude (μV), average frequency (Hz), frequency deviation (Hz), index (%), coefficient of asymmetry (%) and absolute (μV^2/Hz) and relative (%) PSD of basic rhythms: β (35÷13 Hz), α (13÷8 Hz), θ (8÷4 Hz) and δ (4÷0,5 Hz) in all loci, according to the instructions of the device.

Then determine the rate of electronegative nuclei of buccal epithelium (named as Electrokinetic Index) by intracellular microelectrophoresis on the device "Biotest" (VN Karazin National University, Kharkiv), according to the method described [Shakhbazov VG et al., 2000]. Recorded electro-skin conductance in acupuncture points Pg(ND), TR(X) and MC(AVL) Right and Left (device "Medissa") [Chukhrayev NV et al., 2002].

Then determined content in blood plasma of parameters of hormonal status: cortisol, testosterone, triiodothyronine and calcitonin (by the ELISA method with the use of analyzers "Tecan" and "RT-2100C" and corresponding sets of reagents from "Алкор Био", XEMA Co., Ltd and DRG International Inc.); lipids spectrum of plasma: total cholesterol (by a direct method after the classic reaction by Zlatkis-Zack) and content of him in composition of α-lipoproteins (by the enzyme method by Hiller G [1987] after precipitation of notα-lipoproteins; pre-β-lipoproteins (expected by the level of triglycerides, by a certain meta-periodate method); β-lipoproteins (expected by a difference between a total cholesterol and cholesterol in composition α-and pre-β-lipoproteins). In the same portion of plasma determined level of uric acid (by a uricase method), calcium (by a reaction with arsenazo III), magnesium (by a reaction with colgamite), phosphate (by a phosphate-molibdate method), chloride (by a mercurial-rodanide method), sodium and potassium (by the method of flaming photometry) according to instructions [Goryachkovskiy AM, 1998] with the use of analyzers "Reflotron" (BRD), "Pointe-180" (USA), "СФ-46" ПФМУ 4.2 (URSS) and corresponding sets of reagents. After 7 days all tests repeated.

According to calculations by the formula:

$|r|=\{\exp[2t/(n-1,5)^{0,5}]-1\}/\{\exp[2t/(n-1,5)^{0,5}]+1\}$

for a sample of n=40 critical value |r| at $p<0,05$ ($t>2,00$) is 0,31.

Provisional analysis showed that the strength of correlation between diastolic and systolic pressure occupies an intermediate position between moderate and large (Fig. 6). This casts the idea that the two components blood pressure differently associated with neuroendocrine and metabolic parameters.

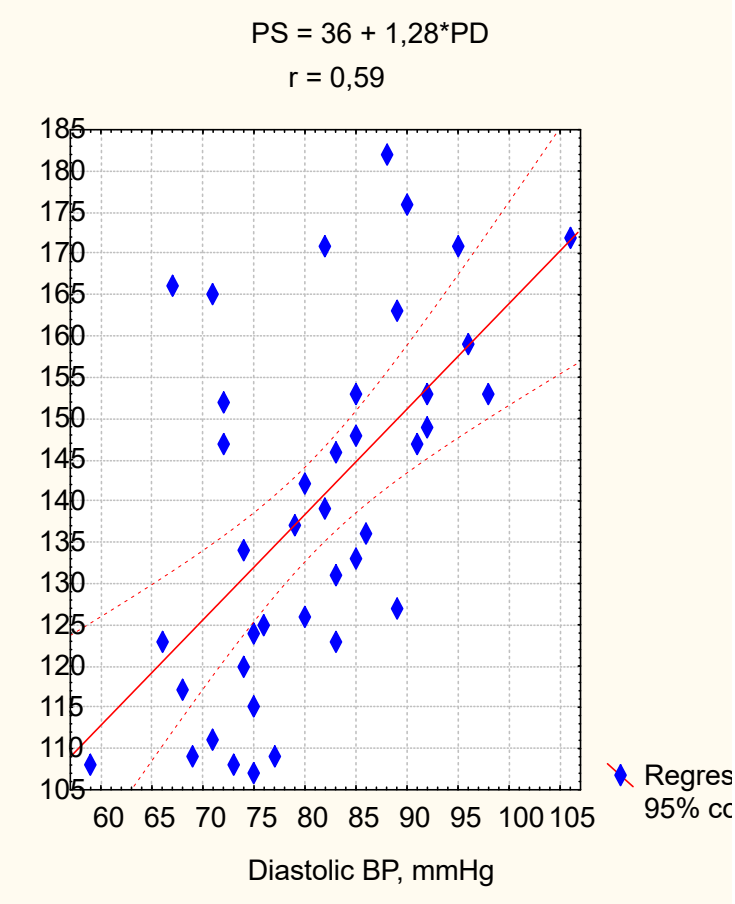

Fig. 6. Relationship between Diastolic (X-line) and Systolic (Y-line) Blood Pressure

Taking as enhanced standards range 80÷120% state that Systolic Blood Pressure in 32 cases was within it (average 102±2%), and only 8 cases exceeded the 3÷13% (an average of 8±1%), while Diastolic Blood Pressure exceeded the upper limit of normal at 2÷40% (mean 13±2%) in 20 cases out of 40, accounting for the other 20 cases 108±1% of the age norm. Thus, the observed contingent characterized generally normal for a particular age or borderline high blood pressure, predominantly diastolic. This correlation between age and age-normalized blood pressure is weak (Fig. 7).

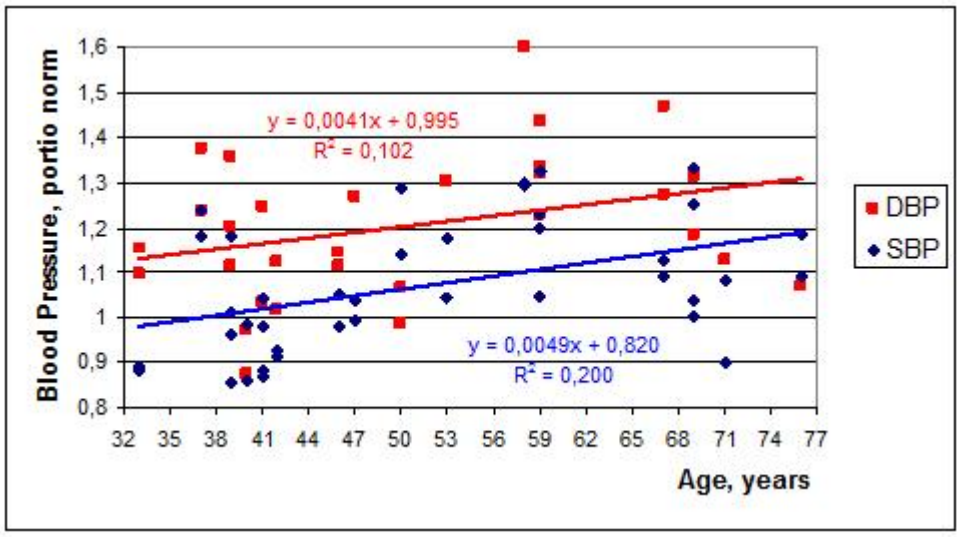

Fig. 7. Normalized levels of Diastolic and Systolic Blood Pressure in Persons of various Age

Instead, current Systolic Blood Pressure correlated with age largely (Fig. 8).

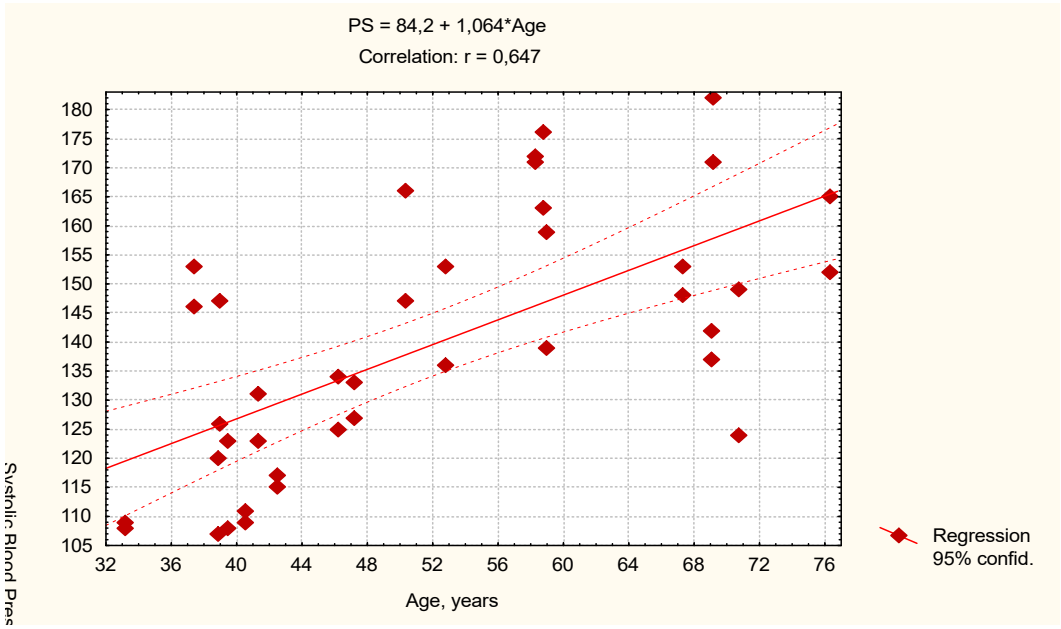

Fig. 8. Relationship between Age (X-line) and Systolic Blood Pressure (Y-line)

In order to quantify the strength of the connection Blood Pressure and Hender we estimated men as 0 and the women as 1. Detected moderate negatively relationship between Systolic Blood Pressure and Hender Index (r=-0,31). Taken together aging and hender factors determines Systolic Blood Pressure on 44% (Table 9).

Table 9. Regression Summary for Dependent Variable SBP and Independent Variables Age and Hender Index

R=0,683; R^2=0,467; Adjusted R^2=0,438; $F_{(2,4)}$=16,2; p=10^{-5}; SE: 16 mmHg

N=40		Beta	St. Err. of Beta	B	St. Err. of B	$t_{(37)}$	p-level
Variables	r		Intercpt	91,7	11,3	8,10	10^{-6}
Age, years	0,65	,615	,121	1,012	,200	5,07	10^{-5}
Hender	-0,31	-,222	,121	-9,48	5,18	-1,83	,075

Dependence Diastolic Blood Pressure on the age weak (r=0,29), instead of the sex much (Fig. 9).

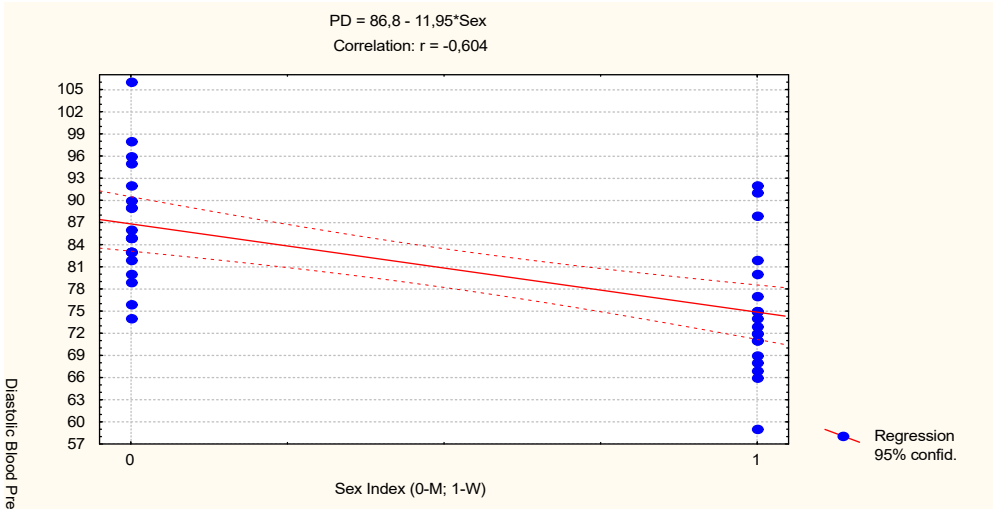

Fig. 9. Relationship between Hender Index (X-line) and Diastolic Blood Pressure (Y-line)

Taken together aging and hender factors determines Diastolic Blood Pressure on 38% (Table 10).

Table 10. Regression Summary for Dependent Variable DBP and Independent Variables Age and Hender Index

R=0,639; R^2=0,409; Adjusted R^2=0,377; $F_{(2,4)}$=12,8; $p<10^{-4}$; SE: 7,9 mmHg

N=40		Beta	St. Err. of Beta	B	St. Err. of B	$t_{(37)}$	p-level
Variables	r		Intercpt	78	5,5	14,1	10^{-6}
Hender	-0,60	-,573	,128	-11,3	2,5	-4,49	10^{-4}
Age, years	0,29	,212	,128	,162	,098	1,66	,105

Now, examine relationships of Systolic Blood Pressure with Neuroendocrine factors. No correlation with Triiodothyronine (r=-0,21), Testosterone (r=0,17) and Cortisol (r=0,13). Detected negatively relationships with HRV markers of vagal tone: MxDMn (r=-0,37), HRV TI (r=-0,32), pNN_{50} (r=-0,23), RMSSD (r=-0,21) while positively dependence from Calcitoninemia, besides sexual normalized (r=0,34) but not current (r=0,12) (mean norm for women 5,5 ng/L, for men 13,95 ng/L). Taken together vagal tone and normalized Calcitonin determine Systolic Blood Pressure on 18,9% (Table 11, Fig. 10).

Table 11. Regression Summary for Dependent Variable SBP and Independent Variables Variation Scope and Calcitonin (portion of norm)

R=0,435; R^2=0,189; Adjusted R^2=0,145; $F_{(2,4)}$=4,3; p=0,021; SE: 19,9 mmHg

N=40		Beta	St. Err. of Beta	B	St. Err. of B	$t_{(37)}$	p-level
Variables	r		Intercpt	147,8	13,1	11,3	10^{-6}
MxDMn, ms	-0,37	-,289	,155	-,081	,044	-1,86	,071
Calcitonin, pn	0,34	,248	,155	8,455	5,292	1,60	,119

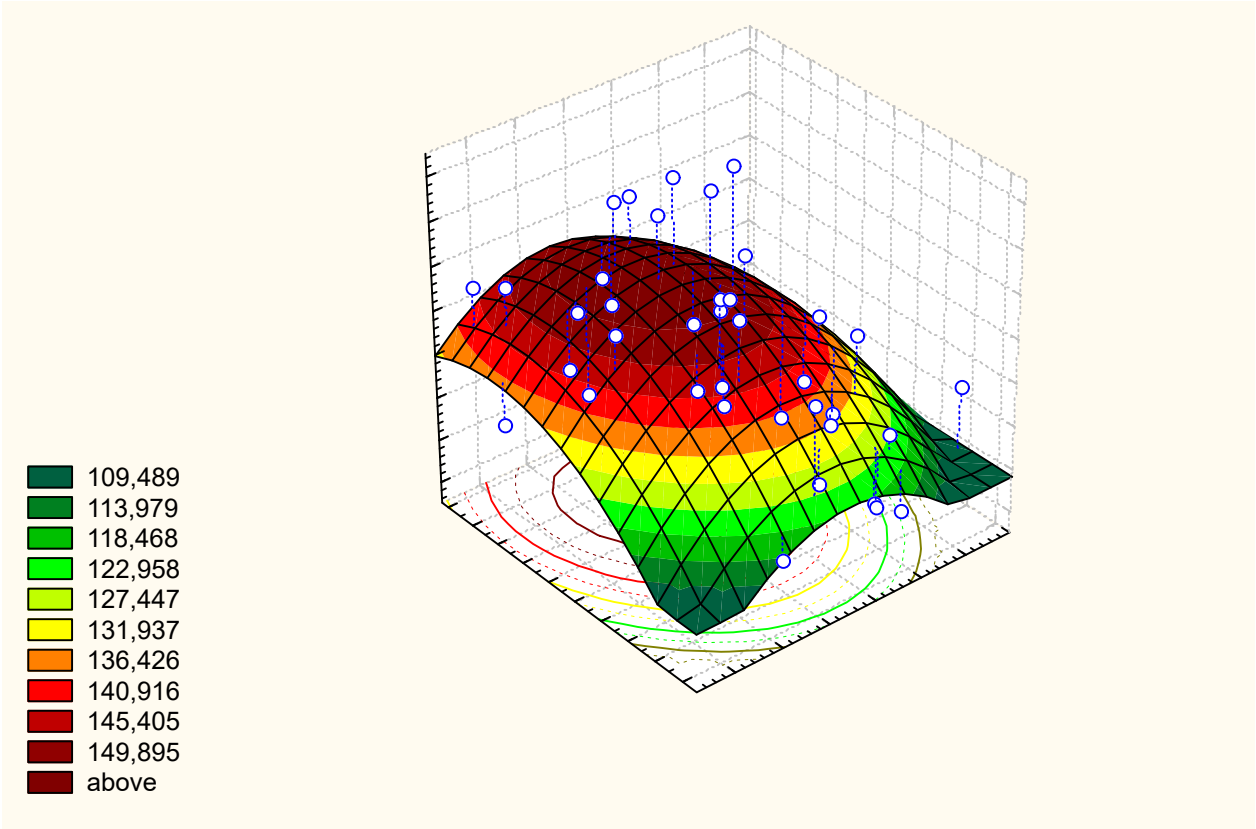

Fig. 10. Relationship between Variation Scope (X-line), normalized Calcitoninemia (Y-line) and Systolic Blood Pressure (Z-line)

By stepwise exclusion in the final regression model were included some more 5 parameters HRV and Index of α-rhythm EEG, which taken together determine Systolic Blood Pressure on 40,5% (Table 12, Fig. 11).

Table 12. Regression Summary for Dependent Variable SBP and Independent Neuroendocrine Variables

R=0,726; R^2=0,527; Adjusted R^2=0,405; $F_{(8,3)}$=4,3; $\chi^2_{(8)}$=25,5; p=0,0014; SE:16,6 mmHg

N=40		Beta	St. Err. of Beta	B	St. Err. of B	$t_{(32)}$	p-level
Variables	r		Intercpt	367	78	4,69	10^{-4}
MxDMn, msec	-0,37	-1,223	,393	-,344	,110	-3,11	,004
PSD LF, % TP	-0,36	-,207	,136	-,334	,219	-1,52	,138
pNN_{50}, %	-0,23	-,879	,585	-1,501	,999	-1,50	,143
α-rhythm Ind, %	-0,22	-,319	,137	-,230	,099	-2,33	,027
RMSSD, msec	-0,21	1,000	,642	1,216	,780	1,56	,129
Calcitonin, port/n	0,34	,436	,141	14,83	4,80	3,09	,004
Baevskiy's SI, ln	0,23	-1,558	,468	-43,66	13,11	-3,33	,002
AMo, %	0,21	,709	,294	,989	,411	2,41	,022

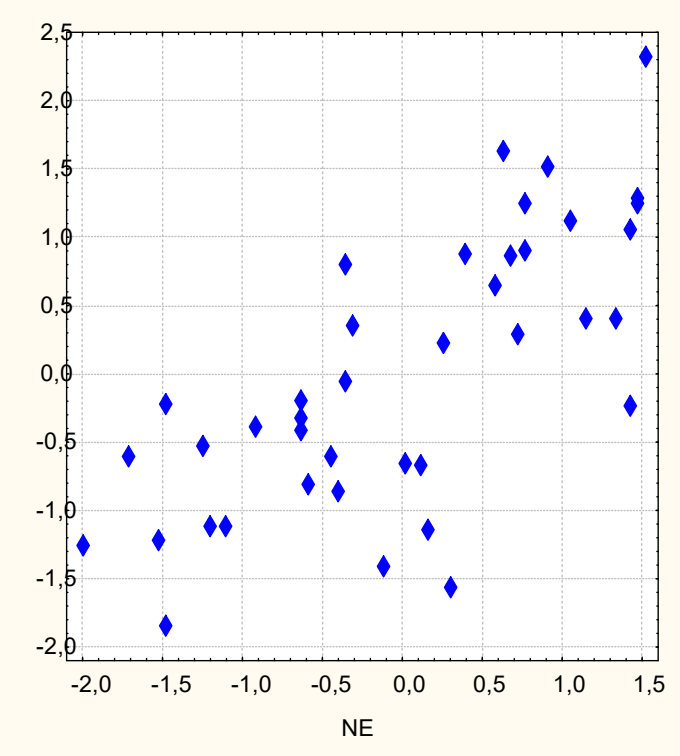

Fig. 11. Canonical correlation between Neuroendocrine factors (X-line) and Systolic Blood Pressure (Y-line)

Among biophysics parameters strong negatively correlate with Systolic Blood Pressure Electrokinetic Index (Fig. 12) as inversely marker of biological age [Shakhbazov VG et al., 1986; Ushakov IB et al., 2008; Kyrylenko IG et al., 2016].

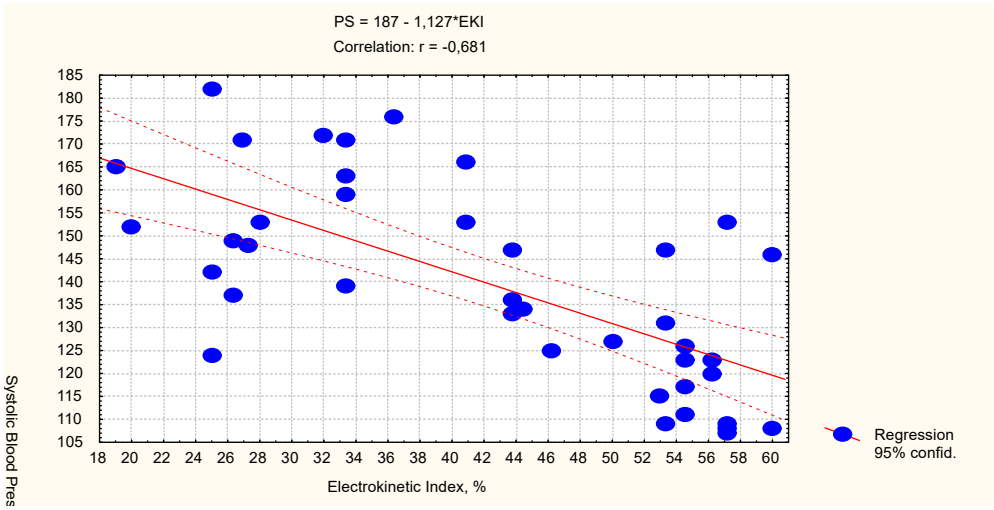

Fig. 12. Relationship between Electrokinetic Index (X-line) and Systolic Blood Pressure (Y-line)

Among electro-skin conductance in 6 points of AP significant correlate with Systolic BP MC(AVL) Left (r=0,33) and TR(X) Right (r=0,30). Last as marker activity of endocrine system [Samosyuk IZ et al., 1994; Hubyts'kyi VYo et al., 2013] together with Electrokinetic Index determinats Systolic Blood Pressure on 50,5% (Table 13, Fig. 13).

Table 13. Regression Summary for Dependent Variable SBP and Independent Biophysics Variables

R=0,729; R^2=0,531; Adjusted R^2=0,505; $F_{(2,4)}$=20,9; $p<10^{-5}$; SE: 15 mmHg.

N=40		Beta	St. Err. of Beta	B	St. Err. of B	$t_{(37)}$	p-level
Variables	r		Intercpt	120	30	3,98	,000312
Electrokinetic Index, %	-0,68	-,667	,113	-1,104	,187	-5,91	,000001
EC AP TR(X) Right, un.	0,30	,259	,113	1,042	,453	2,30	,027297

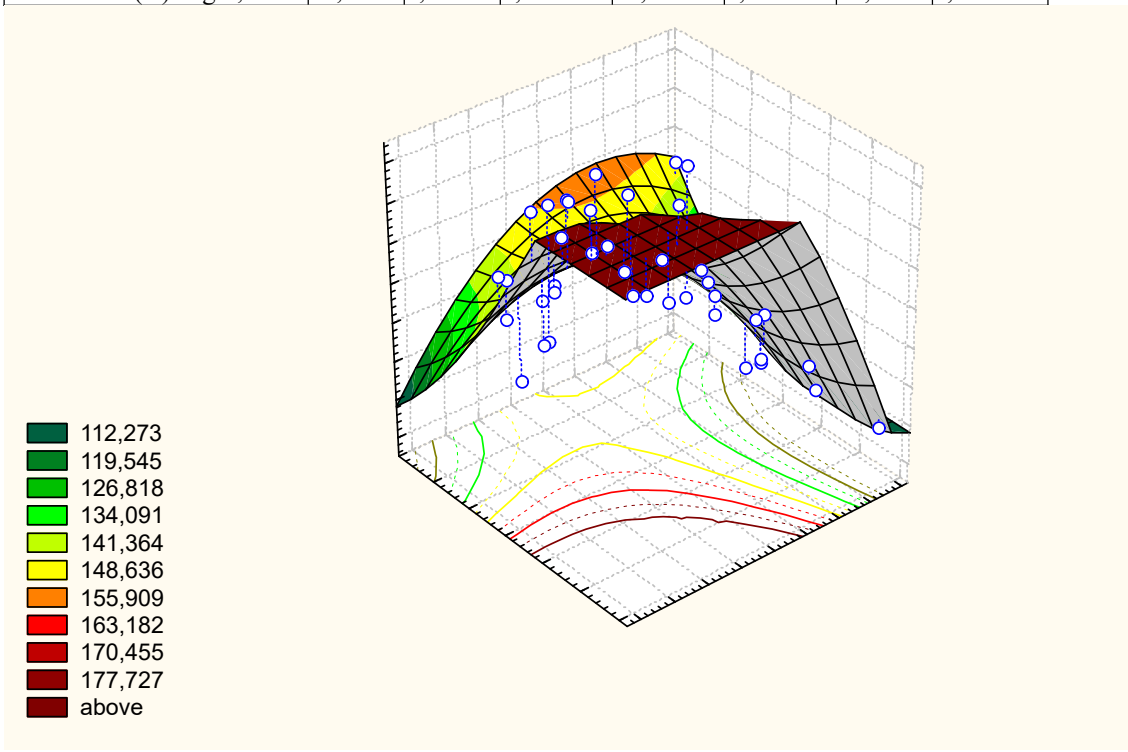

Fig. 13. Relationship between Electrokinetic Index (X-line), conductance in AP TR(X) Right (Y-Line) and Systolic Blood Pressure (Z-line)

Among metabolic parameters strongest influence on Systolic Blood Pressure of total Cholesterol (Fig. 14) as well as its content in low density (r=0,47) and very low density (r=0,41) Lipoproteins. Significantly or borderline correlates with Systolic Blood Pressure Plasma Uric Acid (r=0,42) as endogenous Caffeine [Ivassivka SV et al., 2004], Phosphate (r=0,40) and Calcium (r=0,28) as well as $1/(Pp \bullet Cap)^{0,5}$ Ratio (r=-0,48) as marker of Calcitonin Activity [Popovych IL, 2011], $(Ku/Nau)^{0,5}$ Ratio (r=0,29) as marker of Mineralocorticoid Activity and $(Cap/Kp)^{0,5}$ Ratio (r=0,27) as marker of Sympatho-Vagal Balance [Kazakova M et al., 1979; Fajda OI et al., 2016].

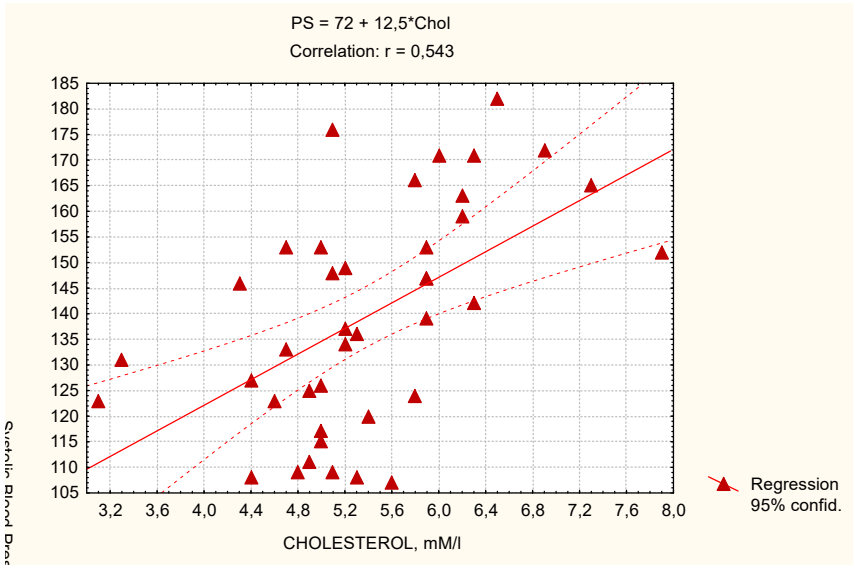

Fig. 14. Relationship between total Cholesterol Plasma (X-line) and Systolic Blood Pressure (Y-line)

By stepwise exclusion in the final regression model were included 5 metabolic and one biophysics parameters, which taken together determine Systolic Blood Pressure on 67% (Table 14, Fig. 15).

Table 14. Regression Summary for Dependent Variable SBP and Independent Metabolic and Biophysics Variables

R=0,849; R^2=0,720; Adjusted R^2=0,670; $F_{(6,3)}$=14,2; $\chi^2_{(6)}$=44,6; $p<10^{-6}$; SE: 12,4 mmHg

N=40		Beta	St. Err. of Beta	B	St. Err. of B	$t_{(33)}$	p-level
Variables	r		Intercpt	839	279	3,00	,005042
Cholesterol, mM/l	0,54	,764	,121	17,58	2,78	6,32	,000000
Uric Acid Plasma, mM/l	0,42	,542	,112	208,25	43,20	4,82	,000031
Phosphate Plasma, mM/l	0,40	-1,542	,564	-173,02	63,32	-2,73	,010023
EC AP TR(X) Right, un.	0,30	,315	,101	1,27	0,41	3,12	,003705
Calcium Plasma, mM/l	0,28	-1,112	,273	-143,05	35,17	-4,07	,000278
CTAP=$(1/Cap \bullet Pp)^{0,5}$	-0,48	-1,907	,621	-659,8	215	-3,07	,004276

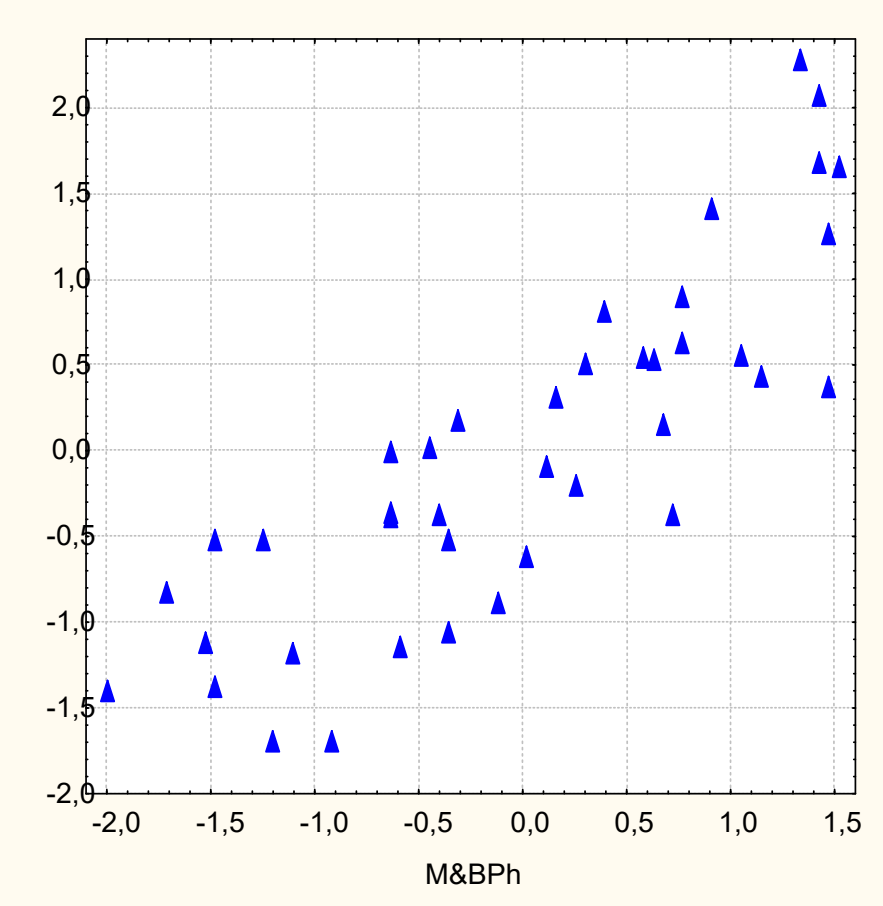

Fig. 15. Canonical correlation between Metabolic and Biophysics factors (X-line) and Systolic Blood Pressure (Y-line)

As a result of screening all parameters HRV, EEG as well as Metabolic and Biophysics parameters in the final regression model were included 4 metabolic, one biophysics and 3 neural parameters (but not age), which taken together determines Systolic Blood Pressure on 77% (Table 15, Fig. 16).

Table 15. Regression Summary for Dependent Variable SBP and Independent Neural, Biophysics and Metabolic Variables

R=0,902; R^2=0,814; Adjusted R^2=0,767; $F_{(8,3)}$=17,0; $\chi^2_{(8)}$=57,3; $p<10^{-6}$; SE: 10 mmHg

N=40		Beta	St. Err. of Beta	B	St. Err. of B	$t_{(31)}$	p-level
Variables	r		Intercpt	73,6	34,1	2,16	,039
Cholesterol Plasma, mM/l	0,54	,685	,097	15,77	2,22	7,10	10^{-6}
Uric Acid Plasma, mM/l	0,42	,537	,096	206,3	36,9	5,58	10^{-5}
Phosphate Plasma, mM/l	0,40	,231	,085	26,0	9,6	2,71	,011
EC AP TR(X) Right, units	0,30	,351	,085	1,413	,342	4,13	10^{-3}
Calcium Plasma, mM/l	0,28	-,570	,116	-73,4	14,9	-4,91	10^{-4}
HRV TI, units	-0,32	-,611	,134	-3,203	,704	-4,55	10^{-4}
α-rhythm Index, %	-0,22	-,363	,091	-,262	,065	-4,01	10^{-3}
RMSSD HRV, msec	-0,21	,436	,131	,530	,159	3,33	,002

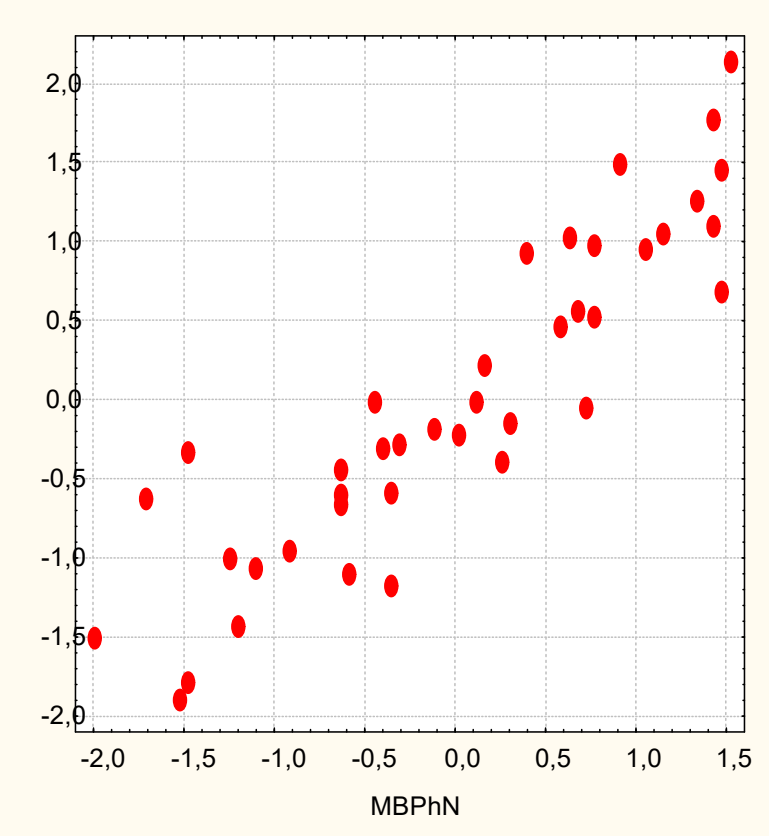

Fig. 16. Canonical correlation between Metabolic, Biophysics and Neural factors (X-line) and Systolic Blood Pressure (Y-line)

Now analyze relationships of Diastolic Blood Pressure with neuroendocrine factors. They were stronger and more numerous compared with Systolic Blood Pressure. In particular, Diastolic Blood Pressure negatively correlate with HRV markers of Vagal tone: Variation Scope (MxDMn) (r=-0,48), PS HF both absolute (r=-0,41) and relative (r=-0,31), HRV TI (r=-0,40), RMSSD (r=-0,39), pNN_{50} (r=-0,35), SDNN (r=-0,31) as well as Mode HRV (r=-0,32) while positively with HRV markers of Sympathetic tone: relative PSD VLF (r=0,30), Amplitude of Mode (r=0,41), Heart Rate (r=0,41) as well as AMo/Mo Ratio (r=0,47) and natural logarithm of Baevskiy's Stress Index (r=0,50) as AMo/2•Mo•MxDMn Ratio (Fig. 17).

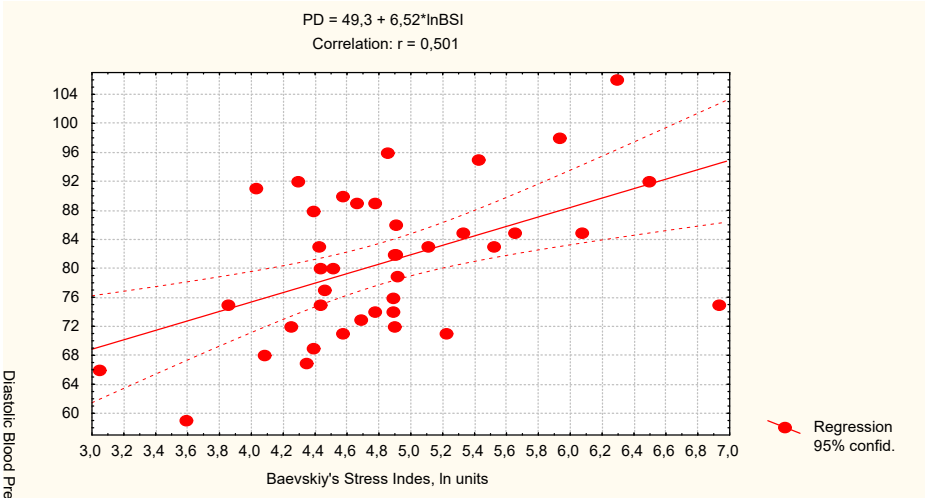

Fig. 17. Relationship between natural logarithm Baevskiy's Stress Index (X-line) and Diastolic Blood Pressure (Y-line)

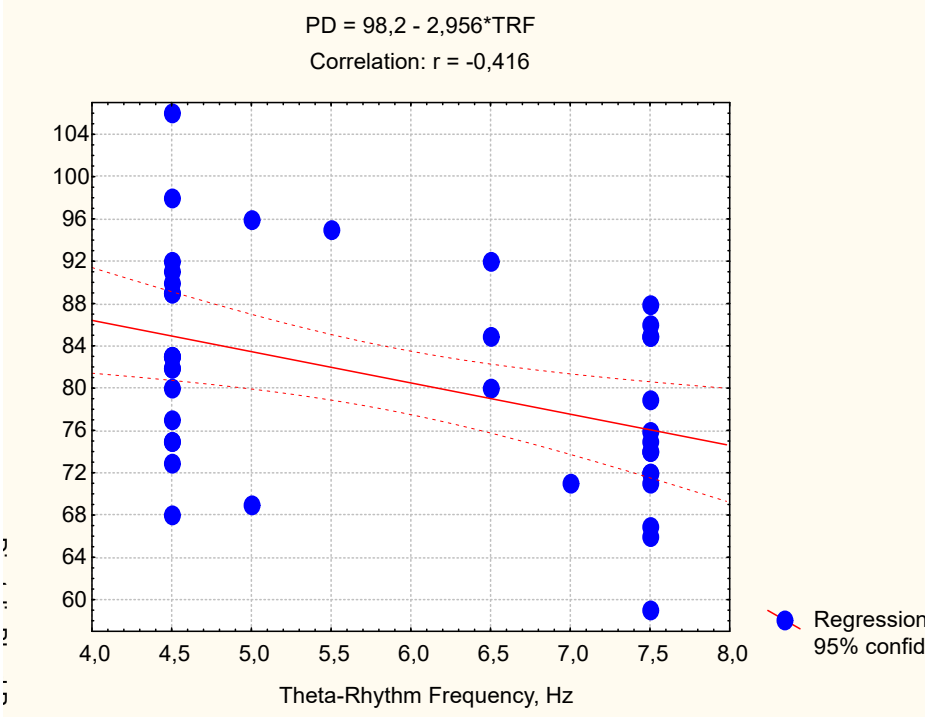

Fig. 18. Relationship between Frequency of θ-rhythm (X-line) and Diastolic Blood Pressure (Y-line)

Among parameters of EEG detected negatively correlation with Frequency of θ-rhythm (Fig. 18), Index (r=-0,41), Deviation (r=-0,40) and Amplitude (r=-0,25) of α-rhythm as well as Deviation of β-rhythm (r=-0,27) while positively correlation with Deviation (r=0,28) and Asymmetry (r=0,27) of δ-rhythm. Previously, we found significant relationships between parameters of HRV and EEG [Popovych IL et al., 2013; Popovych IL et al., 2014]. Taken together Baevskiy's Stress Index and θ-rhythm Frequency determines Systolic Blood Pressure on 38% (Table 16, Fig. 19).

Table 16. Regression Summary for Dependent Variable DBP and Independent Neural Variables

R=0,644; R^2=0,415; Adjusted R^2=0,383; $F_{(2,4)}$=13,1; $p<10^{-4}$; SE: 7,9 mmHg

N=40		Beta	St. Err. of Beta	B	St. Err. of B	$t_{(37)}$	p-level
Variables	r		Intercpt	66,8	9,7	6,89	10^{-6}
Baevskiy Stress Index, ln	0,50	,491	,126	6,391	1,637	3,91	10^{-3}
θ-rhythm Frequency, Hz	-0,42	-,405	,126	-2,872	,893	-3,22	,003

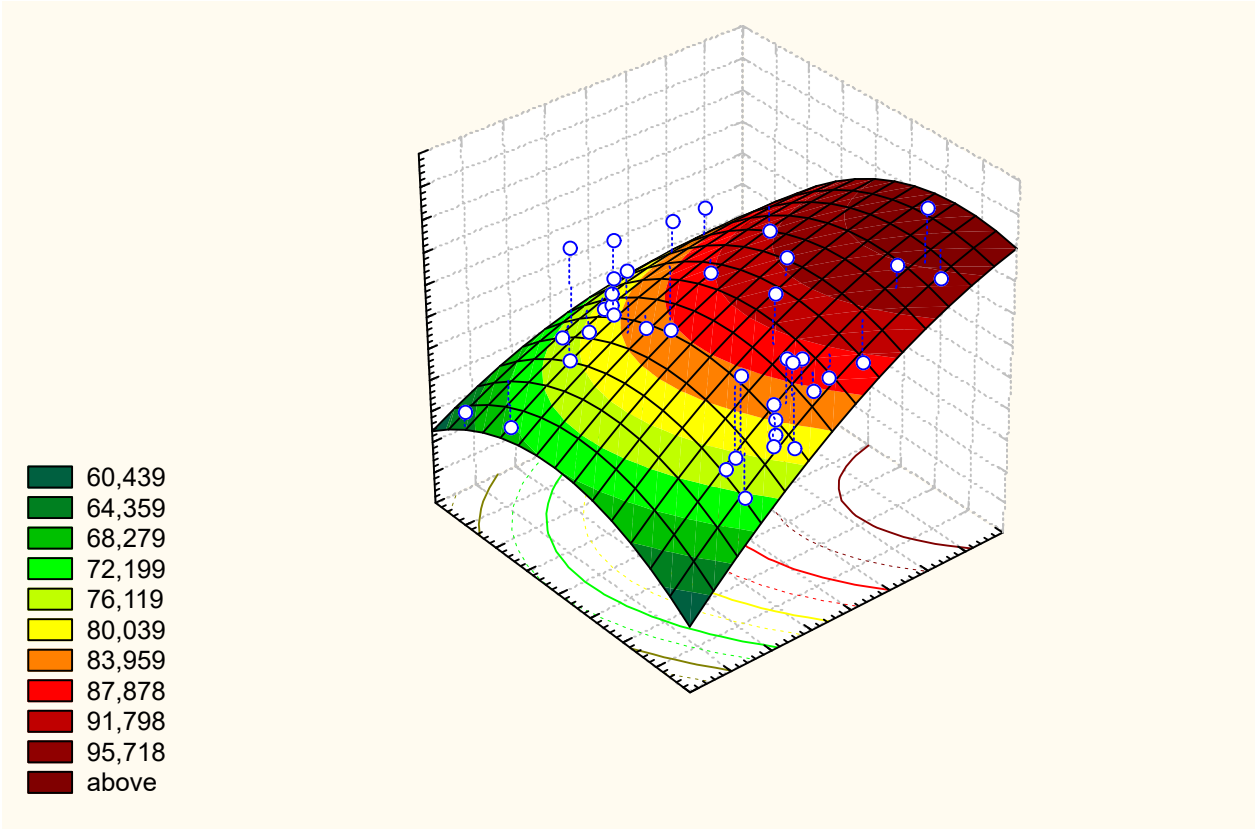

Fig. 19. Relationship between natural logarithm Baevskiy's Stress Index (X-line), Frequency of θ-rhythm (Y-line) and Diastolic Blood Pressure (Z-line)

Among hormones correlates with Diastolic Blood Pressure raw Testosterone (r=0,33) and normalized (r=0,27), but not raw (r=0,24) Calcitonin as well as not Triiodothyronine (r=-0,23), and Cortisol (r=-0,07). Interesting that normalized Testosterone (mean norm for women 2,37 nM/L, for men 25 nM/L) correlate with Diastolic Blood Pressure inversely (r=-0,24).

Taken together Neuroendocrine factors determines Diastolic Blood Pressure on 67% (Table 17, Fig. 20).

Table 17. Regression Summary for Dependent Variable DBP and Independent Neuroendocrine Variables

R=0,888; R^2=0,789; Adjusted R^2=0,670; $F_{(14)}$=6,7; $\chi^2_{(14)}$=48,2; $p<10^{-4}$; SE: 5,7 mmHg

N=40		Beta	St. Err. of Beta	B	St. Err. of B	$t_{(25)}$	p-level
Variables	r		Intercpt	406	117	3,46	,002
Baevskiy's Stress Index, ln	0,50	-3,115	1,438	-40,51	18,71	-2,17	,040
AMo/Mo HRV, units	0,47	1,971	,796	,845	,342	2,47	,020
Testosterone, nM/L	0,33	,186	,129	,374	,259	1,45	,161
PSD VLF, % Total Power	0,30	,510	,172	,285	,096	2,97	,007
Heart Rate, beats/min	0,29	-1,392	,526	-,919	,347	-2,65	,014
Calcitonin, portio norm	0,27	,221	,116	3,496	1,825	1,92	,067
δ-rhythm Asymmetry, %	0,27	,314	,125	,113	,045	2,51	,019
MxDMn HRV, msec	-0,48	-2,288	,773	-,299	,101	-2,96	,007
θ-rhythm Frequence, Hz	-0,42	-,270	,127	-1,919	,901	-2,13	,043
α-rhythm Deviation, Hz	-0,40	-,452	,123	-9,477	2,574	-3,68	,001
HRV TI, units	-0,40	,781	,274	1,900	,666	2,85	,009
Mode HRV, ms	-0,32	-1,443	,584	-,088	,035	-2,47	,021
PSD HF, % Total Power	-0,31	,520	,170	,531	,173	3,06	,005

α-rhythm Amplitude, μV	-0,25	-,313	,161	-,236	,121	-1,95	,063

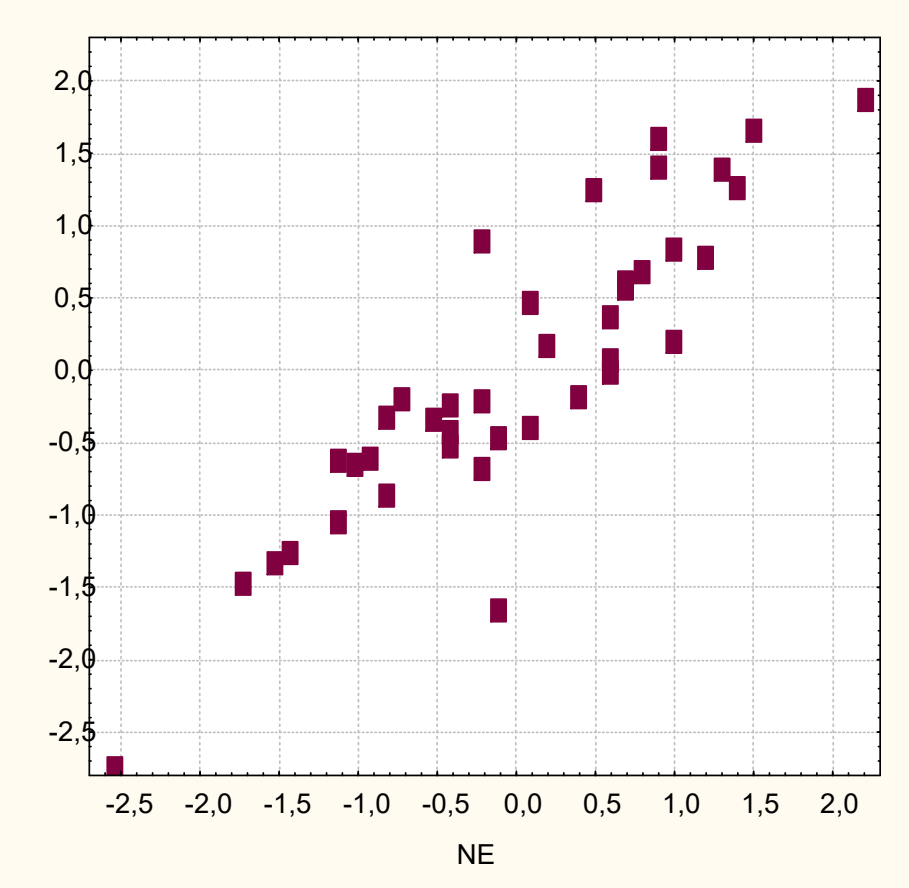

Fig. 20. Canonical correlation between Neuroendocrine factors (X-line) and Diastolic Blood Pressure (Y-line)

Among biophysics parameters significant correlates with Diastolic Blood Pressure electro-skin conductance points of acupuncture TR(X) Right (r=0,37) and Left (r=0,31) as well as Electrokinetics Index (r=-0,33). Among metabolic parameters detected significantly correlation with plasma Chloride (r=-0,39) and Sodium (r=-0,39) as well as $1/(Pp \bullet Cap)^{0,5}$ Ratio (r=-0,31). Taken together they determines Diastolic Blood Pressure on 28% (Table 18, Fig. 21).

Table 18. Regression Summary for Dependent Variable DBP and Independent Metabolic and Biophysics Variables

R=0,579; R^2=0,335; Adjusted R^2=0,280; $F_{(3,4)}$=6,1; $\chi^2_{(3)}$=14,9; p=0,002; SE: 8,5 mmHg

N=40		Beta	St. Err. of Beta	B	St. Err. of B	$t_{(36)}$	p-level
Variables	r		Intercpt	109,8	30,6	3,59	,001
Chloride Plasma, mM/l	-0,39	-,332	,141	-,484	,205	-2,36	,024
Electrokinetic Index, %	-0,33	-,326	,136	-,251	,105	-2,40	,022
EC AP TR(X) Right, un.	0,37	,263	,141	,491	,263	1,87	,070

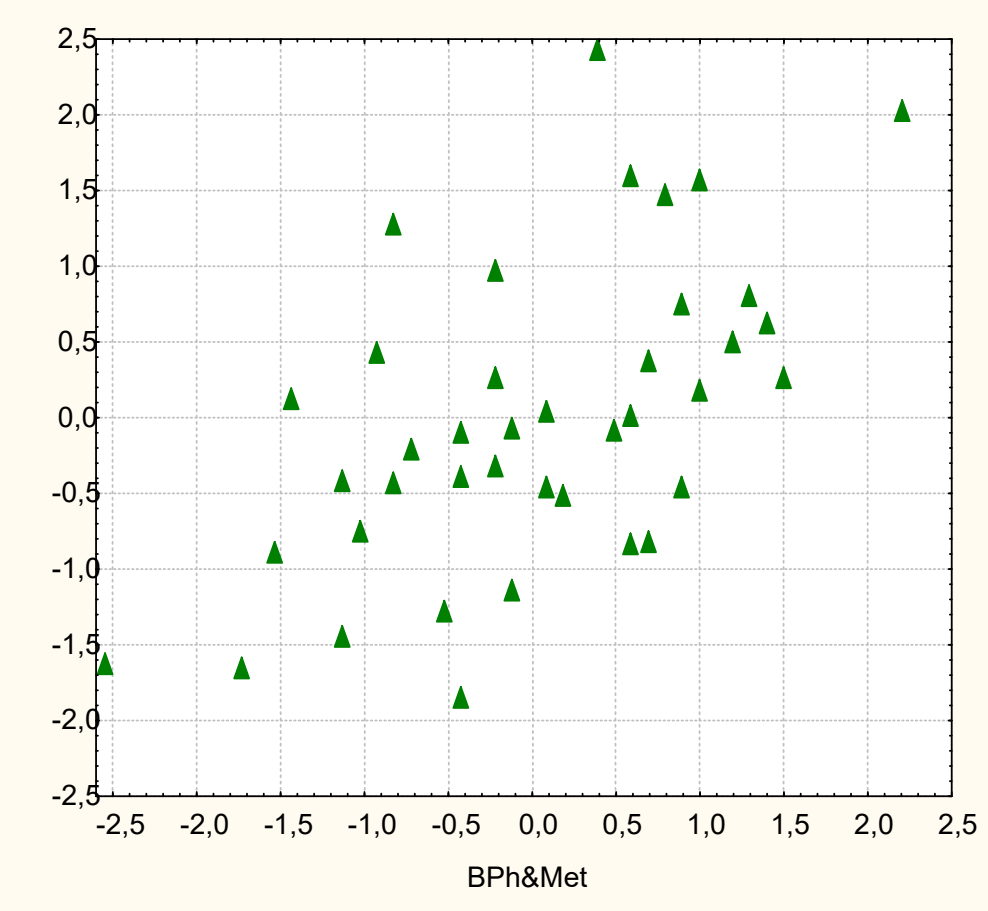

Fig. 21. Canonical correlation between Biophysics and Metabolic factors (X-line) and Diastolic Blood Pressure (Y-line)

Because screening all recorded parameters in the final regression model were included 7 Neural, 2 biophysics and one metabolic parameters as well as Hender Index, which taken together determines Diastolic Blood Pressure on 74% (Table 19, Fig. 22).

Table 19. Regression Summary for Dependent Variable DBP and Independent Neural, Metabolic and Biophysics Variables

$R=0,901$; $R^2=0,811$; Adjusted $R^2=0,737$; $F_{(11)}=10,9$; $\chi^2_{(11)}=54,1$; $p<10^{-5}$; SE: 5,1 mmHg

N=40		Beta	St. Err. of Beta	B	St. Err. of B	$t_{(28)}$	p-level
Variables	r		Intercpt	220,6	73,2	3,01	,005
Baevskiy's Stress Index, ln un.	0,50	-1,844	1,248	-24,0	16,2	-1,48	,151
AMo/Mo HRV, units	0,47	1,412	,760	,606	,326	1,86	,074
EC AP TR(X) Right, units	0,37	,211	,105	,394	,196	2,01	,054
Hender Index (M=0; W=1)	-0,60	-,275	,110	-5,443	2,177	-2,50	,019
MxDMn HRV, msec	-0,48	-,861	,664	-,112	,087	-1,30	,205
θ-rhythm Frequency, Hz	-0,42	-,332	,104	-2,354	,738	-3,19	,004
α-rhythm Deviation, Hz	-0,40	-,250	,096	-5,235	2,017	-2,60	,015
Chloride Plasma, mM/l	-0,39	-,159	,093	-,233	,136	-1,71	,098
Electrokinetics Index, %	-0,33	-,304	,125	-,233	,096	-2,43	,022
PSD HF, % Total Power	-0,31	,265	,105	,270	,107	2,52	,018
α-rhythm Amplitude, μV	-0,25	-,377	,137	-,284	,103	-2,76	,010

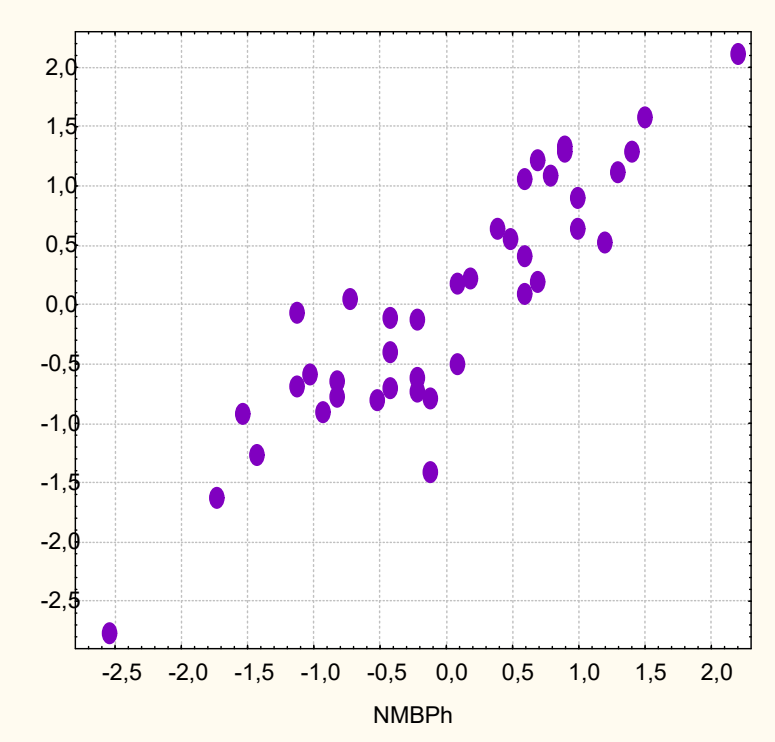

Fig. 22. Canonical correlation between Neural, Metabolic and Biophysics factors (X-line) and Diastolic Blood Pressure (Y-line)

At the final stage of the analysis we conducted canonical correlation between neural, endocrine, metabolic and biophysical parameters, on the one hand, and the two parameters of blood pressure, on the other hand (Table 20).

Table 20. Factor Structure of Canonical Roots

Independent Variables	**Root**
Electrokinetic Index, %	**,574**
Hender Index (Men=0;Women=1)	**,573**
MxDMn HRV, msec	**,516**
HRV TI, units	**,434**
α-rhythm Index, %	**,393**
α-rhythm Deviation, Hz	**,382**
RMSSD HRV, msec	**,375**
PSD HF, % Total Power	**,286**
Chloride Plasma, mM/L	**,284**
θ-rhythm Frequency, Hz	**,260**
α-rhythm Amplitude, μV	**,225**
Baevskiy's Stress Index, ln units	**-,460**
EC AP TR(X) Right, units	**-,403**
AMo/Mo HRV, units	**-,390**
Cholesterol Plasma, mM/l	**-,361**
Phosphate Plasma, mM/l	**-,331**
Uric Acid Plasma, mM/l	**-,288**
Calcium Plasma, mM/l	**-,267**
Dependent Variables	
Diastolic Blood Pressure	**-,924**
Sistolic Blood Pressure	**-,856**
Canon. R=0,935; R^2=0,874; $\chi^2_{(36)}$=116; $p<10^{-6}$	

It notes that the factors associated with **lower** blood pressure are rate of electronegative nuclei of buccal epithelium (inversely marker of biological age), womankind, Vagal tone, Amplitude and Deviation of α-rhythm, Frequency of θ-rhythm EEG as well as Chloridemia, while **increasing** of blood pressure directly related to Sympathetic tone, plasma levels of Cholesterol, Phosphate, Uric Acid and Calcium as well as electro-skin conductance in acupuncture point right, represented endocrine system. Taken together these factors determines Blood Pressure on 87% (Fig. 23).

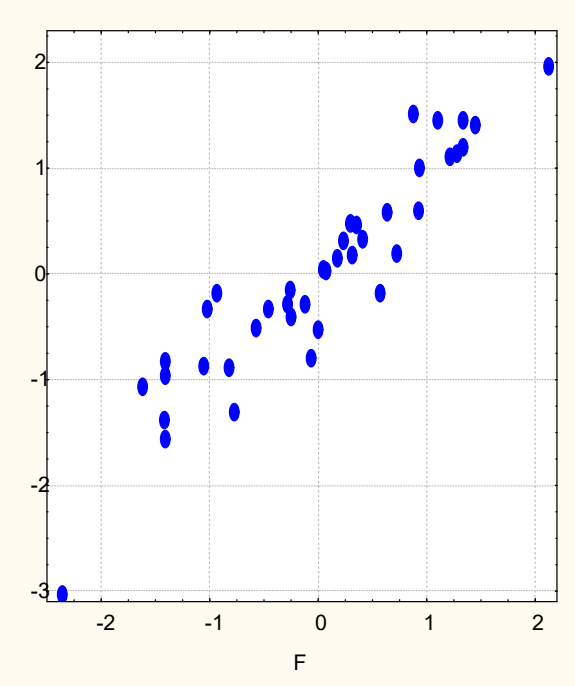

Fig. 23. Canonical correlation between Neural, Metabolic and Biophysics factors (X-line) and Systolic and Diastolic Blood Pressure (Y-line)

A little later, we showed [Kozyavkina NV et al., 2019] that in the same contingent, diastolic blood pressure was determined by EEG spectral parameters by 76.6% (Table 21) and systolic blood pressure by 80.3% (Table 22).

Table 21. Regression summary for dependent variable BP diastolic and PSD EEG

N=40	Regression Summary for Dependent Variable: BPD R=0,875; R^2=0,766; Adjusted R^2=0,674; F(11,3)=8,3; p<10^-5; Std.Error of estimate: 5,7 mmHg					
	Beta	St. Err. of Beta	B	St. Err. of B	t(28)	p-value
Intercpt			112,2844	7,677365	14,62538	0,000000
TF	-0,308	0,136	-2,1851	0,966917	-2,25982	0,031802
DA	-0,664	0,138	-13,9278	2,904958	-4,79450	0,000049
IRA	-0,364	0,211	-0,1219	0,070547	-1,72743	0,095107
F3B%	0,246	0,174	0,2072	0,146263	1,41677	0,167581
F4A%	-0,317	0,250	-0,2087	0,164650	-1,26773	0,215336
F7B%	-0,292	0,181	-0,1720	0,106428	-1,61568	0,117376
T3B%	0,359	0,214	0,2350	0,139993	1,67850	0,104378
T4A%	-0,337	0,270	-0,2606	0,208715	-1,24875	0,222095
C3A%	0,449	0,224	0,2845	0,141609	2,00927	0,054236
T5B	0,289	0,111	0,0590	0,022758	2,59295	0,014960
T6B%	-0,272	0,147	-0,1864	0,100907	-1,84710	0,075325

Table 22. Regression summary for dependent variable BP systolic and PSD EEG

N=40	Regression Summary for Dependent Variable: BPS R=0,896; R^2=0,803; Adjusted R^2=0,650; F(17,2)=5,3; p<0,0002; Std.Error of estimate:12,8 mmHg					
	Beta	St. Err. of Beta	B	St. Err. of B	t(22)	p-value
Intercpt			79,663	31,715	2,51	0,020
FP1H	-0,207	0,195	-30,937	29,202	-1,06	0,301
FP1B%	-0,635	0,443	-0,974	0,679	-1,43	0,166
T5B%	-0,366	0,200	-0,566	0,309	-1,83	0,080
C4B%	0,495	0,303	1,050	0,643	1,63	0,117
F3D%	0,906	0,514	0,877	0,498	1,76	0,092
FP2B%	0,346	0,240	0,495	0,343	1,44	0,163
LIB	-0,447	0,156	-0,310	0,108	-2,86	0,009
FP1D%	-0,663	0,358	-0,625	0,337	-1,85	0,078
F3B%	2,073	0,560	3,763	1,017	3,70	0,001
F4B%	-1,046	0,308	-1,903	0,560	-3,40	0,003
T3H	0,398	0,203	65,774	33,477	1,96	0,062
T3B%	-0,947	0,286	-1,337	0,404	-3,31	0,003
T3D%	-0,844	0,346	-0,893	0,366	-2,44	0,023
C3B%	0,490	0,379	0,937	0,723	1,30	0,209
C3D%	0,683	0,344	0,670	0,338	1,98	0,060
P4B%	-0,486	0,247	-1,070	0,543	-1,97	0,062
O2B%	0,371	0,171	0,696	0,321	2,17	0,041

Based on the analyses and results presented in this Chapter, we can provide an assessment of the hypotheses that were implicitly tested.

1. Hypothesis. There is significant diversity in blood pressure levels among children patients at Truskavets' spa. Result. Confirmed. The study found a range of blood pressure levels, from low normal to hight normal.

2. Hypothesis. Balneotherapy exerts varied effects on blood pressure in different groups of children patients. Result. Confirmed. The study found different patterns of change in blood pressure parameters after balneotherapy for different clusters of children patients.

3. Hypothesis. There is a set of parameters that significantly differentiate clusters of children patients with different changes in blood pressure. Result. Confirmed. Discriminant analysis identified 12 parameters, including HRV, Henchy's and Stange's tests, thrombocytes level as well as elements of luekocytogram that significantly differentiated between blood pressure clusters.

4. Hypothesis. There are significant correlations between changes in blood pressure and some parameters. Result. Partially confirmed. Significant correlations were found between changes in blood pressure and parameters such as thrombocytes level and Henchy's test.

5. Hypothesis. A children patient's initial physiological parameters allow prediction of the nature and magnitude of blood pressure change in response to balneotherapy. Result. Confirmed. The study developed a model that could predict blood pressure changes with 100% accuracy based on 19 initial parameters.

6. Hypothesis. There is significant diversity in blood pressure levels among adult patients at Truskavets' spa. Result. Confirmed. The study found a wide range of blood pressure levels, from low normal to arterial hypertension II.

7. Hypothesis. There are significant correlations between blood pressure and age and hender. Result. Confirmed. Significant correlations were found between blood pressure and age and hender.

8. Hypothesis. Blood pressure levels are linked to markers of sympathetic and parasympathetic activity. Result. Confirmed. Significant correlations were found between blood pressure levels and HRV parameters indicating autonomic nervous system activity.

9. Hypothesis. There are significant correlations between blood pressure levels and concentrations of certain adaptive hormones. Result. Partially confirmed. Some hormones (e.g., testosterone and calcitonin) showed significant correlations with blood pressure, while others did not.

10. Hypothesis. There are significant correlations between blood pressure levels and concentrations of certain metabolites. Result. Confirmed. Some metabolites (cholesterol, uric acid, phosphates, calcium, chloride) showed significant correlations with blood pressure.

11. Hypothesis. There are significant correlations between blood pressure levels and some biophysics parameters. Result. Confirmed. Some biophysics parameters (electrokinetic index, electroconductance at the one acupuncture point) showed significant correlations with blood pressure.

12. Hypothesis. Blood pressure levels are linked to EEG parameters. Result. Confirmed. Significant correlations were found between blood pressure levels and EEG parameters indicating cortical and subcortical structures activity.

In each of these cases, the null hypothesis (no effect or no difference) was implicitly rejected in favor of the alternative hypothesis when statistically significant results were observed (typically $p<0.05$). However, it's important to note that the study does not explicitly frame its findings in terms of null hypothesis significance testing.

The study used various statistical methods (correlation analysis, cluster analysis, discriminant analysis, canonical correlation analysis) to evaluate these hypotheses. When significant results were found (e.g., $p<0.05$ for correlations, high classification accuracy for discriminant analysis), this was taken as evidence to support the alternative hypothesis and reject the null hypothesis of no effect or no difference.

Conclusions

1. Blood Pressure Diversity. The study confirms a wide range of blood pressure levels among patients at Truskavets' spa, from low normal to arterial hypertension II. This diversity suggests that the spa attracts patients with varied cardiovascular profiles.

2. Patient Clusters. Three distinct clusters of children patients were identified based on changes in blood pressure after balneotherapy. This clustering suggests that patients can be categorized into meaningful groups for targeted treatment approaches.

4. Differentiating Parameters. Specific parameters, particularly HRV, thrombocytes level, Henchy’s and Stange’s tests, effectively differentiate between blood pressure dynamics clusters. This finding provides a basis for more precise patient classification and potentially tailored treatments.

5. Predictive Modeling. Initial physiological parameters can predict the nature and magnitude of blood pressure changes in response to balneotherapy with 100% accuracy. This predictive capability could be valuable for personalizing treatment plans.

6. Autonomic and Central Nervous Systems Involvement. Blood pressure levels are linked to markers of sympathetic and parasympathetic activity as well as cortical and subcortical structures activity, as indicated by correlations with HRV and EEG parameters. This underscores the role of the autonomic and central nervous systems in blood pressure regulation.

7. Hormonal Influences. Some adaptive hormones, notably testosterone and calcitonin as well as sex show significant correlations with blood pressure levels. This suggests a complex interplay between the endocrine system and blood pressure regulation.

8. Metabolic Influences. Some metabolites, notably cholesterol, uric acid, phosphates, calcium, and chloride show significant correlations with blood pressure levels. This suggests a complex interplay between the metabolome and blood pressure regulation.

9. Methodological Robustness. The study demonstrates the value of using multiple statistical approaches (cluster analysis, discriminant analysis, canonical correlation) to comprehensively analyze complex physiological data.

10. Integrated Physiological View. The findings support an integrated view of blood pressure regulation, involving neural, endocrine and metabolic factors.

11. Clinical Implications. The results suggest potential for developing more targeted and effective balneotherapy protocols based on individual patient profiles.

12. Future Research Directions. The study opens avenues for further research into the mechanisms underlying the observed relationships and the long-term effects of balneotherapy on cardiovascular health.

13. This pilot study provides a comprehensive characterization of blood pressure profiles and their physiological correlates in patients at Truskavets' spa. It demonstrates the complex, multifaceted nature of blood pressure regulation and the potential for personalized approaches in balneotherapy. The findings lay a foundation for future studies to further elucidate these relationships and translate them into improved clinical practices in spa medicine.

Chapter 1

QUANTITATIVE-QUALITATIVE BLOOD PRESSURE CLUSTERS OF PATIENTS AT TRUSKAVETS' SPA AND THEIR HEMODYNAMIC ACCOMPANIMENT

Abstract

Background. We initiated the project "Neuroendocrine-immune and metabolic mechanisms of the effect of balneotherapy on the blood pressure (BP)". The first swallow of the project is the analysis of a condition of BP and its hemodynamic support of profile patients of a resort. **Materials and methods.** Under an observations were 44 patients with chronic pyelonephritis and cholecystitis in the phase of remission. Testing was performed twice - on admission and after 7-10 days of standard balneotherapy. The main object of the study was BP (tonometer "Omron M4-I", Netherlands). Simultaneously the parameters of hemodynamics were determined (echocamera "Toshiba-140", Japan). **Results**. The optimal level of systolic BP (range 120÷129 mmHg) stated in 18,2% of cases only, high norm (130÷139 mmHg) in 14,8%, arterial hypertension (AH) I (140÷160 mmHg) – in 39,8%, AH II (over 160 mmHg) in 12,5%, however, in 14,8% of cases the BP was lower than 120 mmHg. In order to identify among the registered parameters of hemodynamics, those for which the BP clusters differ from each other, a discriminant analysis was performed. The program forward stepwise included in the discriminant model 13 parameters out of 17. The most informative among them: contractile activity index of left ventricle, heart work per minute, ejection fraction and time as well as end-systolic volume. **Conclusion**. Profile patients of Truskavets' spa are characterized by a wide range of blood pressure - from low norm to arterial hypertension II that correspond to the hemodynamics parameters.

Keywords: blood pressure, hemodynamics, discriminant analysis, Truskavets' spa.

Under an observations were 34 males and 10 females by age 24-76 years with chronic pyelonephritis and cholecystitis in the phase of remission. Testing was performed twice - on admission and after 7-10 days of standard balneotherapy (drinking of Naftussya bioactive water, applications of ozokerite, mineral pools).

The main object of the study was blood pressure (BP). Systolic (Ps) and diastolic (Pd) BP as well as heart rate (HR) was measured (by tonometer "Omron M4-I", Netherlands) in a sitting position three times in a row. After that, the parameters of hemodynamics were determined (by echocamera "Toshiba-140", Japan): ejection time (ET), end-diastolic (EDV) and end-systolic (ESV) volumes of left ventricle with the following ejection fraction (EF), general peripheral vessels resistance (GPVR), cardiac output (CO), heart work per minute (HWM) calculation by classic formulas [Schiller N & Osipov MA, 1993; Bobrov VO et al, 1997; Ruzhylo SV et al, 2003; Popovych IL et al, 2005]:

$EF = 100 \bullet (EDV - ESV)/EDV;$

$GPVR = 80 \bullet (0,67 \bullet Pd + 0,33 \bullet Ps)/HR \bullet (EDV - ESV);$

$CO = (EDV - ESV) \bullet HR;$

$HWM = 0,1332 \bullet 1,055 \bullet (0,67 \bullet Pd + 0,33 \bullet Ps) \bullet (EDV - ESV) \bullet HR.$

In addition, we calculated the contractile activity index of left ventricle by Sagawa K [1981]:

$SCAI = Ps/ESV$

as well as by Ruzhylo SV & Popovych IL [2005]:

$RPCAI = 0,1332 \bullet (0,67 \bullet Pd + 0,33 \bullet Ps) \bullet (EDV-ESV)/EDV \bullet ET.$

Appropriate cardiac output, which is determined by gender, age (A, years), height (H, cm) and body weight (W, kg), was calculated by the formulas [Vinogradova TS, 1986]:

$CO \text{ for females} = (9,56 \bullet W + 1,85 \bullet H + 4,67 \bullet A + 65,09)/281;$

CO for males = (13,75•W + 5•H - 6,75•A + 66,47)/281

Appropriate ejection time, which is determined by cardiac cycle time (C) calculated by the classic formula: ET = 0,109•C + 0,159.

The following research problems and corresponding hypotheses can be identified.

1. Research problem. What is the distribution of blood pressure among patients at Truskavets' spa? Hypothesis. There is significant diversity in blood pressure levels among patients at Truskavets' spa, ranging from low normal to grade II hypertension.

2. Research problem. Is there a relationship between systolic and diastolic blood pressure? Hypothesis: There is a significant correlation between systolic and diastolic blood pressure, but it is not perfect.

For statistical analysis used the software package “Microsoft Excell” and "Statistica 6.4. StatSoft Inc" (Tusla, OK, USA) and "Microsoft Excel". A significance level of $p<0.05$ was used throughout. The methods employed represent a comprehensive multivariate approach to analyzing the complex relationships between blood pressure and various physiological parameters.

The following statistical methods were used.

1. Descriptive Statistics. Mean (M) and standard error (SE) were calculated for various parameters, reported as M±SE. Percentages were used to describe the distribution of blood pressure categories.

2. Discriminant Analysis. Stepwise forward discriminant analysis was used to identify parameters that best distinguish between blood pressure clusters. Wilks' Lambda (Λ), F-values, p-values, and tolerance were reported for variable selection. Standardized and raw coefficients for canonical variables were calculated. Eigenvalues and cumulative proportions were reported for each root. Structural coefficients (correlations variables-roots) were presented. Mahalanobis distances between clusters and corresponding F-values and p-values were computed. Classification functions were derived for predicting group membership. Classification accuracy was assessed via classification matrices.

3. Normalization of Variables. Some variables were normalized relative to age-specific norms.

4. Calculation of Derived Indices. Various hemodynamic indices were calculated from raw measurements.

5. Visualization. Scatter plots of canonical variables were used to visualize the separation of clusters.

6. Significance Testing. P-values were reported throughout, with $p<0.05$ generally considered significant.

These methods represent a comprehensive multivariate approach to analyzing the complex relationships between blood pressure and various hemodynamic parameters. The combination of descriptive and inferential statistics, along with advanced multivariate techniques, allowed for a thorough exploration of the data structure and relationships among variables.

Standards and gradations are still the object of debate [Celis H et al, 2005; Whelton PK et al, 2018; Lin HJ et al, 2020]. If we take the optimal norm of systolic pressure range 120÷129 mmHg, high norm 130÷139, arterial hypertension (AH) I 140÷160, AH II 160÷180, AH III over 180 mmHg and low norm lower 120 mmHg, the quantitative and qualitative characteristics of the observed contingent will be as follows (Fig. 1.1).

In the future, we will refer to the selected groups as clusters, despite the fact that, strictly speaking, they are not, because they were created according to formal characteristics -

intervals of systolic blood pressure, but not according to the result of cluster analysis of systolic and diastolic blood pressure. We will return to this question later.

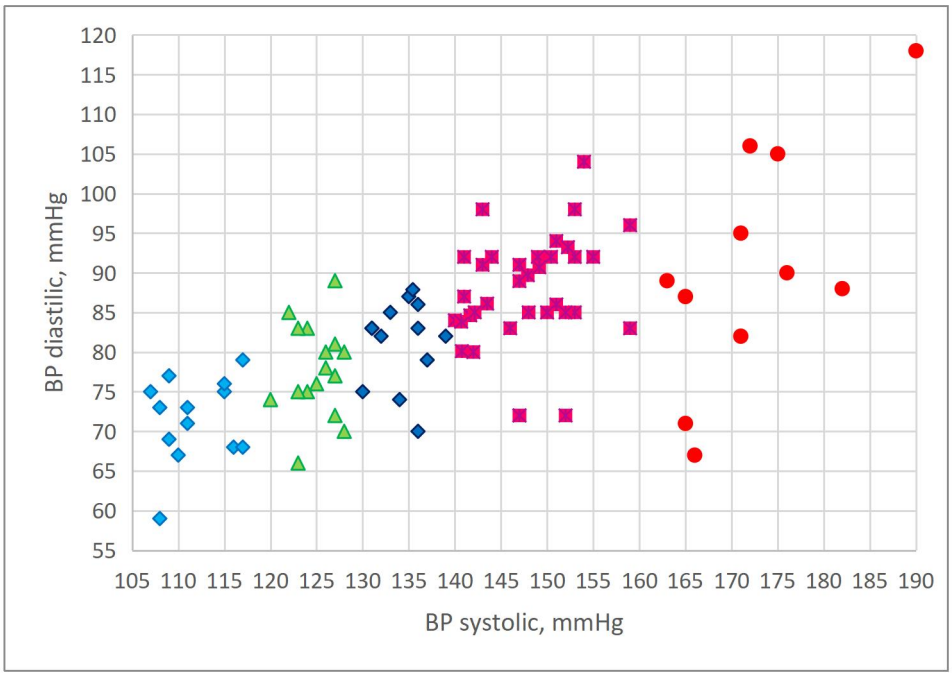

Fig. 1.1. Diagram of scattering of systolic and diastolic blood pressure at patients of Truskavets' spa

As you can see, the optimal systolic pressure is found only in 18,2% of cases, and in the range of the extended norm fall 47,8% of cases. At the same time in 39,8% of cases AH I was stated, and in 12,5% even AH II. Diastolic pressure is strongly associated with systolic, but not very much (r=0,67), so it deserves special attention. For now, we will limit ourselves to stating the different correlation coefficients of both BP parameters with age (0,37 vs 0,18) and sex-index (-0,19 vs -0,44), when M=1 and F=2, for Ps and Pd, respectively.

By recording BP three times in a row, we noticed that Ps2/Ps1, Ps3/Ps1, Pd2/Pd1, Pd3/Pd1 ratio form at least five patterns that correspond to the parameters of neuroendocrine-immune complex and metabolism (this will be the subject of a separate analysis). Therefore, these parameters became the subject of further analysis.

In order to identify among the registered parameters of hemodynamics, those for which the blood pressure clusters differ from each other, a discriminant analysis [Klecka WR, 1989] was performed. The program forward stepwise included in the discriminant model 13 parameters out of 17 (Tables 1.1 and 1.2).

Table 1.1. Discriminant Function Analysis Summary for Hemodynamics Variables, their actual levels for Clusters of Blood Pressure as well as Reference levels and Coefficients of Variability

Step 13, N of vars in model: 13; Grouping: 5 grps; Wilks' Λ: 0,021; approx. $F_{(52)}$=9,2; $p<10^{-6}$

	Clusters of Blood Pressure (n)					Parameters of Wilk's Statistics						
VARIABLES CURRENTLY IN THE MODEL	**AH II (11)**	**AH I (35)**	**High N (13)**	**Norm (16)**	**Low N (13)**	Wilks' Λ	Partial Λ	F-remove (4,7)	p-level	Tolerancy	Reference (44)	Cv
Blood Pressure Systolic, mmHg	172 2,5	148 0,9	134 0,8	125 0,6	112 1,0	0,093	0,223	61,8	10^{-6}	0,588	124,5 2,3	,122
Blood Pressure Diastolic, mmHg	90,7 4,5	87,6 1,2	81,3 1,5	77,8 1,5	71,5 1,5	0,024	0,878	2,47	0,052	0,201	79 1,0	,083
Heart Rate, bpm	70,6 5,2	70,9 2,1	70,6 2,2	68,7 2,4	70,6 2,8	0,023	0,898	2,01	0,102	0,349	68,4 1,2	,120

Heart Work, kJ/min	99 16	83 5	86 5	70 7	65 5	0,022	0,928	1,37	0,253	0,008	72 3	,269
End-diastolic Vol of Left Ventric, mL	122 9	113 2	132 4	111 4	125 5	0,023	0,888	2,25	0,073	0,041	116 2	,115
End-systolic Vol of Left Ventricle, mL	39,4 1,9	38,8 1,4	44,3 1,8	41,8 2,0	47,5 1,3	0,023	0,907	1,83	0,133	0,026	36,2 1,3	,247
Ejection Fraction, %c	66,6 2,2	65,8 1,1	66,2 1,3	62,7 2,3	61,1 2,0	0,024	0,880	2,42	0,056	0,016	67,4 1,9	,189
Cardiac Output, L/min	5,87 0,93	5,46 0,29	6,14 0,37	5,17 0,44	5,40 0,42	0,022	0,941	1,10	0,361	0,009	5,43 0,22	,269
Ejection Time, msec	261 11	275 6	292 6	264 9	303 8	0,025	0,829	3,66	0,009	0,063	252 3	,076
Ruzhylo-Popovych CA Index, kPa/s	34,7 2,4	32,3 1,0	30,2 0,8	32,5 2,1	26,7 0,7	0,025	0,833	3,56	0,010	0,033	35,8 1,2	,223
1000•Ps2/Ps1 Ratio	975 13	922 13	988 29	1000 26	971 16	0,023	0,912	1,72	0,155	0,437	960 13	,089
1000•Ps3/Ps1 Ratio	940 20	934 11	984 17	964 27	953 18	0,023	0,916	1,62	0,179	0,429	951 11	,079
1000•Pd3/Pd1 Ratio	997 21	1023 8	1014 16	996 14	971 10	0,023	0,885	2,30	0,067	0,575	1006 8	,055

VARIABLES CURRENTLY NOT IN THE MODEL	**Clusters of Blood Pressure (n)**					**Parameters of Wilk's Statistics**						
	AH II (11)	**AH I (35)**	**High N (13)**	**Norm (16)**	**Low N (13)**	Wil-ks' Λ	Par-tial Λ	F to en-ter	p-level	Tole-rancy	Refe-rence (44)	Cv
1000•Pd2/Pd1 Ratio	1000 31	1013 11	1001 18	970 16	976 17	0,020	0,947	0,97	0,427	0,377	996 10	,070
Sagawa Contr Act Ind, mmHg/mL	4,48 0,22	4,04 0,21	3,10 0,14	3,11 0,17	2,37 0,06	0,020	0,957	0,79	0,533	0,115	3,63 0,12	,221
Gen Periph Vessel Resist, kPa•s/m^3	18,8 2,0	17,0 0,7	13,3 0,7	16,6 1,9	13,9 1,5	0,020	0,961	0,71	0,586	0,066	16,4 1,0	,415
Stroke Volume of Left Ventricle, mL	82 9	75 2	87 4	73 4	77 5			0,00	1,000		79 3	,271

Table 1.2. Summary of Stepwise Analysis for Hemodynamics Variables, ranked by criterion Lambda

Variables currently in the model	F to enter	p-level	**Λ**	F-va-lue	p-level
Blood Pressure Systolic, mmHg	298	10^{-6}	0,065	298	10^{-6}
Ejection Time, msec	3,39	0,013	0,056	66,2	10^{-6}
Pd3/Pd1 Ratio	2,89	0,027	0,049	38,1	10^{-6}
Ps2/Ps1 Ratio	2,87	0,028	0,043	27,7	10^{-6}
Blood Pressure Diastolic, mmHg	2,07	0,093	0,039	21,9	10^{-6}
End-diastolic Volume of Left Ventricle, mL	2,77	0,033	0,034	18,7	10^{-6}
Ruzhylo&Popovych Contr Activity Ind, kPa/s	1,68	0,162	0,031	16,1	10^{-6}
Ejection Fraction, %c	1,58	0,188	0,029	14,2	10^{-6}
Heart Rate, bpm	1,15	0,340	0,027	12,7	10^{-6}
Heart Work, kJ/min	1,64	0,174	0,025	11,6	10^{-6}
Ps3/Ps1 Ratio	1,25	0,297	0,023	10,7	10^{-6}
End-systolic Volume of Left Ventricle, mL	1,09	0,368	0,022	9,86	10^{-6}
Cardiac Output, L/min	1,11	0,361	0,021	9,17	10^{-6}

Next, the 13-dimensional space of discriminant variables transforms into 4-dimensional space of a canonical roots, which are a linear combination of discriminant variables. The differentiating ability of the root characterizes the canonical correlation coefficient (r*) as a measure of connection, the degree of dependence between groups (clusters) and a discriminant function. It is for Root 1 0,976 (Wilks' Λ=0,021; $\chi^2_{(52)}$=302; p<10^{-6}), for Root 2

0,586 (Wilks' Λ=0,435; $\chi^2_{(36)}$=65; p=0,002), for Root 3 0,462 (Wilks' Λ=0,662; $\chi^2_{(22)}$=32; p=0,075) and for Root 4 0,397 (Wilks' Λ=0,843; $\chi^2_{(10)}$=13; p=0,205). The first root contains 95,3% of discriminative opportunities, the second 2,5%, the third 1,3%, the last 0,9%.

Table 1.3 presents raw (actual) and standardized (normalized) coefficients for discriminant variables. The raw coefficient gives information on the absolute contribution of this variable to the value of the discriminative function, whereas standardized coefficients represent the relative contribution of a variable independent of the unit of measurement. They make it possible to identify those variables that make the largest contribution to the discriminatory function value.

Table 1.3. Standardized and Raw Coefficients and Constants for Hemodynamic Variables

Coefficients	Standardized			Raw		
Variables currently in the model	Root 1	Root 2	Root 3	Root 1	Root 2	Root 3
Blood Pressure Systolic, mmHg	1,170	-0,163	-0,158	0,241	-0,034	-0,033
Ejection Time, msec	0,702	-1,788	2,318	0,022	-0,055	0,072
Pd3/Pd1 Ratio	0,322	0,342	-0,471	6,050	6,434	-8,866
Ps2/Ps1 Ratio	0,299	-0,202	-0,620	3,687	-2,497	-7,652
Blood Pressure Diastolic, mmHg	-0,049	1,232	-0,491	-0,006	0,156	-0,062
End-diastolic Volume of Left Ventricle, mL	1,263	-1,886	-0,076	0,071	-0,106	-0,004
Ruzhylo&Popovych Contr Activity Ind, kPa/s	1,322	-2,177	2,775	0,193	-0,318	0,405
Ejection Fraction, %c	-2,204	2,043	-2,320	-0,308	0,285	-0,324
Heart Rate, bpm	-0,222	-0,844	0,024	-0,019	-0,071	0,002
Heart Work, kJ/min	-2,806	1,146	-1,264	-0,094	0,038	-0,042
Ps3/Ps1 Ratio	-0,382	-0,039	-0,305	-5,135	-0,518	-4,097
End-systolic Volume of Left Ventricle, mL	-1,768	1,000	-0,980	-0,237	0,134	-0,131
Cardiac Output, L/min	2,447	0,234	1,394	1,306	0,125	0,744
			Constants	-27,24	3,719	22,89
			Eigenvalues	20,02	0,52	0,27
			Cumulative proportions	0,953	0,978	0,991

The calculation of the discriminant root values for each person as the sum of the products of raw coefficients to the individual values of discriminant variables together with the constant enables the visualization of each patient in the information space of the roots (Fig. 1.2).

Table 1.4 presents the full structural coefficients, that is, the coefficients of correlation between the discriminant root and variables. The structural coefficient shows how closely variable and discriminant functions are related, that is, what is the portion of information about the discriminant function (root) contained in this variable. There are also average values (centroides) of Roots and Z-scores of Variables.

Table 1.4. Correlations Variables-Canonical Roots, Means of Roots and Z-scores of Hemodynamic Variables

Variables	**Correlations Variables-Roots**			**Low N (13)**	**Nor-mal (16)**	**High N (13)**	**AH I (35)**	**AH II (11)**
Root 1 (95,3%)	**R 1**	**R 2**	**R 3**	-6,76	-3,40	-1,38	2,05	**8,04**
Blood Pressure Systolic	**0,847**	-0,033	-0,005	-0,84	+0,03	+0,64	+1,54	**+3,15**
Blood Pressure Diastolic	**0,177**	0,279	0,047	-1,14	-0,19	+0,35	+1,31	**+1,79**
Ruzhylo&Popovych CA Index	**0,172**	0,185	-0,127	-0,97	-0,22	-0,51	-0,23	**+0,08**
Heart Work	**0,073**	-0,091	-0,142	-0,38	-0,12	+0,69	+0,53	**+1,36**
Ejection Fraction	**0,054**	0,050	-0,130	+0,42	-0,15	-0,53	-0,20	**+0,87**
Heart Rate	**0,006**	-0,022	0,072	+0,23	+0,08	+0,32	+0,23	**+0,31**
Sagawa Contractility Index	currently not in the model			-1,57	-0,65	-0,66	+0,51	**+1,05**
Gener Periph Vessels Resistan	currently not in the model			-0,27	+0,16	-0,35	+0,22	**+0,50**

End-systolic Volume Left Ven	**-0,079**	-0,346	-0,057	+0,76	+0,96	+1,70	+0,65	**+0,21**
Ejection Time	**-0,064**	-0,259	0,227	+2,77	+0,68	+2,21	+1,34	**+0,43**
Root 2 (2,5%)	**R 1**	**R 2**	**R 3**	-0,91	+0,56	-0,40	**+0,58**	-1,11
End-diastolic Vol Left Ventric	-0,023	**-0,416**	-0,292	+1,76	+0,03	+0,67	**-0,28**	+1,04
Cardiac Output	0,015	**-0,130**	-0,140	+1,55	+0,22	-0,04	**-0,03**	+1,28
Ps2/Ps1 Ratio	-0,037	**-0,246**	-0,539	+0,12	+0,46	+0,33	**-0,44**	+0,18
Ps3/Ps1 Ratio	-0,027	**-0,102**	-0,377	+0,02	+0,18	+0,43	**-0,23**	-0,10
Stroke Volume Left Ventricle	currently not in the model			+1,30	+0,06	-0,10	**-0,20**	+1,25
Pd3/Pd1 Ratio	0,044	**0,324**	-0,073	-0,64	-0,18	+0,14	**+0,31**	-0,17
Pd2/Pd1 Ratio	currently not in the model			-0,29	-0,37	+0,07	**+0,25**	+0,05

The localization of the patients with AH II along the first root axis (Fig. 1.2) in the extreme right (positive) zone reflects combination of significantly elevated BP with maximum for sampling levels of myocardial contractility indices, ejection fraction, heart work, and general peripheral resistance of vessels, on the one hand, and minimum ESV and ejection time levels on the other hand. Consecutive decrease in BP is accompanied by a decrease/increase in these hemodynamic parameters. Additional differentiation of patients with AH I occurs along the axis of the second root, the upper position of which reflects the minimum for sampling EDV, cardiac output as well as Ps2/Ps1 and Ps3/Ps1 ratio, while the maximum levels of Pd2/Pd1 and Pd3/Pd1 ratio.

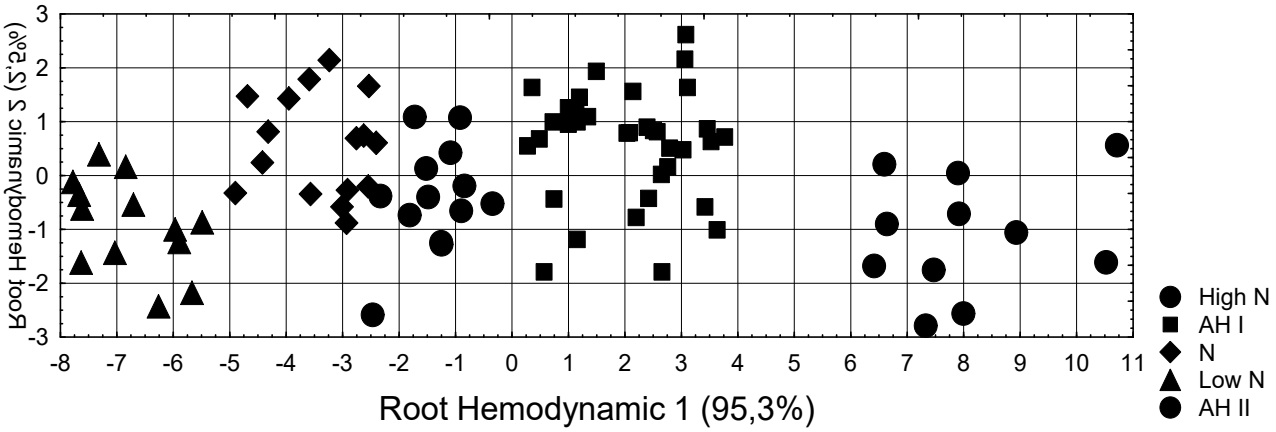

Fig. 1.2. Scattering of individual values of the first and second discriminant hemodynamic roots of patients of different blood pressure clusters

In general, all clusters on the planes of three roots are quite clearly delineated, which is documented by calculating the Mahalanobis distances (Table 1.5).

Table 1.5. Squared Mahalanobis Distances between Blood Pressure Clusters and F-values (df=13,7; for High N/N $p<10^{-3}$, for others $p<10^{-6}$)

Blood Pressure Clusters	High N	AH I	N	Low N	AH II
High N	0	**14,4**	**6,83**	**31,9**	**91,0**
AH I	**8,96**	0	**31,1**	**80,0**	**39,2**
N	**3,22**	**22,5**	0	**15,2**	**134**
Low N	**13,6**	**49,9**	**7,15**	0	**220**
AH II	**35,7**	**21,6**	**57,4**	**86,1**	0

The same discriminant parameters can be used to identify the belonging of one or another person to one or another cluster. This purpose of discriminant analysis is realized with the help of classifying functions (Table 1.6). These functions are special linear combinations that maximize differences between groups and minimize dispersion within groups. An object

belongs to a group with the maximum value of a function calculated by summing the products of the values of the variables by the coefficients of the classifying functions plus the constant.

Table 1.6. Coefficients and Constants for Classification Functions for Blood Pressure Clusters

Blood Pressure Clusters	High N	AH I	Norm	Low N	AH II
Variables currently in the model	p=,148	p=,398	p=,182	p=,148	p=,125
Blood Pressure Systolic, mmHg	6,942	7,683	6,371	5,591	9,177
Ejection Time, msec	0,297	0,400	0,224	0,315	0,592
Pd3/Pd1 Ratio	751,9	765,9	736,0	699,0	791,9
Ps2/Ps1 Ratio	390,6	394,2	384,2	363,9	426,5
Blood Pressure Diastolic, mmHg	-1,737	-1,707	-1,672	-1,917	-2,017
End-diastolic Volume of Left Ventricle, mL	-3,884	-3,751	-4,137	-4,222	-3,145
Ruzhylo&Popovych Contr Activity Index, kPa/s	4,286	5,172	3,889	4,103	6,770
Ejection Fraction, %c	16,51	15,29	17,12	17,44	13,02
Heart Rate, bpm	1,369	1,235	1,334	1,506	1,241
Heart Work, kJ/min	-1,733	-2,035	-1,441	-1,268	-2,605
Ps3/Ps1 Ratio	147,5	121,4	147,8	164,8	89,51
End-systolic Volume of Left Ventricle, mL	16,19	15,34	16,71	17,18	13,73
Cardiac Output, L/min	13,72	18,76	10,35	7,131	25,55
Constants	-1817	-1868	-1725	-1644	-2065

In this case, we can retrospectively recognize patients with AH I and II as well as with low norm BP unmistakably, the patients with high norm BP are classified with one mistake, and with norm BP with two errors. Overall classification accuracy is 96,6% (Table 1.7).

Table 1.7. Classification Matrix for Blood Pressure Clusters

	Rows: Observed classifications Columns: Predicted classifications					
Group	Percent Correct	High N p=,14773	AH I p=,39773	Norm p=,18182	Low N p=,14773	AH II p=,12500
High N	92,3	12	0	1	0	0
AH I	100,0	0	35	0	0	0
Norm	87,5	2	0	14	0	0
Low N	100,0	0	0	0	13	0
AH II	100,0	0	0	0	0	11
Total	96,6	14	35	15	13	11

It is time to return to the clarification of discrepancies between the formal and natural classification of quantitative-qualitative groups of patients. The groups formed by the k-mean clustering method, taking into account both systolic and diastolic blood pressure, that is, the actual clusters, are almost identical both in numerical composition and average values in the cases of Low Norm (Clusters N4) and AH II (Cluster N5). Instead, the other clusters are somewhat different (see Tables 1.1 and 1.8).

Table 1.8. Cluster Means (n)

Variable	Cluster No. 1(18)	Cluster No. 2(21)	Cluster No. 3(23)	Cluster No. 4(15)	Cluster No. 5(11)
PS	141	128	150	113	172
PD	81,9	78,9	91,1	71,3	90,7

At the same time, it is mathematically confirmed that the contribution of systolic pressure to the distribution of the sample into clusters is significantly greater than that of diastolic pressure (Table 1.9).

Table 1.9. Analysis of Variance

Variable	Between SS	df	Within SS	df	F	signif. p
PS	27857	4	2147	83	269	0,000000
PD	4592	4	4190	83	22,7	0,000000

In addition, cluster analysis revealed a subgroup with normal diastolic pressure (Cluster N2) among patients with AH (Table 1.10), but this will not be considered in this study due to the escalating difficulty of simultaneously perceiving even five clusters.

Table 1.10. Cluster Means (n)

Variable	Cluster No. 1(18)	Cluster No. 2(8)	Cluster No. 3(20)	Cluster No. 4(21)	Cluster No. 5(6)	Cluster No. 6(15)
PS	140	159	128	151	178	113
PD	84,8	75,8	78,6	91	100	71,3

Based on the analyses and results presented in this Chapter, we can provide an assessment of the hypotheses that were implicitly tested.

1. Hypothesis. There is significant diversity in blood pressure levels among patients at Truskavets' spa. Verification. Confirmed. The study found a wide range of blood pressure levels, from low normal to grade II hypertension. The optimal systolic pressure was found in only 18.2% of cases, with 39.8% showing grade I hypertension and 12.5% showing grade II hypertension. Null hypothesis rejected. The null hypothesis of uniform blood pressure distribution was rejected in favor of the alternative hypothesis of significant diversity.

2. Hypothesis. There is a significant correlation between systolic and diastolic blood pressure. Verification. Confirmed. A correlation coefficient of r=0.67 was found between systolic and diastolic pressure, indicating a strong but not perfect relationship. Null hypothesis rejected. The null hypothesis of no correlation was rejected in favor of the alternative hypothesis of significant correlation.

In all these cases, the rejection of the null hypothesis was based on statistical significance (typically $p<0.05$) or clear patterns in the data. The study used various statistical methods (correlation analysis, cluster analysis, discriminant analysis) to evaluate these hypotheses. When significant results were found (e.g., $p<0.05$ for correlations, high classification accuracy for discriminant analysis), this was taken as evidence to support the alternative hypothesis and reject the null hypothesis of no effect or no difference.

Conclusions

1. Blood Pressure Distribution. A wide range of blood pressure levels was observed among patients at Truskavets' spa. Only 18.2% of patients had optimal systolic blood pressure (120-129 mmHg). 14.8% had high normal systolic blood pressure (130-139 mmHg) 39.8% exhibited Grade I hypertension (140-160 mmHg). 12.5% showed Grade II hypertension (over 160 mmHg). 14.8% had systolic blood pressure below 120 mmHg.

2. Hemodynamic Clusters. Five distinct clusters of patients were identified based on hemodynamic parameters.

3. Discriminant Analysis. 13 hemodynamic parameters were identified as significant discriminators between blood pressure clusters. The most informative parameters were. a) Contractile activity index of left ventricle. b) Heart work per minute. c) Ejection fraction and time. d) End-systolic volume.

4. Classification Accuracy. The discriminant model achieved high classification accuracy. a) 88% for patients with normal BP. b) 92% for patients with increased BP. c) 100% for patients with decreased BP as well as Grade I and II hypertension. Overall classification accuracy was 97%.

9. Methodological Robustness. The study demonstrated the effectiveness of using multiple statistical approaches (cluster analysis, discriminant analysis) to comprehensively analyze complex physiological data.

10. Clinical Implications The findings suggest potential for developing more targeted and effective balneotherapy protocols based on individual patient hemodynamic profiles.

11. Limitations. The study was observational and exploratory, which limits causal inferences. The sample size for some clusters was relatively small, which may affect the generalizability of results.

12. Future Research Directions. The study opens avenues for further research into the mechanisms underlying the observed relationships. Long-term effects of balneotherapy on cardiovascular health based on initial hemodynamic profiles could be explored. Validation of the predictive model in larger, diverse populations is needed.

This Chapter provides a comprehensive characterization of blood pressure profiles and their hemodynamic correlates in patients at Truskavets' spa. It demonstrates the potential for personalized approaches in balneotherapy. The findings lay a foundation for future studies to further elucidate the neural, endocrine, metabolic and immune accompaniments of blood pressure.

Chapter 2

AUTONOMIC AND ENDOCRINE ACCOMPANIMENTS OF QUANTITATIVE-QUALITATIVE BLOOD PRESSURE CLUSTERS

Abstract

Background. Earlier we showed that profile patients of Truskavets' spa are characterized by a wide range of blood pressure (BP) - from low norm to arterial hypertension III that correspond to the hemodynamics parameters. The **purpose** of this chapter is to clarify the autonomic and endocrine accompaniments of quantitative-qualitative BP clusters in the same contingent. **Materials and methods.** Under an observations were 44 patients with chronic pyelonephritis and cholecystitis in the phase of remission. Testing was performed twice - on admission and after 7-10 days of standard balneotherapy. The parameters of HRV ("CardioLab+HRV", Ukraine), serum levels of Cortisol, Aldosterone, Testosterone, Triiodothyronine, Parathyroid hormone and Calcitonin (ELISA) were determined. **Results**. In order to identify among the registered parameters, those for which the BP clusters differ from each other, a discriminant analysis was performed. The program forward stepwise included in the discriminant model 29 parameters. The most informative among them are HRV-markers of sympathetic tone and sympathetic-vagal balance as well as testosterone and cortisol, whose levels are maximal in patients with hypertension II, while minimal in patients with low norm BP, on the one hand, and markers of vagal tone and Kerdö's vegetative index, the levels of which are polar, on the other hand. The accuracy of patient classification is 98,9%. **Conclusion**. Autonomic and endocrine accompaniments of quantitative-qualitative blood pressure clusters corresponding to the existing ideas about the regulation of blood pressure.

Keywords: blood pressure, HRV, adaptation hormones, discriminant analysis, Truskavets' spa.

Earlier we showed that profile patients of Truskavets' spa are characterized by a wide range of blood pressure - from low norm to arterial hypertension II that correspond to the hemodynamics parameters. Research has shown that the heart communicates to the brain in four major ways: neurologically (through the transmission of nerve impulses), biochemically (via hormones and neurotransmitters), biophysically (through pressure waves) and energetically (through electromagnetic field interactions) [Exploring the Role …, 2016].

The purpose of this chapter is to clarify the autonomic and endocrine accompaniments of quantitative-qualitative blood pressure clusters in the same contingent. Such research remains relevant, as previous research in this area is fragmentary and unsystematic [Ruzhylo SV et al., 2003; Popovych IL et al., 2005; Shakhbazova LV et al., 2005; Shakhbazova LV et al., 2006; Lukovych YuS et al., 2012; Vovchyna YuV & Zukow W, 2014; Vovchyna YuV et al., 2016].

The following research problems and corresponding hypotheses can be inferred.

1. Research problem. What is the relationship between blood pressure and heart rate variability (HRV) parameters? Hypothesis. There are significant correlations between blood pressure levels and various HRV parameters, reflecting autonomic nervous system activity.

2. Research problem. How do endocrine factors relate to blood pressure levels? Hypothesis. Certain hormones (e.g., cortisol, testosterone, triiodothyronine, calcitonin) show significant associations with blood pressure levels.

3. Research problem. Can distinct clusters of patients be identified based on blood pressure and autonomic-endocrine parameters? Hypothesis. It is possible to identify distinct groups of patients characterized by different blood pressure profiles and corresponding autonomic-endocrine patterns.

4. Research problem. Which autonomic and endocrine parameters best differentiate between blood pressure clusters? Hypothesis. A specific set of HRV and hormonal parameters significantly discriminates between different blood pressure clusters.

5. Research problem. Is there a relationship between blood pressure reactivity and autonomic-endocrine factors? Hypothesis. Blood pressure reactivity patterns during repeated measurements are associated with specific autonomic and endocrine parameters.

6. Research problem. How does the Kerdö Vegetative Index relate to blood pressure and other autonomic markers? Hypothesis. The Kerdö Vegetative Index shows significant correlations with blood pressure levels and other markers of autonomic activity.

7. Research problem. Can a predictive model be developed for blood pressure cluster membership based on autonomic and endocrine parameters? Hypothesis. It is possible to create a model that accurately classifies patients into blood pressure clusters using autonomic and endocrine parameters.

8. Research problem. How do autonomic and endocrine profiles differ across various blood pressure categories (from low normal to hypertension II)? Hypothesis. There are significant differences in autonomic and endocrine profiles across the spectrum of blood pressure categories.

We recorded electrocardiogram in II lead for 7 minutes in the supine position and 2 minutes after standing up to assess the parameters of HRV [Heart Rate Variability, 1996; Berntson GG et al., 1997] (software and hardware complex "CardioLab+HRV" produced by "KhAI-MEDICA", Kharkiv, Ukraine). For further analyses the following HRV parameters were selected. Temporal parameters (Time Domain Methods): heart rate (HR), mode (Mo), the standart deviation of all NN intervals (SDNN), the square root of the mean of the sum of the squares of differences between adjacent NN intervals (RMSSD), the percent of interval differences of successive NN intervals greater than 50 msec (pNN_{50}); triangular index (TNN). Spectral parameters (Frequency Domain Methods): power spectral density (PSD) bands of HRV - high-frequency (HF, range 0,4÷0,15 Hz), low-frequency (LF, range 0,15÷0,04 Hz), very low-frequency (VLF, range 0,04÷0,015 Hz) and ultralow-frequency (ULF, range 0,015÷0,003 Hz). We calculated the Entropy of HRV bands [Popadynets' OO et al., 2020] and classical indexes LF/HF, LFnu=100%•LF/(LF+HF), (VLF+LF)/HF as Centralization Index as well as Baevskiy's Stress Index (BSI) and Activity of Regulatory Systems Index (BARSI) for estimate Autonomous Reactivity as the difference between BARSI in standing up and supine positions [Baevskiy RM & Ivanov GG, 2001; Baevskiy RM & Chernikova A, 2017].

Among hormones we determined Cortisol, Aldosterone, Testosterone, Triiodothyronine, Parathyroid hormone and Calcitonin (with ELISA kits according to the SOP provided by the manufacturer "Алкор Био", XEMA Co Ltd and DRG International Inc) with the use of analyzers "Tecan" and "RT-2100C". Finally, the battery of tests included the good old breath-holding Stange's and Henchy's tests, which are traditionally considered markers of the state of the cardio-respiratory system [Ruzhylo SV et al., 2003; Biletskyi SV & Gozhenko AI, 2007] as well as Kerdö's Vegetative Index [Kerdö I, 1966; Fajda OI et al., 2015] and $(Cap/Kp)^{0,5}$ ratio [Fajda OI et al., 2016] as markers of Sympathetic/Vagal balance.

The program forward stepwise included in the discriminant model 29 parameters (Tables 2.1 and 2.2).

Table 2.1. Discriminant Function Analysis Summary for Neuro-Endocrine Variables, their actual levels for Clusters of Blood Pressure as well as Reference levels and Coefficients of Variability

Step 29, N of vars in model: 29; Grouping: 5 grs; Wilks' Λ: 0,0043; approx. $F_{(116)}=5,6$; $p<10^{-6}$

	Clusters of Blood Pressure (n)					Parameters of Wilk's Statistics						
VARIABLES CURRENTLY IN THE MODEL	**AH II (11)**	**AH I (35)**	**High N (13)**	**Norm (16)**	**Low N (13)**	Wilks' Λ	Par-tial Λ	F-re-move (4,55)	p-level	Tole-rancy	Refe-rence (44)	Cv
Blood Pressure Systolic, mmHg	172 2,5	148 0,9	134 0,8	125 0,6	112 1,0	0,004	0,950	0,72	0,580	0,036	124,5 2,3	,122
Blood Pressure Systolic 2, mmHg	168 3,2	136 2,1	132 3,5	125 3,3	108 2,0	0,005	0,849	2,44	0,057	0,003	122,6 2,3	,122
Blood Pressure Systolic 3, mmHg	163 4,5	138 1,9	132 2,2	121 3,4	106 2,3	0,005	0,820	3,02	0,025	0,004	121,4 2,2	,122
Ps2/Ps1 ratio•1000	975 13	922 13	988 29	1000 26	971 16	0,005	0,866	2,13	0,090	0,004	960 13	,089
Ps3/Ps1 ratio•1000	944 20	934 11	984 17	964 27	953 18	0,005	0,797	3,50	0,013	0,005	951 11	,079
Pd2/Pd1 ratio•1000	1000 31	1013 11	1001 18	970 16	976 17	0,005	0,858	2,27	0,073	0,291	996 10	,070
Pd3/Pd1 ratio•1000	997 21	1023 8	1014 16	996 14	971 10	0,005	0,778	3,92	0,007	0,225	1006 8	,055
Mode HRV, msec	864 57	859 22	842 33	845 47	850 30	0,005	0,886	1,77	0,148	0,131	875 15	,116
Triangular Index HRV, units	8,4 0,9	11,1 0,7	10,8 0,7	10,2 1,1	13,7 1,1	0,005	0,845	2,52	0,052	0,087	11,2 0,4	,217
SDNN HRV, msec	38,5 3,8	48,7 3,4	45,4 4,9	45,0 5,3	58,1 4,5	0,005	0,827	2,88	0,031	0,013	56,2 4,4	,516
RMSSD HRV, msec	19,5 3,2	30,2 3,0	26,2 4,1	26,4 5,4	37,5 3,9	0,005	0,854	2,34	0,066	0,009	28,8 2,1	,486
Total Power HRV, msec²	1642 283	2748 354	2402 562	2422 612	3502 558	0,005	0,812	3,18	0,020	0,002	2379 144	,402
VLF band HRV, msec²	814 145	1216 147	1098 110	1050 271	1535 221	0,005	0,874	1,98	0,111	0,007	1250 108	,572
LF band HRV, msec²	527 138	1024 156	683 198	916 191	1157 312	0,005	0,886	1,77	0,147	0,013	625 32	,482
HF band HRV, msec²	210 68	485 85	472 235	373 28	712 190	0,005	0,883	1,82	0,138	0,014	350 38	,713
ULF band HRV, %	4,1 1,4	3,1 0,5	5,7 1,3	4,5 1,7	3,3 0,9	0,005	0,856	2,32	0,068	0,282	5,4 0,7	,816
(VLF+LF)/HF as Centralization Ind	19,9 7,2	10,6 1,6	14,9 4,7	14,1 2,6	6,5 1,6	0,005	0,924	1,13	0,351	0,266	6,8 0,6	,554
LF/HF ratio HRV, units	5,07 1,93	3,74 0,51	4,69 1,57	6,83 1,48	2,36 0,63	0,005	0,887	1,75	0,153	0,051	2,86 0,31	,709
LF band HRV, %	30,3 4,3	33,8 2,4	26,2 2,5	40,8 3,6	29,9 4,5	0,005	0,856	2,30	0,070	0,115	26,1 1,2	,312
LFnu HRV, %	74,9 3,9	71,1 2,5	68,6 5,1	79,4 3,6	58,7 5,7	0,004	0,960	0,58	0,680	0,129	64,2 1,9	,201
Kerdö's Vegetati-ve Index, units	-33 7	-26 3	-17 5	-15 4	-3 3	0,005	0,895	1,61	0,184	0,237	-15 2	**SD 14,6**
$(Cap/Kp)^{0,5}$ as Symp/Vag balance	0,70 0,01	0,73 0,01	0,72 0,01	0,72 0,02	0,68 0,01	0,005	0,814	3,14	0,021	0,518	0,71 0,01	,104
Baevskiy's Stress Index HRV, units	243 71	177 26	125 11	214 59	95 14	0,005	0,872	2,03	0,104	0,008	136 9	,417
Baevskiy's ARSI supine, units	2,64 0,75	3,27 0,43	2,25 0,51	3,43 0,67	2,62 0,60	0,005	0,860	2,24	0,076	0,254	1,50 0,11	,500
Sex Index (M=1; F=2)	1,36 0,15	1,11 0,05	1,00 0,00	1,25 0,11	1,62 0,14	0,005	0,817	3,08	0,023	0,612	1,23 0,06	,343

Testosterone standardized by Sex&Age, Z	0,84 0,57	0,37 0,31	0,74 0,51	-0,35 0,25	-0,11 0,33	0,005	0,913	1,32	0,275	0,677	0 0,30	**SD** 2
Calcitonin standardized by Sex, Z	-0,69 0,30	-0,78 0,09	-0,94 0,19	-0,47 0,33	-0,13 0,35	0,005	0,897	1,59	0,191	0,488	0 0,30	**SD** **2**
Cortisol, nM/L	469 49	374 26	446 56	386 47	391 44	0,005	0,929	1,05	0,391	0,728	370 117	,303
Henchy's Expiration Test, sec	34,5 3,1	31,4 2,0	32,7 3,3	31,1 3,4	33,4 3,7	0,005	0,934	0,97	0,433	0,528	31,0 1,0	,234
VARIABLES CURRENTLY NOT IN THE MODEL	**Clusters of Blood Pressure (n)**					**Parameters of Wilk's Statistics**						
	AH II (11)	**AH I (35)**	**High N (13)**	**Norm (16)**	**Low N (13)**	Wilks' Λ	Partial Λ	F to-enter	p-level	Tolerancy	Reference (44)	Cv
Blood Pressure Diastolic, mmHg	90,7 4,5	87,6 1,2	81,3 1,5	77,8 1,5	71,5 1,5	0,004	0,957	0,61	0,655	0,284	79,0 1,0	,083
Blood Pressure Diastolic 2, mmHg	89,9 3,8	88,7 1,4	81,4 2,0	75,5 2,0	70,0 0,8	0,004	0,971	0,40	0,806	0,275	77,9 1,0	,083
Blood Pressure Diastolic 3, mmHg	90,2 4,2	89,6 1,4	82,5 2,2	77,5 1,9	69,4 1,5	0,004	0,955	0,63	0,643	0,258	76,7 1,0	,083
Baevskiy's ARSI standing up, units	4,83 0,78	4,39 0,35	4,98 0,63	4,64 0,70	4,69 0,46	0,004	0,979	0,29	0,489	0,100	4,60 0,17	,250
Autonomous Reactivity Index	2,19 0,73	1,12 0,44	2,73 0,57	1,21 1,07	2,07 0,98	0,004	0,981	0,87	0,489	0,100	3,10 0,18	,375
pNN_{50} HRV, %	2,8 1,1	10,9 2,1	6,5 2,6	8,4 3,9	14,9 3,8	0,004	0,968	0,44	0,776	0,070	9,0 0,8	,820
ULF band HRV, $msec^2$	81 30	78 22	150 49	83 30	98 26	0,004	0,940	0,87	0,489	0,100	122 12	,892
VLF band HRV, %	54,5 6,5	48,7 2,9	54,8 4,2	44,7 3,6	45,1 5,0	0,004	0,981	0,26	0,900	0,014	53,9 2,2	,277
HF band HRV, %	11,2 3,0	14,4 1,7	13,4 2,9	10,0 1,8	21,7 4,1	0,004	0,980	0,27	0,894	0,036	14,6 1,9	,859
Entropy HRV, units•10^3	674 53	719 19	736 38	714 27	742 24	0,004	0,979	0,29	0,886	0,151	806 14	,113
Parathyroid Hormone, pM/L	3,24 0,24	4,13 0,21	3,34 0,40	3,37 0,22	3,89 0,26	0,004	0,945	0,78	0,544	0,612	3,75 0,13	,230
Aldosterone, pM/L	226 5	229 4	232 11	227 6	221 5	0,004	0,972	0,38	0,820	0,417	238 7	,187
Triiodothyronine, nM/L	1,90 0,16	1,95 0,11	1,72 0,24	2,17 0,31	2,24 0,20	0,004	0,941	0,85	0,502	0,336	2,20 0,08	,227

Table 2.2. Summary of Stepwise Analysis for Blood Pressure and Neuro-Endocrine Variables, ranked by criterion Lambda

Variables currently in the model	F to enter	p-level	**Λ**	F-value	p-value
Blood Pressure Systolic, mmHg	298	10^{-6}	0,065	298	10^{-6}
Sex Index (M=1; F=2)	4,95	0,001	0,052	69,0	10^{-6}
LF band HRV, %	2,99	0,024	0,046	39,5	10^{-6}
Blood Pressure Systolic 2, mmHg	2,89	0,027	0,040	28,6	10^{-6}
Pd3/Pd1 ratio	2,76	0,033	0,035	23,0	10^{-6}
$(Cap/Kp)^{0,5}$ as Sympathetic/Vagal balance	2,33	0,063	0,031	19,4	10^{-6}
ULF band HRV, %	1,56	0,194	0,029	16,6	10^{-6}
Ps3/Ps1 ratio	1,40	0,243	0,027	14,7	10^{-6}
LF/HF as Sympathetic/Vagal balance, units	1,67	0,165	0,025	13,2	10^{-6}
100•(1-Pd/HR) as Kerdö's Vegetative Index	2,22	0,075	0,022	12,2	10^{-6}
Pd2/Pd1 ratio	1,41	0,239	0,021	11,3	10^{-6}
Ps2/Ps1 ratio	1,72	0,156	0,019	10,5	10^{-6}
Testosterone standardized by Sex&Age, Z	1,34	0,265	0,017	9,83	10^{-6}
Cortisol, nM/L	1,87	0,126	0,016	9,35	10^{-6}
Blood Pressure Systolic 3, mmHg	1,22	0,312	0,015	8,81	10^{-6}

Calcitonin standardized by Sex&Age, Z	1,41	0,239	0,014	8,38	10^{-6}
Mode HRV, msec	1,49	0,216	0,012	8,02	10^{-6}
(VLF+LF)/HF as Centralization Index	2,25	0,073	0,011	7,82	10^{-6}
LFnu HRV, %	1,11	0,357	0,010	7,47	10^{-6}
HF band HRV, msec^2	1,32	0,272	0,009	7,19	10^{-6}
Baevskiy's Activity Regulatory Systems Index	1,72	0,157	0,009	7,00	10^{-6}
Triangular Index HRV, units	1,01	0,408	0,008	6,72	10^{-6}
VLF band HRV, msec^2	1,29	0,285	0,007	6,51	10^{-6}
SDNN HRV, msec	1,62	0,181	0,007	6,36	10^{-6}
Total Power HRV, msec^2	1,57	0,194	0,006	6,21	10^{-6}
RMSSD HRV, msec	1,32	0,274	0,006	6,05	10^{-6}
Genchy's Expiration Test, sec	1,03	0,400	0,005	5,87	10^{-6}
Baevskiy's Stress Index HRV, units	1,07	0,378	0,005	5,70	10^{-6}
LF band HRV, msec^2	1,77	0,147	0,004	5,63	10^{-6}

Next, the 29-dimensional space of discriminant variables transforms into 4-dimensional space of a canonical roots. For Root 1 r*=0,986 (Wilks' Λ=0,0043; $\chi^2_{(116)}$=382; p<10^{-6}), for Root 2 r*=0,727 (Wilks' Λ=0,149; $\chi^2_{(84)}$=133; p=0,0005), for Root 3 r*=0,708 (Wilks' Λ=0,315; $\chi^2_{(54)}$=81; p=0,010) and for Root 4 r*=0,607 (Wilks' Λ=0,632; $\chi^2_{(26)}$=32; p=0,188). The first root contains 92,6% of discriminative opportunities, the second 3,1%, the third 2,7%, the last 1,6%.

Table 2.3 presents raw and standardized coefficients for discriminant variables. The calculation of the discriminant root values for each person enables the visualization of each patient in the information space of the roots (Figs. 2.1 and 2.2).

Table 2.3. Standardized and Raw Coefficients and Constants for Variables

Coefficients	Standardized			Raw		
Variables currently in the model	Root 1	Root 2	Root 3	Root 1	Root 2	Root 3
Blood Pressure Systolic, mmHg	-0,555	1,365	-0,034	-0,114	0,281	-0,007
Sex Index (M=1; F=2)	-0,108	-0,727	-0,114	-0,281	-1,900	-0,297
LF band HRV, %	0,512	-0,082	1,238	0,036	-0,0058	0,0881
Blood Pressure Systolic 2, mmHg	-5,961	1,410	-3,733	-0,504	0,119	-0,316
Pd3/Pd1 ratio	-0,363	0,925	-0,685	-6,832	17,40	-12,87
(Cap/Kp)^{0,5} as Sympathetic/Vagal balance	-0,311	-0,120	0,662	-5,690	-2,205	12,12
ULF band HRV, %	0,622	0,224	0,142	0,140	0,051	0,032
Ps3/Ps1 ratio	-3,393	5,410	-4,221	-45,56	72,65	-56,68
LF/HF as Sympathetic/Vagal balance, units	3,321	2,496	2,107	0,014	0,0108	0,0091
100•(1-Pd/HR) as Kerdö's Vegetative Index	0,008	-0,801	-0,416	0,0004	-0,0441	-0,0229
Pd2/Pd1 ratio	-0,627	-0,162	-0,001	-9,096	-2,35	-0,016
Ps2/Ps1 ratio	5,328	-1,646	3,268	65,71	-20,30	40,30
Testosterone standardized by Sex&Age, Z	-0,208	0,017	-0,296	-0,127	0,010	-0,180
Cortisol, nM/L	-0,180	-0,260	-0,238	-0,0011	-0,0015	-0,0014
Blood Pressure Systolic 3, mmHg	3,791	-5,203	3,665	0,329	-0,451	0,318
Calcitonin standardized by Sex&Age, Z	0,267	-0,336	0,407	0,313	-0,393	0,478
Mode HRV, msec	-0,224	-1,132	-0,017	-0,0015	-0,0078	-0,0001
(VLF+LF)/HF as Centralization Index	0,171	-0,410	-0,154	0,013	-0,031	-0,012
LFnu HRV, %	-0,176	0,567	0,435	-0,011	0,036	0,027
HF band HRV, msec^2	1,811	1,406	2,875	0,0030	0,0023	0,0048
Baevskiy's Activity Regulatory Systems Index	0,675	-0,215	0,180	0,279	-0,089	0,074
Triangular Index HRV, units	1,320	-0,173	-0,384	0,354	-0,046	-0,103
VLF band HRV, msec^2	2,588	1,097	4,454	0,0031	0,0014	0,0055
SDNN HRV, msec	1,840	-2,904	2,854	0,099	-0,156	0,153
Total Power HRV, msec^2	-8,527	0,285	-10,22	-0,0042	0,0001	-0,0050
RMSSD HRV, msec	0,684	-1,610	0,879	0,046	-0,107	0,059
Henchy's Expiration Test, sec	-0,274	-0,244	0,115	-0,022	-0,020	0,009
Baevskiy's Stress Index HRV, units	-3,522	-1,841	-1,699	-0,021	-0,011	-0,010
LF band HRV, msec^2	2,342	0,166	2,487	0,0027	0,0002	0,0029

	Constants	33,64	-42,86	8,58
	Eigenvalues	34,03	1,12	1,00
	Cumulative proportions	0,926	0,957	0,984

Table 2.4 shows the correlation coefficients of blood pressure and neuro-endocrine parameters (discriminant variables) with canonical discriminant roots; the cluster centroids of both roots; and Z-scores of the discriminant variables, as well as not included in the discriminant model. The reason for the last step is our experience that not getting a variable into the model does not always indicate a lack of recognition ability, but may be a consequence of redundancy/duplication of information.

Table 2.4. Correlations Variables-Canonical Roots, Means of Roots and Z-scores of Blood Pressure and Neuro-Endocrine Variables

Variables	**Correlations Variables-Roots**			**AH II (11)**	**AH I (35)**	**High N (13)**	**Normal (16)**	**Low N (13)**
Root 1 (92,6%)	**R 1**	**R 2**	**R 3**	**-10,4**	**-2,5**	**+0,8**	**+4,8**	**+8,9**
Blood Pressure Systolic	**-0,648**	-0,106	0,200	**+3,15**	**+1,54**	**+0,64**	**+0,03**	**-0,84**
Blood Pressure Systolic 3	**-0,242**	0,018	-0,054	**+2,79**	**+1,13**	**+0,72**	**-0,06**	**-1,01**
Blood Pressure Systolic 2	**-0,233**	-0,100	-0,075	**+3,04**	**+0,92**	**+0,66**	**+0,16**	**-0,94**
(VLF+LF)/HF	**-0,033**	0,015	-0,068	**+2,74**	+0,93	**+2,02**	+2,05	**+0,04**
Baevskiy's Stress Index	**-0,032**	-0,013	0,151	**+1,51**	**+0,75**	**-0,25**	+1,26	**-0,62**
Testosterone standardized	**-0,032**	-0,017	-0,065	**+0,84**	**+0,37**	**+0,74**	**-0,35**	**-0,11**
Cortisol, nM/L	**-0,015**	-0,042	-0,159	**+0,89**	+0,04	**+0,68**	+0,15	+0,19
Pd3/Pd1 ratio	**-0,035**	0,249	0,069	-0,17	**+0,31**	**+0,14**	**-0,18**	**-0,64**
(Cap/Kp)^{0,5} as S/V balance	**-0,022**	0,279	0,132	-0,15	**+0,24**	**+0,14**	**+0,14**	**-0,48**
Blood Pressure Diastolic	currently not in the model			**+1,79**	**+1,31**	**+0,35**	**-0,19**	**-1,14**
Blood Pressure Diastolic 2	currently not in the model			**+1,86**	**+1,66**	**+0,54**	**-0,37**	**-1,29**
Blood Pressure Diastolic 3	currently not in the model			**+2,09**	**+2,02**	**+0,90**	**+0,12**	**-1,14**
100•(1-Pd/HR) as Kerdö VI	**0,087**	-0,089	-0,123	**-0,42**	**-0,17**	**+0,34**	**+0,41**	**+1,08**
Triangular Index HRV	**0,051**	-0,046	-0,033	**-1,13**	**-0,04**	-0,15	-0,40	**+1,03**
SDNN HRV	**0,037**	-0,053	0,011	**-0,50**	**-0,26**	-0,35	-0,43	**-0,02**
Total Power HRV	**0,032**	-0,021	0,026	**-0,40**	**+0,35**	+0,18	-0,07	**+0,89**
VLF band HRV PSD	**0,030**	-0,033	0,005	**-0,47**	**-0,07**	-0,12	-0,32	**+0,30**
HF band HRV PSD	**0,029**	-0,012	-0,030	**-0,16**	**+0,44**	**+0,54**	-0,16	**+0,87**
LF band HRV PSD	**0,024**	-0,010	0,120	**+0,27**	**+1,39**	+0,34	+0,75	**+1,19**
pNN$_{50}$ HRV	currently not in the model			**-0,75**	**+0,20**	-0,24	-0,06	**+0,76**
Root 2 (3,1%)	**R 1**	**R 2**	**R 3**	-1,59	+0,43	**+1,37**	+0,32	-1,58
Sex Index (M=1; F=2)	0,036	**-0,450**	0,006	+0,32	-0,27	**-0,54**	+0,05	+0,94
Calcitonin standardized	0,034	**-0,169**	0,055	-0,69	-0,78	**-0,94**	-0,47	-0,13
Triiodothyronine	currently not in the model			-0,60	-0,50	**-0,95**	-0,06	+0,09
ULF/TP ratio HRV	0,004	**0,076**	-0,130	-0,46	-0,53	**+0,12**	-0,15	-0,41
Ps3/Ps1 ratio	0,018	**0,070**	-0,150	-0,10	-0,23	**+0,43**	+0,18	+0,02
1/Mode HRV as CA	0,007	**0,021**	-0,019	+0,16	+0,11	**+0,37**	+0,34	+0,21
ULF band HRV PSD	currently not in the model			-0,38	-0,40	**+0,25**	-0,36	-0,22
Aldosterone	currently not in the model			-0,28	-0,20	**-0,14**	-0,24	-0,37
Baevskiy's ARSI standing	currently not in the model			+0,20	-0,18	**+0,33**	+0,03	+0,08
Autonomous Reactivity	currently not in the model			-0,78	-1,71	**-0,32**	-1,63	-0,88
Entropy HRV	currently not in the model			-1,28	-0,94	**-0,75**	-1,07	-0,81
Root 3 (2,7%)	**R 1**	**R 2**	**R 3**	-0,51	+0,61	-1,92	**+1,01**	-0,53
LF/TP ratio HRV	0,010	0,031	**0,297**	+0,87	-0,88	+0,08	**+1,73**	+0,24
LFnu HRV	-0,028	0,126	**0,197**	+0,68	+0,51	+0,34	**+1,28**	-0,34
Baevskiy's ARSI supine	-0,000	0,032	**0,179**	+1,52	+2,36	+1,00	**+2,58**	+1,49
Ps2/Ps1 ratio	0,027	-0,047	**0,150**	+0,18	-0,44	+0,33	**+0,46**	+0,12
LF/HF ratio HRV	-0,031	-0,006	**0,146**	+0,99	+0,44	+0,88	**+1,97**	-0,22
Genchy's test, Z	-0,003	-0,063	**-0,061**	+0,49	+0,06	+0,24	**+0,04**	+0,33
Pd2/Pd1 ratio	-0,032	0,089	**-0,010**	+0,05	+0,25	+0,07	**-0,37**	-0,29

RMSSD HRV	-0,041	-0,032	**-0,089**	-0,16	+0,14	-0,01	**-0,34**	+0,27
VLF/TP ratio HRV	currently not in the model			-0,18	-0,37	-0,01	**-0,58**	-0,48
HF/TP ratio HRV	currently not in the model			-0,10	0,00	-0,19	**-0,39**	+0,36

The localization of the patients with AH II along the first root axis (Fig. 2.1) in the extreme left (negative) zone reflects combination of significantly elevated BP with maximum for sampling levels of HRV-markers of Sympathetic tone and sympathetic/vagal balance as well as Testosterone and Cortisol levels while minimum for sampling levels of HRV-markers of Vagal tone. The extreme right zone of the axis of the first root is occupied by patients with low norm blood pressure. This reflects lower than normal or minimum for sampling levels of parameters that correlate with the root negatively and higher than normal or maximum for sampling levels of positively related parameters.

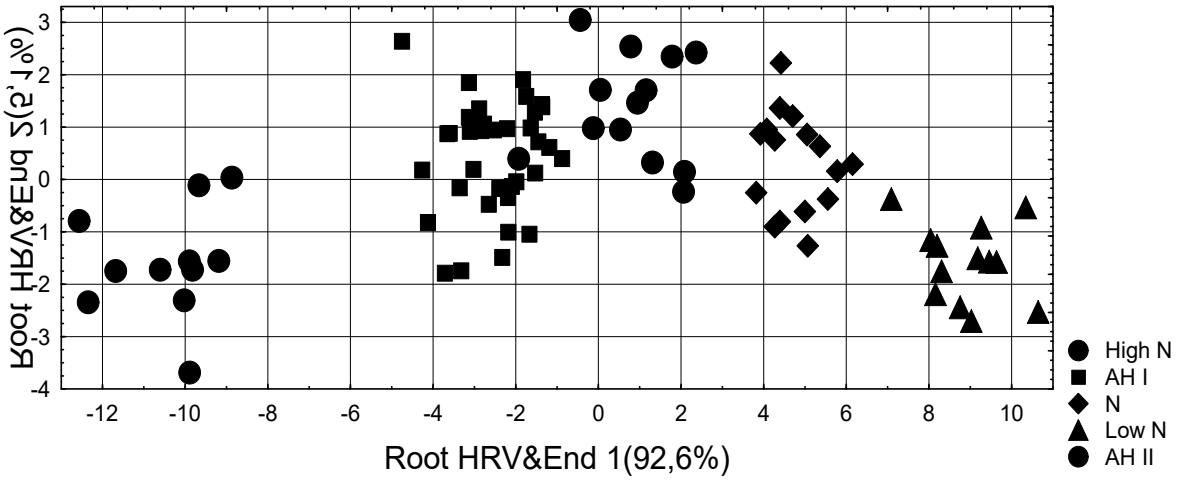

Fig. 2.1. Scattering of individual values of the first and second discriminant autonomic-endocrine roots of patients of different blood pressure clusters

It is time to find out the flashy misunderstanding with one interpretation. According to Kerdö I [1966], author's Vegetative Index [VI=100•(1 - PD/HR)] in terms of euthonia is in the range of 0±15, which displays the optimal average values of PD (80 mmHg) and HR (80 bpm). Under Sympathotonia PD/HR Ratio is less than 1 due to the lower PD and the higher HR, instead, under the conditions of Vagotonia PD/HR Ratio larger than 1 at the expense of the higher PD and the lower HR. According to the instructions to our "Cardiolab+HRV" device, the average level of HR in healthy persons 18÷35 years is 73 bpm and the seniors are 68 bpm, so for our average age sampling 46,5 (24÷76) years referential HR level It is 68,4 bpm, which at the conventional normal level PD 79 mmHg gives the reference level Kerdö's Vegetative Index (M±SD): -15±15. This average is different from the canonical but insignificant. In a special study, we showed that Kerdö's vegetative index (KVI) significantly correlates with a number of EEGs parameters, but neither HRV markers of sympathetic (LFnu, AMo) nor vagal (RMSSD, HF, pNN_{50}, MxDMn) tone as well as sympathetic/vagal balance (LF/HF, Baevskiy's Stress Index) [Fajda OI et al., 2015]. Nevertheless, patients with AH II and AH I have KVI levels significantly lower than the referential, and Low Norm BP persons are significantly higher, which corresponds to sympathotonia and vagotonia respectively by HRV-markers. Our data is consistent with Khramov YuA & Veber VR [1985] about the negative values of KVI in patients with AH II (-21,8÷-45,0) and AH I (-13,8÷-30,4) against quasi-zero (-10,5÷+10,5) in healthy persons. Instead, the data is sharply dissociated with a widespread idea of the positive values of KVI in sympathicotonia and negative - in vagotonia [Andronova TI et al., 1982; Vadziuk SN et al., 1998]. Perhaps such a misunderstanding is the

result of the statement of Kerdö I [1966], that the injection of Adrenaline causes an increase in Vegetative Index, instead, Hydergine reduces it.

Intermediate positions of members of other blood pressure clusters usually reflect intermediate levels of their autonomic and endocrine parameters.

Additional differentiation of patients with High Norm BP occurs along the axis of the second root. The upper position of the cluster members reflects their maximum reduced levels of Calcitonin, Triiodothyronine and Mode HRV (indicating the maximum sampling level of circulating catecholamines and other positive chronotropic factors [Baevskiy RM & Ivanov GG, 2001; Gozhenko AI et al., 2019]) in combination with the maximum sampling levels of Aldosterone and ULF band HRV spectral power as well as the Entropy of HRV bands and Autonomous Reactivity. Interestingly, the gender composition of the cluster is represented exclusively by men (Sex index = 1).

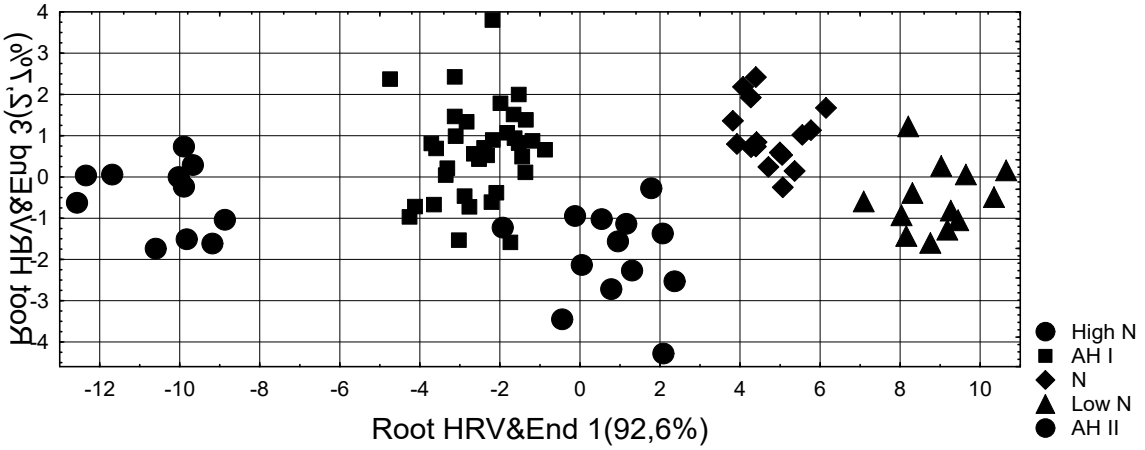

Fig. 2.2. Scattering of individual values of the first and third discriminant autonomic-endocrine roots of patients of different blood pressure clusters

Along the axis of the third root (Fig. 2), the top position is occupied by patients with the optimal level of BP, which is accompanied by the highest (compensatory?) normalized (relative) parameters of LF band HRV and Baevskiy's Activity Regulatory Systems Index in combination with the minimum for sampling relative parameters of VLF and HF bands HRV as well as Henchy's expiratory test.

In general, all clusters on the planes of three roots are clearly delineated, which is documented by calculating the Mahalanobis distances (Table 2.5).

Table 2.5. Squared Mahalanobis Distances between Blood Pressure Clusters and F-values (df=29,6; $p<10^{-5}$ - 10^{-6})

Blood Pressure Clusters	High Norm	AH I	Norm	Low Norm	AH II
High Norm	0	**19,1**	**26,2**	**77,2**	**137**
AH I	**4,15**	0	**56,7**	**136**	**69,5**
Norm	**4,29**	**14,2**	0	**26,5**	**237**
Low Norm	**11,5**	**29,6**	**4,35**	0	**376**
AH II	**18,7**	**13,3**	**35,2**	**51,2**	0

The same discriminant parameters can be used to identify the belonging of one or another person to one or another cluster (Table 2.6).

Table 2.6. Coefficients and Constants for Classification Functions for Blood Pressure Clusters

Blood Pressure Clusters	High N	AH I	Norm	Low N	AH II
Variables currently in the model	p=,148	p=,398	p=,182	p=,148	p=,125
Blood Pressure Systolic, mmHg	165,4	165,4	164,7	163,5	165,9
Sex Index (M=1; F=2)	-28,88	-27,08	-28,67	-26,14	-20,42
LF band HRV, %	0,338	0,396	0,799	0,727	0,097
Blood Pressure Systolic 2, mmHg	-91,28	-90,75	-94,06	-96,38	-86,29
Pd3/Pd1 ratio	2918	2881	2847	2783	2931
$(Cap/Kp)^{0,5}$ as Sympathetic/Vagal balance	-813,8	-757,1	-804,3	-831,9	-729,2
ULF band HRV, %	7,450	6,913	8,160	8,390	5,826
Ps3/Ps1 ratio	10220	10121	9843	9520	10459
LF/HF as Sympathetic/Vagal balance, units	-0,471	-0,508	-0,396	-0,375	-0,651
100•(1-Pd/HR) as Kerdö's Vegetative Index	1,874	1,846	1,867	1,966	1,974
Pd2/Pd1 ratio	-759,5	-720,7	-800,1	-820,5	-654,0
Ps2/Ps1 ratio	13384	13307	13759	14053	12751
Testosterone standardized by Sex&Age, Z	-3,129	-2,991	-4,369	-4,268	-2,093
Cortisol, nM/L	0,0197	0,0208	0,0134	0,0134	0,0343
Blood Pressure Systolic 3, mmHg	-70,60	-70,14	-68,29	-65,85	-72,71
Calcitonin standardized by Sex&Age, Z	-78,46	-77,92	-75,43	-74,09	-80,15
Mode HRV, msec	0,403	0,411	0,409	0,410	0,445
(VLF+LF)/HF as Centralization Index	2,897	2,810	2,996	3,038	2,851
LFnu HRV, %	-1,127	-1,067	-1,114	-1,295	-1,063
HF band HRV, $msec^2$	0,166	0,164	0,190	0,189	0,132
Baevskiy's Activity Regulatory Systems Ind	-41,61	-42,11	-40,37	-38,84	-44,46
Triangular Index HRV, units	16,75	15,33	17,92	19,59	12,78
VLF band HRV, $msec^2$	0,132	0,134	0,160	0,161	0,100
SDNN HRV, msec	-16,13	-15,85	-15,21	-14,58	-16,61
Total Power HRV, $msec^2$	0,0739	0,0748	0,0428	0,0321	0,1138
RMSSD HRV, msec	3,136	3,244	3,587	3,914	3,017
Henchy's Expiration Test, sec	0,0267	0,1566	-0,0285	-0,0702	0,3409
Baevskiy's Stress Index HRV, units	1,089	1,144	0,987	0,934	1,347
LF band HRV, $msec^2$	-0,0078	-0,0094	0,0108	0,0182	-0,0352
Constants	-12988	-13015	-12820	-12594	-13292

In this case, we can retrospectively recognize patients with high norm BP with one mistake and others patients **unmistakably**. Overall classification accuracy is 98,9% (Table 2.7).

Table 2.7. Classification Matrix for Blood Pressure Clusters

	Rows: Observed classifications Columns: Predicted classifications					
Group	Percent Correct	High N p=,14 8	AH I p=,39 8	N p=,18 2	Low N p=,14 8	AH II p=,125
High N	92,3	12	1	0	0	0
AH I	100,0	0	35	0	0	0
N	100,0	0	0	16	0	0
Low N	100,0	0	0	0	13	0
AH II	100,0	0	0	0	0	11
Total	98,9	12	36	16	13	11

In our opinion, the patterns of BP parameters recorded three times in a row deserve special attention. Returning to the Table 2.4, we see that the level of Pd3/Pd1 ratio in patients with AH I is greater than 1 and the maximum for the sample. In contrast, patients with Low Norm BP have a Pd3/Pd1 ratio less than 1 and are associated with low GPRV. Patients in the

other three clusters are characterized by almost identical close to 1 Pd3/Pd1 ratio and quasi-zero GPRV levels.

Hence, it is suggested that in patients with AH I in response to triple occlusion of the shoulder arteries with a tonometer cuff, their endothelium increases the release of vasoconstrictors and/or reduces the release of vasodilators while in patients with Low Norm BP a similar procedure causes increase the release of vasodilators and/or decrease the release of vasoconstrictors. In patients of other clusters, the balance of vasoconstrictors/vasodilators remains stable. Patients with AH I also had the highest level of Pd2/Pd1 ratio, while the lowest level was found in patients with Norm BP, combined with maximum levels of sympathetic markers. Maximal level of Ps3/Ps1 ratio in patients with High Norm BP indicates the minimum for the sample reduction of systolic BP in the third consecutive measurement, which we interpret as the minimum release of vasodilators and/or maximum release of vasoconstrictors in response to occlusion.

In order to check the assumption about the autonomous-endocrine mechanism of the revealed phenomenon, a canonical correlation analysis of the links between the parameters of the triple BP test, on the one hand, and HRV and hormones - on the other, was conducted.

Screening found a significant ($r \geq |0{,}211|$) correlation between Ps3/Ps1 Ratio and HRV-markers of sympathetic tone and sympatho-vagal balance (direct) as well as vagal tone (invers) (Table 2.8 and Fig. 2.3).

Table 2.8. Correlation Matrix for Neuro-endocrine and BP Reactivity variables

	Ps2/Ps1	Ps3/Ps1	Pd2/Pd1	Pd3/Pd1
LF/HF as S/V balance	0,158	**0,436**	0,009	-0,032
LFnu HRV, %	0,181	**0,410**	-0,019	-0,019
(VLF+LF)/HF as CI	0,133	**0,360**	0,007	-0,097
Baevskiy's SI, units	0,047	**0,216**	-0,156	-0,138
HF HRV, %	-0,156	**-0,350**	0,054	-0,002
RMSSD HRV, msec	-0,071	-0,203	0,048	-0,005
HRV Entropy	-0,022	-0,197	-0,010	-0,009
Calcitonin, Z	0,052	0,194	**0,239**	0,135
Calcitonin, ng/L	-0,062	0,152	**0,216**	**0,212**
Testosterone, Z	0,065	-0,039	-0,165	-0,077
Henchy's Test, sec	0,056	0,095	-0,080	-0,192
ULF band HRV, msec^2	0,193	0,062	-0,168	-0,180

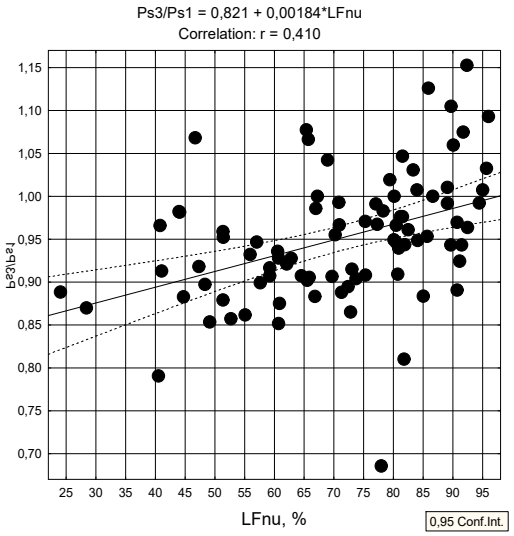

Fig. 2.3. Scatterplot of correlation between Sympathetic tone (X-line) and Ps3/Ps1 ratio (Y-line)

Table 2.9. Factor structure of Neuro-endocrine and BP Reactivity Roots

Left set	R
LF/HF as Symp/Vagal balance	-0,769
LFnu as Sympathetic tone, %	-0,731
Calcitonin row, ng/L	-0,532
Calcitonin normalized, Z	-0,521
Baevskiy's Stress Index, units	-0,240
HF/TP HRV as Vagal tone, %	0,640
Testosterone normalized, Z	0,172
ULF band HRV, msec^2	0,104
Henchy's Test, sec	0,039
Right set	**R**
BPs3/BPs1 ratio	-0,788
BPd2/BPd1 ratio	-0,256
BPs2/BPs1 ratio	-0,239
BPd3/BPd1 ratio	-0,195

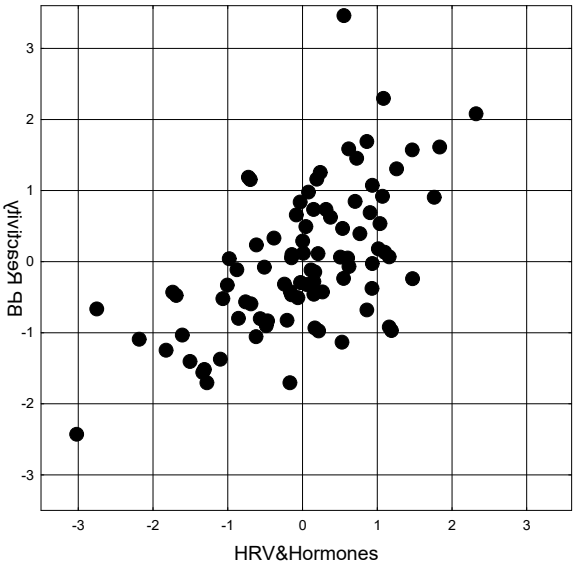

R=0.594; R^2=0.353; $\chi^2_{(36)}$=61; p=0.006; Λ Prime=0.466

Fig. 2.4. Scatterplot of canonical correlation between HRV&Hormonal (X-line) and Blood Pressure Reactivity (Y-line) parameters

In turn, Pd2/Pd1 correlates with the level of calcitonin, both raw and sex-standardized (significant), and testosterone, sex- and age-standardized (marginally significant), and Pd3/Pd1 also correlates with expiratory breath-hold duration. The mechanisms of such connections will be considered in the next chapter. Now let's limit ourselves to stating the fact that BP reactivity in the triplet test is determined by the constellation of autonomous and hormonal influences by 35% (Table 2.9 and Fig. 2.4).

Based on the analyses and results presented in this Chapter, here is a detailed evaluation of the hypotheses and their verification:

1. Hypothesis. It is possible to identify distinct groups of patients characterized by different blood pressure profiles and corresponding autonomic-endocrine patterns. Verification. Confirmed. The study identified five distinct clusters of patients based on blood pressure and autonomic-endocrine parameters. Null hypothesis rejected. The null hypothesis of no distinct clusters was rejected in favor of the alternative hypothesis of distinct patient groups.

2. Hypothesis. A specific set of HRV and hormonal parameters significantly discriminates between different blood pressure clusters. Verification. Confirmed. Discriminant analysis identified 29 parameters that significantly differentiated between blood

pressure clusters. Null hypothesis rejected. The null hypothesis of no differentiating parameters was rejected.

3. Hypothesis. Blood pressure reactivity patterns during repeated measurements are associated with specific autonomic and endocrine parameters. Verification. Confirmed. The study found significant correlations between blood pressure reactivity patterns and various autonomic and endocrine parameters. Null hypothesis rejected. The null hypothesis of no association was rejected.

4. Hypothesis. The Kerdö Vegetative Index shows significant correlations with blood pressure levels and other markers of autonomic activity. Verification. Confirmed, but with unexpected results. The Kerdö Vegetative Index showed significant correlations, but the direction of the relationship was opposite to traditional interpretations. Null hypothesis rejected. The null hypothesis of no correlation was rejected, but the nature of the relationship was different from expected.

5. Hypothesis. It is possible to create a model that accurately classifies patients into blood pressure clusters using autonomic and endocrine parameters. Verification. Confirmed. The classification functions derived from discriminant analysis achieved a high overall accuracy of 98.9%. Null hypothesis rejected. The null hypothesis of no predictive model was rejected in favor of the alternative hypothesis of an accurate classification model.

6. Hypothesis. There are significant differences in autonomic and endocrine profiles across the spectrum of blood pressure categories. Verification. Confirmed. The study found distinct autonomic and endocrine profiles for different blood pressure categories, from low normal to hypertension II. Null hypothesis rejected. The null hypothesis of no differences was rejected in favor of the alternative hypothesis of significant differences across categories.

Conclusions

1. Blood Pressure Distribution. A wide range of blood pressure levels was observed among patients at Truskavets' spa, from low normal to arterial hypertension II. This diversity corresponds to varying hemodynamic and neuro-endocrine parameters.

2. Autonomic Nervous System and Blood Pressure. HRV markers of sympathetic tone (e.g., LFnu) and sympathetic-vagal balance (e.g., LF/HF ratio) were maximal in patients with hypertension II and minimal in patients with low normal BP. Markers of vagal tone (e.g., RMSSD, HF, pNN_{50}) showed an opposite pattern.

3. Endocrine Factors and Blood Pressure. Testosterone and cortisol levels were maximal in patients with hypertension II and minimal in patients with low normal BP. Other hormones (triiodothyronine, calcitonin) showed less clear associations with blood pressure.

4. Kerdö's Vegetative Index. Contrary to traditional interpretations, patients with hypertension II and I had significantly lower Kerdö's Vegetative Index levels than the reference, while those with Low Normal BP had significantly higher levels. This finding challenges the widespread idea of positive values indicating sympathicotonia and negative values indicating vagotonia.

5. Blood Pressure Clusters. Five distinct clusters of patients were identified based on blood pressure and autonomic-endocrine parameters. These clusters were clearly delineated in the space of canonical discriminant roots.

6. Discriminant Analysis. 29 parameters were identified as significant discriminators between blood pressure clusters. The most informative parameters included HRV markers of sympathetic tone and sympathetic-vagal balance, testosterone, cortisol, and markers of vagal tone.

7. Classification Accuracy. The discriminant model achieved a high overall classification accuracy of 98.9%. This suggests that autonomic and endocrine parameters can effectively predict blood pressure cluster membership.

8. Blood Pressure Reactivity. Patterns of blood pressure changes during repeated measurements were associated with specific autonomic and endocrine parameters. These patterns provided additional information beyond static blood pressure measurements.

10. Methodological Robustness. The study demonstrated the effectiveness of using multiple statistical approaches (discriminant analysis, canonical correlation analysis) to comprehensively analyze complex physiological data.

11. Integrated Physiological View. The findings support an integrated view of blood pressure regulation, involving complex interactions between the autonomic nervous system and endocrine factors.

12. Clinical Implications. The results suggest potential for developing more targeted and personalized approaches to blood pressure management based on individual autonomic and endocrine profiles.

13. Limitations. The study was observational and cross-sectional, which limits causal inferences. The sample size, while adequate for the analyses performed, may limit the generalizability of some findings.

14. Future Research Directions. The study opens avenues for further research into the mechanisms underlying the observed relationships between blood pressure, autonomic function, and endocrine factors. Longitudinal studies could help elucidate the temporal dynamics of these relationships. Validation of the predictive model in larger, diverse populations is needed.

This chapter provides a comprehensive characterization of the autonomic and endocrine accompaniments of different blood pressure profiles in patients at Truskavets' spa. It demonstrates the complex, multifaceted nature of blood pressure regulation and the potential for personalized approaches in cardiovascular health management. The findings lay a foundation for future studies to further elucidate these relationships and translate them into improved clinical practices in spa medicine and beyond.

Thus, a wide range of blood pressure in Truskavets’ spa patients is accompanied by an equally wide range of HRV parameters and adaptive hormones. The most informative among them are HRV-markers of sympathetic tone and sympathetic/vagal balance as well as testosterone and cortisol, whose levels are maximal in patients with hypertension II, while minimal in patients with low norm BP, on the one hand, and markers of vagal tone and Kerdö’s vegetative index, the levels of which are polar, on the other hand. Autonomic and endocrine accompaniments of quantitative-qualitative blood pressure clusters corresponding to the existing ideas about the regulation of heart and blood pressure. For the first time, we discovered the informativeness of BP patterns in the conditions of its three-time consecutive measurement.

Chapter 3

ELECTROENCEPHALOGRAPHIC ACCOMPANIMENT OF QUANTITATIVE-QUALITATIVE BLOOD PRESSURE CLUSTERS

Abstract

Background. Earlier we studied the autonomic and endocrine accompaniments of quantitative-qualitative blood pressure (BP) clusters of profile patients of Truskavets' spa. The **purpose** of this chapter is to clarify the electroencephalographic accompaniment in the same contingent. **Materials and methods.** Under an observations were 44 patients with chronic pyelonephritis and cholecystitis in the phase of remission. Testing was performed twice - on admission and after 7-10 days of standard balneotherapy. EEG recorded a hardware-software complex "NeuroCom Standard" (KhAI Medica, Ukraine) monopolar in 16 loci. **Results**. The forward stepwise program identified 30 parameters as characteristic of quantitative-qualitative blood pressure clusters. In addition to BP parameters by default, 5 entropy parameters, 4 delta-rhythm, 6 theta-rhythm, 6 alpha-rhythm and 7 beta-rhythm parameters are included in the discriminant model. The most informative among them are PSD of beta-rhythm in C3 and C4 loci; alpha-rhythm in T4 and F3 loci; delta-rhythm in C3, T5 and P3 loci as well as its deviation. The accuracy of classification is 100%. **Conclusion**. The wide range of blood pressure - from low norm to arterial hypertension II - is accompanied by characteristic EEG conditions.

Keywords: blood pressure, electroencephalogram, discriminant analysis, Truskavets' spa.

Earlier we showed that profile patients of Truskavets' spa are characterized by a wide range of blood pressure - from low norm to arterial hypertension II that correspond to the hemodynamics parameters. In next study we clarified the autonomic and endocrine accompaniments of quantitative-qualitative blood pressure clusters in the same contingent. We have been shown that the most informative among them are HRV-markers of sympathetic tone and sympathetic-vagal balance as well as testosterone and cortisol, whose levels are maximal in patients with hypertension II, while minimal in patients with low norm blood pressure, on the one hand, and markers of vagal tone and Kerdö's vegetative index, the levels of which are polar, on the other hand. The accuracy of patient classification is 98,9%.

Preliminary analysis revealed significant relationships between HRV and EEG parameters [Popovych IL et al., 2013; Popovych IL et al., 2014]. Therefore, the purpose of this chapter is to clarify the electroencephalographic accompaniment of quantitative-qualitative blood pressure clusters in the same contingent.

Based on the content of this Chapter, although not explicitly stated, the following research problems and corresponding hypotheses can be inferred.

1. Research problem. Is there a relationship between blood pressure and electroencephalographic (EEG) parameters? Hypothesis. Significant correlations exist between blood pressure levels and various EEG parameters across different brain regions and frequency bands.

2. Research problem. Can distinct blood pressure clusters be identified based on EEG parameters? Hypothesis. It is possible to identify distinct groups of patients characterized by different blood pressure profiles and corresponding EEG patterns.

3. Research problem. Which EEG parameters best differentiate between blood pressure clusters? Hypothesis. A specific set of EEG parameters significantly discriminates between different blood pressure clusters.

4. Research problem. How do EEG patterns differ across various blood pressure categories (from low normal to hypertension II)? Hypothesis. There are significant differences in EEG profiles across the spectrum of blood pressure categories.

5. Research problem. Is there a relationship between blood pressure and EEG entropy measures? Hypothesis. EEG entropy measures show significant correlations with blood pressure levels.

6. Research problem. How do different EEG frequency bands (delta, theta, alpha, beta) relate to blood pressure levels? Hypothesis. Different EEG frequency bands show distinct patterns of association with blood pressure levels.

7. Research problem. Are there specific EEG laterality or asymmetry patterns associated with different blood pressure levels? Hypothesis. EEG laterality and asymmetry measures are significantly associated with blood pressure levels.

8. Research problem. Can a predictive model be developed for blood pressure cluster membership based on EEG parameters? Hypothesis. It is possible to create a model that accurately classifies patients into blood pressure clusters using EEG parameters.

9. Research problem. How do EEG parameters interact with other physiological measures (e.g., autonomic, endocrine) in relation to blood pressure? Hypothesis. There are significant interactions between EEG parameters and other physiological measures in their association with blood pressure.

10. Research problem. Are there specific EEG biomarkers that could be indicative of hypertension risk or severity? Hypothesis. Certain EEG parameters or patterns can serve as biomarkers for hypertension risk or severity.

These research problems and hypotheses are not explicitly stated in the text of this Chapter, but they can be inferred from the analyses conducted and the results presented. The study appears to have an exploratory nature, which explains the lack of formally stated hypotheses at the beginning of the chapter. The research aims to uncover the electroencephalographic accompaniments of different blood pressure profiles, potentially providing new insights into the neural correlates of blood pressure regulation.

EEG recorded a hardware-software complex “NeuroCom Standard” (KhAI Medica, Kharkiv, Ukraine) monopolar in 16 loci (Fp1, Fp2, F3, F4, F7, F8, C3, C4, T3, T4, P3, P4, T5, T6, O1, O2) by 10-20 international system, with the reference electrodes A and Ref on the earlobes. Two minutes after the eyes had been closed, 25 sec of artifact free EEG data were collected by computer. Among the options considered the average EEG amplitude (μV), average frequency (Hz), frequency deviation (Hz), index (%), absolute (μV^2/Hz) and relative (%) PSD of basic rhythms: β (35÷13 Hz), α (13÷8 Hz), θ (8÷4 Hz) and δ (4÷0,5 Hz) in all loci, according to the instructions of the device. In addition, calculated coefficient of Asymmetry (As) and Laterality Index (LI) for PSD each Rhythm using formulas [Newberg AB et al., 2001]:

As, % = 100•(Max – Min)/Min; LI, % = Σ [200•(Right – Left)/(Right + Left)]/8.

We calculated for each locus EEG the Entropy (h) of normalized PSD using Popovych’s IL [Ruzhylo SV et al., 2015] formula based on classic Shannon’s CE [1948] formula:

$hEEG = - [PSD\alpha \bullet \log_2 PSD\alpha + PSD\beta \bullet \log_2 PSD\beta + PSD\theta \bullet \log_2 PSD\theta + PSD\delta \bullet \log_2 PSD\delta]/\log_2 4$.

Reference values are taken from the database of our laboratory (n=112).

Following the pre-accepted algorithm, the recorded BP&EEG parameters were subjected to discriminant analysis. The forward stepwise program identified 30 parameters as characteristic of quantitative-qualitative blood pressure clusters. In addition to BP parameters by default, 5 **entropy** parameters, 4 **delta-rhythm**, 6 **theta-rhythm**, 6 **alpha-rhythm** and 7 **beta-rhythm** parameters are included in the discriminant model. Another 2 EEG parameters were found to be out of the model, despite the clear recognition ability (Tables 3.1 and 3.2).

Table 3.1. Discriminant Function Analysis Summary for BP&EEG Variables, their actual levels (Mean±SE) for Clusters as well as Reference levels and Coefficients of Variability

Step 30, N of vars in model: 30; Grouping: 5 grs; Wilks' Λ: 0,0031; approx. $F_{(120)}$=6,0; $p<10^{-6}$

	Clusters of Blood Pressure (n)					Parameters of Wilk's Statistics						
Variables currently in the model	**AH II (11)**	**AH I (35)**	**High N (13)**	**No-rm (16)**	**Low N (13)**	Wilks' Λ	Par-tial Λ	F-re-move (4,54)	p-level	Tole-rancy	Refe-rence (44)	Cv
BP systolic, mmHg	172 2,5	148 0,9	134 0,8	125 0,6	112 1,0	0,027	0,113	106	10^{-6}	0,509	124,5 2,3	,122
BP diastolic, mmHg	90,7 4,5	87,6 1,2	81,3 1,5	77,8 1,5	71,5 1,5	0,004	0,770	4,03	0,006	0,484	79,0 1,0	,083
Entropy PSD C3	0,82 0,04	0,89 0,01	0,78 0,04	0,87 0,02	0,78 0,05	0,003	0,931	1,00	0,416	0,289	0,862 0,015	,115
Entropy PSD O2	0,76 0,06	0,81 0,02	0,78 0,04	0,67 0,05	0,75 0,03	0,004	0,707	5,582	0,001	0,140	0,776 0,021	,178
Entropy PSD P3	0,80 0,05	0,82 0,02	0,81 0,03	0,82 0,02	0,77 0,05	0,004	0,859	2,21	0,080	0,128	0,802 0,020	,167
Entropy PSD T3	0,83 0,04	0,90 0,01	0,75 0,04	0,78 0,04	0,76 0,05	0,003	0,889	1,68	0,168	0,361	0,857 0,017	,131
Entropy PSD T5	0,74 0,08	0,83 0,02	0,77 0,04	0,81 0,05	0,73 0,04	0,003	0,899	1,52	0,210	0,183	0,825 0,019	,156
Deviation-δ, Hz	0,64 0,07	0,70 0,04	0,55 0,04	0,66 0,08	0,85 0,10	0,004	0,807	3,23	0,019	0,611	0,67 0,04	,395
P3-δ PSD, %	25,2 6,0	27,7 2,8	26,0 5,6	24,8 3,5	36,7 7,1	0,004	0,805	3,27	0,018	0,120	25,6 2,7	,694
T5-δ PSD, %	32,5 9,2	25,8 3,2	29,9 7,0	40,9 6,0	41,6 8,2	0,003	0,942	0,835	0,509	0,065	26,3 2,8	,696
C3-δ PSD, %	30,4 6,8	27,9 2,7	37,5 7,5	28,8 3,3	43,5 7,4	0,004	0,792	3,56	0,012	0,098	28,0 2,5	,602
Amplitude-θ, μV	7,7 1,0	9,7 0,9	7,7 0,6	9,4 0,9	8,6 1,0	0,004	0,861	2,18	0,083	0,287	7,75 0,4	,376
C4-θ PSD, %	9,4 1,1	13,9 1,1	9,5 1,4	9,8 1,1	11,9 1,3	0,004	0,750	4,50	0,003	0,157	11,1 0,7	,442
O1-θ PSD, %	8,5 1,6	8,2 0,8	8,2 1,4	7,0 0,9	10,3 1,7	0,004	0,746	4,60	0,003	0,207	8,2 0,7	,584
F8-θ PSD, %	7,2 1,2	11,3 1,2	7,3 0,6	8,1 1,3	10,5 2,0	0,003	0,905	1,42	0,241	0,250	9,8 0,7	,492
P4-θ PSD, %	9,4 1,6	10,2 0,9	7,2 0,8	7,3 0,7	9,3 1,3	0,004	0,744	4,64	0,003	0,135	8,75 0,7	,545
O2-θ PSD, %	6,8 1,3	7,5 0,8	7,3 1,4	6,1 0,9	7,45 1,4	0,003	0,883	1,79	0,144	0,141	7,1 0,6	,554
Index-α, %	49,5 8,5	48,4 5,7	47,3 8,7	62,6 6,0	53,4 6,6	0,004	0,795	3,47	0,014	0,125	50,7 4,3	,560
Deviation-α, Hz	0,86 0,10	1,11 0,12	0,91 0,10	0,81 0,10	1,23 0,15	0,004	0,835	2,67	0,042	0,500	1,02 0,08	,527
F7-α PSD, %	28,9 6,1	27,1 2,5	21,1 3,9	18,4 3,4	26,6 3,7	0,004	0,776	3,89	0,008	0,168	27,6 2,2	,522
T4-α PSD, %	31,6 5,9	29,3 2,5	22,0 4,4	26,7 3,1	24,5 4,7	0,003	0,911	1,32	0,274	0,137	29,0 2,3	,500
F3-α PSD, %	31,6 5,8	29,5 2,2	30,1 6,1	30,9 4,3	27,0 5,7	0,004	0,766	4,12	0,006	0,061	33,2 2,4	,479
Fp2-α PSD, %	27,9 4,2	31,3 2,4	27,2 4,1	34,3 4,7	31,9 5,1	0,004	0,837	2,61	0,045	0,131	32,9 2,2	,448
Laterality-	-34	-3,1	-13,0	-13	-6,2	0,004	0,810	3,18	0,020	0,518	-0,9	**SD**

β, %	6,4	4,7	10,8	5,5	7,2						5,1	**34**
T3-β PSD, %	28,6 3,7	28,5 2,1	38,5 6,1	19,5 3,3	28,55 5,1	0,003	0,884	1,77	0,148	0,247	30,7 2,1	,462
F3-β PSD, %	25,5 3,6	27,0 2,4	27,8 3,5	15,6 2,6	17,1 2,7	0,003	0,949	0,73	0,575	0,264	26,7 1,9	,463
O1-β PSD, %	31,6 4,8	28,0 3,2	26,1 4,4	16,4 3,1	18,4 2,7	0,004	0,814	3,09	0,023	0,159	26,3 2,2	,542
T5-β PSD, %	26,4 4,9	31,2 3,2	35,4 5,9	19,9 2,5	24,9 5,3	0,004	0,863	2,14	0,088	0,061	29,0 2,3	,536
C4-β PSD, %	25,8 3,2	25,6 1,8	29,0 3,9	22,2 3,3	17,1 2,2	0,003	0,890	1,66	0,172	0,129	25,9 1,6	,405
T4-β PSD, %	26,6 3,2	29,3 2,7	39,7 5,7	24,5 4,0	26,9 4,5	0,003	0,919	1,18	0,329	0,198	30,4 2,2	,483
Variables currently not in model	**AH II (11)**	**AH I (35)**	**High N (13)**	**No-rm (16)**	**Low N (13)**	Wil ks' Λ	Par-tial Λ	F to enter	p-level	Tole-rancy	Refe-rence (44)	Cv
Fp1-θ PSD, %	9,4 1,6	13,4 1,6	6,65 0,8	7,7 0,9	10,8 2,1	0,003	0,985	0,21	0,933	0,203	10,4 0,9	,588
C3-β PSD, %	27,1 3,6	26,3 2,0	26,7 3,8	21,6 2,8	16,6 2,4	0,003	0,983	0,23	0,922	0,060	25,45 1,6	,420

Table 3.2. Summary of Stepwise Analysis for BP&EEG Variables, ranked by criterion Λ

Variables currently in the model	F to enter	p-level	**Λ**	F-value	p-value
BP systolic, mmHg	298	10^{-6}	0,065	298	10^{-6}
T3-β PSD, %	3,83	0,007	0,055	67,0	10^{-6}
Entropy PSD C3	3,73	0,008	0,046	39,2	10^{-6}
C4-θ PSD, %	2,97	0,024	0,040	28,5	10^{-6}
BP diastolic, mmHg	2,68	0,037	0,036	22,8	10^{-6}
Deviation-δ, Hz	2,24	0,072	0,032	19,2	10^{-6}
Laterality-β, %	2,06	0,094	0,029	16,7	10^{-6}
F7-α PSD, %	1,95	0,111	0,026	14,9	10^{-6}
P3-δ PSD, %	3,80	0,007	0,022	14,0	10^{-6}
F3-β PSD, %	1,65	0,171	0,020	12,8	10^{-6}
Index-α, %	2,00	0,104	0,018	11,9	10^{-6}
O1-θ PSD, %	2,44	0,054	0,016	11,3	10^{-6}
F8-θ PSD, %	2,58	0,045	0,014	10,8	10^{-6}
Amplitude-θ, μV	1,33	0,268	0,013	10,1	10^{-6}
Deviation-α, Hz	1,06	0,383	0,012	9,50	10^{-6}
O1-β PSD, %	1,09	0,370	0,011	8,96	10^{-6}
T5-β PSD, %	2,02	0,101	0,010	8,66	10^{-6}
T5-δ PSD, %	1,32	0,271	0,009	8,28	10^{-6}
Entropy PSD O2	1,51	0,209	0,009	7,97	10^{-6}
T4-α PSD, %	1,24	0,302	0,008	7,66	10^{-6}
F3-α PSD, %	1,39	0,246	0,007	7,39	10^{-6}
Fp2-α PSD, %	2,03	0,102	0,006	7,25	10^{-6}
P4-θ PSD, %	1,53	0,205	0,006	7,05	10^{-6}
Entropy PSD P3	1,37	0,256	0,005	6,85	10^{-6}
C3-δ PSD, %	1,54	0,202	0,005	6,69	10^{-6}
C4-β PSD, %	1,42	0,239	0,004	6,52	10^{-6}
Entropy PSD T3	1,63	0,180	0,004	6,40	10^{-6}
O2-θ PSD, %	1,25	0,299	0,004	6,24	10^{-6}
Entropy PSD T5	1,40	0,248	0,003	6,11	10^{-6}
T4-β PSD, %	1,18	0,329	0,003	5,96	10^{-6}

Next, the 30-dimensional space of discriminant variables transforms into 4-dimensional space of a canonical roots. For Root 1 r*=0,979 (Wilks' Λ=0,0031; $\chi^2_{(120)}$=402; p<10^{-6}), for Root 2 r*=0,849 (Wilks' Λ=0,075; $\chi^2_{(87)}$=180; p=10^{-6}), for Root 3 r*=0,722 (Wilks' Λ=0,270;

$\chi^2_{(56)}$=91; p=0,002) and for Root 4 r*=0,660 (Wilks' Λ=0,564; $\chi^2_{(27)}$=40; p=0,053). The first root contains 84,1% of discriminative opportunities, the second 9,3%, the third 3,8%, the last 2,8%.

The calculation of the discriminant root values for each person as the sum of the products of raw coefficients to the individual values of discriminant variables together with the constant (Table 3.3) enables the visualization of each patient in the information space of the roots (Fig. 3.1).

Table 3.3. Standardized and Raw Coefficients and Constants for BP&EEG Variables

Coefficients	Standardized				Raw			
Variables currently in the model	Root 1	Root 2	Root 3	Root 4	Root 1	Root 2	Root 3	Root 4
BP systolic, mmHg	-1,344	0,105	-0,007	0,079	-0,277	0,022	-0,001	0,016
T3-β PSD, %	0,303	-0,053	-0,387	0,830	0,021	-0,004	-0,027	0,058
Entropy PSD C3	-0,163	-0,123	0,470	-0,447	-1,462	-1,099	4,211	-4,000
C4-θ PSD, %	0,141	0,866	-1,379	0,320	0,030	0,184	-0,292	0,068
BP diastolic, mmHg	0,258	-0,392	-0,688	-0,352	0,033	-0,049	-0,087	-0,044
Deviation-δ, Hz	0,068	0,249	0,660	-0,301	0,272	0,994	2,630	-1,199
Laterality-β, %	-0,030	0,469	-0,630	-0,060	-0,001	0,019	-0,025	-0,002
F7-α PSD, %	0,556	0,991	0,482	-0,687	0,040	0,071	0,035	-0,049
P3-δ PSD, %	0,269	0,945	-1,275	0,397	0,015	0,054	-0,073	0,023
F3-β PSD, %	-0,208	0,200	-0,465	-0,160	-0,019	0,018	-0,041	-0,014
Index-α, %	-0,506	1,370	-0,097	0,295	-0,019	0,052	-0,004	0,011
O1-θ PSD, %	-0,700	0,757	0,721	0,407	-0,157	0,170	0,162	0,091
F8-θ PSD, %	0,014	-0,482	-0,346	-0,586	0,003	-0,090	-0,065	-0,109
Amplitude-θ, μV	0,096	-0,737	-0,396	0,069	0,026	-0,199	-0,107	0,019
Deviation-α, Hz	0,242	0,507	-0,294	-0,317	0,502	1,051	-0,609	-0,658
O1-β PSD, %	-0,076	-1,016	0,892	-0,099	-0,005	-0,072	0,063	-0,007
T5-β PSD, %	0,069	1,562	-0,196	-1,020	0,004	0,098	-0,012	-0,064
T5-δ PSD, %	0,440	0,342	0,036	-1,193	0,019	0,015	0,002	-0,052
Entropy PSD O2	-0,104	1,683	0,092	0,241	-0,739	12,01	0,659	1,718
T4-α PSD, %	0,233	0,640	0,596	-0,522	0,016	0,045	0,042	-0,037
F3-α PSD, %	-0,342	1,410	-1,177	1,901	-0,021	0,087	-0,072	0,117
Fp2-α PSD, %	0,089	-1,063	-0,440	-0,850	0,006	-0,072	-0,030	-0,057
P4-θ PSD, %	-0,207	1,128	1,190	-0,676	-0,050	0,275	0,290	-0,165
Entropy PSD P3	0,030	-0,323	-1,067	0,992	0,249	-2,679	-8,846	8,231
C3-δ PSD, %	-0,408	1,555	0,570	0,348	-0,022	0,083	0,030	0,019
C4-β PSD, %	0,305	0,995	0,217	0,240	0,029	0,095	0,021	0,023
Entropy PSD T3	-0,109	-0,584	0,100	-0,312	-0,865	-4,636	0,872	-2,475
O2-θ PSD, %	0,258	-0,829	-0,716	0,109	0,063	-0,203	-0,176	0,027
Entropy PSD T5	0,335	-0,732	-0,109	-0,345	2,126	-4,646	-0,692	-2,189
T4-β PSD, %	-0,290	0,187	-0,648	0,432	-0,020	+0,013	-0,044	0,029
				Constants	35,88	-15,51	14,64	2,254
				Eigenvalues	23,58	2,587	1,088	0,774
				Cumulative proportions	0,841	0,934	0,972	1

Following the algorithm, at the next stage of the analysis, the actual values of the variables were recalculated into Z-scores (Table 3.4).

Table 3.4. Correlations Variables-Canonical Roots, Means of Roots and Z-scores of Blood Pressure and EEG Variables

Variables	Correlations Variables-Roots				AH II (11)	AH I (35)	High N (13)	No-rm (16)	Low N (13)
Root 1 (84,1%)	**R 1**	**R 2**	**R 3**	**R 4**	**-8,9**	-2,1	+1,2	**+3,7**	+7,3
BP systolic	**-0,780**	0,010	-0,079	-0,090	+3,15	+1,54	+0,64	+0,03	**-0,84**
BP diastolic	**-0,162**	-0,017	-0,231	-0,098	+1,79	+1,31	+0,35	-0,19	**-1,14**

C4-β PSD	**-0,046**	-0,026	-0,164	0,184	-0,01	-0,02	+0,29	-0,35	**-0,84**
C3-β PSD	currently not in the model				+0,16	+0,08	+0,11	-0,36	**-0,83**
T4-α PSD	**-0,032**	-0,024	0,042	-0,116	+0,18	+0,02	-0,48	-0,15	**-0,31**
F3-α PSD	**-0,011**	-0,038	0,005	0,033	-0,10	-0,24	-0,20	-0,14	**-0,39**
C3-δ PSD	**0,035**	0,116	0,106	0,017	0,14	-0,01	+0,33	+0,04	**+0,92**
T5-δ PSD	**0,036**	-0,042	0,162	-0,004	+0,34	-0,03	+0,20	+0,80	**+0,84**
Deviation-δ	**0,032**	0,089	0,102	-0,256	-0,13	+0,10	-0,47	-0,05	**+0,67**
P3-δ PSD	**0,026**	0,101	0,048	-0,086	-0,02	+0,12	+0,03	-0,04	**+0,63**
Root 2 (9,3%)	**R 1**	**R 2**	**R 3**	**R 4**	+0,18	+0,25	+0,7	**-3,0**	+2,2
Entropy PSD O2	-0,028	**0,152**	-0,153	-0,027	-0,15	+0,24	+0,04	**-0,78**	-0,18
T3-β PSD	-0,014	**0,168**	-0,114	0,228	-0,15	-0,15	+0,55	**-0,79**	-0,15
T5-β PSD	-0,021	**0,109**	-0,179	0,113	-0,16	+0,15	+0,42	**-0,58**	-0,26
T4-β PSD	-0,003	**0,075**	-0,159	0,228	-0,26	-0,07	+0,64	**-0,40**	-0,24
F3-β PSD	-0,062	**0,105**	-0,202	0,114	-0,10	+0,02	+0,09	**-0,90**	-0,78
O1-β PSD	-0,068	**0,087**	-0,062	0,050	+0,37	+0,12	-0,01	**-0,70**	-0,56
F7-α PSD	-0,028	**0,116**	0,046	-0,115	+0,09	-0,03	-0,45	**-0,63**	-0,07
Deviation-α	0,019	**0,146**	-0,044	-0,173	-0,29	+0,17	-0,21	**-0,39**	+0,39
O1-θ PSD	0,011	**0,124**	0,069	-0,039	+0,05	-0,01	-0,01	**-0,26**	+0,43
O2-θ PSD	-0,001	**0,067**	-0,046	-0,023	-0,08	+0,11	+0,05	**-0,24**	+0,10
Index-α	0,021	**-0,094**	0,064	-0,037	-0,04	-0,08	-0,12	**+0,42**	+0,09
Fp2-α PSD	0,018	**-0,053**	0,003	-0,106	-0,34	-0,11	-0,39	**+0,09**	-0,07
Entropy PSD P3	-0,012	**-0,068**	-0,093	-0,005	-0,02	+0,17	+0,06	**+0,16**	-0,26
Root 3 (3,8%)	**R 1**	**R 2**	**R 3**	**R 4**	**+1,8**	-0,85	-0,85	+0,4	+1,1
Laterality-β	0,043	0,041	**-0,230**	-0,169	**-0,97**	-0,07	-0,36	-0,37	-0,16
Entropy PSD T5	-0,006	-0,070	**-0,155**	-0,093	**-0,64**	+0,05	-0,45	-0,15	-0,70
F8-θ PSD	0,013	0,072	**-0,109**	-0,250	**-0,55**	+0,30	-0,52	-0,35	+0,14
Root 4 (2,8%)	**R 1**	**R 2**	**R 3**	**R 4**	+0,4	**-0,7**	**+1,9**	0,0	-0,4
C4-θ PSD	-0,000	0,086	-0,175	**-0,286**	-0,34	**+0,59**	**-0,34**	-0,29	+0,16
P4-θ PSD	-0,024	0,094	-0,011	**-0,205**	+0,14	**+0,31**	**-0,32**	-0,30	+0,12
Fp1-θ PSD	currently not in the model				-0,16	**+0,50**	**-0,61**	-0,44	+0,06
Amplitude-θ	0,010	**-0,051**	-0,084	**-0,165**	-0,01	**+0,65**	**-0,02**	+0,57	+0,30
Entropy PSD T3	-0,057	0,012	-0,157	**-0,294**	-0,21	**+0,42**	**-0,98**	-0,70	-0,84
Entropy PSD C3	-0,023	-0,146	-0,155	**-0,227**	-0,44	**+0,27**	**-0,80**	+0,10	-0,80

The localization along the first root axis of the patients with **Low Norm** BP (Fig. 3.2) in the extreme right (positive) zone reflects combination of minimum for sampling BP levels with **maximally suppressed** PSD of beta-rhythm in C3 and C4 loci and alpha-rhythm in T4 and F3 loci. At the opposite pole of the axis of the first root, there are patients with **AH II**, whose maximum BP is accompanied by normal and, as a rule, maximum levels for the sample of the listed variables. On the other hand, **Low Norm** BP is accompanied by a **maximally increased** PSD of delta-rhythm in C3, T5 and P3 loci as well as its deviation (variability), while in patients with **AH II** such variables are again normal and, as a rule, minimal for the sample. Clusters of patients with intermediate BP levels are also characterized by intermediate levels of the listed variables. Therefore, all 5 clusters are quite clearly demarcated already in the space of the major root.

Additional demarcation of patients with **Norm BP** occurs along the axis of the second root, the bottommost position of which reflects the **maximally suppressed** entropy in O2 locus; PSD of beta-rhythm in T3, T5, T4, F3 and O1 loci; PSD of alpha-rhythm in F7 loci and its deviation; PSD of theta-rhythm in O1 and O2 loci, on the one hand, instead, **normal** and at the same time **maximal** for the sample the index and PSD of alpha-rhythm in Fp2 locus as well as entropy PSD in P3 locus.

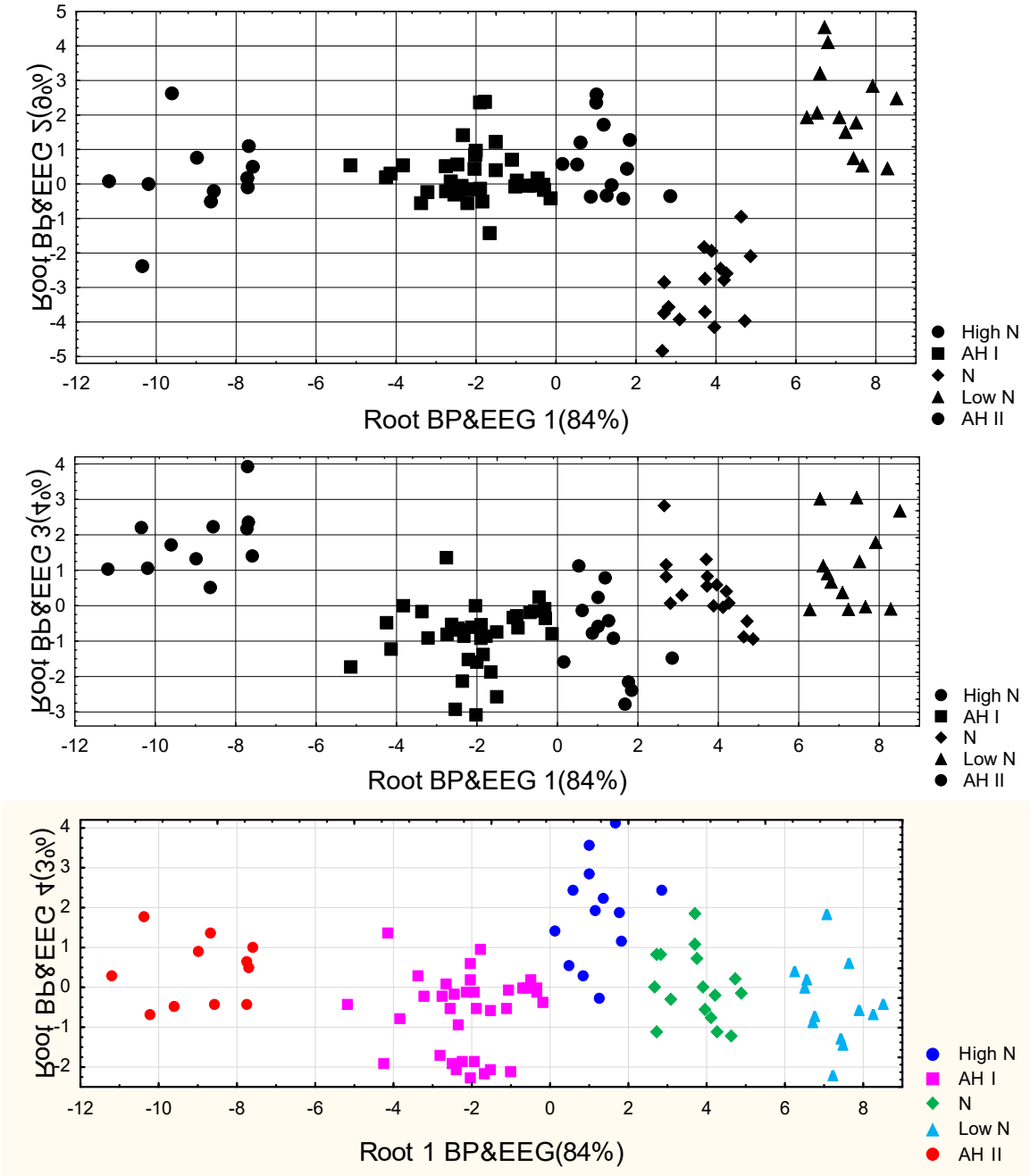

Fig. 3.1. Scattering of individual values of the discriminant BP&EEG roots of patients of different blood pressure clusters

Patients with **AH II**, in turn, are additionally distinguished from others along the axis of the third root due to a clearly expressed left lateralization of the beta rhythm, as well as **maximally suppressed** entropy in T5 locus and PSD of theta-rhythm in F8 locus.

Finally, along the axis of the fourth root, the polar positions are occupied by clusters of patients with **AH I** and **High N**, which reflects their maximum and minimum levels of theta-rhythm amplitude and its PSD in C4, P4 and Fp1 loci as well as entropy PSD in T3 and C3 loci.

In general, all clusters on the planes of four roots are clearly delineated, which is documented by calculating the Mahalanobis distances (Table 3.5).

Table 3.5. Squared Mahalanobis Distances between Blood Pressure Clusters and F-values (df=30,5; for High N-AH I $p<10^{-4}$; for High N-N $p<10^{-5}$; for rest $p<10^{-6}$)

Blood Pressure Clusters	High Norm	AH I	Norm	Low Norm	AH II
High Norm	0	**17,5**	**25,1**	**47,7**	**113**
AH I	**3,60**	0	**46,3**	**94,9**	**55,3**
Norm	**3,91**	**11,0**	0	**40,0**	**173**
Low Norm	**6,72**	**19,5**	**6,22**	0	**268**
AH II	**14,6**	**10,0**	**24,4**	**34,6**	0

The same discriminant parameters can be used to identify the belonging of one or another person to one or another cluster (Table 3.6).

Table 3.6. Coefficients and Constants for Classification Functions for BP Clusters

Blood Pressure Clusters	**High N**	**AH I**	**Norm**	**Low N**	**AH II**
Variables currently in the model	p=,148	p=,398	p=,182	p=,148	p=,125
BP systolic, mmHg	10,06	10,92	9,253	8,376	12,83
T3-β PSD, %	-0,493	-0,709	-0,570	-0,558	-0,868
Entropy PSD C3	86,15	101,6	99,44	93,23	118,8
C4-θ PSD, %	7,734	7,381	6,630	7,449	6,454
BP diastolic, mmHg	0,243	0,270	0,481	0,298	-0,228
Deviation-δ, Hz	-17,13	-15,47	-14,58	-6,104	-11,60
Laterality-β, %	0,673	0,675	0,574	0,649	0,613
F7-α PSD, %	0,228	0,187	0,199	0,755	-0,049
P3-δ PSD, %	1,880	1,746	1,581	1,855	1,464
F3-β PSD, %	1,299	1,389	1,161	1,165	1,390
Index-α, %	2,415	2,426	2,150	2,342	2,556
O1-θ PSD, %	4,560	4,771	3,573	3,968	6,362
F8-θ PSD, %	-1,359	-1,051	-0,896	-1,349	-1,348
Amplitude-θ, μV	-2,110	-2,151	-1,475	-2,496	-2,585
Deviation-α, Hz	22,69	22,20	20,48	27,56	16,39
O1-β PSD, %	-1,773	-1,704	-1,426	-1,769	-1,502
T5-β PSD, %	4,189	4,290	3,939	4,480	4,157
T5-δ PSD, %	2,412	2,473	2,504	2,674	2,291
Entropy PSD O2	194,4	187,0	145,6	204,8	194,9
T4-α PSD, %	1,481	1,498	1,476	1,812	1,458
F3-α PSD, %	4,331	4,066	3,646	3,919	4,132
Fp2-α PSD, %	-0,387	-0,229	-0,036	-0,382	-0,404
P4-θ PSD, %	1,176	1,630	0,702	2,221	2,566
Entropy PSD P3	230,9	210,6	214,9	192,1	193,8
C3-δ PSD, %	3,093	3,080	2,734	3,099	3,325
C4-β PSD, %	1,885	1,686	1,587	2,187	1,559
Entropy PSD T3	-170,6	-159,3	-149,7	-175,1	-153,3
O2-θ PSD, %	0,823	0,641	1,465	0,503	-0,223
Entropy PSD T5	-45,45	-44,81	-19,67	-35,70	-63,21
T4-β PSD, %	2,183	2,169	1,978	1,931	2,215
Constants	-1234,9	-1350,8	-1081,8	-1043,8	-1594,7

The classification accuracy is absolute (100%).

Now let's return to the announced consideration of the neuro-endocrine mechanism of BP patterns with a triplet test. First of all, retrospectively reveal the basis of the non-obvious inclusion in the factor structure of the causal HRV-Edocrine canonical root of the Henchy's test. It has been found that the duration of breath delay on exhalation is significantly determined by the EEG (Fig. 3.2 and Table 3.7) parameters, so the Henchy's test is a neurogenic marker.

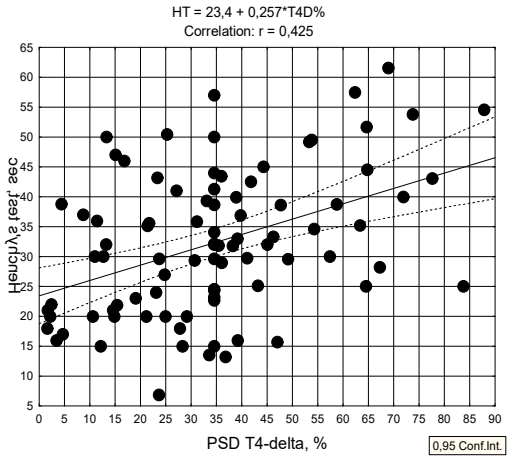

Fig. 3.2. Scatterplot of correlation between PSD of delta-rhythm in T4 locus (X-line) and Henhchy's test (Y-line)

Table 3.7. Regression Summary for Henchy's test
R=0,567; R^2=0,322; Adjusted R^2=0,272; $F_{(6,8)}$=6,4; $p<10^{-5}$

N=88		Beta	St. Err. of Beta	B	St. Err. of B	$t_{(81)}$	p-level
Variables	r		Intercpt	36,5	6,4	5,70	10^{-6}
T4-δ PSD, %	**0,43**	0,537	0,138	0,324	0,083	3,89	10^{-4}
Asymmetry-δ, %	**0,30**	0,232	0,096	0,124	0,051	2,42	0,018
P4-δ PSD, μV²/Hz	**0,23**	0,240	0,106	0,013	0,006	2,26	0,026
C4-δ PSD, %	**0,23**	-0,335	0,173	-0,211	0,109	-1,93	0,057
F3-δ PSD, %	**0,23**	-0,297	0,175	-0,170	0,100	-1,69	0,094
C3-α PSD, %	**-0,29**	-0,394	0,142	-0,300	0,108	-2,78	0,007

However, the weight of Henchy's test turned out to be insufficient to include it in the factor structure of the new causal root, expanded due to EEG parameters. According to the results of the canonical analysis, two pairs of roots were selected (Tables 3.8-3.9 and Figs. 3.3-3.4).

Table 3.8. Factor structure of first pair of EEG and BP Reactivity Roots

Left set	**R1**
Fp2-δ PSD, μV²/Hz	**0,800**
F7-δ PSD, μV²/Hz	**0,801**
F8-δ PSD, μV²/Hz	**0,614**
F4-δ PSD, μV²/Hz	**0,589**
F3-δ PSD, μV²/Hz	**0,556**
Fp1-δ PSD, %	**0,702**
HF/TP ratio, %	**0,328**
Amplitude-θ, μV	**0,302**
C4-θ PSD, μV²/Hz	**0,258**
F4-θ PSD, μV²/Hz	**0,231**
F3-θ PSD, μV²/Hz	**0,239**
C4-θ PSD, %	**0,250**
LF/HF ratio	**-0,414**
LFnu HRV, %	**-0,368**
(VLF+LF)/HF ratio	**-0,334**
Calcitonin normalized, Z	**-0,120**
F4-β PSD, %	**-0,350**
Index-β, %	**0,346**
Right set	**R1**
BPs3/BPs1 ratio	**-0,732**
BPd3/BPd1 ratio	**0,248**

BPd2/BPd1 ratio	0,203

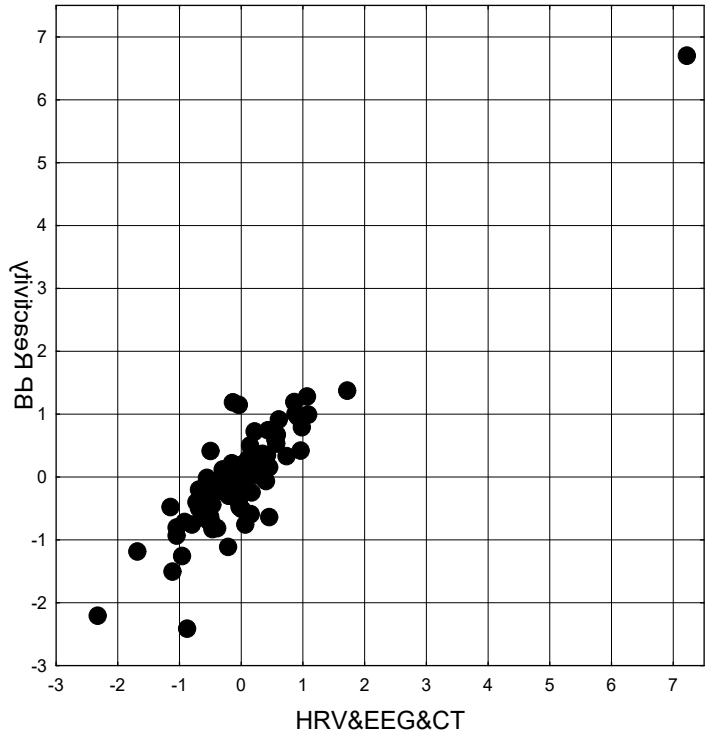

R=0,907; R^2=0,823; $\chi^2_{(80)}$=255; p<10^{-6}; Λ Prime=0,032

Fig. 3.3. Scatterplot of canonical correlation between EEG (X-line) and Blood Pressure Reactivity (Y-line) parameters. First pair of Roots

The causal neuro-endocrine root of the first pair (Table 3.8) receives significant factor loads from delta-rhythm generating nuclei and moderate loads from theta-rhythm and vagal tone generating, which together exert a downregulating influence on the Ps3/Ps1 ratio, which dominates the factor structure of effective root. Instead, sympathetic tone and calcitonin have the upregulating effect. The minor components of the effective root are subject to the downregulating influence of the beta-rhythm generating nuclei, which are projected on the F4 locus, but upregulation by the beta-rhythm index.

Taken together, neuro-endocrine factors determine BP reactivity on 82% (Fig. 3.3).

The factor structure of the effective root of the second pair (Table 3.9) is dominated by the Pd2/Pd1 and Pd3/Pd1 ratio. Entropy PSD in Fp2 locus and variability of beta-rhythm were added to their downregulating factors. The Ps2/Ps1 ratio is subject to the downregulating influence of the same theta-rhythm generating nuclei as the Ps3/Ps1 ratio, instead, the same delta-rhythm generating nuclei exert an upregulating influence on the Ps2/Ps1 ratio. Such a constellation of neuro-endocrine factors determines BP reactivity on 59% (Fig. 3.4).

Table 3.9. Factor structure of second pair of EEG and BP Reactivity Roots

Left set	R2
Index-β, %	-0,595
Entropy PSD Fp2	-0,557
Deviation-β, Hz	-0,472
Calcitonin normalized, Z	-0,185
F4-β PSD, %	0,484
F7-δ PSD, μV^2/Hz	0,416
Fp2-δ PSD, μV^2/Hz	0,377
Fp1-δ PSD, %	0,358
F8-δ PSD, μV^2/Hz	0,357
Amplitude-θ, μV	-0,383

C4-θ PSD, μV²/Hz	-0,390
F4-θ PSD, μV²/Hz	-0,326
F3-θ PSD, μV²/Hz	-0,302
C4-θ PSD, %	-0,266
Right set	**R2**
BPd2/BPd1 ratio	-0,851
BPd3/BPd1 ratio	-0,402
BPs2/BPs1 ratio	0,662

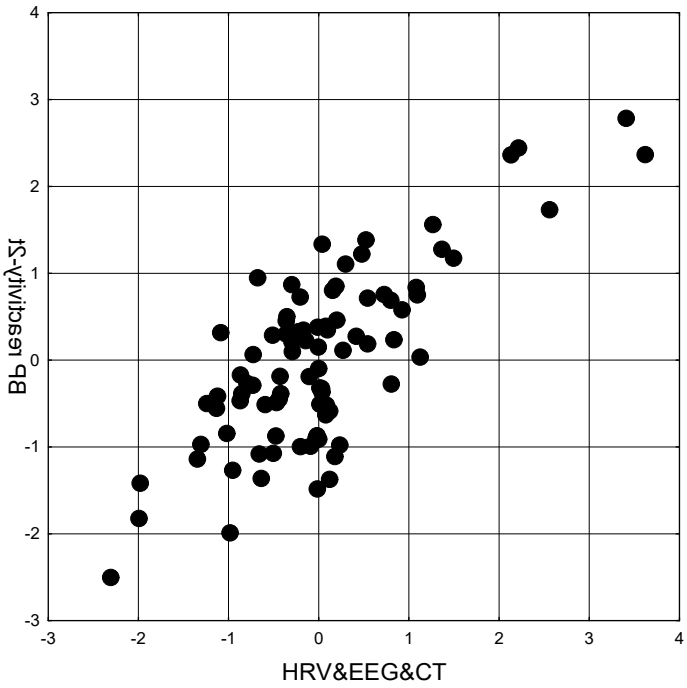

R=0,766; R^2=0,587; $\chi^2_{(57)}$=126; p<10^{-6}; Λ Prime=0,184

Fig. 3.4. Scatterplot of canonical correlation between EEG (X-line) and Blood Pressure Reactivity (Y-line) parameters. Second pair of Roots

Based on the analyses and results presented in this Chapter, here is a detailed evaluation of the hypotheses and their verification.

1. Hypothesis. Significant correlations exist between blood pressure levels and various EEG parameters across different brain regions and frequency bands. Verification. Confirmed. The study found significant correlations between blood pressure and various EEG parameters, including power spectral density in different frequency bands and brain regions. Null hypothesis rejected. The null hypothesis of no correlation was rejected in favor of the alternative hypothesis of significant correlations.

2. Hypothesis. It is possible to identify distinct groups of patients characterized by different blood pressure profiles and corresponding EEG patterns. Verification. Confirmed. The study successfully identified five distinct clusters of patients based on blood pressure and EEG parameters. Null hypothesis rejected. The null hypothesis of no distinct clusters was rejected in favor of the alternative hypothesis of distinct patient groups.

3. Hypothesis. A specific set of EEG parameters significantly discriminates between different blood pressure clusters. Verification. Confirmed. The discriminant analysis identified 30 EEG parameters that significantly differentiated between blood pressure clusters. Null hypothesis rejected. The null hypothesis of no differentiating parameters was rejected.

4. Hypothesis. There are significant differences in EEG profiles across the spectrum of blood pressure categories. Verification. Confirmed. The study found distinct EEG profiles for different blood pressure categories, from low normal to hypertension II. Null hypothesis

rejected. The null hypothesis of no differences was rejected in favor of the alternative hypothesis of significant differences across categories.

5. Hypothesis. EEG entropy measures show significant correlations with blood pressure levels. Verification. Confirmed. The study included 5 entropy parameters in the discriminant model, indicating their significance in differentiating blood pressure clusters. Null hypothesis rejected. The null hypothesis of no correlation was rejected.

6. Hypothesis. Different EEG frequency bands show distinct patterns of association with blood pressure levels. Verification. Confirmed. The study found different patterns of association for delta, theta, alpha, and beta bands with blood pressure levels. Null hypothesis rejected. The null hypothesis of no distinct patterns was rejected.

7. Hypothesis. EEG laterality and asymmetry measures are significantly associated with blood pressure levels. Verification. Partially confirmed. The study included laterality of beta rhythm in the discriminant model, suggesting some association with blood pressure levels. Null hypothesis partially rejected. The null hypothesis was rejected for some laterality measures but not comprehensively for all asymmetry patterns.

8. Hypothesis. It is possible to create a model that accurately classifies patients into blood pressure clusters using EEG parameters. Verification. Confirmed. The classification functions derived from discriminant analysis achieved 100% accuracy. Null hypothesis rejected. The null hypothesis of no predictive model was strongly rejected in favor of the alternative hypothesis of an accurate classification model.

9. Hypothesis. There are significant interactions between EEG parameters and other physiological measures in their association with blood pressure. Verification. Not directly addressed in this chapter. This hypothesis would require integration with results from other chapters. Null hypothesis. Neither rejected nor accepted based on the information in this chapter alone.

10. Hypothesis. Certain EEG parameters or patterns can serve as biomarkers for hypertension risk or severity. Verification. Partially confirmed. The study identified several EEG parameters strongly associated with different blood pressure levels, suggesting potential biomarkers. Null hypothesis partially rejected. The null hypothesis was rejected for some EEG parameters, but further validation would be needed to establish them as definitive biomarkers.

While these hypotheses were not explicitly stated in the chapter, they are inferred from the analyses conducted and the results presented. The exploratory nature of the study allowed for the discovery of these relationships without formal a priori hypothesis testing.

Conclusions

Based on a thorough review of this Chapter, here are the detailed conclusions drawn from the study.

1. EEG Parameter Selection. The forward stepwise discriminant analysis identified 30 EEG parameters as characteristic of quantitative-qualitative blood pressure clusters. These parameters included 5 entropy measures, 4 delta-rhythm, 6 theta-rhythm, 6 alpha-rhythm, and 7 beta-rhythm parameters.

2. Most Informative EEG Parameters. Power Spectral Density (PSD) of beta-rhythm in C3 and C4 loci. PSD of alpha-rhythm in T4 and F3 loci. PSD of delta-rhythm in C3, T5, and P3 loci. Deviation of delta-rhythm.

3. Classification Accuracy. The discriminant model achieved 100% classification accuracy, indicating a strong relationship between EEG parameters and blood pressure clusters.

4. Blood Pressure Clusters and EEG Characteristics.

a) Low Normal BP Cluster. Characterized by maximally suppressed PSD of beta-rhythm in C3 and C4 loci. Maximally suppressed PSD of alpha-rhythm in T4 and F3 loci. Maximally increased PSD of delta-rhythm in C3, T5, and P3 loci. Maximally increased delta-rhythm deviation.

b) Arterial Hypertension II Cluster. Showed opposite patterns to the Low Normal BP cluster. Normal or maximal levels of beta and alpha PSD in specific loci. Minimal levels of delta PSD and its deviation.

c) Intermediate BP Clusters. Characterized by intermediate levels of the aforementioned EEG parameters.

5. Secondary Discriminating Factors. The second discriminant root provided additional separation, particularly for the Normal BP cluster. This cluster showed maximally suppressed entropy in O2 locus, PSD of beta-rhythm in various loci, and other specific EEG patterns.

6. Lateralization Findings. Patients with Arterial Hypertension II showed a clearly expressed left lateralization of the beta rhythm.

7. Theta Rhythm Patterns. Clusters of patients with Arterial Hypertension I and High Normal BP showed distinct patterns in theta-rhythm amplitude and its PSD in specific loci.

8. EEG Entropy. EEG entropy measures in various loci (C3, O2, P3, T3, T5) were found to be significant discriminators between blood pressure clusters.

9. Frequency Band Specificity. Different frequency bands (delta, theta, alpha, beta) showed distinct patterns of association with blood pressure levels across various brain regions.

10. Spatial Distribution of EEG Effects. The study revealed that EEG changes associated with blood pressure are not uniformly distributed across the scalp but show specific spatial patterns.

11. Potential Neural Mechanisms. The findings suggest involvement of various brain regions and neural networks in blood pressure regulation, including cortical and subcortical structures.

12. Methodological Robustness. The study demonstrated the effectiveness of using discriminant analysis to comprehensively analyze complex EEG data in relation to blood pressure.

13. Clinical Implications. The strong association between EEG parameters and blood pressure clusters suggests potential for using EEG as a tool in hypertension assessment or risk prediction.

14. Limitations. The study was observational and cross-sectional, limiting causal inferences. The sample size, while adequate for the analyses performed, may limit the generalizability of some findings.

15. Future Research Directions. The study opens avenues for further research into the neurophysiological mechanisms underlying the observed relationships between EEG patterns and blood pressure. Longitudinal studies could help elucidate the temporal dynamics of these relationships. Validation of the EEG-based classification model in larger, diverse populations is needed.

This chapter provides a comprehensive characterization of the electroencephalographic accompaniments of different blood pressure profiles in patients at Truskavets' spa. It demonstrates complex relationships between brain activity patterns and blood pressure regulation, suggesting potential neural mechanisms involved in hypertension. The findings lay a foundation for future studies to further elucidate these relationships and potentially translate them into novel diagnostic or prognostic tools in cardiovascular health management.

Thus, a wide range of blood pressure in Truskavets’ spa patients is accompanied by an equally wide range of EEG and HRV parameters and adaptive hormones. For the first time, we found close relationships between the parameters of HRV ECG and Blood Pressure Reactivity during the triplet test.

Chapter 4

IMMUNE ACCOMPANIMENT OF QUANTITATIVE-QUALITATIVE BLOOD PRESSURE CLUSTERS

Abstract

Background. Earlier we studied the neural and endocrine accompaniments of quantitative-qualitative blood pressure (BP) clusters of profile patients of Truskavets' spa. The **purpose** of this study is to clarify the immune accompaniment in the same contingent. **Materials and methods.** Under an observations were 44 patients with chronic pyelonephritis and cholecystitis in the phase of remission. Testing was performed twice - on admission and after 7-10 days of standard balneotherapy. We determined in the blood the relative content of leukocyte forms, of T-lymphocytes and their killer, helper and regulatory subpopulations as well as NK- and B-lymphocytes; in serum - the concentration of C-reactive protein, Tumor Necrosis Factor-α, Interleukins 1β and 6, immunoglobulins classes G, A, and M as well as circulating immune complexes; in saliva - IgG, IgA, and secretory IgA. In addition, we determined parameters of phagocytosis by neutrophils of *Staph. aureus* and *E. coli*; components of stool and urine microbiota. **Results**. The forward stepwise program identified 18 parameters as characteristic of quantitative-qualitative blood pressure clusters. In addition to BP parameters by default, the most informative among them are serum levels of IL-6 and TNF-α as well as activity and intensity of phagocytosis by neutrophils of *Staph. aureus*. The accuracy of patient classification is 96,6%. **Conclusion**. The quantitative-qualitative blood pressure clusters have a characteristic immune accompaniment.

Keywords: blood pressure, immunity, discriminant analysis, Truskavets' spa.

Earlier we showed that profile patients of Truskavets' spa are characterized by a wide range of blood pressure - from low norm to arterial hypertension II - that correspond to the hemodynamic and neuro-endocrine parameters. It is well known about the close relationships between the nervous, endocrine and immune systems within the framework of the triune neuro-endocrine-immune complex, which are carried out through neurotransmitters, hormones and cytokines, which are simultaneously released by neurons, endocrinocytes and immunocytes [Besedovsky H & Sorkin E, 1977; Besedovsky H & del Rey A, 1996; Nance DM & Sanders VM, 2007; Tracey KJ, 2007; Thayer JF & Sternberg EM, 2010; Chavan SS et al., 2017; Pavlov VA et al., 2018; Korneva EA, 2020]. By the way, this concept is cornerstone of Truskavetsian Scientific School of Balneology [Popovych IL, 2009; Popovych IL, 2011; Popovych IL et al., 2020; Popovych IL et al., 2022; Popovych IL et al., 2023].

Therefore, the purpose of this chapter is to clarify the immune accompaniments of quantitative-qualitative blood pressure clusters in the same contingent.

In this Chapter, the following research problems and corresponding hypotheses can be inferred.

1. Research problem. Can distinct blood pressure clusters be identified based on immune parameters? Hypothesis. It is possible to identify distinct groups of patients characterized by different blood pressure profiles and corresponding immune patterns.

2. Research problem. Which immune parameters best differentiate between blood pressure clusters? Hypothesis. A specific set of immune parameters significantly discriminates between different blood pressure clusters.

3. Research problem. How do immune profiles differ across various blood pressure categories (from low normal to hypertension II)? Hypothesis. There are significant differences in immune profiles across the spectrum of blood pressure categories.

4. Research problem. Can a predictive model be developed for blood pressure cluster membership based on immune parameters? Hypothesis. It is possible to create a model that accurately classifies patients into blood pressure clusters using immune parameters.

The study appears to have an exploratory nature, which explains the lack of formally stated hypotheses at the beginning of the chapter. The research aims to uncover the immunological accompaniments of different blood pressure profiles, potentially providing new insights into the immune correlates of blood pressure regulation and hypertension.

Immune status evaluated as described in the manuals [Khaitov RM et al., 1995; Lapovets' LY & Lutsyk BD, 2002]. For phenotyping subpopulations of lymphocytes used the methods of rosette formation with sheep erythrocytes on which adsorbed monoclonal antibodies against receptors CD3, CD4, CD8, CD25, CD22 and CD56 from company "Granum" (Kharkiv) with visualization under light microscope with immersion system. Subpopulation of T cells with receptors high affinity determined by test of "active" rosette formation. The state of humoral immunity judged by the concentration in serum of Immunoglobulins of classes G, A, M (ELISA, analyser "Immunochem", USA) and circulating immune complexes (by polyethylene glycol precipitation method) as well as C-reactive protein (by the ELISA with the use of analyzer "RT-2100C"), Tumor Necrosis Factor-α, Interleukins 1β and 6 (ELISA, analyzer "Stat Fax 303", USA, reagents from "Vector-Best", RF).

Based on the normalized values of humoral (5 parameters) and cellular (4 parameters) links, the integral index of immunity was calculated as the average of nine Z-scores.

The set of immune parameters of saliva was IgG, IgA, and secretory IgA (ELISA, analyser "Immunochem", USA).

In portion of the capillary blood we counted up Leukocytogram and calculated the Entropy (h) of Leukocytogram (LCG) as well as its Strain Index using equations [Popovych IL, 2007; Popovych IL, 2022]:

$$hLCG = - [L \bullet \log_2 L + M \bullet \log_2 M + E \bullet \log_2 E + SNN \bullet \log_2 SNN + StubN \bullet \log_2 StubN]/\log_2 5;$$

$$\text{Strain Index-1} = [(Eos/3,5\text{-}1)^2 + (StubN/3,5\text{-}1)^2 + (Mon/5,5\text{-}1)^2 + (Leuk/6\text{-}1)^2]/4.$$

Parameters of phagocytic function of neutrophils estimated as described by Kovbasnyuk MM [Kul'chyns'kyi AB, Kovbasnyuk MM et al., 2016; Popovych IL et al., 2018]. The objects of phagocytosis served daily cultures of *Staphylococcus aureus* (ATCC N 25423 F49) as typical specimen for Gram-positive Bacteria and *Escherichia coli* (O55 K59) as typical representative of Gram-negative Bacteria. Take into account the following parameters of Phagocytosis: activity (percentage of neutrophils, in which found microbes - Hamburger's Phagocytic Index PhI), intensity (number of microbes absorbed one phagocytes - Microbial Count MC or Right's Index) and completeness (percentage of dead microbes - Killing Index KI). On the basis of the registered partial parameters of phagocytosis, taking into account the content of neutrophils (N) in 1 L of blood, the integral parameter such as the BacteriCidal Capacity of Neutrophils was calculated by the equation:

$$BCCN\ (10^9\ Bact/L) = N\ (10^9/L) \bullet PhI\ (\%) \bullet MC\ (Bact/Phag) \bullet KI\ (\%) \bullet 10^{-4}.$$

The condition of Microbiota was evaluated on the results of sowing of feces. The levels of Bacteriuria, Leukocyturia, and Erythrocyturia were also assessed by routine methods.

Reference values of variables are taken from the database of the Truskavetsian Scientific School of Balneology.

In order to identify among the registered parameters, those for which the blood pressure clusters differ from each other, a discriminant analysis was performed. The program forward stepwise included in the discriminant model 18 parameters. In addition to BP parameters by default, the following variables were identified as characteristic: 2 **proinflammatory cytokines**, 6 immune parameters of **blood** and **saliva**, 5 parameters of **phagocytosis**, 2 markers of **pyelonephritis** as well as strain index of leukocytogram. A number of parameters

that were found to be outside the discriminant model are also worthy of attention (Tables 4.1 and 4.2).

Table 4.1. Discriminant Function Analysis Summary for Immune Variables, their actual levels (Mean±SE) for Clusters as well as Reference levels and Coefficients of Variability
Step 18, N of vars in model: 18; Grouping: 5 grs; Wilks' Λ: 0,0155; approx. $F_{(72)}$=6,85; $p<10^{-6}$

Variables currently in the model	Clusters of Blood Pressure (n)					Parameters of Wilk's Statistics						
	AH II (11)	AH I (35)	High N (13)	No-rm (16)	Low N (13)	Wilks' Λ	Par-tial Λ	F-re-move (4,66)	p-level	Tole-rancy	Refe-rence (44)	Cv
BP Systolic, mmHg	172 2,5	148 0,9	134 0,8	125 0,6	112 1,0	0,166	0,094	159	10^{-6}	0,658	124,5 2,3	,122
BP Diasto-lic, mHg	90,7 4,5	87,6 1,2	81,3 1,5	77,8 1,5	71,5 1,5	0,017	0,911	1,61	0,181	0,697	79,0 1,0	,086
Interleukin-6, ng/L	7,22 0,76	4,62 0,55	4,76 0,91	3,64 0,81	4,61 0,88	0,019	0,802	4,08	0,005	0,368	4,25 0,21	,324
TNF-α, ng/L	6,94 0,42	6,06 0,25	6,29 0,60	5,15 0,46	5,97 0,33	0,019	0,839	3,17	0,019	0,355	4,90 0,24	,326
Immunity Integral Ind	0,24 0,13	-0,15 0,08	0,10 0,12	0,01 0,13	0,24 0,15	0,020	0,788	4,43	0,003	0,276	0 0,30	**SD 2**
CIC, units	42 6	34 2	30 3	34 4	43 5	0,017	0,926	1,32	0,270	0,784	45 2,6	,389
IgA Serum, g/L	2,03 0,05	1,58 0,09	1,91 0,14	1,78 0,11	1,92 0,12	0,017	0,906	1,71	0,158	0,404	1,875 0,05	,167
Secretory IgA, mg/L	505 20	491 9	464 20	495 17	504 13	0,018	0,882	2,21	0,077	0,400	622 14	,153
IgA Saliva, mg/L	149 9	123 5	136 10	133 10	156 12	0,017	0,889	2,05	0,097	0,328	163 6	,241
Rod shaped Neutrop, %	2,85 0,38	2,40 0,17	3,10 0,36	2,64 0,27	2,80 0,25	0,017	0,904	1,75	0,150	0,497	4,25 0,09	,147
Monocytes, %	5,05 0,48	6,55 0,36	6,39 0,55	5,38 0,49	5,15 0,61	0,016	0,951	0,85	0,500	0,614	5,50 0,11	,186
Popovych's Strain Ind-1	0,11 0,02	0,18 0,02	0,14 0,02	0,16 0,03	0,11 0,02	0,017	0,936	1,13	0,351	0,613	0,10 0,01	,559
Phag Ind vs *St. aur.*, %	98,5 0,34	98,62 0,24	99,34 0,21	99,2 0,19	98,91 0,32	0,018	0,883	2,19	0,080	0,370	98,3 0,27	,018
Killing vs *St. aur.*, %	46,1 1,5	49,6 1,4	53,8 3,0	47,3 2,3	50,4 1,8	0,018	0,856	2,78	0,034	0,348	58,9 1,3	,142
Mic Cou *St. aur.*, B/Ph	59,7 1,9	61,3 1,6	63,2 1,9	64,1 1,9	63,9 1,9	0,017	0,929	1,27	0,292	0,398	61,6 1,5	,160
Phagoc Ind vs *E. coli*,%	99,2 0,18	98,62 0,26	99,61 0,18	98,9 0,47	99,38 0,18	0,017	0,929	1,27	0,291	0,336	98,3 0,27	,012
Leukocytu-ria, lgL/mL	3,75 0,16	3,35 0,10	3,12 0,23	3,35 0,18	3,28 0,19	0,018	0,860	2,69	0,038	0,429	3,00 0,03	,070
Erhytrocyt-uria, lg/mL	2,99 0,10	3,07 0,04	3,05 0,07	3,06 0,11	3,02 0,09	0,017	0,939	1,08	0,376	0,691	2,70 0,03	,078
Variables currently't in model	**AH II (11)**	**AH I (35)**	**High N (13)**	**No-rm (16)**	**Low N (13)**	Wilks' Λ	Par-tial Λ	F to enter	p-level	Tole-rancy	Refe-rence (88)	Cv
C-Reactive Prot., µg/L	2,92 0,18	2,54 0,11	2,64 0,26	2,14 0,20	2,50 0,15	0,015	0,956	0,752	0,560	0,274	2,18 0,11	,324
$CD4^+CD25^+$ T-regul., %	18,8 1,1	21,1 0,6	19,1 1,1	20,8 1,2	17,6 1,3	0,015	0,977	0,378	0,823	0,386	16,4 0,4	,153
$CD4^+$ T-hel-per Lym, %	33,7 1,9	27,4 1,0	33,1 1,9	30,5 2,2	35,9 2,6	0,015	0,968	0,544	0,704	0,052	39,5 0,9	,164
Bifidobacte-ria,lgCFU/g	5,35 0,30	5,69 0,19	5,78 0,24	5,52 0,36	5,38 0,35	0,015	0,978	0,367	0,832	0,468	6,94 0,01	,011
Lactobacilli lg CFU/g	6,00	6,48	6,69	6,22	6,09	0,015	0,978	0,368	0,831	0,432	8,10	,015

	0,38	0,23	0,26	0,45	0,45						0,02	
***E. coli* com., lg CFU/g**	8,16 0,06	8,30 0,04	8,33 0,07	8,26 0,07	5,24 0,09	0,015	0,987	0,206	0,934	0,415	8,66 0,06	,045

Table 4.2. Summary of Stepwise Analysis for Variables, ranked by criterion Lambda

Variables currently in the model	F to enter	p-level	**Λ**	F-value	p-value
BP Systolic, mmHg	298	10^{-6}	0,065	298	10^{-6}
Immunity Integral Index	3,83	0,007	0,055	67,0	10^{-6}
Monocytes, %	2,13	0,084	0,050	37,8	10^{-6}
Interleukin-6, ng/L	2,52	0,047	0,044	27,2	10^{-6}
Leukocyturia, lgLeu/mL	1,49	0,213	0,041	21,3	10^{-6}
Circulating Immune Complex, units	1,65	0,170	0,038	17,7	10^{-6}
Tumor Necrosis Factor-α, ng/L	1,35	0,260	0,035	15,2	10^{-6}
BP Diastolic, mHg	1,59	0,186	0,033	13,5	10^{-6}
Rod shaped Neutrophils, %	1,61	0,180	0,030	12,2	10^{-6}
Killing Index vs *Staph. aureus*, %	1,47	0,220	0,028	11,1	10^{-6}
IgA Serum, g/L	1,48	0,217	0,026	10,2	10^{-6}
Phagocytose Index vs *St. aureus*, %	1,49	0,213	0,024	9,55	10^{-6}
Secretory IgA Saliva, g/L	1,54	0,200	0,022	8,97	10^{-6}
IgA Saliva, g/L	1,44	0,229	0,020	8,47	10^{-6}
Popovych's Strain Index-1	1,28	0,288	0,019	8,00	10^{-6}
Microbian Count for *St. aureus*, B/Ph	1,09	0,367	0,018	7,57	10^{-6}
Phagocytose Index vs *E. coli*, %	1,13	0,351	0,017	7,19	10^{-6}
Erhytrocyturia, lgEr/mL	1,08	0,376	0,016	6,85	10^{-6}

Next, the 18-dimensional space of discriminant variables transforms into 4-dimensional space of a canonical roots. For Root 1 r*=0,976 (Wilks' Λ=0,0155; $\chi^2_{(72)}$=314; p<10^{-6}), for Root 2 r*=0,637 (Wilks' Λ=0,330; $\chi^2_{(51)}$=84; p=0,003), for Root 3 r*=0,572 (Wilks' Λ=0,556; $\chi^2_{(32)}$=44; p=0,072), and for Root 4 r*=0,416 (Wilks' Λ=0,827; $\chi^2_{(15)}$=14; p=0,498). The first root contains 93,6% of discriminative opportunities, the second 3,2%, the third 2,2%, the last 1,0% only, therefore will be ignored in the future.

Table 4.3 presents raw and standardized coefficients for discriminant variables, which are used for the calculation of the discriminant root values for each person, which enables the visualization of each patient in the information space of the roots (Figs. 4.2 and 4.3).

Table 4.3. Standardized and Raw Coefficients and Constants for Variables

Coefficients	**Standardized**			**Raw**		
Variables currently in the model	Root 1	Root 2	Root 3	Root 1	Root 2	Root 3
BP Systolic, mmHg	-1,202	-0,003	-0,049	-0,248	-0,001	-0,010
Immunity Integral Index	-0,363	-0,817	0,860	-0,675	-1,518	1,599
Monocytes, %	0,113	0,339	-0,223	0,055	0,166	-0,109
Interleukin-6, ng/L	-0,481	-0,796	0,245	-0,192	-0,318	0,098
Leukocyturia, lg Leu/mL	-0,578	-0,043	-0,133	-0,878	-0,065	-0,203
Circulating Immune Complex, units	0,022	-0,250	-0,059	0,001	-0,016	-0,004
Tumor Necrosis Factor-α, ng/L	0,354	0,583	-0,683	0,218	0,359	-0,421
BP Diastolic, mmHg	0,299	0,319	-0,022	0,038	0,040	-0,003
Rod shaped Neutrophils, %	0,198	0,498	-0,386	0,181	0,457	-0,354
Killing Index vs *Staph. aureus*, %	-0,097	0,414	-0,992	-0,012	0,049	-0,117
IgA Serum, g/L	0,260	0,078	-0,711	0,566	0,169	-1,547
Phagocytose Index vs *St. aureus*, %	-0,279	0,439	0,445	-0,241	0,379	0,384
Secretory IgA Saliva, mg/L	0,0004	-0,291	0,883	0,00001	-0,005	0,015
IgA Saliva, mg/L	0,113	-0,348	-0,803	0,003	-0,010	-0,024
Popovych's Strain Index-1	0,141	0,402	0,208	1,293	3,682	1,901
Microbian Count for *St. aureus*, B/Ph	0,199	0,100	-0,597	0,024	0,012	-0,073
Phagocytose Index vs *E. coli*, %	0,247	0,245	-0,614	0,184	0,183	-0,458
Erythrocyturia, lg Er/mL	0,303	-0,050	-0,005	0,977	-0,162	-0,015

	Constants	32,830	-61,01	22,48
	Eigenvalues	20,25	0,683	0,487
	Cumulative proportions	0,936	0,968	0,990

Table 4.4 shows the correlation coefficients of blood pressure and immune parameters with canonical discriminant roots; the cluster centroids of roots; and Z-scores of the variables.

Table 4.4. Correlations Variables-Canonical Roots, Means of Roots and Z-scores of Blood Pressure and Immune Variables

Variables currently in the model	Correlations Variables-Roots			AH II (11)	AH I (35)	High N (13)	Norm (16)	Low N (13)
Root 1 (93,6%)	**R 1**	**R 2**	**R 3**	**-8,5**	-1,8	+1,5	+3,3	**+6,6**
BP Systolic	**-0,840**	0,254	-0,064	**+3,15**	+1,54	+0,64	+0,04	**-0,84**
BP Diastolic	**-0,174**	0,320	0,087	**+1,79**	+1,31	+0,35	-0,19	**-1,14**
Interleukin-6	**-0,063**	-0,193	-0,204	**+2,16**	+0,27	+0,37	-0,44	+0,26
Tumor Necrosis Factor-α	**-0,049**	-0,063	-0,307	**+1,28**	+0,73	+0,87	+0,15	+0,67
C-Reactive Protein				**+1,05**	+0,57	+0,65	-0,05	+0,45
Phagocytose Index vs *St. aureus*	**0,040**	0,024	-0,070	**+0,14**	+0,18	+0,59	+0,53	+0,35
Microbial Count for *Staph. aur.*	**0,041**	-0,008	0,012	**-0,19**	-0,03	+0,16	+0,26	+0,23
Root 2 (3,2%)	**R 1**	**R 2**	**R 3**	**-1,4**	+0,6	+0,7	-0,3	**-1,0**
IgA Saliva	0,022	**-0,384**	-0,242	**-0,36**	-1,03	-0,68	-0,77	**-0,17**
Secretory IgA Saliva	-0,005	**-0,193**	0,150	**-1,23**	-1,38	-1,66	-1,34	**-1,24**
Immunity Integral Index	0,003	**-0,363**	-0,314	**+0,24**	-0,15	+0,10	-0,01	**+0,24**
IgA Serum	0,005	**-0,337**	-0,298	**+0,50**	-0,94	+0,13	-0,31	**+0,13**
Circulating Immune Complex	-0,001	**-0,309**	-0,017	**-0,17**	-0,62	-0,84	-0,60	**-0,11**
CD4⁺ T-helper Lymphocytes				**-0,89**	-1,87	-0,99	-1,39	**-0,55**
CD4⁺CD25⁺ T-regulatory Lym				**+0,95**	+1,85	+1,07	+1,74	**+0,47**
Monocytes	-0,013	**0,383**	-0,035	**-0,60**	+1,40	+1,19	-0,16	**-0,47**
Popovych's Strain Index-1	-0,002	**0,263**	0,197	**+0,18**	+1,43	+0,86	+1,18	**+0,26**
Erythrocyturia	0,005	**0,105**	0,060	**+1,12**	+1,46	+1,38	+1,42	**+1,25**
***Lactobacilli* feces**				**-1,45**	-1,12	-0,97	-1,29	**-1,38**
***Bifidobacteria* feces**				**-1,39**	-1,10	-1,02	-1,25	**-1,37**
Root 3 (2,2%)	**R 1**	**R 2**	**R 3**	-0,3	+0,3	**-1,2**	+1,0	-0,4
Phagocytose Index vs *E. coli*	0,021	-0,132	**-0,327**	+0,75	+0,27	**+1,11**	+0,50	+0,92
Killing Index vs *Staph. aureus*	0,026	0,192	**-0,279**	-1,53	-1,11	**-0,60**	-1,37	-1,01
Rod shaped Neutrophils	0,010	-0,103	**-0,249**	-2,24	-2,96	**-1,85**	-2,57	-2,32
***Escherichia coli* feces**				-1,27	-0,93	**-0,85**	-1,02	-1,07
Leukocyturia	-0,043	-0,196	**0,108**	+1,49	+0,70	**+0,23**	+0,71	+0,56

The clear separation of the AH II cluster along the axis of the major root reflects the accompaniment of maximum BP levels by elevated levels of pro-inflammatory cytokines and normal, but minimal for the sample, activity and intensity of phagocytosis of gram-positive bacteria (Table 4.4 and Fig. 4.2).

A cluster of patients with minimal BP is located at the opposite pole of the axis of the major root. However, the other variables mentioned are not min/max (extreme) for the sample. However, both extreme clusters are separated from the other three along the axis of the second root. Their lowest localization reflects their normal, but minimal for the sample, levels of serum and saliva IgA, circulating immune complexes, integral immunity index as well as maximally reduced levels of salivary secretory IgA and blood T-helper subpopulations - on the one hand, while minimally increased levels of regulatory T-lymphocytes and Erythrocyturia, normal, but minimal for the sample Leukocytary Strain-index as well as maximally reduced levels of Monocytes in the blood and probiotics in the intestines/feces - on the one hand.

Finally, patients with High Norm BP are distinguished from others along the axis of the third root. Their lowest localization reflects a minimally reduced blood level of Rod shaped

Neutrophils and a minimally reduced Bactericidal activity of neutrophils against *Staphylococcus aureus* as well as a maximally increased Activity of phagocytosis by blood neutrophils of *Escherichia coli* and a minimally reduced content of the latter in the intestines/feces. This is accompanied by the minimum for the sample Leukocyturia level.

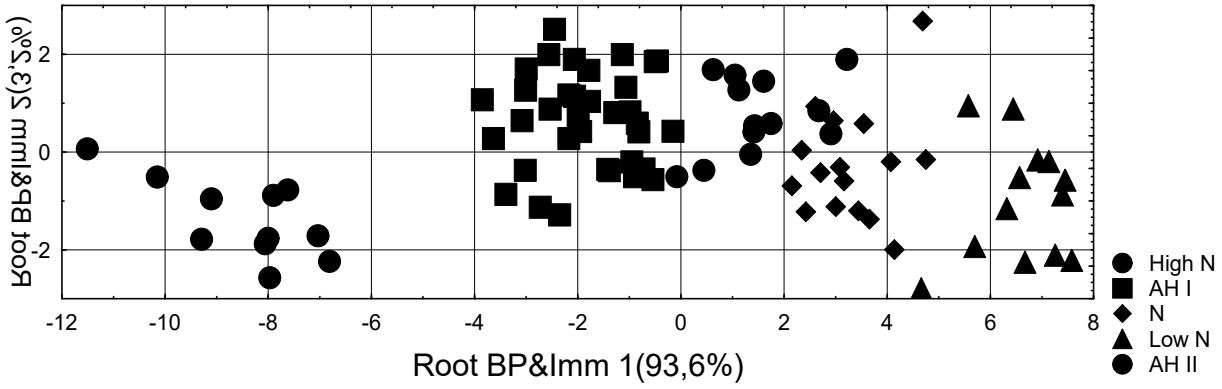

Fig. 4.2. Scattering of individual values of the first&second discriminant roots of patients of different blood pressure clusters

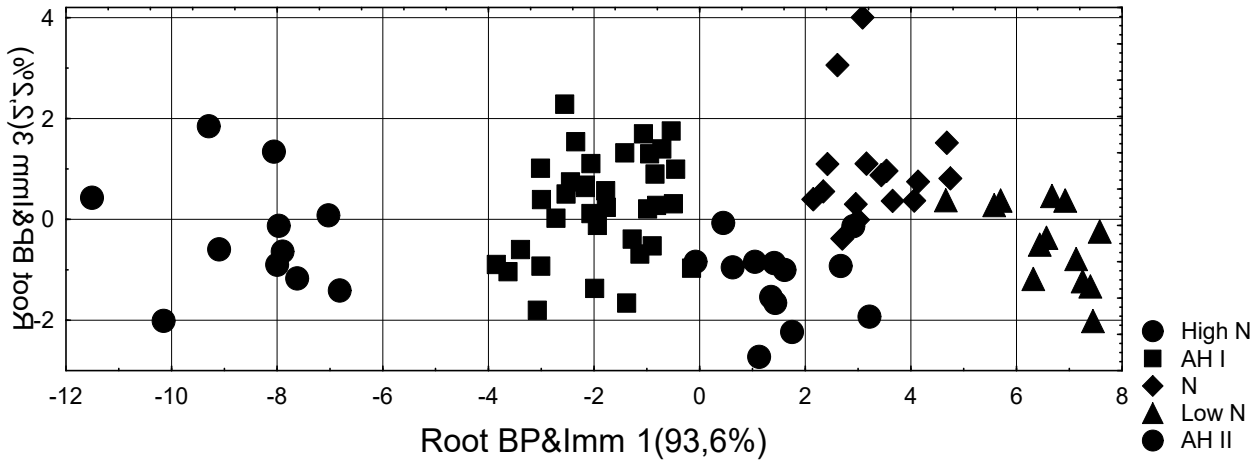

Fig. 4.3. Scattering of individual values of the first&third discriminant roots of patients of different blood pressure clusters

In general, all clusters on the planes of three roots are clearly delineated, which is documented by calculating the Mahalanobis distances (Table 4.5).

Table 4.5. Squared Mahalanobis Distances between Blood Pressure Clusters and F-values (df=18,7; for High N-N $p<10^{-3}$; for Low N-N $p<10^{-5}$; for other pairs $p<10^{-6}$)

Blood Pressure Clusters	High Norm	AH I	Norm	Low Norm	AH II
High Norm	0	**14,2**	**9,07**	**30,8**	**105**
AH I	**5,94**	0	**28,6**	**74,5**	**48,8**
Norm	**2,87**	**13,9**	0	**14,7**	**142**
Low Norm	**8,83**	**31,2**	**4,31**	0	**228**
AH II	**27,7**	**18,0**	**40,4**	**40,9**	0

The same discriminant parameters can be used to identify the belonging of one or another person to one or another blood pressure cluster (Table 4.6).

In this case, we can retrospectively recognize patients with high norm and low norm BP with two and one mistakes while others patients unmistakably. Overall classification accuracy is 96,6% (Table 4.7).

Table 4.6. Coefficients and Constants for Classification Functions for Clusters

Blood Pressure Clusters	High N	AH I	Norm	Low N	AH II
Variables currently in the model	p=,148	p=,398	p=,182	p=,148	p=,125
BP Systolic, mmHg	7,486	8,301	7,021	6,219	9,954
Immunity Integral Index	-101,9	-98,53	-97,99	-103,2	-91,06
Monocytes, %	13,16	12,87	12,85	13,15	12,18
Interleukin-6, ng/L	-1,335	-0,691	-1,136	-1,897	1,266
Leukocyturia, lg Leu/L	121,2	123,7	119,3	116,5	129,9
Circulating Immune Complex, units	-0,036	-0,009	-0,026	0,041	-0,004
Tumor Necrosis Factor-α, ng/L	7,977	6,871	7,072	8,483	4,775
BP Diastolic, mmHg	0,840	0,713	0,860	0,969	0,378
Rod shaped Neutrophils, %	2,198	0,873	1,282	1,863	-0,975
Killing Index vs *Staph. aureus*, %	4,826	4,716	4,497	4,628	4,742
IgA Serum, g/L	-38,87	-43,05	-41,42	-37,45	-46,31
Phagocytose Index vs *St. aureus*, %	120,4	121,2	120,5	118,1	122,2
Secretory IgA Saliva, mg/L	-0,633	-0,608	-0,595	-0,610	-0,608
IgA Saliva, mg/L	-2,292	-2,321	-2,327	-2,255	-2,318
Popovych's Strain Index-1	-115,1	-118,4	-112,3	-115,3	-134,7
Microbian Count for *St. aureus*, B/Ph	-8,149	-8,302	-8,279	-8,056	-8,470
Phagocytose Index vs *E. coli*, %	83,59	82,41	82,73	84,03	81,00
Erythrocyturia, lg Er/L	-19,82	-22,98	-17,94	-14,42	-29,21
Constants	-10430	-10465	-10264	-10116	-10628

Table 4.7. Classification Matrix for Blood Pressure Clusters

	Classification Matrix Rows: Observed classifications Columns: Predicted classifications					
Group	Percent Correct	High N p=,14773	AH I p=,39773	N p=,18182	Low N p=,14773	AH II p=,12500
High N	84,6	11	1	1	0	0
AH I	100,0	0	35	0	0	0
N	100,0	0	0	16	0	0
Low N	92,3	0	0	1	12	0
AH II	100,0	0	0	0	0	11
Total	96,6	11	36	18	12	11

The results obtained in this study are consistent with existing data summarized in a number of excellent reviews [McMaster WG et al., 2015; Agita A & Alsagaff MT, 2017; Rodriguez-Iturbe B et al., 2017; Mikolajczyk TP & Guzik TJ, 2019; Rai A et al., 2020; Zhang RM et al., 2021]. Numerous cells of the immune system, both innate and adaptive immunity, have been indicated to play an important role in the development and maintenance of hypertension. In response to hypertensive stimuli such as Ang II and high salt, T cells become pro-inflammatory and they infiltrate the brain, blood vessel adventitia and periadventitial fat, heart, and the kidney. Pro-inflammatory T cell-derived cytokines such as IFN-γ and TNF-α (from $CD8^+$ and $CD4^+$Th1) and IL-17A (from the γδ-T cell and $CD4^+$Th17) exacerbate hypertensive responses mediating both endothelial dysfunction. Th-1 and Th-17 effectors participate in inflammation which leads to increased blood pressure. One part of $CD4^+$ is the regulatory T cells (Tregs) that suppress immune response activation as they produce immunosuppressive cytokines, such as TGF-β and IL-10. Moreover, cross-talk among natural

killer cells, adaptive immune cells (T cells and B cells), and innate immune cells (i.e. monocytes, macrophages, neutrophils, and dendritic cells) contributes to end-cardiovasculature damage and dysfunction in hypertension. Clinical and experimental studies on the diagnostic potential of T-cell subsets revealed that blood regulatory T cells, CD4 cells, and CD8 T cells show promise as biomarkers of hypertension. Therapeutic interventions to suppress activation of these cells may prove beneficial in reducing end-organ damage and preventing consequences of cardiovascular failure, including hypertension.

The above mostly applies to patients with AH II, while in persons with AH I and quasi-normal BP, its immune support is less pronounced.

Based on the analyses and results presented in this Chapter, here is a detailed evaluation of the hypotheses and their verification.

1. Hypothesis. It is possible to identify distinct groups of patients characterized by different blood pressure profiles and corresponding immune patterns. Verification. Confirmed. The study successfully identified five distinct clusters of patients based on blood pressure and immune parameters. Null hypothesis rejected. The null hypothesis of no distinct clusters was rejected in favor of the alternative hypothesis of distinct patient groups.

2. Hypothesis. A specific set of immune parameters significantly discriminates between different blood pressure clusters. Verification. Confirmed. The discriminant analysis identified 18 parameters that significantly differentiated between blood pressure clusters. Null hypothesis rejected. The null hypothesis of no differentiating parameters was rejected.

3. Hypothesis. There are significant differences in immune profiles across the spectrum of blood pressure categories. Verification. Confirmed. The study found distinct immune profiles for different blood pressure categories, from low normal to hypertension II. Null hypothesis rejected. The null hypothesis of no differences was rejected in favor of the alternative hypothesis of significant differences across categories.

4. Hypothesis. It is possible to create a model that accurately classifies patients into blood pressure clusters using immune parameters. Verification. Confirmed. The classification functions derived from discriminant analysis achieved 96.6% accuracy. Null hypothesis rejected. The null hypothesis of no predictive model was strongly rejected in favor of the alternative hypothesis of an accurate classification model.

11. Hypothesis. There are significant interactions between immune parameters and other physiological measures in their association with blood pressure. Verification. Not directly addressed in this chapter. This hypothesis would require integration with results from other chapters. Null hypothesis. Neither rejected nor accepted based on the information in this chapter alone.

Based on a thorough review of this Chapter, here are the detailed conclusions drawn from the study.

1. Immune Parameter Selection. The forward stepwise discriminant analysis identified 18 parameters as characteristic of quantitative-qualitative blood pressure clusters. These included 2 proinflammatory cytokines, 6 immune parameters of blood and saliva, 5 parameters of phagocytosis, 2 markers of pyelonephritis, and the strain index of leukocytogram.

2. Most Informative Immune Parameters. Serum levels of IL-6 and TNF-α were among the most informative parameters. Activity and intensity of phagocytosis by neutrophils against *Staphylococcus aureus* were highly significant.

3. Classification Accuracy. The discriminant model achieved a high overall classification accuracy of 96.6%, indicating a strong relationship between immune parameters and blood pressure clusters.

4. Blood Pressure Clusters and Immune Characteristics. a) Arterial Hypertension II Cluster. Characterized by elevated levels of pro-inflammatory cytokines (IL-6 and TNF-α). Normal, but minimal for the sample, activity and intensity of phagocytosis of gram-positive bacteria. b) Low Normal BP Cluster. Located at the opposite pole of the major discriminant root. Did not show extreme values for the mentioned immune parameters. c) Other BP Clusters. Showed intermediate levels of the aforementioned immune parameters.

5. Salivary Immune Markers. Levels of serum and salivary IgA, as well as secretory IgA, were found to be significant discriminators between blood pressure clusters.

6. Systemic Inflammation. Circulating immune complexes were included in the discriminant model, indicating their relevance to blood pressure categorization.

7. Leukocyte Parameters. The strain index of leukocytogram and specific leukocyte subpopulations (e.g., rod-shaped neutrophils, monocytes) were significant in differentiating blood pressure clusters.

8. Phagocytic Activity. Parameters of phagocytosis against both *Staphylococcus aureus* and *Escherichia coli* were important in distinguishing between blood pressure groups.

9. Markers of Pyelonephritis. Leukocyturia and erythrocyturia were included in the discriminant model, suggesting a potential link between urinary tract health and blood pressure.

10. Integral Immunity Index. An integral index of immunity was found to be a significant discriminator between blood pressure clusters.

11. Microbiota Influence. While not among the most significant discriminators, some parameters related to gut microbiota were included in the analysis, suggesting a potential role in blood pressure regulation.

12. Patterns Across BP Spectrum. The study revealed distinct immune profiles across the spectrum of blood pressure categories, from low normal to hypertension II.

13. Potential Mechanisms. The results imply that both innate (e.g., phagocytosis) and adaptive (e.g., immunoglobulins) immune responses are involved in blood pressure regulation.

15. Clinical Implications. The strong association between immune parameters and blood pressure clusters suggests potential for using immune markers in hypertension assessment or risk prediction.

16. Methodological Robustness. The study demonstrated the effectiveness of using discriminant analysis to comprehensively analyze complex immune data in relation to blood pressure.

17. Limitations. The study was observational and cross-sectional, limiting causal inferences. The sample size, while adequate for the analyses performed, may limit the generalizability of some findings.

18. Future Research Directions. The study opens avenues for further research into the immunological mechanisms underlying the observed relationships with blood pressure. Longitudinal studies could help elucidate the temporal dynamics of these relationships. Validation of the immune-based classification model in larger, diverse populations is needed.
This chapter provides a comprehensive characterization of the immunological accompaniments of different blood pressure profiles in patients at Truskavets' spa. It demonstrates complex relationships between various components of the immune system and blood pressure regulation, suggesting potential immune mechanisms involved in hypertension. The findings lay a foundation for future studies to further elucidate these relationships and potentially translate them into novel diagnostic or therapeutic approaches in cardiovascular health management.

Thus, a wide range of blood pressure in Truskavets' spa patients is accompanied by an equally wide range of neural, endocrine and immune parameters. A detailed analysis and discussion will be conducted in next chapters.

Chapter 5

METABOLIC ACCOMPANIMENT OF QUANTITATIVE-QUALITATIVE BLOOD PRESSURE CLUSTERS

Abstract

Background. Earlier we studied the neural, endocrine and immune accompaniments of quantitative-qualitative blood pressure (BP) clusters of profile patients of Truskavets' spa. The **purpose** of this study is to clarify the metabolic accompaniment in the same contingent. **Materials and methods.** Under an observations were 44 patients with chronic pyelonephritis and cholecystitis in the phase of remission. Testing was performed twice - on admission and after 7-10 days of standard balneotherapy. The plasma levels of lipids, lipids peroxidation, glucose, nitrogenous metabolites and electrolytes as well as urinary excretion of last two were determined. In addition, the electrokinetic and cholecystokinetic indexes were determined. **Results**. The forward stepwise program identified 24 parameters as characteristic of quantitative-qualitative blood pressure clusters. In addition to BP parameters by default, the most informative among them are sodium, chloride and uric acid daily excretion as well as plasma phosphate and diene conjugates, whose levels are maximal in patients with hypertension, while minimal in patients with low norm BP, on the one hand, and activity of antioxidant enzymes and electrokinetic index, the level of which are polar, on the other hand. The accuracy of patient classification is 98,9%. **Conclusion**. The quantitative-qualitative blood pressure clusters have a characteristic metabolic accompaniment.

Keywords: blood pressure, electrolytes, nitrogenous metabolites, lipids, electrokinetic and cholecystokinetic indexes, discriminant analysis, Truskavets' spa.

Earlier we showed that profile patients of Truskavets' spa are characterized by a wide range of blood pressure - from low norm to arterial hypertension II - that correspond to the hemodynamics parameters. Than we clarified the neural, endocrine and immune accompaniments of quantitative-qualitative blood pressure clusters in the same contingent.

The **purpose** of this chapter, given the previous data about relationships between hemodynamics and metabolism [Popovych IL et al., 2005], is to clarify the metabolic accompaniments of quantitative-qualitative blood pressure clusters in the same contingent.

In this Chapter the following research problems and corresponding hypotheses can be inferred, although they are not explicitly stated.

1. Research problem. Can distinct blood pressure clusters be identified based on metabolic parameters? Hypothesis. It is possible to identify distinct groups of patients characterized by different blood pressure profiles and corresponding metabolic patterns.
2. Research problem. Which metabolic parameters best differentiate between blood pressure clusters? Hypothesis. A specific set of metabolic parameters significantly discriminates between different blood pressure clusters.
3. Research problem. How do metabolic profiles differ across various blood pressure categories (from low normal to hypertension II)? Hypothesis. There are significant differences in metabolic profiles across the spectrum of blood pressure categories.
4. Research problem. Can a predictive model be developed for blood pressure cluster membership based on metabolic parameters? Hypothesis. It is possible to create a model that accurately classifies patients into blood pressure clusters using metabolic parameters.

Daily urine was collected, in which was determined the concentration of electrolytes: calcium (by reaction with arsenase III), magnesium (by reaction with colgamite), phosphates

(phosphate-molybdate method), chloride (mercury-rhodanidine method), sodium and potassium (flamming photometry); nitric metabolites: creatinine (by Jaffe's color reaction by Popper's method), urea (urease method by reaction with phenolhypochlorite), uric acid (uricase method). Urine lithogenicity index (Lith) was also calculated by the Tiselius' HS [1978] formula modifed by Flyunt VR et al. [2017; 2021].

Lith = (Uric acid•Calcium/Magnesium•Creatinine)^{0,25}.

The same metabolic parameters were determined in plasma as well as glucose (glucose-oxidase method), triglycerides (by a certain meta-periodate method), total cholesterol (by a direct method after the classic reaction by Zlatkis-Zack) and its content in composition of α-lipoproteins (HDLP) (by the enzyme method after precipitation of notα-lipoproteins); pre-β-lipoproteins (VLDLP) (calculated by the level of triglycerides); β-lipoproteins (LDLP) (calculated by a difference between a total cholesterol and cholesterol in composition α-and pre-β-lipoproteins).

Based on them, two Atherogenic Index Plasma (AIP) were calculated: TG/HDL-Ch named as Dobiásová&Frohlich [Dobiásová M & Frohlich J, 2001] as well as previously widely used Klimov's AIP as ratio (VLDLCh + LDLCh)/HDLCh [Klimov AN, 1995].

State of lipid peroxidation assessed the content in the serum its products: diene conjugates (spectrophotometry of heptane phase of lipids extract) [Gavrilov VB & Mishkorudnaya MI, 1983] and malondialdehyde (test with thiobarbituric acid) [Andreyeva LI et al., 1988], as well as the activity of antioxidant enzymes: catalase serum (by the speed of decomposition hydrogen peroxide) [Korolyuk MA et al., 1988] and superoxide dismutase erythrocytes (by the degree of inhibition of nitroblue tetrazolium recovery in the presence of N-methylphenazone metasulfate and NADH) [Dubinina YYet al., 1988; Makarenko YeV, 1988].

The analysis carried out according to instructions [Goryachkovskiy AM, 1998] with the use of analyzers "Reflotron" (BRD) and "Pointe-180" (USA) and corresponding sets of reagents.

Given its integral physiological nature [Honcharenko MS, 1992; Honcharenko MS & Yereshchenko YA, 2011; Kyrylenko IG, 2018; Kyrylenko IG et al., 2016; 2018; 2022], we determined also the electrokinetic index (EKI) as rate of electronegative nuclei of buccal epithelium by intracellular microelectrophoresis on the device "Biotest" (VN Karazin National University, Kharkiv), according to the method described [Shakhbazov VG et al., 2000].

On the tone and motility of gall-bladder judged by its volume on an empty stomach in the morning and after 5, 15 and 30 min after ingestion cholekinetic (50 ml of 40% solution of xylitol). The method echoscopy (echocamera "Radmir") applicated. To quantify cholekinetics, the area between the cholecystovolumogram and the basal line was calculated [Marfiyan OM & Zukow W, 2015; Marfiyan OM et al., 2015].

Reference values of variables are taken from the instructions and/or database of the Truskavetsian Scientific School of Balneology.

The program forward stepwise included in the discriminant model 24 parameters. In addition to BP parameters by default, the following variables were identified as characteristic: **sex** index (as a ratio between the number of male and female in the cluster), **electrokinetic** index, **body mass** index, as well as 11 parameters of **plasma**, 6 parameters of **urine**, and 2 parameters of cholekinetics (Tables 5.1 and 5.2).

Table 5.1. Discriminant Function Analysis Summary for Metabolic Variables, their actual levels (Mean±SE) for Clusters as well as Reference levels and Coefficients of Variability

Step 24, N of vars in model: 24; Grouping: 5 grs; Wilks' Λ: 0,0060; approx. $F_{(96)}$=6,6; $p<10^{-6}$

	Clusters of Blood Pressure (n)					Parameters of Wilk's Statistics						
Variables currently in the model	**AH II (11)**	**AH I (35)**	**High N (13)**	**Norm (16)**	**Low N (13)**	Wilks' Λ	Partial Λ	F-remove (4,62)	p-level	Tolerancy	Reference (44)	Cv
BP Systolic, mmHg	172 2,5	148 0,9	134 0,8	125 0,6	112 1,0	0,011	0,525	13,58	10^{-6}	0,234	124,5 2,3	,122
Catalase, µM/L•h	92 15	90 9	117 9	146 7	151 19	0,008	0,702	6,354	10^{-3}	0,472	125 9	,458
Sex Index (M=1; F=2)	1,36 0,15	1,11 0,05	1,00 0,00	1,25 0,11	1,62 0,14	0,007	0,889	1,882	0,125	0,485	1,23 0,06	,343
Potassium P, mM/L	4,49 0,14	4,22 0,09	4,35 0,15	4,22 0,14	4,72 0,16	0,007	0,854	2,563	0,047	0,653	4,55 0,07	,104
Sodium P, mM/L	149 2,8	140 1,5	140,4 2,1	145 2,0	148,2 1,2	0,006	0,924	1,229	0,308	0,540	145,0 0,7	,034
Calcium Ex, mM/24 h	3,74 0,72	6,17 0,60	4,88 0,86	3,92 0,44	4,82 0,79	0,007	0,916	1,373	0,254	0,525	4,38 0,14	,214
VLD LP Ch Plasma, Z	0,19 0,21	0,39 0,16	-0,51 0,19	0,16 0,26	-0,41 0,18	0,007	0,912	1,444	0,231	0,132	0 0,30	**SD 2**
Klimov's AI, Z	0,92 0,51	0,22 0,28	0,16 0,45	0,01 0,35	0,41 0,45	0,006	0,931	1,115	0,358	0,339	0 0,30	**SD 2**
Cholecysto-kinetics Ind	615 43	569 25	635 40	613 35	559 31	0,007	0,902	1,622	0,181	0,481	624 12	,131
Creatinine Ex, mM/24h	10,5 1,3	8,2 0,7	6,5 0,6	7,1 0,8	8,6 1,1	0,007	0,871	2,231	0,076	0,472	11,0 0,5	,300
Magnesium P, mM/L	0,85 0,02	0,83 0,01	0,84 0,01	0,84 0,01	0,82 0,01	0,007	0,875	2,141	0,087	0,636	0,90 0,01	,056
BP Diastolic, mHg	90,7 4,5	87,6 1,2	81,3 1,5	77,8 1,5	71,5 1,5	0,006	0,932	1,087	0,371	0,482	79,0 1,0	,086
Superox dis-mut, un/mL	49 8	67 4	76 3	88 4	90 8	0,007	0,893	1,807	0,139	0,114	62,0 2,6	,286
Diene conju, E^{232}/mL	1,72 0.05	1,58 0,04	1,49 0,03	1,50 0,04	1,47 0,05	0,006	0,947	0,835	0,508	0,273	1,90 0,08	,279
Urea P, mM/L	5,37 0,26	6,22 0,21	6,22 0,41	5,69 0,21	6,08 0,28	0,007	0,910	1,477	0,220	0,278	5,00 0,25	,330
Electrokine-tic Ind, %	31,7 2,1	44,7 2,3	42,7 2,6	46,6 2,7	50,1 2,5	0,009	0,721	5,795	0,001	0,328	40,9 1,5	,250
Body Mass Index, kg/m²	27,5 1,3	27,2 0,7	27,4 0,8	27,9 0,9	25,5 0,6	0,007	0,865	2,340	0,065	0,401	24,2 0,5	,133
Uric acid Ex, mM/24h	4,01 0,56	4,25 0,25	3,71 0,45	3,44 0,30	3,29 0,38	0,008	0,790	3,988	0,006	0,222	3,00 0,11	,250
Calcium P, mM/L	2,19 0,04	2,22 0,04	2,24 0,05	2,17 0,04	2,13 0,02	0,007	0,902	1,629	0,179	0,556	2,30 0,02	,065
Gallbladder Volume, mL	51,2 2,2	45,0 2,1	43,9 4,9	48,7 5,2	46,1 4,5	0,007	0,893	1,801	0,140	0,632	41,0 3,1	,500
Urea Excr., mM/24 h	516 64	632 39	551 78	531 58	489 45	0,007	0,843	2,785	0,034	0,166	458 13	,186
Dobiásová& Frohlich AI	0,55 0,25	0,76 0,33	-0,40 0,47	0,57 0,56	-0,33 0,35	0,007	0,913	1,438	0,233	0,099	0 0,30	**SD 2**
Sodium Ex, mM/24 h	238 37	221 14	189 21	217 24	194 22	0,007	0,870	2,241	0,075	0,040	154 5	,211
Chloride Ex, mM/24 h	247 41	236 16	209 25	233 27	207 24	0,007	0,897	1,713	0,159	0,042	167,5 4	,172
Variables	**AH**	**AH**	**High**	**No-**	**Low**	Wil	Par-	F to	p-	Tole-	Refe-	Cv

currently not in model	II (11)	I (35)	N (13)	rm (16)	N (13)	ks' Λ	tial Λ	enter	level	rancy	rence (44)	
Phosphate P, mM/L	1,08 0,07	1,02 0,03	1,09 0,07	1,00 0,04	0,90 0,09						1,20 0,02	,167
Lithogenici-ty Urine	0,74 0,05	0,89 0,03	0,89 0,03	0,88 0,04	0,79 0,04						0,73 0,03	,300

Table 5.2. Summary of Stepwise Analysis for Blood Pressure and Metabolic Variables, ranked by criterion Lambda

Variables currently in the model	F to enter	p-level	Λ	F-va-lue	p-value
BP Systolic, mmHg	298	10^{-6}	0,065	298	10^{-6}
Catalase, µM/L•h	7,995	10^{-4}	0,047	74,20	10^{-6}
Sex Index (M=1; F=2)	4,814	0,002	0,038	43,76	10^{-6}
Potassium Plasma, mM/L	2,494	0,049	0,034	31,16	10^{-6}
Sodium Plasma, mM/L	1,956	0,109	0,031	24,46	10^{-6}
Calcium Excretion, mM/24 h	2,022	0,100	0,028	20,43	10^{-6}
VLD LP Cholesterol Plasma, Z	1,935	0,113	0,025	17,69	10^{-6}
Klimov's Atherogenic Index, Z	2,391	0,058	0,022	15,87	10^{-6}
Cholecystokinetics Index, units	1,296	0,279	0,021	14,18	10^{-6}
Creatinine Excretion, mM/24h	1,601	0,183	0,019	12,94	10^{-6}
Magnesium Plasma, mM/L	1,290	0,282	0,018	11,87	10^{-6}
BP Diastolic, mHg	1,314	0,273	0,017	11,00	10^{-6}
Superoxide dismutase Erythrocytes, un/mL	1,125	0,351	0,016	10,23	10^{-6}
Diene conjugates, E^{232}/mL	1,619	0,179	0,014	9,67	10^{-6}
Urea Plasma, mM/L	1,479	0,218	0,013	9,16	10^{-6}
Electrokinetics Index, %	1,475	0,220	0,012	8,72	10^{-6}
Body Mass Index, kg/m^2	1,874	0,125	0,011	8,41	10^{-6}
Uric acid Excretion, mM/24h	1,280	0,287	0,010	8,03	10^{-6}
Calcium Plasma, mM/L	1,625	0,178	0,009	7,75	10^{-6}
Gallbladder Volume, mL	1,176	0,330	0,009	7,44	10^{-6}
Urea Excretion, mM/24 h	1,625	0,179	0,008	7,22	10^{-6}
Dobiásová's & Frohlich's Atherogen Ind, Z	1,397	0,246	0,007	6,99	10^{-6}
Sodium Excretion, mM/24 h	1,287	0,285	0,007	6,76	10^{-6}
Chloride Excretion, mM/24 h	1,713	0,159	0,006	6,62	10^{-6}

Next, the 24-dimensional space of discriminant variables transforms into 4-dimensional space of a canonical roots. For Root 1 r*=0,980 (Wilks' Λ=0,0060; $\chi^2_{(96)}$=371; p<10^{-6}), for Root 2 r*=0,827 (Wilks' Λ=0,1485; $\chi^2_{(69)}$=138; p=0,000002), for Root 3 r*=0,606 (Wilks' Λ=0,470; $\chi^2_{(44)}$=55; p=0,130), and for Root 4 r*=0,507 (Wilks' Λ=0,743; $\chi^2_{(21)}$=22; p=0,426). The first root contains 88,6% of discriminative opportunities, the second 8,0%, the third 2,1%, the last 1,3% only, therefore will be ignored in the future.

Table 5.3 presents raw and standardized coefficients for discriminant variables. The calculation of the discriminant root values for each person as the sum of the products of raw coefficients to the individual values of discriminant variables together with the constant enables the visualization of each patient in the information space of the roots (Fig. 5.1).

Table 5.3. Standardized and Raw Coefficients and Constants for Blood Pressure and Metabolic Variables

Coefficients	Standardized			Raw		
Variables currently in the model	Root 1	Root 2	Root 3	Root 1	Root 2	Root 3
BP Systolic, mmHg	1,313	0,711	0,251	0,271	0,147	0,052
Catalase, µM/L•h	-0,426	0,769	-0,373	-0,014	0,025	-0,012
Sex Index (M=1; F=2)	0,089	0,297	0,599	0,233	0,776	1,563
Potassium Plasma, mM/L	-0,287	0,387	0,298	-0,537	0,725	0,559
Sodium Plasma, mM/L	-0,023	0,381	0,246	-0,003	0,048	0,031

Calcium Excretion, mM/24 h	-0,178	-0,356	0,326	-0,059	-0,119	0,109
VLD LP Ch Plasma, Z	-0,497	0,418	0,783	-0,570	0,478	0,897
Klimov's Atherogenic Index, Z	0,048	0,455	0,074	0,030	0,284	0,046
Cholecystokinetics Index, units	-0,066	-0,048	-0,728	-0,0005	-0,0003	-0,0052
Creatinine Excretion, mM/24h	0,100	0,492	0,471	0,028	0,136	0,130
Magnesium Plasma, mM/L	0,241	-0,301	-0,462	6,223	-7,752	-11,90
BP Diastolic, mHg	-0,099	-0,265	0,363	-0,013	-0,034	0,046
Superoxide dismutase Erythr., un/mL	0,177	0,940	0,740	0,016	0,084	0,066
Diene conjugates, E^{232}/mL	-0,015	0,334	-0,168	-0,104	2,266	-1,139
Urea Plasma, mM/L	0,044	0,341	0,790	0,039	0,301	0,698
Electrokinetics Index, %	0,597	-0,837	-0,082	0,053	-0,075	-0,007
Body Mass Index, kg/m^2	0,370	-0,473	-0,021	0,104	-0,133	-0,006
Uric acid Excretion, mM/24h	-0,769	0,683	0,256	-0,516	0,458	0,171
Calcium Plasma, mM/L	0,280	-0,281	0,307	1,571	-1,578	1,722
Gallbladder Volume, mL	0,278	0,106	-0,336	0,018	0,007	-0,022
Urea Excretion, mM/24 h	0,611	-0,817	-0,553	0,0027	-0,0036	-0,0024
Dobiásová's & Frohlich's Ather Ind, Z	0,478	-0,811	-0,758	0,689	-1,169	-1,093
Sodium Excretion, mM/24 h	-0,395	1,254	0,163	-0,004	0,014	0,002
Chloride Excretion, mM/24 h	0,336	-0,771	-0,250	0,0033	-0,0077	-0,0025
			Constants	-48,18	-26,65	-14,66
			Eigenvalues	23,93	2,168	0,580
			Cumulative proportions	0,886	0,966	0,987

Table 5.4 shows the correlation coefficients of blood pressure and metabolic parameters (discriminant variables) with canonical discriminant roots; the cluster centroids of roots; and Z-scores of the discriminant variables.

Table 5.4. Correlations Variables-Canonical Roots, Means of Roots and Z-scores of Blood Pressure and Metabolic Variables

Variables currently in the model	Correlations Variables-Roots			AH II (11)	AH I (35)	High N (13)	Norm (16)	Low N (13)
Root 1 (88,6%)	**R 1**	**R 2**	**R 3**	**+8,2**	+2,5	-1,3	-3,7	**7,8**
Blood Pressure Systolic	**0,773**	0,163	0,035	**+3,15**	+1,51	+0,64	+0,04	**-0,84**
Blood Pressure Diastolic	**0,165**	-0,121	0,075	**+1,79**	+1,31	+0,35	-0,19	**-1,14**
Sodium Excretion	**0,028**	0,019	0,023	**+2,58**	+2,07	+1,07	+1,95	**+1,23**
Chloride Excretion	**0,025**	-0,002	0,033	**+2,74**	+2,37	+1,45	+2,29	**+1,36**
Uric acid Excretion	**0,045**	-0,080	0,119	+1,35	+1,67	+0,95	+0,58	**+0,38**
Dobiásová's&Frohlich's AI	**0,050**	-0,039	0,005	+0,55	+0,76	-0,40	+0,57	**-0,33**
Diene conjugates	**0,179**	0,055	0,112	**-0,35**	-0,61	-0,76	-0,76	**-0,82**
Phosphate Plasma				**-0,58**	-0,89	-0,57	-0,98	**-1,49**
Superoxide dismutase	**-0,407**	-0,038	-0,046	**-0,75**	+0,28	+0,81	+1,45	**+1,59**
Catalase	**-0,288**	0,307	-0,332	**-0,58**	-0,62	-0,15	+0,37	**+0,45**
Electrokinetics Index	**-0,081**	-0,131	0,194	**-0,90**	+0,38	+0,18	+0,56	**+0,89**
Root 2 (8,0%)	**R 1**	**R 2**	**R 3**	**+2,80**	-1,14	-0,91	-0,05	**+1,68**
Sex Index	-0,045	**0,289**	0,239	**+0,32**	-0,27	-0,54	+0,05	**+0,94**
Sodium Plasma	-0,026	**0,307**	-0,056	**+0,71**	-1,05	-0,93	+0,07	**+0,65**
Klimov's Atherogenic Ind	0,019	**0,092**	0,051	**+0,92**	+0,22	+0,16	-0,01	**+0,41**
Gallbladder Volume	0,008	**0,083**	-0,067	**+0,50**	+0,19	+0,14	+0,38	**+0,25**
Potassium Plasma	-0,026	**0,183**	0,125	**-0,12**	-0,69	-0,43	-0,70	**+0,35**
Creatinine Excretion	0,037	**0,154**	0,197	**-0,15**	-0,85	-1,35	-1,20	**-0,73**
Lithogenicity Urine				**+0,02**	+0,69	+0,70	+0,66	**+0,27**
Urea Excretion	0,025	**-0,138**	0,116	**+0,68**	+2,04	+1,09	+0,86	**+0,37**
Calcium Plasma	0,027	**-0,102**	-0,037	**-0,74**	-0,51	-0,40	-0,90	**-1,14**
Root 3 (2,4%)	**R 1**	**R 2**	**R 3**	-0,31	**+0,55**	-0,98	**-0,92**	**+0,89**
Magnesium Plasma	0,017	0,065	**-0,294**	-1,02	**-1,49**	-1,21	-1,15	**-1,56**
Cholecystokinetics Indexs	0,005	0,015	**-0,260**	-0,11	**-0,67**	+0,13	-0,13	**-0,80**
Body Mass Index	0,020	-0,052	**-0,200**	+1,02	**+0,93**	+1,00	+1,15	**+0,41**

Calcium Excretion	0,012	-0,162	**0,293**	-0,68	**+1,92**	+0,54	-0,48	**+0,47**
Urea Plasma	-0,014	-0,141	**0,166**	+0,22	**+0,74**	+0,74	+0,42	**+0,65**

The localization along the first root axis of the patients with **Low Norm** BP (Fig. 5.1) in the extreme left (negative) zone reflects combination of minimum for sampling BP levels with minimum for sampling sodium, chloride and uric acid excretion; maximally decreased levels of diene conjugates and phosphate as well as Dobiásová's & Frohlich's atherogenic index, instead maximally increased activities of catalase and superoxide dismutase as well as electrokinetics index. At the opposite pole of the axis of the first root, there are patients with **AH II**, whose maximum BP is accompanied by maximum/minimum for sampling levels of the listed variables. Clusters of patients with intermediate BP levels are also characterized by intermediate levels of the listed variables. Therefore, all 5 clusters are quite clearly demarcated already in the space of the major root.

Both extreme clusters are separated from the other three also along the axis of the second root. Theirs bottommost position reflects, on the one hand, the increased levels of plasma sodium and Klimov's atherogenic index; maximum for sampling gallbladder volumes and plasma potassium and creatinineuria levels, as well as the highest proportion of women in the cluster. On the other hand, these clusters are characterized by normal and at the same time minimal for the sample levels of lithogenicity of urine and urea excretion, as well as maximally reduced levels of plasma calcium.

Along the axis of the third root, clusters of patients with **AH I** and **Low Norm** BP are further distinguished from other clusters due to maximally decreased magnesiemia and cholecystokinetics index as well as minimally elevated body mass index levels, instead maximally elevated levels of calciuria and plasma urea.

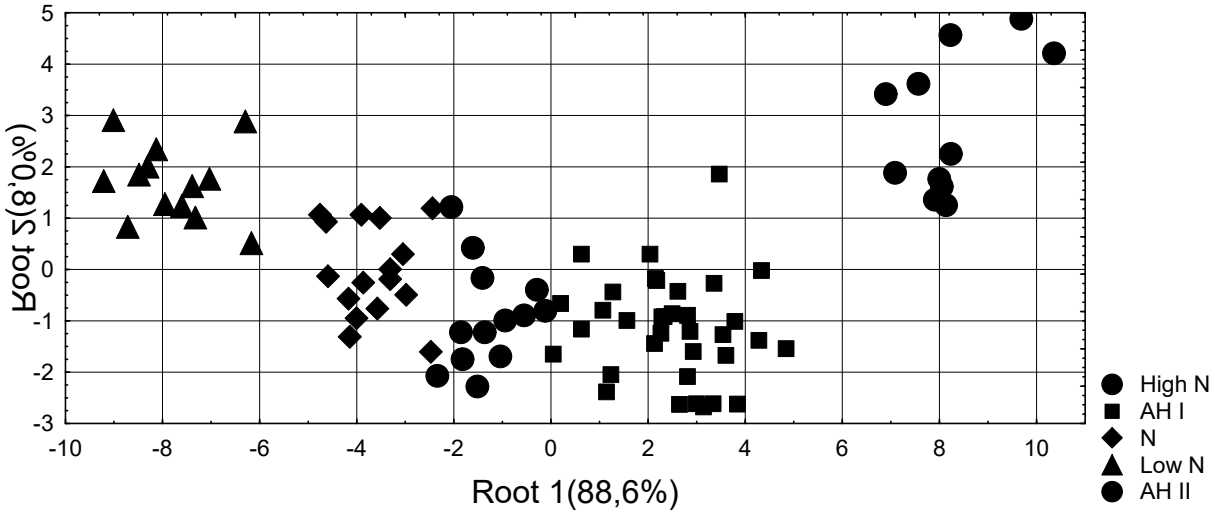

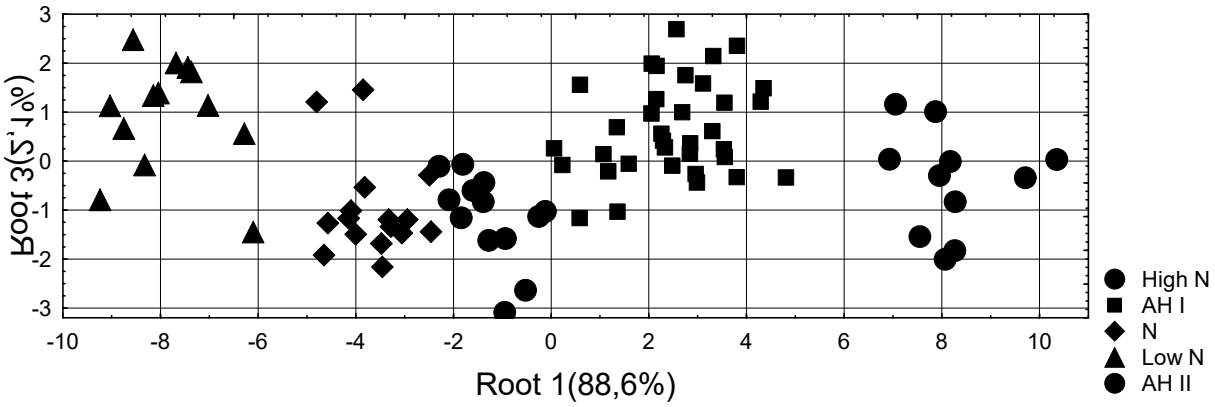

Fig. 5.1. Scattering of individual values of the discriminant metabolic roots at patients of different blood pressure clusters

In general, all clusters on the planes of three roots are clearly delineated, which is documented by calculating the Mahalanobis distances (Table 5.5).

Table 5.5. Squared Mahalanobis Distances between Blood Pressure Clusters and F-values (df=24,6; p for all<10^{-6}; for High N-N p=0,007

Blood Pressure Clusters	High Norm	AH I	Norm	Low Norm	AH II
High Norm	0	**18,1**	**10,2**	**53,3**	**105**
AH I	**5,18**	0	**41,8**	**114**	**49,0**
Norm	**2,20**	**13,8**	0	**26,4**	**143**
Low Norm	**10,4**	**32,6**	**5,35**	0	**251**
AH II	**18,9**	**12,3**	**29,5**	**46,5**	0

The same discriminant parameters can be used to identify the belonging of one or another person to one or another cluster (Table 5.6).

Table 5.6. Coefficients and Constants for Classification Functions for Blood Pressure Clusters

Blood Pressure Clusters	High N	AH I	Norm	Low N	AH II
Variables currently in the model	p=,148	p=,398	p=,182	p=,148	p=,125
BP Systolic, mmHg	39,20	40,31	38,75	37,94	42,38
Catalase, µM/L•h	-0,09	-0,17	-0,04	0,04	-0,14
Sex Index (M=1; F=2)	108,5	112,6	110,44	112,61	115,53
Potassium P, mM/L	-17,72	-19,49	-16,48	-11,57	-20,12
Sodium P, mM/L	7,98	8,05	8,10	8,21	8,19
Calcium Excretion, mM/24 h	-3,46	-3,54	-3,49	-3,21	-4,43
VLD LP Ch Plasma, Z	-16,76	-16,87	-13,66	-9,60	-19,12
Klimov's Atherogenic Index, Z	-18,54	-18,77	-18,94	-18,15	-17,47
Cholecystokinetics Index, units	-0,14	-0,14	-0,13	-0,14	-0,14
Creatinine Excretion, mM/24h	5,32	5,51	5,24	5,68	6,10
Magnesium Plasma, mM/L	1231	1237	1207	1147	1252
BP Diastolic, mHg	0,89	0,97	0,98	1,01	0,72
Superoxide dismutase Erythr., un/mL	25,09	25,30	25,24	25,38	25,66
Diene conjugates, E^{232}/mL	842,9	845,4	853,6	850,8	854,1
Urea Plasma, mM/L	133,3	134,7	133,9	135,3	135,5
Electrokine-tic Ind, %	4,75	4,99	4,62	4,22	5,01
Body Mass Index, kg/m²	20,09	20,65	19,97	19,15	20,71
Uric acid Excretion, mM/24h	-41,56	-43,65	-40,41	-36,89	-44,89
Calcium Plasma, mM/L	410,1	420,5	407,5	400,0	421,6
Gallbladder Volume, mL	2,33	2,39	2,34	2,21	2,54
Urea Excretion, mM/24 h	0,14	0,15	0,13	0,11	0,15
Dobiásová's & Frohlich's Ather Ind, Z	-29,27	-27,96	-31,79	-38,76	-27,70
Sodium Excretion, mM/24 h	-0,15	-0,13	-0,06	-0,05	-0,10
Chloride Excretion, mM/24 h	-0,13	-0,15	-0,19	-0,19	-0,15
Constants	-6552	-6790	-6530	-6391	-7187

In this case, we can retrospectively recognize patients with one mistake only. Overall classification accuracy is 98,9% (Table 5.7).

Table 5.7. Classification Matrix for Blood Pressure Clusters

	Rows: Observed classifications Columns: Predicted classifications					
Group	Percent Correct	High N p=,14773	AH I p=,39773	N p=,18182	Low N p=,14773	AH II p=,12500
High N	100,0	13	0	0	0	0
AH I	97,1	1	34	0	0	0
N	100,0	0	0	16	0	0
Low N	100,0	0	0	0	13	0
AH II	100,0	0	0	0	0	11
Total	98,9	14	34	16	13	11

Based on the analyses and results presented in this Chapter, here is a detailed evaluation of the hypotheses and their verification.

1. Hypothesis. It is possible to identify distinct groups of patients characterized by different blood pressure profiles and corresponding metabolic patterns. Verification. Confirmed. The study successfully identified five distinct clusters of patients based on blood pressure and metabolic parameters. Null hypothesis rejected. The null hypothesis of no distinct clusters was rejected in favor of the alternative hypothesis of distinct patient groups.

3. Hypothesis. A specific set of metabolic parameters significantly discriminates between different blood pressure clusters. Verification. Confirmed. The discriminant analysis identified 24 parameters that significantly differentiated between blood pressure clusters. Null hypothesis rejected. The null hypothesis of no differentiating parameters was rejected.

4. Hypothesis. There are significant differences in metabolic profiles across the spectrum of blood pressure categories. Verification. Confirmed. The study found distinct metabolic profiles for different blood pressure categories, from low normal to hypertension II. Null hypothesis rejected. The null hypothesis of no differences was rejected in favor of the alternative hypothesis of significant differences across categories.

5. Hypothesis. It is possible to create a model that accurately classifies patients into blood pressure clusters using metabolic parameters. Verification. Confirmed. The classification functions derived from discriminant analysis achieved 98.9% accuracy. Null hypothesis rejected. The null hypothesis of no predictive model was strongly rejected in favor of the alternative hypothesis of an accurate classification model.

Conclusions

Based on a thorough review of Chapter 5, here are the detailed conclusions drawn from the study.

1. Blood Pressure Distribution. The study confirmed a wide range of blood pressure levels among patients at Truskavets' spa, from low normal to arterial hypertension II.

2. Metabolic Parameter Selection. The forward stepwise discriminant analysis identified 24 parameters as characteristic of quantitative-qualitative blood pressure clusters. These included sex index, electrokinetic index, body mass index, 11 parameters of plasma, 6 parameters of urine, and 2 parameters of cholekinetics.

3. Most Informative Metabolic Parameters. Sodium, chloride, and uric acid daily excretion. Plasma phosphate and diene conjugates. Activity of antioxidant enzymes (catalase and superoxide dismutase). Electrokinetic index.

4. Blood Pressure Clusters and Metabolic Characteristics. a) Low Normal BP Cluster. Characterized by minimum levels of sodium, chloride, and uric acid excretion. Maximally decreased levels of diene conjugates and phosphate. Maximally decreased Dobiásová's & Frohlich's atherogenic index. Maximally increased activities of catalase and superoxide dismutase. Maximally increased electrokinetic index. b) Arterial Hypertension II Cluster. Showed opposite patterns to the Low Normal BP cluster. Maximum levels of sodium, chloride, and uric acid excretion. Maximally increased levels of diene conjugates and phosphate. Maximally increased Dobiásová's & Frohlich's atherogenic index. Minimally increased activities of catalase and superoxide dismutase. Minimally increased electrokinetic index. c) Intermediate BP Clusters. Characterized by intermediate levels of the aforementioned metabolic parameters.

5. Secondary Discriminating Factors. The second discriminant root provided additional separation, particularly for the extreme clusters (Low Normal BP and AH II). These clusters showed increased levels of plasma sodium and Klimov's atherogenic index, maximum gallbladder volumes, and plasma potassium and creatinineuria levels. They also had the highest proportion of women and minimal levels of urinary lithogenicity and urea excretion.

6. Tertiary Discriminating Factors. The third discriminant root further distinguished clusters of patients with AH I and Low Normal BP. These clusters showed maximally decreased magnesiemia and cholecystokinetics index, minimally elevated body mass index levels, and maximally elevated levels of calciuria and plasma urea.

7. Classification Accuracy. The discriminant model achieved a high overall classification accuracy of 98.9%, indicating a strong relationship between metabolic parameters and blood pressure clusters.

8. Lipid Metabolism. Atherogenic indices (Klimov's and Dobiásová's & Frohlich's) were significant discriminators between blood pressure clusters, suggesting a link between lipid metabolism and blood pressure regulation.

9. Oxidative Stress. Markers of oxidative stress (diene conjugates) and antioxidant activity (catalase, superoxide dismutase) showed significant associations with blood pressure levels, implying a role of oxidative balance in blood pressure regulation.

10. Electrolyte Exchange. Urinary excretion of sodium, chloride, and uric acid, as well as plasma levels of electrolytes, were important discriminators, highlighting the role of electrolyte balance in blood pressure regulation.

11. Biological Age. The electrokinetic index, as a marker of biological age, showed significant associations with blood pressure clusters, suggesting a link between aging processes and blood pressure regulation.

12. Gallbladder Function. Gallbladder volume and cholecystokinetics index were included in the discriminant model, indicating a potential relationship between gallbladder function and blood pressure regulation.

13. Body Mass. Body Mass Index was a significant discriminator, suggesting a link between body mass and blood pressure.

14. Sex Differences. The sex index was included in the discriminant model, indicating potential sex-related differences in the relationship between metabolic parameters and blood pressure.

15. Methodological Robustness. The study demonstrated the effectiveness of using discriminant analysis to comprehensively analyze complex metabolic data in relation to blood pressure.

16. Clinical Implications. The strong association between metabolic parameters and blood pressure clusters suggests potential for using metabolic profiles in hypertension assessment or risk prediction.

17. Limitations. The study was observational and cross-sectional, limiting causal inferences. The sample size, while adequate for the analyses performed, may limit the generalizability of some findings.

18. Future Research Directions. The study opens avenues for further research into the metabolic mechanisms underlying the observed relationships with blood pressure. Longitudinal studies could help elucidate the temporal dynamics of these relationships. Validation of the metabolic-based classification model in larger, diverse populations is needed.

This Chapter provides a comprehensive characterization of the metabolic accompaniments of different blood pressure profiles in patients at Truskavets' spa. It demonstrates complex relationships between various metabolic parameters and blood pressure regulation, suggesting potential metabolic mechanisms involved in hypertension. The findings lay a foundation for future studies to further elucidate these relationships and potentially translate them into novel diagnostic or therapeutic approaches in cardiovascular health management.

Chapter 6

TENSIOREGULOME AS AN ACCOMPANIMENT OF QUANTITATIVE-QUALITATIVE BLOOD PRESSURE CLUSTERS

Abstract

Background. Earlier we studied the neural, endocrine, immune, microbiome and metabolome accompaniments of quantitative-qualitative blood pressure (BP) clusters of profile patients of Truskavets' spa. The obtained results give us grounds to put forward the concept of ***tensioregulome*** by analogy with the metabolome and the microbiome. The purpose of this study is detailing this concept. **Materials and methods.** Under an observations were 44 patients with chronic pyelonephritis and cholecystitis in the phase of remission. Testing was performed twice - on admission and after 7-10 days of standard balneotherapy. The main object of the study was BP. We determined parameters of EEG and HRV, levels of adaptation hormones, electrolytes, lipids, and nitrogenous metabolites, components of humoral, cellular, and phagocytic links of immunity and markers of pyelonephritis. **Results**. The forward stepwise program identified 26 tensioregulome parameters as characteristic of quantitative-qualitative blood pressure clusters: 10 EEG, 6 metabolic, 6 immune, testosterone, cortisol, sympathetic tone as well as sex. The accuracy of patient classification is 98,9%. Another 24 parameters were found to be characteristic, but were outside the discriminant model, including 11 EEG, 1 HRV, 5 metabolic, 4 immune, bacteriuria, body mass index, and age. Both linear and non-linear correlations between the BP and tensioregulome parameters were revealed. **Conclusion**. The quantitative-qualitative blood pressure clusters have a characteristic accompaniment named tensioregulome.

Keywords: blood pressure, EEG, HRV, immunity, metabolome, pyelonephritis.

Earlier we showed that profile patients of Truskavets' spa are characterized by a wide range of blood pressure - from low norm to arterial hypertension II - that correspond to the hemodynamics parameters. Than we clarified the neural, endocrine, metabolome, immune, and microbiome accompaniments of quantitative-qualitative blood pressure clusters in the same contingent. The obtained results give us grounds to put forward the concept of ***tensioregulome***

by Popovych IL (2022). The term was first introduced by Popovych IL in 2022 by analogy with the metabolome and the microbiome. The purpose of this chapter is detailing this concept.

In this Capter the following research problems and hypotheses appear to have been addressed.

Research Problems.

1. What are the neuro-endocrine, immune, and metabolic accompaniments (termed the "tensioregulome") of different quantitative-qualitative blood pressure clusters in patients at Truskavets' spa?
2. To what extent can blood pressure levels be determined or predicted by tensioregulome parameters?
3. What are the key components and relationships within the tensioregulome that relate to blood pressure regulation?

Hypotheses.

1. There are distinct neuro-endocrine, immune, and metabolic profiles (tensioregulomes) associated with different blood pressure clusters.
2. Blood pressure levels can be significantly determined or predicted by a combination of tensioregulome parameters.

3. Certain EEG parameters have significant relationships with blood pressure levels.

4. Immune parameters, especially related to inflammation and phagocytosis, play an important role in the tensioregulome's relationship to blood pressure.

5. Metabolic factors, particularly related to electrolytes, lipids, and oxidative stress, are key components of the tensioregulome affecting blood pressure.

6. There are both linear and non-linear relationships between tensioregulome parameters and blood pressure levels.

7. The tensioregulome provides a more comprehensive model for understanding blood pressure regulation compared to individual physiological systems alone.

The Chapter aims to detail and validate the concept of the tensioregulome as a multifaceted physiological accompaniment to blood pressure levels, integrating neural, endocrine, immune, and metabolic factors.

The following statistical methods were used.

1. Descriptive Statistics. a) Arithmetic means - used to present average values of variables for each blood pressure cluster. b) Standard errors of means - provided alongside means to indicate precision of population mean estimates. c) Coefficients of variation (Cv) - calculated as the ratio of standard deviation to mean, expressed as percentages. They inform about relative variability of features.

2. Discriminant Analysis. a) Stepwise discriminant analysis (forward stepwise) - applied to identify variables best differentiating blood pressure clusters. b) Wilks' Lambda statistic - used to assess statistical significance of the discriminant model and individual variables. c) Partial Wilks' Lambda - evaluates unique contribution of each variable to discrimination, controlling for other variables in the model. d) F-remove - F statistic for removing a variable from the model. e) Tolerance - measures redundancy of a variable relative to other variables in the model. f) Standardized coefficients of discriminant functions - show relative contribution of each variable to the discriminant function. g) Raw coefficients of discriminant functions - used to calculate discriminant function values for individual cases. h) Classification function coefficients - used to assign new cases to clusters. i) Mahalanobis distances - measure distance between cluster centroids in multidimensional space. j) Classification matrix - shows accuracy of case classification into clusters.

3. Canonical Correlation Analysis. a) Canonical correlation coefficients - measure strength of relationship between sets of variables. b) Chi-square test - assesses statistical significance of canonical correlations. c) Structure coefficients (canonical loadings) - show correlations between variables and canonical variables.

4. Multiple Regression Analysis. a) Stepwise regression analysis - applied to identify best predictors of blood pressure. b) Coefficient of determination R^2 - informs about proportion of variance explained by the model. c) Adjusted R^2 - accounts for number of predictors in the model. d) Standard error of estimate - measures average deviation of predicted values from actual ones. e) Standardized regression coefficients (Beta) - show relative impact of predictors. f) Raw regression coefficients (B) - used to construct regression equation. g) F-test - assesses overall significance of regression model. h) t-tests - evaluate significance of individual predictors.

5. Nonlinear Relationship Analysis. a) Second- and third-order curve approximation - applied to model nonlinear relationships between tensioregulome variables and blood pressure.

6. Graphical Presentation of Results. a) Scatter plots - used to visualize relationships between canonical variables and between predictors and blood pressure. b) Bar charts - present mean values of variables in blood pressure clusters.

7. Significance Levels. a) p-values - provided for statistical significance tests, with adopted α level of 0.05.

These methods allowed for a comprehensive analysis of multidimensional relationships between tensioregulome parameters and blood pressure, enabling identification of key factors and patterns in the data.

Under an observations were 34 males and 10 females by age 24-76 years with chronic pyelonephritis and cholecystitis in the phase of remission. Testing was performed twice - on admission and after 7-10 days of standard balneotherapy (drinking of bioactive water Naftussya, applications of ozokerite, mineral pools).

Systolic and diastolic BP was measured in a sitting position three times in a row. We determined parameters of EEG and HRV, levels of adaptation hormones, electrolytes, lipids, and nitrogenous metabolites, components of humoral, cellular, and phagocytic links of immunity and markers of pyelonephritis.

Reference values of variables are taken from the database of the Truskavetsian Scientific School of Balneology.

In order to identify among the registered parameters, those for which the blood pressure clusters differ from each other, a discriminant analysis was performed. The forward stepwise program identified 26 ***tensioregulome*** parameters as characteristic: 10 EEG, 6 metabolic, 6 immune, as well as testosterone, cortisol, sympathetic tone and the sex (more precisely, the sex index) (Tables 6.1 and 6.2). Another 2 parameters were found to be characteristic, but were outside the discriminant model, including 11 EEG, 1 HRV, 5 metabolic, 4 immune, as well as bacteriuria, body mass index and the age (Table 6.3).

Obviously, this distribution is caused by duplication and/or redundancy of recognition information, the strongest evidence of which is the failure to include diastolic BP in the model.

Table 6.1. Discriminant Function Analysis Summary for Variables, their actual levels for Clusters of Blood Pressure as well as Reference levels and Coefficients of Variability

Step 27, N of vars in model: 27; Grouping: 5 grs; Wilks' Λ: 0,0023; approx. $F_{(108)}=7,7$; $p<10^{-6}$

Variables currently in the model	Clusters of Blood Pressure (n)					Parameters of Wilk's Statistics						
	AH II (11)	AH I (35)	High N (13)	No-rm (16)	Low N (13)	Wil-ks Λ	Par-tial Λ	F-re-move (4,57)	p-level	Tole-rancy	Refe-rence (88)	Cv
BP Systolic, mmHg	172 2,5	148 0,9	134 0,8	125 0,6	112 1,0	0,041	0,055	245	10^{-6}	0,511	124,5 1,6	,122
Sex Index (M=1;F=2)	1,36 0,15	1,11 0,05	1,00 0,00	1,25 0,11	1,62 0,14	0,004	0,622	8,64	10^{-4}	0,372	1,23 0,04	,343
Deviation-δ, Hz	0,64 0,07	0,70 0,04	0,55 0,04	0,66 0,08	0,85 0,10	0,003	0,802	3,52	0,012	0,727	0,67 0,03	,395
C3-δ PSD, %	30,4 6,8	27,9 2,7	37,5 7,5	28,8 3,3	43,5 7,4	0,003	0,866	2,21	0,080	0,200	28,0 1,8	,602
P3-δ PSD, %	25,2 6,0	27,7 2,8	26,0 5,6	24,8 3,5	36,7 7,1	0,003	0,906	1,47	0,222	0,232	25,6 1,9	,694
O1-θ PSD, %	8,5 1,6	8,2 0,8	8,2 1,4	7,0 0,9	10,3 1,7	0,003	0,815	3,24	0,018	0,492	8,2 0,5	,584
Index-α, %	49,5 8,5	48,4 5,7	47,3 8,7	62,6 6,0	53,4 6,6	0,003	0,773	4,19	0,005	0,185	50,7 3,0	,560
Deviation-α, Hz	0,86 0,10	1,11 0,12	0,91 0,10	0,81 0,10	1,23 0,15	0,003	0,878	1,97	0,111	0,738	1,02 0,06	,527
Fp2-α PSD, %	27,9 4,2	31,3 2,4	27,2 4,1	34,3 4,7	31,9 5,1	0,003	0,893	1,70	0,163	0,218	32,9 1,6	,448
F7-α PSD, %	28,9 6,1	27,1 2,5	21,1 3,9	18,4 3,4	26,6 3,7	0,003	0,731	5,24	0,001	0,231	27,6 1,5	,522
F8-β PSD, %	26,3 4,6	33,4 3,9	31,7 5,9	18,9 4,0	26,8 4,1	0,003	0,835	2,81	0,034	0,435	29,4 1,8	,567
T3-β PSD, %	28,6 3,7	28,5 2,1	38,5 6,1	19,5 3,3	28,55 5,1	0,003	0,785	3,91	0,007	0,335	30,7 1,5	,462

LF PSD nu, %	74,9 3,9	71,1 2,5	68,6 5,1	79,4 3,6	58,7 5,7	0,003	0,720	5,53	0,001	0,584	64,2 1,4	,201
Cortisol, nM/L	469 49	374 26	446 56	386 47	391 44	0,002	0,909	1,43	0,237	0,689	370 12	,303
Testostero-ne, Z	0,84 0,71	0,37 0,46	0,74 0,74	-0,35 0,34	-0,11 0,41	0,003	0,843	2,66	0,042	0,479	0	
Sodium P, mM/L	149 2,8	140 1,5	140,4 2,1	145 2,0	148,2 1,2	0,004	0,609	9,15	10^{-5}	0,505	145 0,5	,034
Potassium P, mM/L	4,49 0,14	4,22 0,09	4,35 0,15	4,22 0,14	4,72 0,16	0,003	0,781	3,99	0,006	0,359	4,55 0,05	,104
Magnesium P, mM/L	0,85 0,02	0,83 0,01	0,84 0,01	0,84 0,01	0,82 0,01	0,002	0,918	1,27	0,291	0,421	0,90 0,01	,056
Phosphate P, mM/L	1,08 0,07	1,02 0,03	1,09 0,07	1,00 0,04	0,90 0,05	0,003	0,877	1,99	0,108	0,570	1,20 0,02	,167
Potassium Ex, mM/d	72 8	79 7	71 13	66 5	63 9	0,003	0,895	1,67	0,171	0,385	65 2	,269
Calcium Ex, mM/d	3,74 0,72	6,17 0,60	4,88 0,86	3,92 0,44	4,82 0,79	0,003	0,816	3,21	0,019	0,408	4,38 0,10	,214
$CD4^+CD25^+$ T-regs, %	18,8 1,1	21,1 0,6	19,1 1,1	20,8 1,2	17,6 1,3	0,003	0,843	2,65	0,042	0,311	16,4 0,3	,153
$CD4^+$ T-hel-per Lym, %	33,7 1,9	27,4 1,0	33,1 1,9	30,5 2,2	35,9 2,6	0,003	0,850	2,51	0,052	0,239	39,5 0,7	,164
CIC, units	42 6	34 2	30 3	34 4	43 5	0,003	0,777	4,08	0,006	0,575	45 2	,389
IgA Serum, g/L	2,03 0,05	1,58 0,09	1,91 0,14	1,78 0,11	1,92 0,12	0,003	0,803	3,49	0,013	0,434	1,875 0,03	,167
Phag Ind vs St. aur., %	98,5 0,34	98,6 0,24	99,3 0,21	99,2 0,19	98,9 0,32	0,003	0,727	5,34	0,001	0,288	98,3 0,19	,018
Mic Cou St. aur., B/Ph	59,7 1,9	61,3 1,6	63,2 1,9	64,1 1,9	63,9 1,9	0,003	0,904	1,52	0,209	0,391	61,6 1,1	,160

Table 6.2. Summary of Stepwise Analysis for Variables, ranked by criterion Lambda

Variables currently in the model	F to enter	p-level	Λ	F-value	p-value
BP Systolic, mmHg	298	10^{-6}	0,065	298	10^{-6}
Sex Index (M=1;F=2)	4,95	0,001	0,052	68,99	10^{-6}
Sodium P, mM/L	4,29	0,003	0,043	40,71	10^{-6}
T3-β PSD, %	3,77	0,007	0,036	29,97	10^{-6}
IgA Serum, g/L	3,48	0,011	0,031	24,33	10^{-6}
Phagocytosis Index vs Staph. aur., %	2,86	0,029	0,027	20,68	10^{-6}
Potassium Plasma, mM/L	3,39	0,013	0,023	18,42	10^{-6}
Deviation-δ, Hz	3,07	0,021	0,020	16,72	10^{-6}
P3-δ PSD, %	2,70	0,037	0,017	15,35	10^{-6}
F7-α PSD, %	2,83	0,030	0,015	14,32	10^{-6}
LF PSD nu, %	3,36	0,014	0,013	13,64	10^{-6}
$CD4^+$ T-helper Lymphocytes, %	2,39	0,059	0,011	12,87	10^{-6}
Potassium Excretion, mM/d	2,25	0,073	0,010	12,21	10^{-6}
Calcium Excretion, mM/d	2,28	0,069	0,009	11,66	10^{-6}
Circulating Immune Complex, units	2,11	0,088	0,008	11,16	10^{-6}
Testosterone, Z	1,82	0,135	0,007	10,67	10^{-6}
$CD4^+CD25^+$ T-regulatory Lymphoc, %	1,78	0,143	0,006	10,24	10^{-6}
Deviation-α, Hz	1,67	0,167	0,006	9,842	10^{-6}
Cortisol, nM/L	1,58	0,191	0,005	9,472	10^{-6}
O1-θ PSD, %	1,38	0,250	0,005	9,107	10^{-6}
Index-α, %	2,42	0,057	0,004	8,956	10^{-6}
C3-δ PSD, %	1,87	0,127	0,004	8,735	10^{-6}
F8-β PSD, %	2,44	0,056	0,003	8,632	10^{-6}
Fp2-α PSD, %	1,53	0,206	0,003	8,396	10^{-6}
Microbial Count Staph. aur., Bac/Ph	1,41	0,242	0,003	8,162	10^{-6}

Phosphate Plasma, mM/L	1,25	0,301	0,002	7,921	10^{-6}
Magnesium Plasma, mM/L	1,27	0,291	0,002	7,704	10^{-6}

Table 6.3. Variables currently not in model

Variables	AH II (11)	AH I (35)	High N (13)	No-rm (16)	Low N (13)	Wilks' Λ	Par-tial Λ	F to enter	p-level	Tole-rancy	Refe-rence (88)	Cv SD
BP Diasto-lic, mmHg	90,7 4,5	87,6 1,2	81,3 1,5	77,8 1,5	71,5 1,5	0,002	0,969	0,45	0,772	0,530	79,0 0,7	,083
Age, years	61,3 2,5	49,2 2,6	50,9 2,5	47,3 2,6	43,1 2,1	0,002	0,988	0,18	0,949	0,442	49,7 1,4	,257
Fp1-θ PSD, %	9,4 1,6	13,4 1,6	6,65 0,8	7,7 0,9	10,8 2,1	0,002	0,946	0,80	0,532	0,532	10,4 0,7	,588
C4-θ PSD, %	9,4 1,1	13,9 1,1	9,5 1,4	9,8 1,1	11,9 1,3	0,002	0,958	0,61	0,656	0,287	11,1 0,5	,442
O2-θ PSD, %	6,8 1,3	7,5 0,8	7,3 1,4	6,1 0,9	7,45 1,4	0,003	0,837	0,91	0,197	0,089	7,1 0,4	,554
F3-α PSD, %	31,6 5,8	29,5 2,2	30,1 6,1	30,9 4,3	26,9 5,7	0,015	0,978	0,37	0,831	0,432	33,2 1,7	,479
F4-α PSD, %	27,2 5,7	28,7 2,0	27,5 6,5	31,1 4,0	28,1 5,6	0,002	0,961	0,43	0,789	0,307	31,1 1,6	,485
T4-α PSD, %	31,6 5,9	29,3 2,5	22,0 4,4	26,7 3,1	24,5 4,7	0,002	0,940	0,89	0,476	0,412	29,0 1,6	,500
F3-β PSD, %	25,5 3,6	27,0 2,4	27,8 3,5	15,6 2,6	17,1 2,7	0,002	0,946	0,80	0,532	0,250	26,7 1,3	,463
C3-β PSD, %	27,1 3,6	26,3 2,0	26,7 3,8	21,6 2,8	16,6 2,4	0,002	0,971	0,41	0,799	0,192	25,45 1,1	,420
T5-β PSD, %	26,4 4,9	31,2 3,2	35,4 5,9	19,9 2,5	24,9 5,3	0,002	0,971	0,41	0,799	0,192	29,0 1,7	,536
O1-β PSD, %	31,6 4,8	28,0 3,2	26,1 4,4	16,4 3,1	18,4 2,7	0,002	0,958	0,61	0,656	0,287	26,3 1,5	,542
Entropy PSD O2	0,76 0,06	0,81 0,02	0,78 0,04	0,67 0,05	0,75 0,03	0,002	0,940	0,89	0,476	0,412	0,776 0,015	,178
Triangular Index, un.	8,5 0,9	11,1 0,7	10,8 0,7	10,2 1,1	13,7 1,0	0,002	0,946	0,80	0,532	0,250	11,2 0,26	,217
Body Mass Index,kg/m^2	27,5 1,3	27,2 0,7	27,4 0,8	27,9 0,9	25,5 0,6	0,003	0,893	0,929	0,290	0,288	24,2 0,3	,133
Cholesterol, mM/L	5,93 0,24	5,43 0,15	5,55 0,35	4,88 0,27	5,36 0,20	0,002	0,979	0,29	0,881	0,644	5,37 0,11	,192
Uric acid Ex, mM/d	4,01 0,56	4,25 0,25	3,71 0,45	3,44 0,30	3,29 0,38	0,002	0,940	0,89	0,476	0,412	3,00 0,08	,250
Sodium Ex, mM/d	238 37	221 14	189 21	217 24	194 22	0,002	0,953	0,69	0,601	0,323	154 3	,211
Chloride Ex, mM/d	206 26	235 19	186 20	187 20	190 22	0,002	0,930	0,79	0,539	0,160	167,5 3	,172
Chloride P, mM/L	106 2,2	99,3 1,2	99,8 1,7	104 1,6	106,0 1,0	0,004	0,978	0,37	0,832	0,468	101,5 0,4	,032
C-Reactive Prot., µg/L	2,92 0,18	2,54 0,11	2,64 0,26	2,14 0,20	2,50 0,15	0,002	0,981	0,28	0,893	0,644	2,18 0,08	,324
TNF-α, ng/L	6,94 0,42	6,06 0,25	6,29 0,60	5,15 0,46	5,97 0,33	0,002	0,981	0,28	0,893	0,644	4,90 0,17	,326
Interleukin-1, ng/L	4,69 0,30	5,06 0,21	4,62 0,30	4,49 0,35	4,78 0,43	0,002	0,943	0,85	0,500	0,232	4,51 0,08	,172
Interleukin-6, ng/L	7,22 0,76	4,62 0,55	4,76 0,91	3,64 0,81	4,61 0,88	0,002	0,955	0,65	0,626	0,673	4,25 0,15	,324
Bacteriuria, lgCFU/mL	0,59 0,26	1,55 0,17	1,13 0,25	1,23 0,27	1,24 0,25	0,003	0,961	0,43	0,789	0,307	0	**,98**

The 27-dimensional space of discriminant variables transforms into 4-dimensional space

of a canonical roots. For Root 1 r*=0,981 (Wilks' Λ=0,0023; $\chi^2_{(108)}$=432; p<10^{-6}), for Root 2 r*=0,855 (Wilks' Λ=0,0609; $\chi^2_{(78)}$=199; p<10^{-6}), for Root 3 r*=0,776 (Wilks' Λ=0,227; $\chi^2_{(50)}$=105; p<10^{-5}), and for Root 4 r*=0,655 (Wilks' Λ=0,571; $\chi^2_{(24)}$=40; p=0,022). The first root contains 83,8% of discriminative opportunities, the II 8,9%, the III 5,0%, the last 2,3%.

Table 6.4 presents raw and standardized coefficients for discriminant variables, which are used for the calculation of the discriminant root values for each person, which enables the visualization of each patient in the information space of the roots (Fig. 6.1).

Table 6.4. Standardized and Raw Coefficients and Constants for Variables

Coefficients	Standardized			Raw		
Variables currently in the model	Root 1	Root 2	Root 3	Root 1	Root 2	Root 3
BP Systolic, mmHg	-1,382	-0,101	0,060	-0,285	-0,021	0,012
Sex Index (Male=1;Female=2)	0,030	-0,784	0,906	0,079	-2,047	2,366
Sodium P, mM/L	0,248	-0,917	0,255	0,031	-0,115	0,032
T3-β PSD, %	-0,036	-0,188	-1,001	-0,0025	-0,0132	-0,070
IgA Serum, g/L	0,178	-0,156	-0,724	0,387	-0,339	-1,574
Phagocytosis Index vs Staph. aur., %	0,009	1,053	-0,348	0,008	0,909	-0,301
Potassium Plasma, mM/L	0,361	-0,764	0,307	0,677	-1,432	0,574
Deviation-δ, Hz	0,251	-0,419	0,261	1,000	-1,671	1,040
P3-δ PSD, %	0,368	-0,361	-0,453	0,021	-0,021	-0,026
F7-α PSD, %	0,680	-0,406	-0,985	0,049	-0,029	-0,071
LF PSD nu, %	0,108	0,275	0,821	0,007	0,017	0,052
CD4⁺ T-helper Lymphocytes, %	-0,329	0,137	-0,564	-0,046	0,019	-0,079
Potassium Excretion, mM/d	0,020	-0,597	-0,049	0,0006	-0,016	-0,0014
Calcium Excretion, mM/d	0,047	0,558	-0,598	0,016	0,186	-0,199
Circulating Immune Complex, units	0,066	-0,603	0,390	0,0043	-0,039	0,025
Testosterone, Z	-0,278	0,057	-0,646	-0,169	0,035	-0,393
CD4⁺CD25⁺ T-regulatory Lymphoc, %	-0,248	0,576	-0,523	-0,061	0,142	-0,129
Deviation-α, Hz	0,001	0,241	-0,209	0,0029	0,501	-0,433
Cortisol, nM/L	0,011	-0,207	0,076	0,0001	-0,0012	0,0004
O1-θ PSD, %	-0,576	-0,041	-0,285	-0,129	-0,009	-0,064
Index-α, %	-0,692	-0,003	-1,056	-0,026	-0,0001	-0,040
C3-δ PSD, %	-0,442	-0,011	-0,891	-0,024	-0,0006	-0,048
F8-β PSD, %	-0,232	-0,234	-0,679	-0,013	-0,013	-0,039
Fp2-α PSD, %	-0,250	0,508	0,603	-0,017	0,034	0,041
Microbial Count Staph. aur., Bac/Ph	-0,179	-0,371	0,399	-0,022	-0,045	0,049
Phosphate Plasma, mM/L	-0,004	0,452	-0,132	-0,022	2,282	-0,668
Magnesium Plasma, mM/L	0,088	0,343	-0,122	2,267	8,847	-3,150
			Constants	33,79	-68,69	30,55
			Eigenvalues	25,85	2,727	1,514
			Cumulative proportions	0,838	0,927	0,976

Table 6.5 shows the correlation coefficients of BP and tensioregulome with canonical discriminant roots; the cluster centroids of roots; and Z-scores of the variables. In addition, in view of the previously stated remark, extra-model variables are also included in the table.

Table 6.5. Correlations Variables-Canonical Roots, Means of Roots and Z-scores of Blood Pressure and Neuro-Endocrine, Immune and Metabolic (Tensioregulome) Variables

Variables currently in the model	Correlations Variables-Roots			AH II (11)	AH I (35)	High N (13)	Norm (16)	Low N (13)
Root 1 (83,8%)	**R 1**	**R 2**	**R 3**	**-8,8**	-2,4	+1,1	**+3,8**	**+8,1**
BP systolic	**-0,744**	-0,111	0,015	**+3,15**	+1,54	+0,64	+0,04	**-0,84**
BP diastolic				**+1,79**	+1,31	+0,35	-0,19	**-1,14**
Sodium Excretion				**+2,58**	+2,07	+1,07	+1,95	+1,23

Chloride Excretion				+2,74	+2,37	+1,45	+2,29	+1,36
Age				+0,92	-0,04	+0,10	-0,18	-0,52
Testosterone	-0,036	-0,025	-0,059	+0,84	+0,37	+0,74	-0,35	-0,11
Cortisol	-0,015	-0,039	-0,045	+0,89	+0,04	+0,68	+0,15	+0,19
C3-β PSD				+0,16	+0,08	+0,11	-0,36	-0,83
T4-α PSD				+0,18	+0,02	-0,48	-0,15	-0,31
F3-α PSD				-0,10	-0,24	-0,20	-0,14	-0,39
Phosphate Plasma	-0,044	0,075	-0,043	-0,58	-0,89	-0,57	-0,98	-1,49
Magnesium Plasma	-0,017	0,014	0,075	-1,02	-1,49	-1,21	-1,15	-1,56
C3-δ PSD	0,035	-0,108	-0,088	+0,14	-0,01	+0,33	0,04	+0,92
P3-δ PSD	0,026	-0,084	-0,061	-0,02	+0,12	+0,03	-0,04	+0,63
Deviation-δ	0,033	-0,124	0,023	-0,13	+0,10	-0,47	-0,05	+0,67
Triangular Index HRV				-1,13	-0,04	-0,15	-0,40	+1,03
Phagocytose Index vs St. aur.	0,035	0,069	-0,009	+0,14	+0,18	+0,59	+0,53	+0,35
Microbial Count for St. aur.	0,036	0,025	0,114	-0,19	-0,03	+0,16	+0,26	+0,23
Root 2 (8,9%)	R 1	R 2	R 3	-2,4	+0,6	+1,5	+1,3	-2,7
Sex Index	0,043	**-0,272**	0,118	+0,32	-0,27	-0,54	+0,05	+0,94
Sodium Plasma	0,023	**-0,222**	0,167	+0,71	-1,05	-0,93	+0,07	+0,65
Chloride Plasma				+1,45	-0,67	-0,54	+0,69	+1,38
Potassium Plasma	0,024	**-0,182**	-0,071	-0,12	-0,69	-0,43	-0,70	+0,35
CD4⁺ T-helper Lymphocytes	0,036	**-0,180**	-0,068	-0,89	-1,87	-0,99	-1,39	-0,55
Circulating Immune Compl	0,004	**-0,168**	0,053	-0,17	-0,62	-0,84	-0,60	-0,11
IgA Serum	0,009	**-0,127**	-0,025	+0,50	-0,94	+0,13	-0,31	+0,13
O1-θ PSD	0,012	**-0,104**	-0,092	+0,05	-0,01	-0,01	**-0,26**	+0,43
F7-α PSD	-0,026	**-0,104**	-0,068	+0,09	-0,03	-0,45	**-0,63**	-0,07
Root 3 (5,0%)	R 1	R 2	R 3	+0,6	-0,2	-2,0	+2,0	-0,5
T3-β PSD	-0,014	-0,008	-0,286	-0,15	-0,15	+0,55	-0,79	-0,15
F8-β PSD	-0,020	0,010	-0,181	-0,19	+0,24	+0,14	-0,63	-0,15
F3-β PSD				-0,10	+0,02	+0,09	-0,90	-0,78
T5-β PSD				-0,16	+0,15	+0,42	-0,58	-0,26
O1-β PSD				+0,37	+0,12	-0,01	-0,70	-0,56
Deviation-α	0,018	-0,074	-0,115	-0,29	+0,17	-0,21	-0,39	+0,39
Entropy PSD O2				-0,15	+0,24	+0,04	-0,78	-0,18
O2-θ PSD				-0,08	+0,11	+0,05	-0,24	+0,10
Cholesterol				+0,27	+0,12	+0,13	-0,43	+0,05
Body Mass Index				+1,15	+1,02	+0,93	+0,41	+1,00
Interleukin-6				+2,16	+0,27	+0,37	-0,44	+0,26
Tumor Necrosis Factor-α				+1,28	+0,73	+0,87	+0,15	+0,67
C-Reactive Protein				+1,05	+0,57	+0,65	-0,05	+0,45
LF PSD nu	-0,035	0,125	0,220	+0,68	+0,51	+0,34	+1,28	-0,34
Index-α	0,021	0,018	0,131	-0,04	-0,08	-0,12	+0,42	+0,09
Fp2-α PSD	0,017	0,017	0,088	-0,34	-0,11	-0,39	+0,09	-0,07
F4-α PSD				-0,26	-0,16	-0,24	+0,00	-0,20
Root 4 (2,3%)	R 1	R 2	R 4	-0,9	+0,9	-1,2	-0,5	+0,3
Calcium Excretion	-0,010	0,062	0,320	-0,68	+1,92	+0,54	-0,48	+0,47
Potassium Excretion	-0,025	0,038	0,107	+0,43	+0,80	+0,36	+0,05	-0,11
Uric acid Excretion				+1,35	+1,67	+0,95	+0,58	+0,38
CD4⁺CD25⁺ T-regulatory Ly	-0,014	0,109	0,117	+0,95	+1,85	+1,07	+1,74	+0,47
Interleukin-1				+0,17	+0,65	+0,09	-0,07	+0,29
C4-θ PSD				-0,36	+0,59	-0,34	-0,29	+0,16
Fp1-θ PSD				-0,16	+0,50	-0,61	-0,44	+0,06
Bacteriuria				+0,60	+1,58	+1,15	+1,25	+1,26

The localization along the major root axis of the patients with **AH II** (Fig. 6,1) in the extreme left (negative) zone reflects combination of maximum for sampling BP levels with **maximally increased** sodium and chloride excretion, plasma testosterone and cortisol levels, normal, but maximum for the sample levels of PSD of beta-rhythm in C3 locus and alpha-

rhythm in T4 and F3 loci, as well as minimally decreased plasma phosphate and magnesium levels. In addition, such patients are the oldest in the sample.

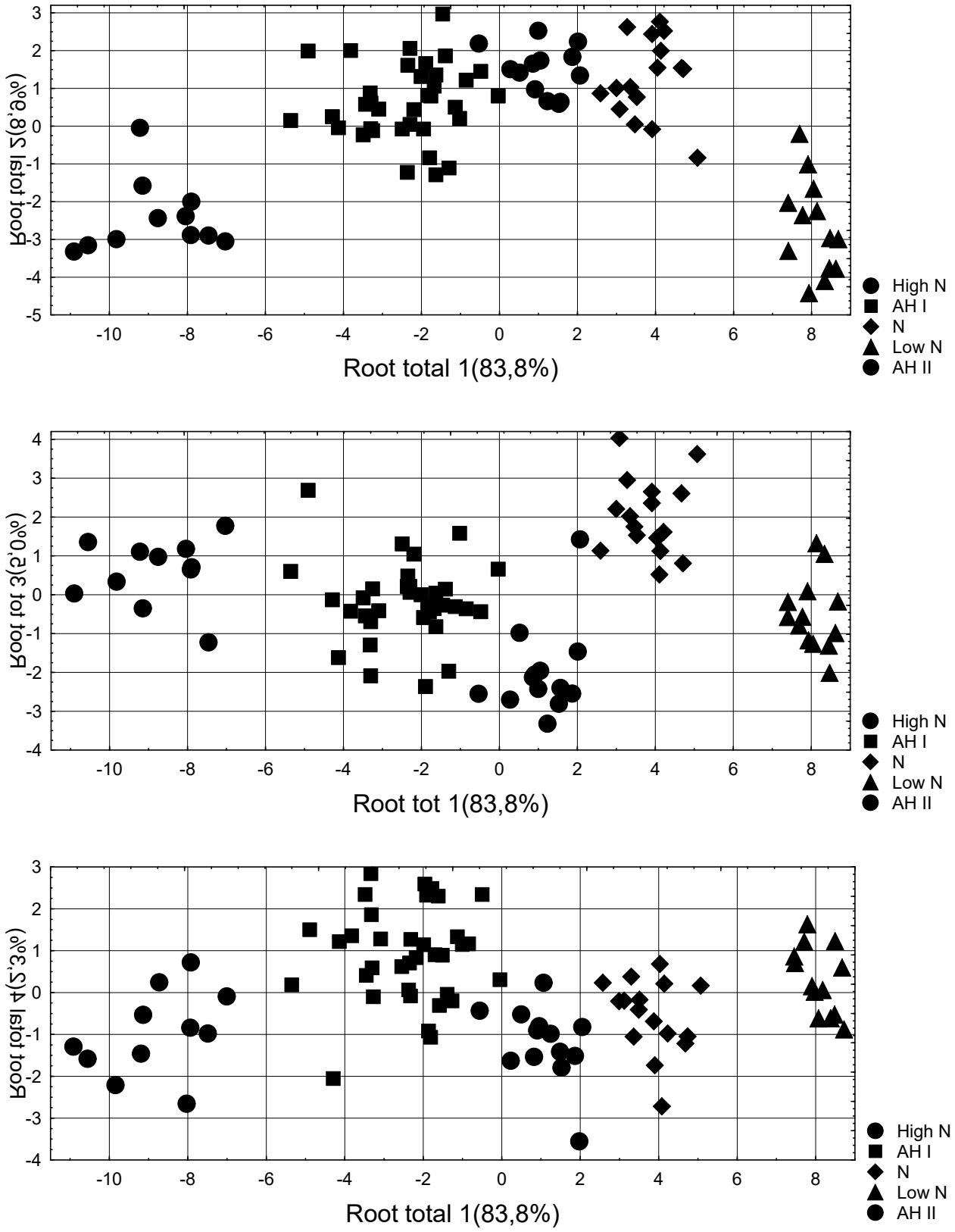

Fig. 6.1. Scattering of individual values of the discriminant roots of patients of different blood pressure clusters

On the other hand, **AH II** is accompanied by a **decreased** vagal tone (triangular index as marker), normal, but minimum for the sample levels of deviation of delta-rhythm and its PSD in C3 and P3 loci as well as activity and intensity of phagocytosis of Staph. aureus. At the opposite pole of the axis of the first root, there are patients with **Low Norm** BP, whose minimum BP is accompanied by, as a rule, **minimum** for the sample levels of the listed variables correlated with root inversely while **maximally** levels of variables correlated with root direct. In addition, such patients are the youngest in the sample. Clusters of patients with intermediate BP levels are also characterized by intermediate levels of the listed variables. Therefore, all 5 clusters are quite clearly demarcated already in the space of the major root.

Additional demarcation of patients with **AH II** and **Low Norm** BP occurs along the axis of the second root, the bottommost position of which reflects the **maximal** for the sample the PSD of alpha-rhythm in F7 locus and theta-rhythm in O1 locus, plasma levels of sodium, chloride and potassium, serum levels of IgA and CIC as well as minimal decreased blood level of T-helper lymphocytes. In addition, among the patients of both clusters, the share of women is the maximum for the sample (positive sex index).

Patients with **Norm** BP, in turn, are additionally distinguished from others along the axis of the third root due to a **maximally suppressed** deviation of alpha-rhythm, PSD of beta-rhythm in 5 loci and theta-rhythm in O2 locus, entropy of PSD in O2 locus, plasma cholesterol and IL-6 levels as well as minimum for the sample levels of TNF-alpha and C-RP, and body mass index.

On the other hand, a normal BP level is accompanied by normal, but maximum for the sample the index and PSD of alpha-rhythm in Fp2 and F4 loci, as well as maximally increased sympathetic tone, which is quite surprising, but the fact. This will be the subject of a special discussion in the future, and now we will limit ourselves to indicating the leading role in this situation the enhancing of beta-adrenergic vasodilatory outflows, reduction of ACE2 in the brain [Hirooka Y, 2020] and decrease in production of pro-inflammatory cytokines, however increasing anti-inflammatory cytokines such as IL-10 while alpha-adrenergic receptors have predominantly pro-inflammatory and vasoconstrictory actions [Stolk RF et al., 2016].

Finally, along the axis of the fourth root, the top positions are occupied by clusters of patients with **AH I**, which reflects their **maximum increased** levels of calcium, potassium and uric acid excretion, PSD of theta-rhythm in C4 and Fp1 loci, blood content of T-regulatory lymphocytes and IL-1 as well as bacteriuria as marker of pyelonephritis.

In general, all clusters on the planes of four roots are clearly delineated, which is documented by calculating the Mahalanobis distances (Table 6.6).

Table 6.6. Squared Mahalanobis Distances between Blood Pressure Clusters and F-values (df=27,6; for High N-N $p=10^{-6}$; for other pairs $p<10^{-6}$)

Blood Pressure Clusters	High Norm	AH I	Norm	Low Norm	AH II
High Norm	0	**20,6**	**24,0**	**70,4**	**120**
AH I	**4,96**	0	**45,8**	**121**	**54,2**
Norm	**4,38**	**12,8**	0	**40,7**	**175**
Low Norm	**11,6**	**29,1**	**7,43**	0	**287**
AH II	**18,2**	**11,6**	**29,0**	**43,5**	0

The same discriminant parameters can be used to identify the belonging of one or another person to one or another blood pressure cluster (Table 6.7).

Table 6.7. Coefficients and Constants for Classification Functions for Blood Pressure Clusters

Blood Pressure Clusters	High N	AH I	Norm	Low N	AH II

Variables currently in the model	p=,148	p=,398	p=,182	p=,148	p=,125
BP Systolic, mmHg	7,735	8,793	7,024	5,874	10,67
Sex Index (M=1;F=2)	-186,1	-178,1	-175,2	-171,9	-172,5
Sodium P, mM/L	-8,579	-8,630	-8,371	-7,905	-8,365
T3-β PSD, %	1,660	1,530	1,366	1,576	1,552
IgA Serum, g/L	-12,20	-18,19	-18,07	-11,94	-19,04
Phagocytosis Index vs Staph. aur., %	210,8	210,1	209,6	207,1	206,5
Potassium Plasma, mM/L	-85,29	-85,34	-80,81	-73,72	-84,89
Deviation-δ, Hz	-65,16	-62,72	-57,05	-47,79	-65,50
P3-δ PSD, %	-0,394	-0,453	-0,422	-0,167	-0,584
F7-α PSD, %	2,420	2,173	2,284	2,797	1,870
LF PSD nu, %	0,650	0,721	0,877	0,713	0,651
$CD4^+$ T-helper Lymphocytes, %	-2,295	-2,545	-2,820	-2,993	-2,151
Potassium Excretion, mM/d	-0,322	-0,304	-0,320	-0,245	-0,266
Calcium Excretion, mM/d	17,17	16,67	16,39	16,26	15,78
Circulating Immune Complex, units	-3,349	-3,252	-3,217	-3,097	-3,170
Testosterone, Z	22,10	21,92	20,05	20,17	22,62
$CD4^+CD25^+$ T-regulatory Lymphoc, %	19,64	19,35	18,88	18,33	19,34
Deviation-α, Hz	50,34	51,18	49,16	49,12	47,49
Cortisol, nM/L	-0,153	-0,157	-0,153	-0,151	-0,148
O1-θ PSD, %	0,605	1,009	0,020	-0,307	1,760
Index-α, %	2,931	2,988	2,712	2,717	3,091
C3-δ PSD, %	3,954	3,963	3,703	3,730	4,069
F8-β PSD, %	1,167	1,172	0,984	1,085	1,252
Fp2-α PSD, %	-0,715	-0,643	-0,615	-0,938	-0,580
Microbial Count Staph. aur., Bac/Ph	-16,01	-15,86	-15,88	-15,94	-15,49
Phosphate Plasma, mM/L	179,1	172,2	174,6	165,7	168,1
Magnesium Plasma, mM/L	-109,2	-155,5	-125,8	-153,2	-177,6
Constants	-9960	-9988	-9744	-9444	-9988

In this case, we can retrospectively recognize patients with one mistake only. Overall classification accuracy is 98,9% (Table 6.8).

Table 6.8. Classification Matrix for Blood Pressure Clusters

Group	Rows: Observed classifications Columns: Predicted classifications Percent Correct	High N p=,14773	AH I p=,39773	N p=,18182	Low N p=,14773	AH II p=,12500
High N	92,3	12	0	1	0	0
AH I	100,0	0	35	0	0	0
N	100,0	0	0	16	0	0
Low N	100,0	0	0	0	13	0
AH II	100,0	0	0	0	0	11
Total	98,9	12	35	17	13	11

At the next stage, an analysis of the correlations between the average Z-scores of systolic and diastolic BP, on the one hand, and the variables whose information is condensed in four discriminant roots, as well as not included in the model (see please Table 6.5), on the other hand, was performed.

A strong positive linear relationship between BP and the constellation of 3 EEG, 2 endocrine and 4 metabolic (more precisely, electrolyte) variables as well as age (Fig. 6.2), which obviously has an upregulating effect on the BP, was revealed.

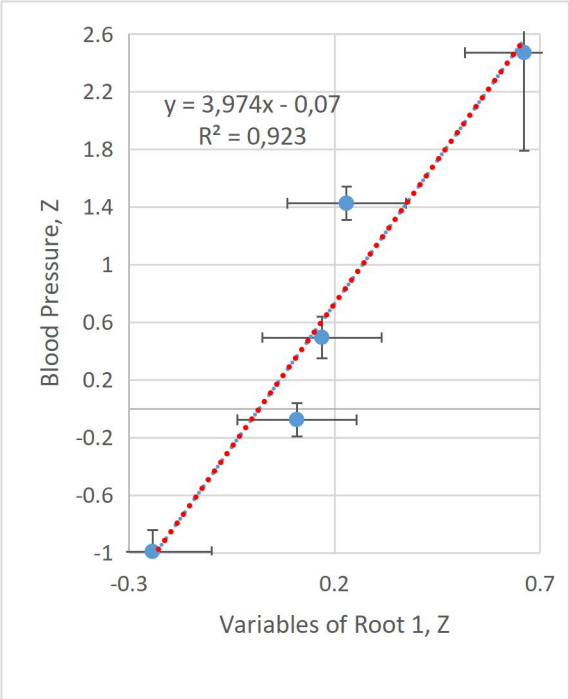

Fig. 6.2. Scatterplot of correlation between means of 10 variables of Root 1 (X-line) and means of systolic and diastolic blood pressure (Y-line)

Instead, the activity of delta-rhythm generating brain structures, vagal tone as well as the activity of microphages-neutrophils are negatively correlated with BP (Fig. 6.3).

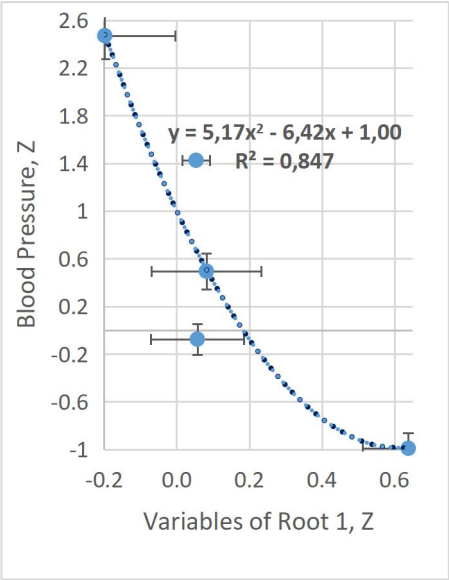

Fig. 6.3. Scatterplot of correlation between means of 6 variables of Root 1 (X-line) and means of systolic and diastolic blood pressure (Y-line)

If the downregulating vagal effect is quite expected and understandable, then the physiological basis of the negative relationship between phagocytosis and BP needs clarification and will be the subject of discussion.

In contrast to the described quazi-linear both direct and inverse relationships between BP and 16 variables, its relationship with 9 variables associated with the second root is non-linear, and satisfactorily approximated only by a third-order curve (Fig. 6.4). There is a paradoxical situation when the “extremes converge”, that is, patients with extreme BP levels (AH II and Low Norm) are characterized by almost identical and maximal for the sample levels of

variables. In particular, increased plasma levels of sodium and chloride, quasi-normal levels of potassium, IgA and CIC as well as PSD of O1-θ and F7-α rhythms, and reduced levels of T-helper lymphocytes. In addition, women predominate in both clusters. Instead, the intermediate values of the same variables decrease linearly from patients with AH I to Norm BP.

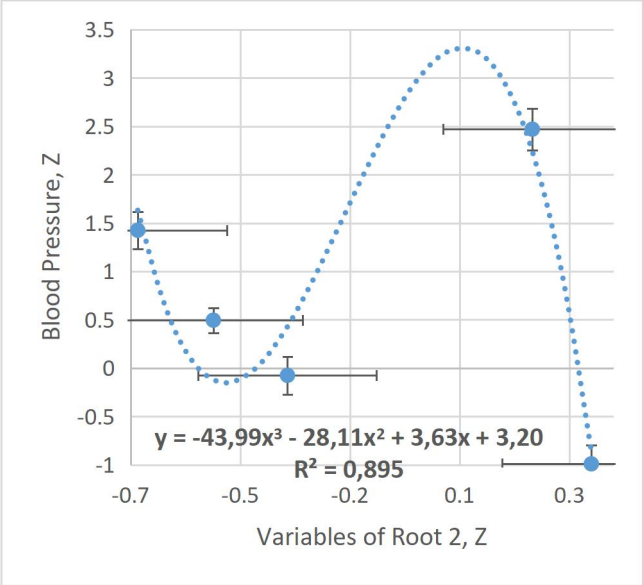

Fig. 6.4. Scatterplot of correlation between means of 9 variables of Root 2 (X-line) and means of systolic and diastolic blood pressure (Y-line)

Relationships of BP with variables related to the third root are approximated by curves of the second order (Figs. 6.6 and 6.6).

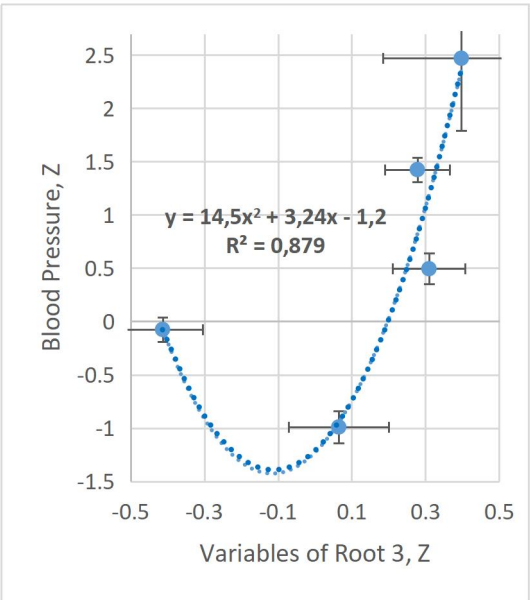

Fig. 6.5. Scatterplot of correlation between means of 13 variables of Root 3 (X-line) and means of systolic and diastolic blood pressure (Y-line)

Fig. 6.5 illustrates that patients with normal BP are characterized by reduced levels of PSD of beta-rhythm in 5 loci and entropy in O2 locus, as well as normal, but minimal for the sample PSD of theta-rhythm in O2 locus and deviation of alpha-rhythm. This is combined with normal, but minimal for the sample, levels of body mass index, cholesterol and pro-

inflammatory factors. It is interesting that these same parameters increase not only as BP increases, but also when it decreases.

An almost mirror-image Fig. 6.6 illustrates the presence in normotensive patients of increased sympathetic tone and normal, but maximal for the sample of three parameters of the alpha-rhythm, while these parameters are lower in both hypotensive and hypertensive patients.

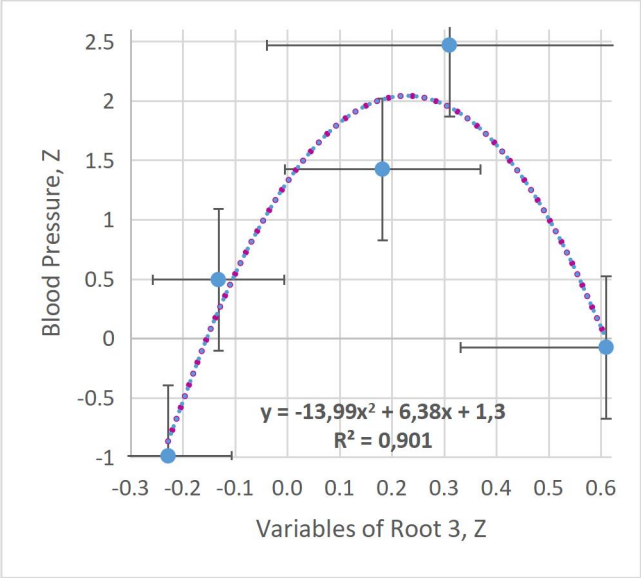

Fig. 6.6. Scatterplot of correlation between means of 5 variables of Root 3 (X-line) and means of systolic and diastolic blood pressure (Y-line)

The U-shaped form of the graph shown in Fig. 6.7, illustrates situations in which 2 EEGs, 3 metabolic, and 2 immune variables, as well as bacteriuria are equally minimal in patients with both AH II and Norm BP, slightly higher and also the same in both High Norm and Low Norm BP, instead, are maximally increased in patients with AH I.

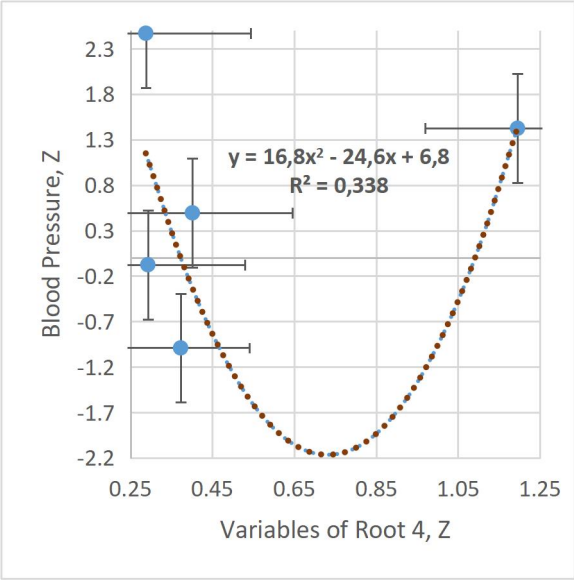

Fig. 6.7. Scatterplot of correlation between means of 8 variables of Root 4 (X-line) and means of systolic and diastolic blood pressure (Y-line)

In this Chapter is description of the hypothesis verification.

1. Hypothesis. There are distinct neuro-endocrine, immune, and metabolic profiles (tensioregulomes) associated with different blood pressure clusters.

Verification. This hypothesis was strongly confirmed. The discriminant analysis identified 42 tensioregulome parameters that significantly differentiated between blood pressure clusters ($p<10^{-6}$). The null hypothesis of no difference between clusters was rejected in favor of the alternative hypothesis.

2. Hypothesis. Blood pressure levels can be significantly determined or predicted by a combination of tensioregulome parameters.

Verification. This hypothesis was confirmed. The canonical correlation analysis showed that tensioregulome parameters could determine blood pressure levels with high accuracy ($R=0.983$, $R^2=0.966$, $p<10^{-6}$). The null hypothesis of no relationship was rejected.

3. Hypothesis. Certain EEG parameters have significant relationships with blood pressure levels.

Verification. This hypothesis was confirmed. EEG parameters, especially those related to beta and alpha rhythms, were found to be significant predictors of blood pressure in the regression models ($p<0.05$ for several EEG variables). The null hypothesis of no relationship was rejected for these parameters.

4. Hypothesis. Immune parameters, especially related to inflammation and phagocytosis, play an important role in the tensioregulome's relationship to blood pressure.

Verification. This hypothesis was partially confirmed. Some immune parameters, such as interleukin-6 and phagocytosis indices, were found to be significant in the models ($p<0.05$). However, not all immune parameters showed strong relationships. The null hypothesis was rejected for some, but not all, immune parameters.

5. Hypothesis. Metabolic factors, particularly related to electrolytes, lipids, and oxidative stress, are key components of the tensioregulome affecting blood pressure.

Verification. This hypothesis was confirmed. Metabolic factors, including electrolytes (e.g., sodium, potassium), lipids (e.g., cholesterol), and oxidative stress markers (e.g., superoxide dismutase), were significant predictors in the models ($p<0.05$). The null hypothesis of no relationship was rejected for these factors.

6. Hypothesis. There are both linear and non-linear relationships between tensioregulome parameters and blood pressure levels.

Verification. This hypothesis was confirmed. The analysis revealed both linear relationships (in regression models) and non-linear relationships (approximated by second- and third-order curves) between tensioregulome parameters and blood pressure. The null hypothesis of only linear relationships was rejected.

7. Hypothesis. The tensioregulome provides a more comprehensive model for understanding blood pressure regulation compared to individual physiological systems alone.

Verification. This hypothesis was confirmed. The combined tensioregulome model explained a higher proportion of blood pressure variance ($R^2=0.966$) compared to models based on individual systems (e.g., EEG alone: $R^2=0.941$, metabolic alone: $R^2=0.808$). The null hypothesis that the combined model is not superior was rejected.

Most of the hypotheses were confirmed, with strong statistical evidence ($p<0.05$ or lower) leading to the rejection of the corresponding null hypotheses. The tensioregulome concept was largely validated as a comprehensive approach to understanding blood pressure regulation.

Conclusions

Based on the detailed analysis presented in this Chapter, here are the key conclusions drawn from the study.

1. Tensioregulome Concept Validation. The study strongly supports the concept of the tensioregulome - a complex set of neuro-endocrine, immune, and metabolic parameters that accompany and potentially regulate blood pressure. This multifaceted approach provides a

more comprehensive understanding of blood pressure regulation than considering individual physiological systems alone.

2. Cluster Differentiation. The study identified distinct tensioregulome profiles associated with different blood pressure clusters (Low Normal, Normal, High Normal, AH I, and AH II). These clusters are clearly delineated in the multidimensional space of tensioregulome parameters, suggesting unique physiological states associated with each blood pressure level.

3. Predictive Power of Tensioregulome. The combination of tensioregulome parameters demonstrated high predictive power for blood pressure levels. The model explained 83.7% of the variance in blood pressure, indicating that blood pressure can be reliably estimated using tensioregulome parameters without direct measurement.

4. Key Components of Tensioregulome. a) EEG Parameters: Electrical activity of the brain, particularly beta and alpha rhythms in various loci, showed significant associations with blood pressure regulation. b) Immune Factors: Inflammatory markers (e.g., IL-6, C-reactive protein) and immune cell activities (e.g., phagocytosis) were identified as important components of the tensioregulome. c) Metabolic Factors: Electrolytes (sodium, potassium), lipids (cholesterol), and oxidative stress markers (superoxide dismutase, catalase) emerged as crucial elements in blood pressure regulation. d) Endocrine Factors: Hormones such as cortisol, testosterone, and calcitonin were found to be significant components of the tensioregulome.

5. Non-linear Relationships. The study revealed complex, non-linear relationships between many tensioregulome parameters and blood pressure. These relationships were often best described by second- or third-order curves, highlighting the intricate nature of blood pressure regulation.

6. Sex and Age Differences. The analysis identified significant effects of sex and age on the tensioregulome and its relationship to blood pressure, underscoring the importance of considering these demographic factors in blood pressure research and management.

7. Integration of Physiological Systems. The tensioregulome model demonstrates the intricate interplay between neural, endocrine, immune, and metabolic systems in blood pressure regulation, emphasizing the need for an integrated approach in hypertension research and treatment.

8. Potential for New Diagnostic and Therapeutic Approaches. The comprehensive tensioregulome model suggests potential new avenues for diagnosing hypertension risk and developing targeted therapies that address multiple physiological systems simultaneously.

9. Methodological Innovation. The study showcases the power of advanced statistical techniques, particularly discriminant analysis and canonical correlation analysis, in unraveling complex physiological relationships.

10. Confirmation of Known Factors and Discovery of New Ones. While confirming the role of well-established factors in blood pressure regulation (e.g., age, sex, sympathetic tone, testosterone, cortisol, cholesterol, sodium and uric acid levels, oxidative stress and inflammation markers), the study also identified less recognized factors (e.g., specific EEG patterns) as potentially important in blood pressure control.

12. Individualized Approach to Blood Pressure Management. The identification of distinct tensioregulome profiles associated with different blood pressure clusters suggests the potential for more personalized approaches to hypertension prevention and treatment.

These conclusions collectively underscore the complexity of blood pressure regulation and the potential of the tensioregulome concept to advance our understanding and management of hypertension.

So, the qualitative-quantitative clusters of blood pressure are very clearly different from each other by age, sex and the constellation of neuro-endocrine, immune and metabolic variables, which we called the ***Tensioregulome.***

Chapter 7

EVALUATION OF QUANTITATIVE-QUALITATIVE LEVELS OF BLOOD PRESSURE BY TENSIOREGULOME

Abstract

Background. Earlier we showed that the qualitative-quantitative clusters of blood pressure (BP) are very clearly different from each other by age, sex and the constellation of neuro-endocrine, immune and metabolic variables, which we called the **Tensioregulome** by analogy with the metabolome and the microbiome. The purpose of this study is detailing this concept. **Materials and methods.** Under an observations were 44 patients with chronic pyelonephritis and cholecystitis in the phase of remission. Testing was performed twice - on admission and after 7-10 days of standard balneotherapy. The main object of the study was BP. We determined parameters of EEG and HRV, plasma levels of adaptation hormones, electrolytes, lipids, and nitrogenous metabolites, components of humoral, cellular, and phagocytic links of immunity and microbiota as well as markers of pyelonephritis. **Results**. The forward stepwise program identified 42 Tensioregulome parameters as characteristic of quantitative-qualitative blood pressure clusters: 25 EEGs, sympathetic tone, cortisol, calcitonin, *Bifidobacteria* faeces, 5 metabolic and 5 immune parameters as well as sex and age. The accuracy of patient classification is 97,7%. Another 15 parameters were found to be characteristic, but were outside the discriminant model. Non-linear correlations between the BP and Tensioregulome parameters were revealed. **Conclusion**. The Tensioregulome allows us to reliably evaluate quantitative-qualitative levels of blood pressure without measuring it with a tonometer.

Keywords: blood pressure, Tensioregulome, EEG, HRV, hormones, immunity, metabolome, pyelonephritis.

Earlier we showed that the qualitative-quantitative clusters of blood pressure are very clearly different from each other by age, sex and the constellation of neuro-endocrine, immune and metabolic variables, which we called the **Tensioregulome** by analogy with the metabolome and the microbiome. The purpose of this chapter is detailing this concept.

In this Chapter, here are the research problems and hypotheses that appear to have been addressed.

Research Problems.

1. Can quantitative-qualitative levels of blood pressure be evaluated accurately using tensioregulome parameters **without direct blood pressure measurement**?
2. What is the relative importance of different components of the tensioregulome (EEG, HRV, hormones, immunity, metabolome) in determining blood pressure levels?
3. How do **changes** in tensioregulome parameters relate to **changes** in blood pressure following balneotherapy?
4. Are there non-linear relationships between tensioregulome parameters and blood pressure levels?
5. Can the tensioregulome concept provide a more comprehensive understanding of blood pressure regulation than individual physiological systems alone?

Hypotheses.

1. Quantitative-qualitative levels of blood pressure can be accurately evaluated using a combination of tensioregulome parameters without direct blood pressure measurement.
2. Different components of the tensioregulome (EEG, HRV, hormones, immunity, metabolome) have varying degrees of importance in determining blood pressure levels.
3. Changes in tensioregulome parameters following balneotherapy are significantly correlated with changes in blood pressure.

4. There are significant non-linear relationships between certain tensioregulome parameters and blood pressure levels.

5. The combined tensioregulome model provides a more comprehensive and accurate prediction of blood pressure levels compared to models based on individual physiological systems.

6. Specific EEG parameters are significant predictors of blood pressure levels.

7. Immune and metabolic parameters, especially those related to inflammation and oxidative stress, play a crucial role in blood pressure regulation within the tensioregulome framework.

8. The tensioregulome concept can reveal complex interactions between different physiological systems in blood pressure regulation.

These research problems and hypotheses reflect the study's aim to validate and expand upon the tensioregulome concept introduced in the previous chapter, with a particular focus on its predictive power and the relative importance of its components in blood pressure regulation.

The author of the concept of stress-age syndrome Frolkis VV [1990] proposed a stress coefficient, the numerator of which is represented by the catecholamines, ACTH, cortisol, vasopressin, and the denominator is the sex steroid hormones, thyroxine, TSH, as well as anti-stress neuropeptides. The authors of the concept of general adaptation reactions Garkavi LKh et al. [1990] added aldosterone to the list of anti-stress hormones. Based on the available data and the algorithm of the Truskavetsian Scientific School of Balneology [Gozhenko AI et al., 2021; Popovych IL et al., 2022], we offer our own modification of the neuro-hormonal stress index (NHSI) by combining Z-scores of BSI and hormones:

Frolkis's NHSI = (**BSI + cortisol - testosterone – triiodothyronine**)/4;

Garkavi's NHSI = (**BSI + cortisol - testosterone – triiodothyronine - aldosterone**)/5.

We again applied discriminant analysis, but this time deliberately did not include either systolic or diastolic BP in the list of variables. The program forward stepwise included in the discriminant model 42 parameters. The following variables were identified as characteristic. Integral parameters of the organism: **age** and **sex index** (as a ratio between the number of the male and female in the cluster); 25 EEG parameters that reflect main rhythms: **delta** (5), **theta** (5), **alpha** (6) and **beta** (4) as well as **entropy** (5); HRV-marker of **sympathetic tone**, two hormones such as **cortisol** (raw) and **calcitonin** (standardized by sex), 5 parameters of **immunity** and 5 parameters of **metabolome** as well as ***Bifidobacteria*** as representative of microbiome (Tables 7.1 and 7.2).

Table 7.1. Discriminant Function Analysis Summary for Variables, their actual levels for Clusters of Blood Pressure as well as Reference levels and Coefficients of Variability

Step 42, N of vars in model: 42; Grouping: 5 grs; Wilks' Λ: 0,0018; approx. $F_{(168)}$=3,9; $p<10^{-6}$

Variables currently in the model	Clusters of Blood Pressure (n)					Parameters of Wilk's Statistics						
	Norm (16)	High N (13)	AH I (35)	Low N (13)	AH II (11)	Wilks' Λ	Partial Λ	F-remove (4,42)	p-level	Tolerancy	Reference (88)	Cv
Sex Index (M=1; F=2)	1,25 0,11	1,00 0,00	1,11 0,05	1,62 0,14	1,36 0,15	0,003	0,664	5,31	0,001	0,285	1,23 0,04	,343
Age, years	47,3 2,6	50,9 2,5	49,2 2,6	43,1 2,1	61,3 2,5	0,002	0,862	1,68	0,172	0,332	49,7 1,4	,257
Deviation-δ, Hz	0,66 0,08	0,55 0,04	0,70 0,04	0,85 0,10	0,64 0,07	0,003	0,709	4,30	0,005	0,365	0,67 0,03	,395
F4-δ PSD, %	40,5 6,5	35,5 8,4	30,2 3,0	44,1 8,0	40,1 9,3	0,003	0,550	8,61	10^{-4}	0,025	31,25 2,1	,624
T3-δ PSD, %	44,3 6,4	27,3 5,8	29,6 2,1	40,9 7,7	28,8 6,6	0,002	0,823	2,25	0,079	0,088	28,6 1,8	,596

C3-δ PSD, %	28,8 3,3	37,5 7,5	27,9 2,7	43,5 7,4	30,4 6,8	0,003	0,578	7,68	10^{-4}	0,032	28,0 1,8	,602
P3-δ PSD, %	24,8 3,5	26,0 5,6	27,7 2,8	36,7 7,1	25,2 6,0	0,003	0,683	4,88	0,003	0,088	25,6 1,9	,694
Amplitude-θ, μV	9,4 0,9	7,7 0,6	9,7 0,9	8,6 1,0	7,7 1,0	0,003	0,718	4,13	0,007	0,184	7,75 0,3	,376
F8-θ PSD, %	8,1 1,3	7,3 0,6	11,3 1,2	10,5 2,0	7,2 1,2	0,003	0,615	6,56	10^{-3}	0,131	9,8 0,5	,492
C4-θ PSD, %	9,8 1,1	9,5 1,4	13,9 1,1	11,9 1,3	9,4 1,1	0,003	0,636	6,01	0,001	0,110	11,1 0,5	,442
P4-θ PSD, %	7,3 0,7	7,2 0,8	10,2 0,9	9,3 1,3	9,4 1,6	0,004	0,432	13,8	10^{-6}	0,073	8,75 0,5	,545
O1-θ PSD, %	7,0 0,9	8,2 1,4	8,2 0,8	10,3 1,7	8,5 1,6	0,003	0,699	4,52	0,004	0,167	8,2 0,5	,584
Index-α, %	62,6 6,0	47,3 8,7	48,4 5,7	53,4 6,6	49,5 8,5	0,003	0,714	4,20	0,006	0,099	50,7 3,0	,560
Deviation-α, Hz	0,81 0,10	0,91 0,10	1,11 0,12	1,23 0,15	0,86 0,10	0,003	0,604	6,89	10^{-3}	0,313	1,02 0,06	,527
Fp2-α PSD, %	34,3 4,7	27,2 4,1	31,3 2,4	31,9 5,1	27,9 4,2	0,003	0,720	4,09	0,007	0,078	32,9 1,6	,448
F4-α PSD, %	31,1 4,0	27,5 6,5	28,7 2,0	28,1 5,6	27,2 5,7	0,002	0,783	2,91	0,033	0,025	31,1 1,6	,485
F7-α PSD, %	18,4 3,4	21,1 3,9	27,1 2,5	26,6 3,7	28,9 6,1	0,003	0,591	7,26	10^{-4}	0,138	27,6 1,5	,522
T4-α PSD, %	26,7 3,1	22,0 4,4	29,3 2,5	24,5 4,7	31,6 5,9	0,003	0,600	7,01	10^{-3}	0,072	29,0 1,6	,500
Laterality-β, %	-13 5,5	-13,0 10,8	-3,1 4,7	-6,2 7,2	-34 6,4	0,003	0,539	9,00	10^{-4}	0,268	-0,9 3,6	**SD 34**
T3-β PSD, %	19,5 3,3	38,5 6,1	28,5 2,1	28,55 5,1	28,6 3,7	0,003	0,576	7,74	10^{-4}	0,072	30,7 1,5	,462
C3-β PSD, %	21,6 2,8	26,7 3,8	26,3 2,0	16,6 2,4	27,1 3,6	0,004	0,515	9,89	10^{-5}	0,029	25,45 1,1	,420
O1-β PSD, %	16,4 3,1	26,1 4,4	28,0 3,2	18,4 2,7	31,6 4,8	0,003	0,677	5,02	0,002	0,167	26,3 1,5	,542
Entropy PSD F3	0,78 0,05	0,81 0,04	0,89 0,02	0,76 0,05	0,81 0,04	0,003	0,559	8,29	10^{-4}	0,126	0,862 0,012	,130
Entropy PSD T3	0,78 0,04	0,75 0,04	0,90 0,01	0,76 0,05	0,83 0,04	0,004	0,512	10,0	10^{-5}	0,111	0,857 0,012	,131
Entropy PSD T5	0,81 0,05	0,77 0,04	0,83 0,02	0,73 0,04	0,74 0,08	0,002	0,851	1,83	0,140	0,256	0,825 0,014	,156
Entropy PSD T6	0,76 0,05	0,80 0,03	0,83 0,03	0,85 0,02	0,74 0,07	0,002	0,777	3,01	0,028	0,160	0,825 0,013	,149
Entropy PSD P3	0,82 0,02	0,81 0,03	0,82 0,02	0,77 0,05	0,80 0,05	0,002	0,758	3,35	0,018	0,132	0,802 0,014	,167
LF PSD nu, %	79,4 3,6	68,6 5,1	71,1 2,5	58,7 5,7	74,9 3,9	0,003	0,533	9,19	10^{-4}	0,324	64,2 1,4	,201
Cortisol, nM/L	386 47	446 56	374 26	391 44	469 49	0,002	0,897	1,21	0,321	0,474	370 12	,303
Calcitonin, Z	-0,47 0,33	-0,94 0,19	-0,78 0,09	-0,13 0,35	-0,69 0,30	0,002	0,862	1,68	0,172	0,481	0 0,21	
Interleukin-6, ng/L	3,64 0,81	4,76 0,91	4,62 0,55	4,61 0,88	7,22 0,76	0,002	0,810	2,46	0,060	0,346	4,25 0,15	,324
CIC, units	34 4	30 3	34 2	43 5	42 6	0,002	0,776	3,03	0,028	0,461	45 2	,389
$CD4^+$ T-helper Lym, %	30,5 2,2	33,1 1,9	27,4 1,0	35,9 2,6	33,7 1,9	0,002	0,835	2,07	0,102	0,189	39,5 0,7	,164
Phag Ind vs St. aur., %	99,2 0,19	99,3 0,21	98,6 0,24	98,9 0,32	98,5 0,34	0,002	0,764	3,25	0,021	0,224	98,3 0,19	,018
Micr. Count	64,1	63,2	61,3	63,9	59,7	0,002	0,837	2,05	0,105	0,327	61,6	,160

St. aur., B/Ph	1,9	1,9	1,6	1,9	1,9						1,1	
Sodium Plasma, mM/L	145 2,0	140,4 2,1	140 1,5	148,2 1,2	149 2,8	0,004	0,452	12,7	10^{-6}	0,288	145 0,5	,034
Magnesium P, mM/L	0,84 0,01	0,84 0,01	0,83 0,01	0,82 0,01	0,85 0,02	0,003	0,700	4,50	0,004	0,279	0,90 0,01	,056
Phosphate P, mM/L	1,00 0,04	1,09 0,07	1,02 0,03	0,90 0,05	1,08 0,07	0,004	0,453	12,7	10^{-6}	0,127	1,20 0,02	,167
Potassium P, mM/L	4,22 0,14	4,35 0,15	4,22 0,09	4,72 0,16	4,49 0,14	0,004	0,452	12,7	10^{-6}	0,288	4,55 0,05	,104
Potassium Excr, mM/d	66 5	71 13	79 7	63 9	72 8	0,002	0,868	1,60	0,192	0,374	65 2	,269
Calcium Excretion, mM/d	3,92 0,44	4,88 0,86	6,17 0,60	4,82 0,79	3,74 0,72	0,002	0,845	1,93	0,123	0,454	4,38 0,10	,214
Bifidobacteria, lgCFU/g	5,52 0,36	5,78 0,24	5,69 0,19	5,38 0,35	5,35 0,30	0,002	0,846	1,92	0,125	0,282	6,94 0,01	,011

Table 7.2. Summary of Stepwise Analysis for Variables, ranked by criterion Lambda

Variables currently in the model	F to enter	p-level	Λ	F-value	p-value
Sex Index (M=1; F=2)	5,61	10^{-3}	0,787	5,61	10^{-3}
Sodium Plasma, mM/L	4,45	0,003	0,647	4,99	10^{-4}
Entropy PSD T3	4,29	0,003	0,534	4,79	10^{-6}
Age, years	3,69	0,008	0,451	4,56	10^{-6}
Deviation-δ, Hz	3,63	0,009	0,381	4,44	10^{-6}
Phagocytic Ind vs St. aur., %	3,52	0,011	0,323	4,36	10^{-6}
$CD4^+$ T-helper Lymphoc, %	3,23	0,017	0,276	4,27	10^{-6}
LF PSD nu, %	3,79	0,007	0,230	4,31	10^{-6}
T3-β PSD, %	2,79	0,032	0,201	4,21	10^{-6}
P3-δ PSD, %	2,53	0,048	0,176	4,10	10^{-6}
F7-α PSD, %	2,11	0,089	0,158	3,96	10^{-6}
O1-β PSD, %	2,24	0,073	0,141	3,86	10^{-6}
Laterality-β, %	2,51	0,050	0,123	3,82	10^{-6}
Phosphate Plasma, mM/L	2,67	0,039	0,107	3,81	10^{-6}
Magnesium Plasma, mM/L	3,02	0,024	0,091	3,84	10^{-6}
Interleukin-6, ng/L	2,51	0,050	0,079	3,82	10^{-6}
F8-θ PSD, %	2,42	0,057	0,069	3,80	10^{-6}
Fp2-α PSD, %	2,27	0,071	0,061	3,77	10^{-6}
CIC, units	1,89	0,123	0,055	3,71	10^{-6}
O1-θ PSD, %	2,12	0,089	0,048	3,69	10^{-6}
T3-δ PSD, %	1,87	0,127	0,043	3,64	10^{-6}
Deviation-α, Hz	2,08	0,095	0,038	3,62	10^{-6}
Calcium Excretion, mM/d	2,07	0,095	0,033	3,60	10^{-6}
F4-α PSD, %	1,97	0,110	0,030	3,58	10^{-6}
C4-θ PSD, %	2,03	0,102	0,026	3,57	10^{-6}
Amplitude-θ, μV	2,44	0,057	0,022	3,60	10^{-6}
Index-α, %	2,23	0,077	0,019	3,61	10^{-6}
P4-θ PSD, %	2,90	0,030	0,016	3,69	10^{-6}
Entropy PSD P3	3,29	0,017	0,013	3,80	10^{-6}
Entropy PSD T6	2,83	0,033	0,011	3,87	10^{-6}
Entropy PSD F3	2,40	0,061	0,009	3,91	10^{-6}
$CD4^+CD25^+$ T-regulatory, %	2,09	0,095	0,008	3,92	10^{-6}
Microb Count St. aur., B/Ph	1,74	0,156	0,007	3,90	10^{-6}
Cortisol, nM/L	1,77	0,150	0,006	3,88	10^{-6}
F4-δ PSD, %	1,73	0,159	0,005	3,87	10^{-6}
T4-α PSD, %	1,78	0,148	0,005	3,86	10^{-6}
C3-β PSD, %	1,47	0,225	0,004	3,83	10^{-6}
C3-δ PSD, %	4,29	0,005	0,003	4,06	10^{-6}
Calcitonin, Z	1,36	0,263	0,003	4,01	10^{-6}

Entropy PSD T5	1,53	0,211	0,002	3,99	10^{-6}
***Bifidobacteria* feces, lgCFU/g**	1,21	0,322	0,002	3,94	10^{-6}
Potassium Excretion, mM/d	1,60	0,192	0,002	3,93	10^{-6}

Another 13 variables also were found to be characteristic, but were outside the discriminant model due to duplication/redundancy of information (Table 7.3).

Table 7.3. Summary for Variables currently not in the model

Variables	Norm (16)	High N (13)	AH I (35)	Low N (13)	AH II (11)	Wilks' Λ	Partial Λ	F to enter	p-level	Tolerancy	Reference (88)	Cv
Electrokinetic Index, %	46,6 2,7	42,7 2,6	44,7 2,3	50,1 2,5	31,7 2,1	0,002	0,836	2,06	0,103	0,291	40,9 1,1	,250
T5-β PSD, %	19,9 2,5	35,4 5,9	31,2 3,2	24,9 5,3	26,4 4,9	0,143	0,939	0,64	0,634	0,394	29,0 1,7	,536
Triangular Index, units	10,2 1,1	10,8 0,7	11,1 0,7	13,7 1,0	8,5 0,9	0,002	0,682	4,89	0,002	0,102	11,2 0,26	,217
Testostero-ne, Z	-0,35 0,34	0,74 0,74	0,37 0,46	-0,11 0,41	0,84 0,71	0,140	0,920	0,86	0,494	0,395	0 0,21	
Aldosterone, pM/L	227 6	232 11	229 4	221 5	226 5	0,149	0,976	0,24	0,913	0,286	238 5	,187
Triiodothyronine, nM/L	2,17 0,31	1,72 0,24	1,95 0,11	2,24 0,20	1,90 0,16	0,147	0,964	0,38	0,825	0,292	2,20 0,05	,227
Frolkis's NHSI	0,46 0,35	0,23 0,25	0,23 0,19	-0,10 0,22	0,54 0,29	0,002	0,827	2,19	0,086	0,093	0 0,21	
Garkavi's NHSI	0,41 0,28	0,21 0,20	0,22 0,15	-0,01 0,18	0,49 0,25	0,002	0,903	1,13	0,357	0,160	0 0,21	
Popovych's Strain Ind-1	0,16 0,03	0,14 0,02	0,18 0,02	0,11 0,02	0,11 0,02	0,143	0,939	0,64	0,634	0,394	0,10 0,01	,559
Monocytes, %	5,38 0,49	6,39 0,55	6,55 0,36	5,15 0,61	5,05 0,48	0,144	0,948	0,54	0,704	0,449	6,00 0,05	,166
IgA Serum, g/L	1,78 0,11	1,91 0,14	1,58 0,09	1,92 0,12	2,03 0,05	0,147	0,966	0,36	0,837	0,312	1,875 0,03	,167
Cholesterol, mM/L	4,88 0,27	5,55 0,35	5,43 0,15	5,36 0,20	5,93 0,24	0,002	0,697	4,57	0,004	0,284	5,37 0,11	,192
VLD LP Cholester, Z	0,16 0,26	-0,51 0,19	0,39 0,16	-0,41 0,18	0,19 0,21	0,002	0,682	4,89	0,002	0,102	0	

The 42-dimensional space of discriminant variables transforms into 4-dimensional space of a canonical roots. For Root 1 r*=0,956 (Wilks' Λ=0,0018; $\chi^2_{(168)}$=401; $p<10^{-6}$), for Root 2 r*=0,908 (Wilks' Λ=0,0207; $\chi^2_{(123)}$=246; $p<10^{-6}$), for Root 3 r*=0,825 (Wilks' Λ=0,118; $\chi^2_{(80)}$=136; $p=10^{-4}$), and for Root 4 r*=0,794 (Wilks' Λ=0,370; $\chi^2_{(39)}$=63; p=0,008). The first root contains 55,2% of discriminative opportunities, the II 24,6%, the III 12,2%, the last 9,0%.

Table 7.4 presents standardized and raw coefficients for discriminant variables, which are used for the calculation of the discriminant root values for each person, that enables the visualization of each patient in the information space of the roots.

Table 7.4. Standardized and Raw Coefficients and Constants for Variables

Coefficients	Standardized				Raw			
Variables in the model	Root 1	Root 2	Root 3	Root 4	Root 1	Root 2	Root 3	Root 4
Sex Index (M=1; F=2)	-0,539	0,175	-1,140	0,031	-1,407	0,457	-2,978	0,080
Sodium Plasma, mM/L	-1,397	0,196	-0,341	-0,118	-0,176	0,025	-0,043	-0,015
Entropy PSD T3	-0,301	-2,072	-0,671	0,855	-2,391	-16,44	-5,320	6,779
Age, years	0,573	0,229	0,158	-0,297	0,048	0,0193	0,0133	-0,0249
Deviation-δ, Hz	-0,752	-0,123	-0,592	0,206	-2,998	-0,492	-2,360	0,820
Phagoc. Ind vs St. aur., %	0,710	-0,439	0,700	0,406	0,613	-0,379	0,605	0,351
$CD4^+$ T-helper Lymph, %	-0,861	-0,057	0,333	-0,432	-0,120	-0,008	0,046	-0,060

LF PSD nu, %	0,657	-0,933	-0,681	0,152	0,041	-0,059	-0,043	0,010
T3-β PSD, %	1,606	2,057	-0,284	0,199	0,113	0,145	-0,020	0,014
P3-δ PSD, %	0,621	1,914	0,612	-0,037	0,036	0,110	0,035	-0,002
F7-α PSD, %	-1,573	-0,165	0,800	0,631	-0,113	-0,012	0,058	0,045
O1-β PSD, %	-1,128	-0,936	-0,250	-0,092	-0,080	-0,066	-0,018	-0,006
Laterality-β, %	-0,022	1,337	0,562	0,224	-0,001	0,053	0,022	0,009
Phosphates Plasma, mM/L	1,347	1,499	0,431	-1,026	6,800	7,569	2,175	-5,181
Magnesium Plasma, mM/L	0,657	0,479	0,429	-0,761	16,93	12,35	11,08	-19,61
Interleukin-6, ng/L	-0,741	-0,119	0,228	0,005	-0,296	-0,048	0,091	0,002
F8-θ PSD, %	0,933	-1,528	-0,414	0,385	0,174	-0,285	-0,077	0,072
Fp2-α PSD, %	1,770	-0,192	-1,018	0,150	0,120	-0,013	-0,069	0,010
CIC, units	-0,197	0,628	-0,421	0,083	-0,013	0,040	-0,027	0,005
O1-θ PSD, %	-0,756	1,182	0,076	-0,449	-0,170	0,265	0,017	-0,101
T3-δ PSD, %	0,831	0,142	-1,147	0,858	0,042	0,007	-0,058	0,044
Deviation-α, Hz	0,862	0,631	0,465	0,419	1,789	1,308	0,965	0,869
Calcium Excretion, mM/d	0,444	0,117	0,379	0,291	0,148	0,039	0,126	0,097
F4-α PSD, %	-2,541	0,761	1,660	-0,811	-0,159	0,048	0,104	-0,051
C4-θ PSD, %	0,884	1,545	0,965	-0,014	0,187	0,327	0,204	-0,003
Amplitude-θ, μV	0,678	-1,087	-0,415	0,207	0,183	-0,294	-0,112	0,056
Index-α, %	0,300	1,644	0,754	0,562	0,011	0,062	0,028	0,021
P4-θ PSD, %	-2,806	-0,450	0,162	0,820	-0,684	-0,110	0,040	0,200
Entropy PSD P3	1,005	0,812	-0,147	-0,738	8,335	6,735	-1,219	-6,124
Entropy PSD T6	0,626	0,999	0,525	-0,191	4,183	6,672	3,504	-1,275
Entropy PSD F3	-1,753	-0,836	0,403	0,001	-12,75	-6,080	2,932	0,007
CD4$^+$CD25$^+$ T-regulator, %	-0,026	-0,639	0,451	-0,034	-0,006	-0,157	0,111	-0,008
Micr Count St. aur., B/Ph	-0,141	0,016	-0,795	-0,284	-0,017	0,002	-0,097	-0,035
Cortisol, nM/L	-0,345	0,018	-0,036	-0,414	-0,002	0,0001	-0,0002	-0,0024
F4-δ PSD, %	-3,947	-1,438	1,639	-0,335	-0,167	-0,061	0,069	-0,014
T4-α PSD, %	-2,291	-0,633	0,801	0,121	-0,161	-0,044	0,056	0,009
C3-β PSD, %	-3,618	-0,781	2,312	0,802	-0,342	-0,074	0,218	0,076
C3-δ PSD, %	-3,216	-0,440	2,224	0,808	-0,172	-0,023	0,119	0,043
Calcitonin, Z	0,461	0,208	-0,281	-0,078	0,540	0,244	-0,330	-0,091
Entropy PSD T5	0,750	0,200	0,058	-0,230	4,760	1,272	0,368	-1,457
***Bifidobacteria* fec, lgCFU/g**	0,608	-0,034	-0,456	-0,327	0,521	-0,029	-0,390	-0,281
Potassium Excretio, mM/d	-0,365	0,095	0,404	0,424	-0,010	0,003	0,011	0,012
				Constants	-30,81	23,14	-70,51	-12,82
				Eigenvalues	10,49	4,688	2,135	1,706
				Cumulative proportions	0,552	0,798	0,910	1

The localization along the major root axis of the patients with **AH II** (Fig. 7.1) in the extreme left (negative) zone reflects combination of maximum for sampling BP levels with **maximally increased** plasma IL-6 and testosterone levels, as well as normal, but maximum for the sample levels of cholesterol and PSD of beta-rhythm in O1 locus and alpha-rhythm in F7 locus. On the other hand, **AH II** is accompanied by normal, but minimum for the sample levels of the index and PSD of alpha-rhythm in F4 locus, amplitude of theta-rhythm, PSD of delta-rhythm in T3 locus as well as intensity of phagocytosis of Staph. aureus (Table 7.5).

At the opposite pole of the axis of the first root, there are patients with **Norm** BP, which are characterized, as a rule, by the **minimum**/**maximum** levels of the listed variables comparable to those in patients with **AH II**. It is interesting that in the latter patients (as well as with **AH I**), the sex- and age-normalized testosterone levels are increased almost equally in men and women, while among patients with **Norm** BP, the testosterone level in men is in the lower normal range, and in women - in the upper range.

The projections of patients with **High Norm** BP on the axis of the first root are only slightly shifted to the left and are densely intertwined, which is understandable, instead, the

cluster of patients with **Low Norm** BP is localized close to patients with **AH II** (a situation where the extremes paradoxically converge).

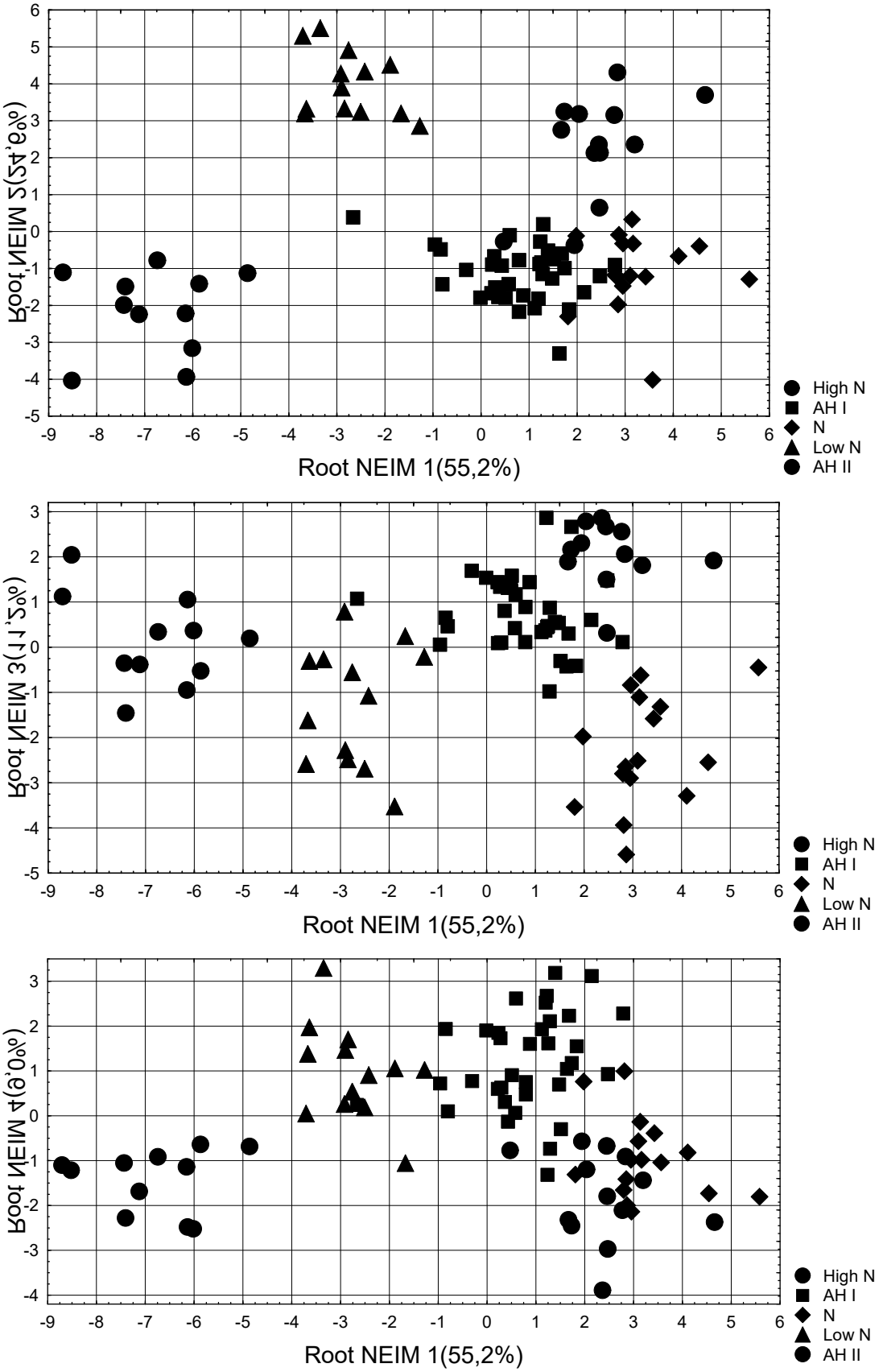

Fig. 7.1. Scattering of individual values of the discriminant roots of patients of different blood pressure clusters

The separation of this cluster from others occurs along the axis of the second root. The top position of patients with minimum BP reflects, first of all, their youngest age as well as **maximally decreased** levels of plasma phosphate and magnesium, PSD of beta-rhythm in C3 locus, entropy of PSD in F3 and T5 loci, **minimum** for the sample lower border levels of entropy of PSD in P3 locus, sympathetic tone markers, and aldosterone as well as normal, but minimum for the sample levels of T-regulatory lymphocytes, potassium excretion and Frolkis's and Garkavi's NHSI.On the other hand, minimum BP is accompanied by maximum electrokinetic index (which reflects, first of all, biological age [Honcharenko MS, 2011; Kyrylenko IG et al., 2016; 2018; 2022], upper limit levels of vagal tone, PSD of delta-rhythm in F4, C3 and P3 loci, theta-rhythm in O1 locus, entropy of PSD in T6 locus, deviation of alpha-rhythm as well as normal, but maximum for the sample levels of plasma potassium and blood T-helper lymphocytes.

Demarcation of cluster with **High Norm** BP, whose members are exclusively men, occurs along the axis of the third root. The bottommost position of patients reflects their **minimally decreased** level of *Bifidobacteria* in faeces and normal, but maximum for the sample levels of the PSD of beta-rhythm in T3 and T5 loci, on the one hand, while **minimum** for the sample lower border levels of the PSD of alpha-rhythm in Fp2 and T4 loci and deviation of delta-rhythm, as well as **maximally decreased** levels of circulating immune complexes, triiodothyronine and calcitonin.

Finally, along the axis of the fourth root, the top positions are occupied by cluster of patients with **AH I,** which reflects their normal, but maximum for the sample levels of the PSD of theta-rhythm in C4, F8 and P4 loci, entropy of PSD in T3 locus and plasma VLD LP cholesterol as well as **maximally increased** levels of plasma calcium, blood monocytes and Popovych's Strain Index of leukocytogram as marker of maladaptation [Popovych IL et al., 2022]. The symmetry of the beta- rhythm is also characteristic, in contrast to its left-sided asymmetry in other clusters. On the other hand, such patients are characterized by normal, but **minimum** for the sample levels of cortisol and activity of phagocytosis of *Staph. aureus* by neutrophils as well as **maximally decreased** plasma levels of sodium, chloride and IgA.

Table 7.5. Correlations Variables-Canonical Roots, Means of Roots and Z-scores of Variables

Variables of Tensioregulome	Correlations Variables-Roots				Norm (16)	High N (13)	AH I (35)	Low N (13)	AH II (11)
Root 1 (55,2%)	R 1	R 2	R 3	R 4	+3,2	+2,4	+0,8	-2,7	-6,8
See Fig. 7.2									
Interleukin-6	-0,093	-0,046	0,087	-0,080	-0,44	+0,37	+0,27	+0,26	+2,16
Cholesterol total					-0,43	+0,13	+0,12	+0,05	+0,27
F7-α PSD	-0,062	-0,008	0,067	0,096	-0,63	-0,45	-0,03	-0,07	+0,09
O1-β PSD	-0,052	-0,071	0,199	-0,003	-0,70	-0,01	+0,12	-0,56	+0,37
Testosterone total					-0,35	+0,74	+0,37	-0,11	+0,84
Testosterone Male					-0,59	+0,74	+0,35	-0,50	+0,91
Testosterone Female					+0,37		+0,50	+0,13	+0,71
See Fig. 7.3									
Amplitude-θ	0,034	-0,030	-0,047	-0,086	+0,57	-0,02	+0,65	+0,30	-0,03
T3-δ PSD	0,025	0,033	**-0,207**	0,009	+0,92	-0,07	+0,06	+0,72	+0,01
Index-α	0,022	-0,008	**-0,123**	-0,028	+0,42	-0,12	-0,08	+0,09	-0,04
F4-α PSD	0,016	-0,011	-0,037	0,002	+0,00	-0,24	-0,16	-0,20	-0,26
Microb Cou St. aur.	0,033	0,057	-0,069	-0,026	+0,26	+0,16	-0,03	+0,23	-0,19
Root 2 (24,6%)	R 1	R 2	R 3	R 4	-1,1	+2,3	-1,15	+4,0	-2,1
See Fig. 7.3									
Age	-0,070	-0,112	0,110	-0,166	-0,18	+0,10	-0,04	-0,52	+0,92

LF PSD nu	0,037	-0,154	-0,056	-0,126	+1,28	+0,34	+0,51	-0,34	+0,68
C3-β PSD	0,002	-0,099	0,164	-0,067	-0,36	+0,11	+0,08	-0,83	+0,16
Entropy PSD F3	0,016	-0,075	0,134	0,109	-0,73	-0,48	+0,22	-0,89	-0,50
Entropy PSD T5	0,047	-0,059	0,016	0,060	-0,15	-0,45	+0,05	-0,70	-0,64
Entropy PSD P3	0,030	-0,055	0,020	-0,009	+0,16	+0,06	+0,17	-0,26	-0,02
$CD4^+CD25^+$ T-regs	0,046	-0,090	-0,013	0,047	+1,74	+1,07	+1,85	+0,47	+0,95
Phosphate Plasma	0,003	-0,071	0,127	-0,133	-0,98	-0,57	-0,89	-1,49	-0,58
Magnesium Plasma	-0,009	-0,043	-0,023	-0,181	-1,15	-1,21	-1,49	-1,56	-1,02
Potassium Excretion	0,004	-0,047	0,084	0,055	+0,05	+0,36	+0,80	-0,11	+0,43
Aldosterone					-0,24	-0,14	-0,20	-0,37	-0,28
Frolkis's NHSI					+0,46	+0,23	+0,23	-0,10	+0,54
Garkavi's NHSI					+0,41	+0,21	+0,22	-0,01	+0,49
See Fig. 7.4									
C3-δ PSD	-0,030	0,115	-0,033	0,030	+0,04	+0,33	-0,01	+0,92	+0,14
P3-δ PSD	-0,021	0,079	-0,026	0,095	-0,04	+0,03	+0,12	+0,63	-0,02
F4-δ PSD	-0,022	0,041	-0,093	-0,049	+0,48	+0,22	-0,05	+0,66	+0,45
O1-θ PSD	-0,041	0,071	0,013	0,066	-0,26	-0,01	-0,01	+0,43	+0,05
Deviation-α	-0,019	0,071	0,031	0,186	-0,39	-0,21	+0,17	+0,39	-0,29
Entropy PSD T6	0,008	0,068	0,032	0,143	-0,51	-0,22	+0,03	+0,23	-0,69
Electrokinetic Index					+0,56	+0,18	+0,38	+0,89	-0,90
Triangular Ind HRV					-0,40	-0,15	-0,04	+1,03	-1,13
Potassium Plasma					-0,70	-0,43	-0,69	+0,35	-0,12
$CD4^+$ T-helper Lym	-0,070	0,145	-0,076	0,168	-1,39	-0,99	-1,87	-0,55	-0,89
Root 3 (12,2%)	**R 1**	**R 2**	**R 3**	**R 4**	-2,3	+2,0	+0,7	-1,3	+0,1
See Fig. 7.5									
T3-β PSD	-0,017	0,075	0,218	-0,033	-0,79	+0,55	-0,15	-0,15	-0,15
T5-β PSD					-0,58	+0,42	+0,15	-0,26	-0,16
Bifidobacteria feces	0,030	-0,005	0,065	0,010	-1,25	-1,02	-1,10	-1,37	-1,39
See Fig. 7.6									
Sex Index	-0,099	0,097	-0,235	0,057	+0,05	-0,54	-0,27	+0,94	+0,32
Deviation-δ	-0,032	0,064	-0,104	0,177	-0,05	-0,47	-0,10	+0,67	-0,13
Fp2-α PSD	0,021	-0,007	-0,085	0,045	+0,09	-0,39	-0,11	-0,07	-0,34
T4-α PSD	-0,029	-0,076	-0,005	0,033	-0,15	-0,48	+0,02	-0,31	+0,18
Calcitonin total	-0,018	0,058	-0,154	0,047	-0,47	-0,94	-0,78	-0,12	-0,69
Calcitonin Male					-0,74	-0,94	-0,83	-0,70	-1,26
Calcitonin Female					+0,35		-0,37	+0,25	+0,32
Triiodothyronine					-0,06	-0,95	-0,50	+0,09	-0,60
CIC	-0,074	0,027	-0,090	0,036	-0,60	-0,84	-0,62	-0,11	-0,17
Root 4 (9,0%)	**R 1**	**R 2**	**R 3**	**R 4**	-0,95	-1,8	+1,2	+1,0	-1,4
See Fig. 7.7									
C4-θ PSD	0,010	-0,007	0,059	0,250	-0,29	-0,34	+0,59	+0,16	-0,36
F8-θ PSD	0,008	0,016	0,009	0,212	-0,35	-0,52	+0,30	0,14	-0,55
P4-θ PSD	-0,043	-0,024	0,050	0,155	-0,30	-0,32	+0,31	+0,12	+0,14
Entropy PSD T3	-0,014	-0,134	0,102	0,192	-0,70	-0,98	+0,42	-0,84	-0,21
Laterality-β	0,067	0,058	0,012	0,195	-0,37	-0,36	-0,07	-0,16	-0,97
Calcium Excretion	0,028	-0,010	0,127	0,202	-0,48	+0,54	+1,92	+0,47	-0,68
VLD LP Cholesterol					+0,16	-0,51	+0,39	-0,41	+0,19
Monocytes Blood					-0,62	+0,39	+0,55	-0,86	-0,96
Popovych's Strain-1					+1,18	+0,86	+1,43	+0,26	+0,18
See Fig. 7.8									
Cortisol	-0,033	0,008	0,043	-0,131	+0,15	+0,68	+0,04	+0,19	+0,89
Sodium Plasma	-0,093	0,049	-0,223	-0,113	+0,07	-0,93	-1,05	+0,65	+0,71
Chloride Plasma					+0,69	-0,54	-0,67	+1,38	+1,45
Phag. Ind. vs *St. aur.*	0,049	0,061	-0,042	-0,131	+0,53	+0,59	+0,18	+0,35	+0,14
IgA Serum					-0,31	+0,13	-0,94	+0,13	+0,50

In general, all clusters on the planes of four roots are clearly delineated, which is documented by calculating the Mahalanobis distances (Table 7.6).

Table 7.6. Squared Mahalanobis Distances between Blood Pressure Clusters, F-values (df=42,4) and p-levels

Blood Pressure Clusters	High Norm	AH I	Norm	Low Norm	AH II
High Norm	0	24,8	31,2	47,9	108
AH I	2,83 10^{-3}	0	19,7	43,0	66,0
Norm	2,70 10^{-3}	2,60 10^{-2}	0	66,2	108
Low Norm	3,75 10^{-4}	4,91 10^{-6}	5,72 10^{-6}	0	62,0
AH II	7,73 10^{-6}	6,66 10^{-6}	8,49 10^{-6}	4,45 10^{-5}	0

The same discriminant parameters can be used to identify the belonging of one or another person to one or another BP cluster. These functions are special linear combinations that maximize differences between groups and minimize dispersion within groups. The coefficients of the classifying functions are not standardized therefore they are not interpreted. An object belongs to a group with the maximum value of a function calculated by summing the products of the values of the variables by the coefficients of the classifying functions plus the constant (Table 7.7). In this case, we can retrospectively recognize patients with high norm BP with two mistake and others patients **unmistakably**. Overall classification accuracy is 97,7% (Table 7.8).

Table 7.7. Coefficients and Constants for Classification Functions for Blood Pressure Clusters

Blood Pressure Clusters	High N	AH I	Norm	Low N	AH II
Variables currently in the model	p=,148	p=,398	p=,182	p=,148	p=,125
Sex Index (M=1; F=2)	-298,9	-294,2	-288,7	-280,9	-282,3
Sodium Plasma, mM/L	-11,31	-11,10	-11,36	-10,26	-9,722
Entropy PSD T3	281,3	368,3	363,0	301,4	388,1
Age, years	1,877	1,642	1,774	1,550	1,315
Deviation-δ, Hz	-282,4	-270,4	-272,4	-257,8	-247,9
Phagocytic Index vs *Staph. aureus*, %	272,1	272,7	271,6	267,3	267,1
$CD4^+$ T-helper Lymphocytes, %	-5,945	-5,966	-6,270	-5,665	-4,916
LF PSD nu, %	0,514	0,731	0,937	0,369	0,476
T3-β PSD, %	3,683	3,076	3,391	3,460	2,050
P3-δ PSD, %	0,389	-0,094	-0,102	0,276	-0,490
F7-α PSD, %	6,536	6,820	6,272	7,033	7,540
O1-β PSD, %	-2,050	-1,694	-1,824	-1,716	-0,995
Laterality-β, %	0,595	0,414	0,329	0,643	0,332
Phosphate Plasma, mM/L	41,26	-13,73	7,844	-2,036	-60,62
Magnesium Plasma, mM/L	-134,1	-276,2	-225,6	-290,4	-372,4
Interleukin-6, ng/L	12,81	13,33	12,33	13,95	15,57
F8-θ PSD, %	7,509	8,516	9,002	6,578	7,331
Fp2-α PSD, %	1,550	1,521	1,999	1,169	0,638
Circulating Immune Complexes, units	-3,368	-3,435	-3,393	-3,130	-3,376
O1-θ PSD, %	-9,562	-10,52	-10,75	-8,570	-9,236
T3-δ PSD, %	2,814	2,929	3,116	2,926	2,521
Deviation-α, Hz	133,1	127,1	126,8	125,4	109,4
Calcium Excretion, mM/d	16,18	15,94	15,71	15,34	14,45
F4-α PSD, %	11,92	11,73	11,14	12,33	12,96
C4-θ PSD, %	30,31	28,63	28,49	29,24	26,76
Amplitude-θ, μV	-4,008	-2,987	-2,339	-4,932	-4,172
Index-α, %	2,889	2,686	2,586	2,902	2,466
P4-θ PSD, %	-14,93	-12,91	-15,13	-11,19	-8,149

Entropy PSD P3	311,7	258,6	296,2	267,7	205,4
Entropy PSD T6	-36,82	-74,55	-71,82	-61,75	-111,7
Entropy PSD F3	-322,8	-285,4	-325,8	-277,7	-184,2
$CD4^+CD25^+$ T-regulatory Lymph, %	25,38	25,76	25,42	24,75	25,92
Microbial Count for *St. aur.*, Bac/Phag	-21,27	-21,23	-20,90	-20,96	-20,95
Cortisol, nM/L	-0,360	-0,364	-0,363	-0,355	-0,342
F4-δ PSD, %	7,874	8,218	7,627	8,357	9,544
T4-α PSD, %	4,799	5,161	4,577	5,385	6,373
C3-β PSD, %	21,85	22,60	20,93	22,97	24,94
C3-δ PSD, %	12,94	13,27	12,40	13,51	14,41
Calcitonin, Z	-14,91	-16,46	-13,93	-16,42	-20,37
Entropy PSD T5	-372,1	-388,9	-375,2	-399,5	-422,7
***Bifidobacteria* feces, lgCFU/g**	-14,07	-15,15	-12,09	-16,29	-18,11
Potassium Excretion, mM/d	0,960	0,988	0,904	1,012	1,025
Constants	-13098	-13067	-12908	-12707	-12805

Table 7.8. Classification Matrix for Blood Pressure Clusters

Group	Rows: Observed classifications Columns: Predicted classifications Percent Correct	High N p=,14773	AH I p=,39773	N p=,18182	Low N p=,14773	AH II p=,12500
High N	84,6	11	2	0	0	0
AH I	100,0	0	35	0	0	0
N	100,0	0	0	16	0	0
Low N	100,0	0	0	0	13	0
AH II	100,0	0	0	0	0	11
Total	97,7	11	37	16	13	11

At the next stage, an analysis of the correlations between the average Z-scores of systolic and diastolic BP, on the one hand, and the variables whose information is condensed in four discriminant roots, as well as not included in the model (see please Table 7.5), on the other hand, was performed.

Figures 7.2-7.9 illustrate that there are correlations between blood pressure and elements of the Tensioregulome, but they are non-linear and approximated by curves of only the second/third orders.

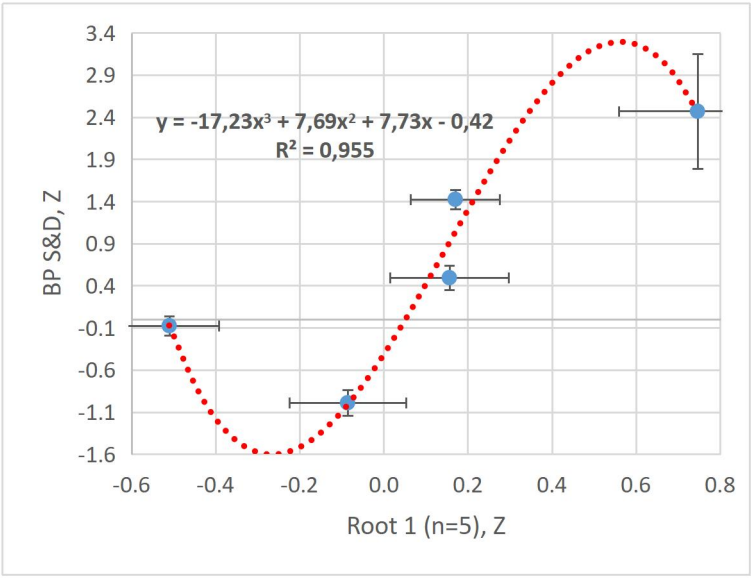

Fig. 7.2. Scatterplot of correlation between means of 5 variables of Root 1 (X-line) and means of systolic and diastolic blood pressure (Y-line)

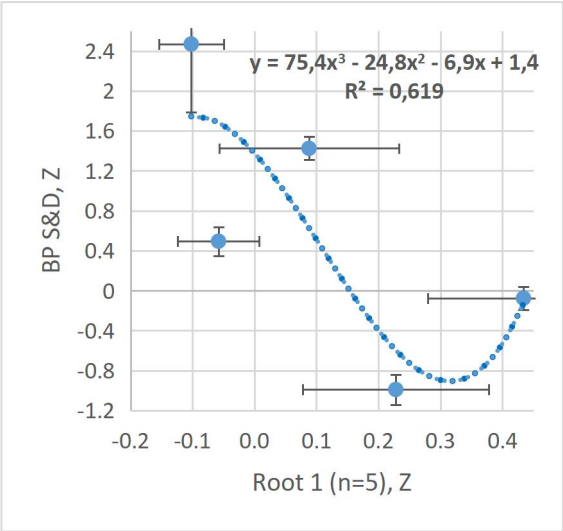

Fig. 7.3. Scatterplot of correlation between means of 5 variables of Root 1 (X-line) and means of systolic and diastolic blood pressure (Y-line)

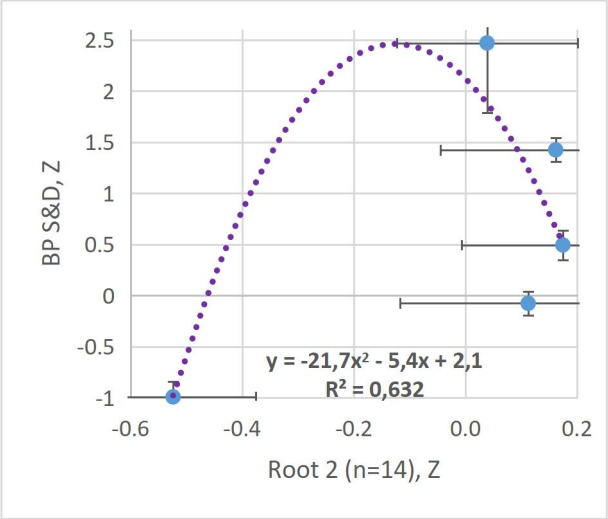

Fig. 7.4. Scatterplot of correlation between means of 14 variables of Root 2 (X-line) and means of systolic and diastolic blood pressure (Y-line)

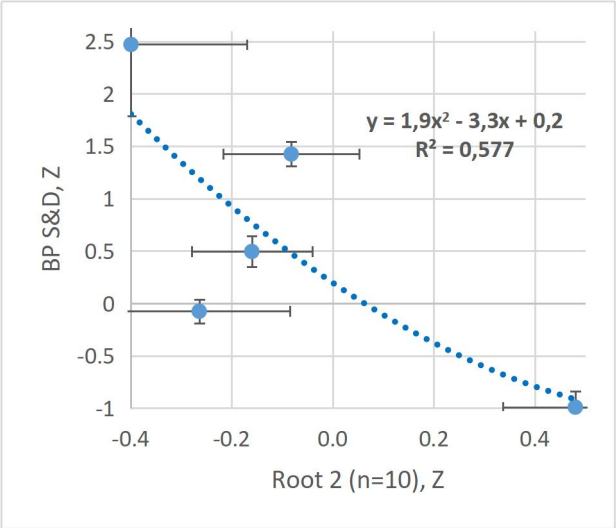

Fig. 7.5. Scatterplot of correlation between means of 10 variables of Root 2 (X-line) and means of systolic and diastolic blood pressure (Y-line)

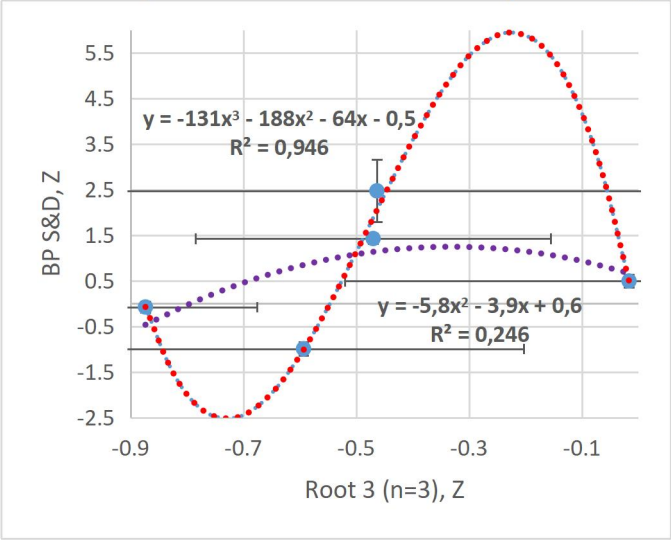

Fig. 7.6. Scatterplot of correlation between means of 3 variables of Root 3 (X-line) and means of systolic and diastolic blood pressure (Y-line)

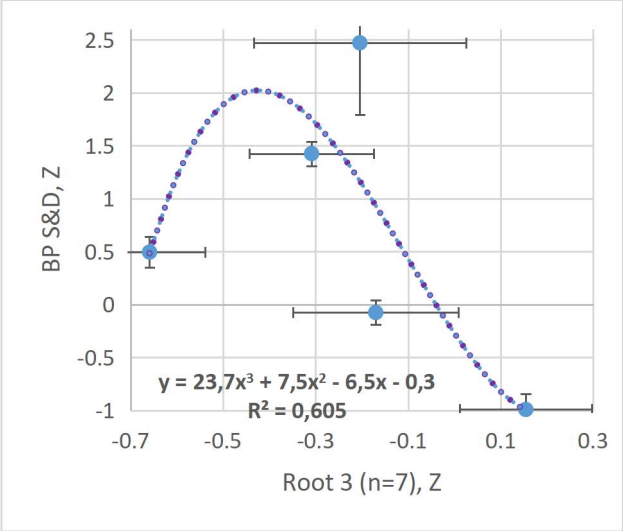

Fig. 7.7. Scatterplot of correlation between means of 7 variables of Root 3 (X-line) and means of systolic and diastolic blood pressure (Y-line)

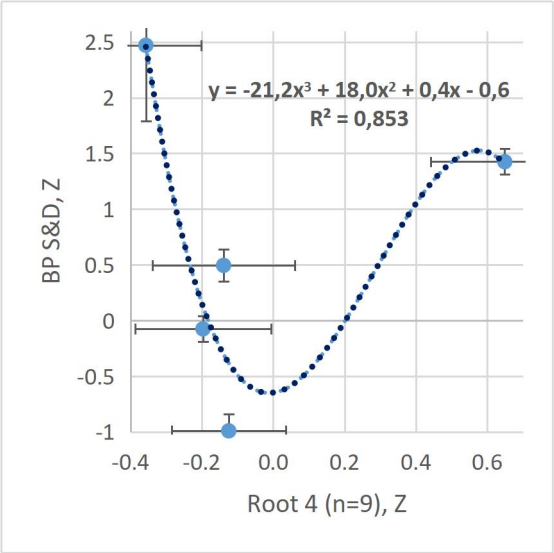

Fig. 7.8. Scatterplot of correlation between means of 9 variables of Root 4 (X-line) and means of systolic and diastolic blood pressure (Y-line)

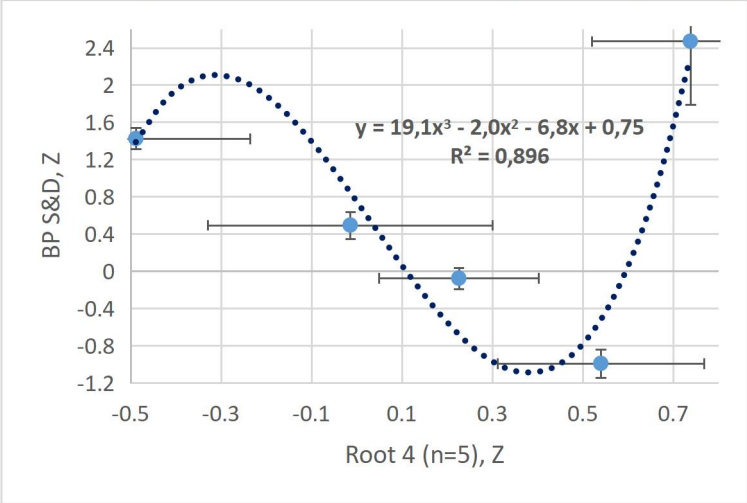

Fig. 7.9. Scatterplot of correlation between means of 5 variables of Root 4 (X-line) and means of systolic and diastolic blood pressure (Y-line)

The goal of the final stage was to build regression models for estimating blood pressure levels based on constellations of variables of the neuro-endocrine-immune complex and the metabolome. First, based on the results of the screening, a correlation matrix was created for the EEG variables, based on the critical value of the r module of 0,21 (Table 7.9).

Table 7.9. Correlation Matrix for EEG and Blood Pressure Variables

EEG Variables	BP systolic	BP diastolic
Amplitude θ, μV	-0,08	-0,23
Deviation β, Hz	0,21	-0,21
Index α, %	-0,15	-0,28
Laterality β, %	-0,20	-0,03
Laterality α, %	-0,22	-0,08
PSD Fp1-β, %	0,26	0,32
PSD Fp1-δ, %	-0,26	-0,12
PSD Fp2-β, %	0,22	0,36
PSD F3-β, %	0,31	0,34
PSD F3-δ, %	-0,23	-0,14
PSD F4-β, %	0,20	0,31

PSD F7-β, %	0,11	0,24
PSD F7-α, %	0,20	0,10
PSD F7-δ, %	-0,23	-0,24
PSD F8-β, %	0,10	0,22
PSD F8-β, μV²/Hz	0,06	0,22
PSD T3 Entropy	0,24	0,04
PSD T3-θ, %	0,21	-0,03
PSD T3-δ, μV²/Hz	-0,27	-0,18
PSD C3-β, %	0,30	-0,24
PSD C4-β, %	0,25	0,23
PSD C4-δ, %	-0,20	-0,13
PSD T5-β, %	0,12	0,23
PSD T5-δ, %	-0,21	-0,18
PSD T6 Entropy	-0,11	-0,21
PSD T6-β, %	0,13	0,28
PSD P4-β, %	0,16	0,22
PSD O1-β, %	0,33	0,28
PSD O2-β, %	0,21	0,32
PSD O2-α, μV²/Hz	-0,14	-0,23
PSD O2-θ, μV²/Hz	-0,07	-0,24

After step-by-step elimination until the maximum value of Adjusted R^2 was reached, 9 upregulating and 6 downregulating variables remained in the regression model for systolic BP. Pseudostaining clearly illustrates the **hypertensive** effect, first of all, of neurons that generate β-rhythm and, to a lesser extent, θ- and α-rhythms as well as entropy in T3 locus. Instead, the **hypotensive** effect is exerted by neurons that generate the δ-rhythm and, to a lesser extent, the left lateralization (symmetry shift) of the β- and α-rhythms.

The listed variables, taken together, determines systolic BP level by 49,0% and make it possible to estimate it with an error of 16 mmHg (Table 7.10 and Fig. 7.10).

Table 7.10. Regression Summary for Blood Pressure Systolic
R=0,700; R^2=0,490; Adjusted R^2=0,345; $F_{(16,6)}$=3,4; p=0,0004; SE=16 mmHg

N=73		Beta	St. Err. of Beta	B	St. Err. of B	$t_{(56)}$	p-level
Variables	r		Intercpt	55,3	21,0	2,63	0,011
PSD O1-β, %	**0,33**	0,185	0,161	0,148	0,128	1,15	0,254
PSD C4-β, %	**0,25**	-0,164	0,156	-0,602	0,573	-1,05	0,298
PSD T3 Entropy	**0,24**	0,366	0,154	0,480	0,202	2,38	0,021
PSD Fp2-β, %	**0,22**	0,439	0,236	0,499	0,269	1,86	0,068
PSD O2-β, %	**0,21**	0,500	0,176	0,634	0,224	2,83	0,006
Deviation β, Hz	**0,21**	0,294	0,107	8,430	3,085	2,73	0,008
PSD T3-θ, %	**0,21**	0,416	0,155	57,26	21,32	2,69	0,009
PSD F4-β, %	0,20	0,364	0,279	0,317	0,243	1,30	0,198
PSD F7-α, %	0,20	-0,824	0,292	-1,113	0,394	-2,82	0,007
Laterality β, %	-0,20	0,186	0,175	0,130	0,122	1,07	0,291
Laterality α, %	**-0,22**	-0,692	0,198	-0,481	0,138	-3,50	0,001
PSD C4-δ, %	-0,20	-0,385	0,262	-0,672	0,457	-1,47	0,147
PSD T5-δ, %	**-0,21**	-0,912	0,285	-0,873	0,272	-3,20	0,002
PSD F3-δ, %	**-0,23**	0,583	0,260	0,924	0,413	2,24	0,029
PSD Fp1-δ, %	**-0,26**	0,490	0,209	0,429	0,183	2,34	0,023

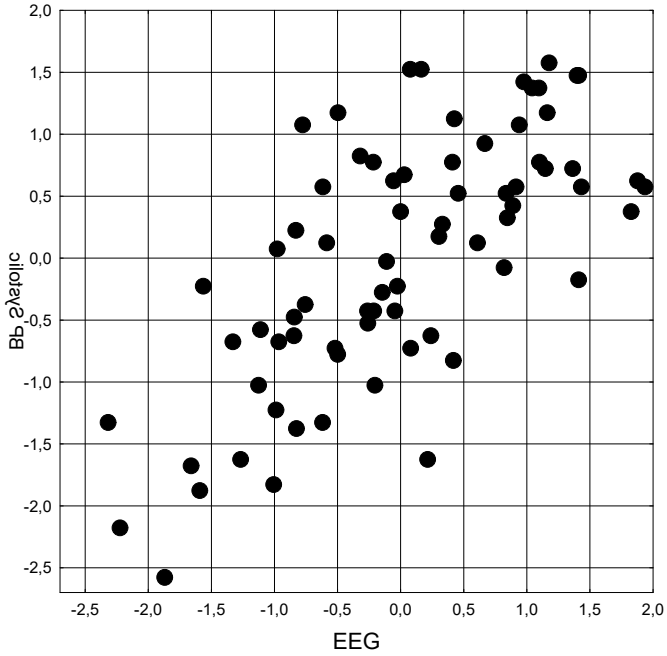

R=0,700; R^2=0,490; $\chi^2_{(16)}$=42; p=0,0004; Λ Prime=0,5096

Fig. 7.10. Scatterplot of canonical correlation between EEG variables (X-line) and Blood Pressure Systolic (Y-line)

A similar situation with regard to hypertensive and hypotensive factors was also found for diastolic BP, however, the measure of neurogenic determination is smaller and, accordingly, the relative error for the estimate is larger (Table 7.11 and Fig. 7.11).

Table 7.11. Regression Summary for Blood Pressure Diastolic
R=0,604; R^2=0,365; Adjusted R^2=0,274; $F_{(9,6)}$=4,0; p=0,0004; SE=9 mmHg

N=73		Beta	St. Err. of Beta	B	St. Err. of B	$t_{(63)}$	p-level
Variables	r		Intercpt	91,3	6,2	14,8	10^{-6}
PSD F3-β, %	**0,34**	0,318	0,152	0,265	0,127	2,10	0,040
PSD O1-β, %	**0,28**	0,240	0,160	0,160	0,107	1,51	0,137
PSD F7-β, %	**0,24**	-0,303	0,214	-0,163	0,115	-1,42	0,161
PSD T5-β, %	**0,23**	-0,317	0,204	-0,189	0,122	-1,55	0,126
PSD F8-β, μV^2/Hz	**0,22**	0,428	0,117	0,105	0,029	3,66	0,001
Deviation β, Hz	**-0,21**	-0,278	0,103	-4,201	1,554	-2,70	0,009
PSD O2-α, μV^2/Hz	**-0,23**	-0,176	0,135	-0,004	0,003	-1,30	0,199
PSD O2-θ, μV^2/Hz	**-0,24**	-0,269	0,137	-0,051	0,026	-1,96	0,054
PSD F7-δ, %	**-0,24**	-0,323	0,164	-0,131	0,067	-1,97	0,053

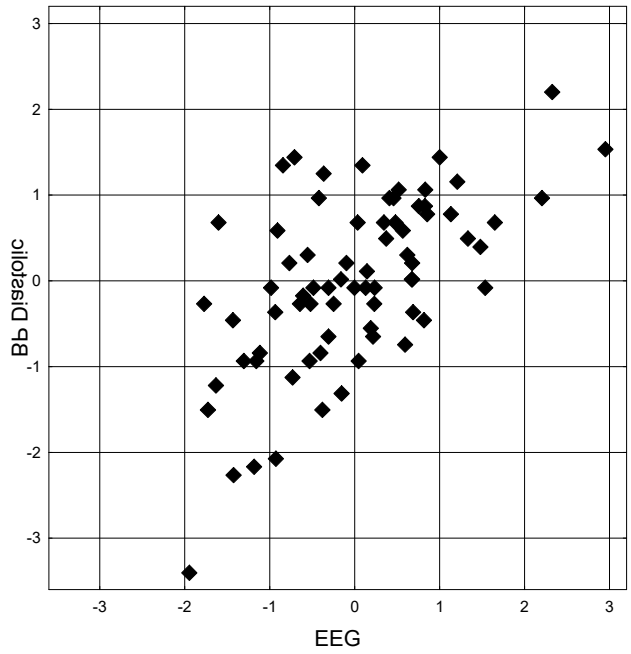

R=0,604; R^2=0,365; $\chi^2_{(9)}$=30; p=0,0004; Λ Prime=0,6349

Fig. 7.11. Scatterplot of canonical correlation between EEG variables (X-line) and Blood Pressure Diastolic (Y-line)

Based on the analysis of the canonical correlation between the EEG variables, on the one hand, and both BP parameters, on the other hand, two pairs of canonical roots were selected. The EEG Root of the first pair is represented, first of all, by the variability of the β-rhythm, which upregulates systolic BP while downregulates diastolic BP (Table 7.12). The next two triads of factors downregulates only systolic BP without affecting diastolic BP. Instead, β-rhythm generating neurons, which project to F8 and F7 loci, upregulates, while θ-rhythm generating neurons, which project to O2 locus, downregulates only diastolic BP without affecting systolic BP.

Table 7.12. Factor structure of first pair of EEG and Blood Pressure Roots

Left set	R1
Deviation β, Hz	0,674
PSD T3-θ, %	0,399
PSD T3 Entropy	0,341
PSD F7-α, %	0,187
Laterality β, %	-0,299
Laterality α, %	-0,269
PSD Fp1-δ, %	-0,238
PSD F8-β, μV^2/Hz	-0,241
PSD F7-β, %	-0,208
PSD O2-θ, μV^2/Hz	0,256
Right set	R1
BP Systolic	0,506
BP Diastolic	-0,302

The listed variables, taken together, determines both BP level by 59,6% (Fig. 7.12).

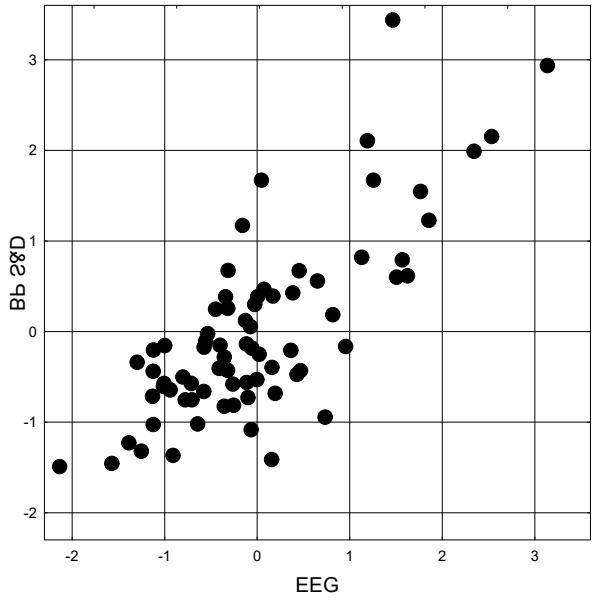

R=0,772; R^2=0,596; $\chi^2_{(44)}$=98; p<10^{-5}; Λ Prime=0,1941

Fig. 7.12. Scatterplot of canonical correlation between EEG variables (X-line) and Blood Pressure Systolic&Diastolic (Y-line). First pair of Roots

The second pair of canonical roots, despite a slightly lower correlation coefficient, seems to us to be more interesting than the first (Table 7.13).

Table 7.13. Factor structure of second pair of EEG and Blood Pressure Roots

Left set	R2
PSD F4-β, %	-0,398
PSD F3-β, %	-0,494
PSD F3-δ, %	0,262
PSD Fp2-β, %	-0,461
PSD Fp1-δ, %	0,256
PSD F8-β, μV²/Hz	-0,238
PSD F7-β, %	-0,284
PSD F7-α, %	-0,219
PSD F7-δ, %	0,349
PSD O1-β, %	-0,449
PSD O2-β, %	-0,416
PSD O2-α, μV²/Hz	0,291
PSD O2-θ, μV²/Hz	0,263
PSD C4-β, %	-0,350
PSD C4-δ, %	0,232
PSD T5-β, %	-0,279
PSD T5-δ, %	0,288
PSD T3 Entropy	-0,182
Laterality α, %	0,215
Right set	R1
BP Diastolic	-0,953
BP Systolic	-0,862

First, both BP parameters receive factor loadings of the same sign, which simplifies interpretation. Second, and this is the most important, we managed to detect opposite effects on the BP of neurons that project to the same loci, but generate rhythms of different frequencies. In particular, these are loci F3, F7, C4, and T5, whose β-rhythm generating neurons upregulates BP, while δ-rhythm generating neurons downregulates BP.

In addition, the hypertensive effect of β-rhythm generating neurons, which are projected to the F7 and O2 loci, in contrast to the hypotensive effects of neighboring neurons generating α- and θ-rhythms, was revealed. The hypertensive effects of β-rhythm generating neurons projecting to the contralateral F4, F8 and O1 loci are also noteworthy.

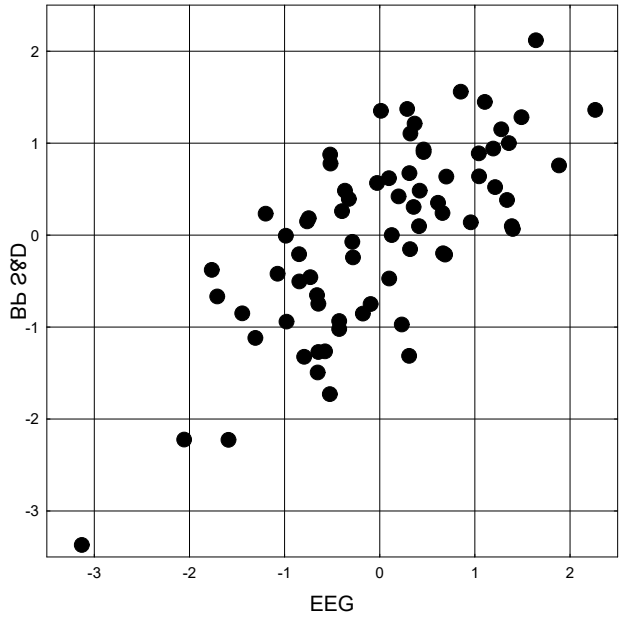

R=0,721; R^2=0,520; $\chi^2_{(21)}$=44; p=0,0026; Λ Prime=0,4800

Fig. 7.13. Scatterplot of canonical correlation between EEG variables (X-line) and Blood Pressure Systolic&Diastolic (Y-line). Second pair of Roots

Looking ahead, we hope that the presented findings will help explain the inconsistency of the conclusions of numerous studies collected in systematic reviews [Beissner F et al., 2013; Matusik PS et al., 2023] regarding the strength and nature of associations of brain morphology (cortical thickness or volume) or region activity (measured as BOLD signals) with HRV-markers of vagal and sympathetic activity: in these studies, the nature of EEG rhythms was not taken into account.

It is time to move on to the analysis of connections with the BP of the parameters of the autonomic and endocrine systems. Given the well-known effects of both sex and age on the level of parameters of both systems, these variables were included specifically in the endocrine-autonomic set (Table 7.14).

Table 7.14. Correlation Matrix for Endocrine&HRV and Blood Pressure Variables

Endocrine&HRV Variables	**BP systolic**	**BP diastolic**
Triiodothyronine, nM/L	-0,15	-0,23
Calcitonin standardized, Z	-0,17	-0,24
Testosterone raw, nM/L	0,16	0,21
Sex Index (M=1; F=2)	-0,19	-0,44
Age, years	0,37	0,18
Triangular Index, units	-0,26	-0,28
1/Mode HRV, 1/msec	0,00	0,29
Baevskiy's Stress Index, ln un	0,23	0,32
Heart Rate, beats/min	0,02	0,27
SDNN, msec	-0,21	-0,24
RMSSD, msec	-0,21	-0,26
pNN_{50}, %	-0,20	-0,25

Total Power HRV, msec²	-0,20	-0,22
PSD VLF band, msec²	-0,19	-0,25
PSD HF band, msec²	-0,19	-0,25
(VLF + LF)/HF Ratio	0,18	0,21
PSD HF band, %	-0,17	-0,25
PSD LFnu band, %	0,18	0,25

Table 7.15. Regression Summary for Blood Pressure Systolic

R=0,461; R^2=0,212; Adjusted R^2=0,164; $F_{(5,8)}$=4,4; p=0,0013; SE=17 mmHg

N=88		Beta	St. Err. of Beta	B	St. Err. of B	$t_{(82)}$	p-level
Variables	r		Intercpt	118	14,4	8,17	10^{-6}
Age, years	**0,37**	0,343	0,105	0,504	0,155	3,26	0,002
PSD LFnu band, %	0,18	0,127	0,103	0,141	0,115	1,23	0,221
Sex Index (M=1; F=2)	-0,19	-0,177	0,101	-7,812	4,467	-1,75	0,084
SDNN, msec	**-0,21**	0,297	0,228	0,290	0,223	1,30	0,197
Triangular Index, un	**-0,26**	-0,344	0,223	-1,632	1,060	-1,54	0,127

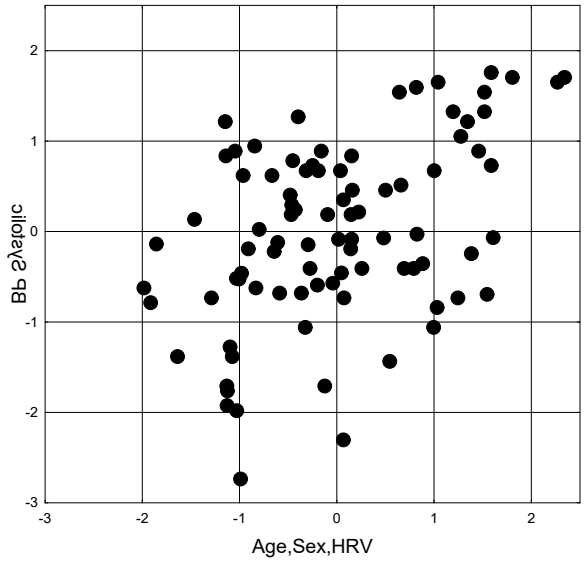

R=0,461; R^2=0,212; $\chi^2_{(5)}$=20; p=0,0013; Λ Prime=0,7876

Fig. 7.14. Scatterplot of canonical correlation between Endocrine&HRV variables (X-line) and Blood Pressure Systolic (Y-line)

It is significant that in relation to systolic BP, age turned out to be a more significant hypertensive factor than sympathetic tone, and female sex as a hypotensive factor was only marginally inferior to HRV-markers of vagal tone. However, the degree of determination of systolic BP by these factors is very insignificant, making up 21,2% (Table 7.15 and Fig. 7.14).

Instead, the autonomic-endocrine determination of diastolic BP is twice as powerful (Table 7.16 and Fig. 7.15). Hypertensive factors are Baevskiy's Stress Index as a marker of sympatho-vagal balance and 1/Mode as a marker of circulating catecholamines (as well as other humoral chronotropic substances), and again age. Female gender was the most significant hypotensive factor, and less significant factors were markers of vagal tone, triiodothyronine and calcitonin standardized by sex, but no raw.

Interestingly, neither raw nor sex- and age-standardized testosterone levels were included in the regression model despite a significant correlation coefficient for testosterone raw level (Table 7.14). Undoubtedly, there would be female sex hormones in the model, but they were not determined in this study.

Table 7.16. Regression Summary for Blood Pressure Diastolic

R=0,655; R^2=0,429; Adjusted R^2=0,364; $F_{(9,8)}$=6,5; $p<10^{-5}$; SE=8 mmHg

N=88		Beta	St. Err. of Beta	B	St. Err. of B	$t_{(78)}$	p-level
Variables	r		Intercpt	65,3	15,5	4,21	10^{-4}
Baevskiy's Stress Index, ln un	**0,32**	0,394	0,169	5,227	2,242	2,33	0,022
1/Mode HRV, 1/msec	**0,29**	0,178	0,104	0,013	0,007	1,71	0,091
Age, years	0,18	0,244	0,100	0,194	0,080	2,43	0,017
Total Power HRV, msec²	**-0,22**	1,262	0,375	0,006	0,002	3,36	0,001
Triiodothyronine, nM/L	**-0,23**	-0,164	0,100	-2,044	1,245	-1,64	0,105
Calcitonin standardized, Z	**-0,24**	-0,243	0,100	-2,825	1,167	-2,42	0,018
PSD VLF band, msec²	**-0,25**	-0,487	0,265	-0,006	0,003	-1,84	0,070
PSD HF band, msec²	**-0,25**	-0,519	0,205	-0,009	0,003	-2,53	0,013
Sex Index (M=1; F=2)	**-0,44**	-0,329	0,101	-7,844	2,403	-3,26	0,002

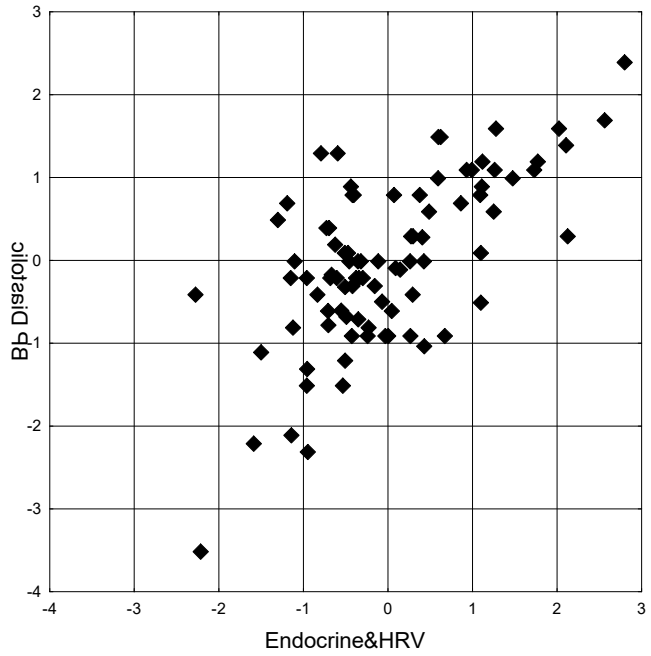

R=0,655; R^2=0,429; $\chi^2_{(9)}$=46; $p=10^{-6}$; Λ Prime=0,5706

Fig. 7.15. Scatterplot of canonical correlation between Endocrine&HRV variables (X-line) and Blood Pressure Diastolic (Y-line)

Combining both regression models in the process of canonical analysis almost did not affect the measure of endocrine-autonomous determination of blood pressure, which was 43,9% (Table 7.17 and Fig. 7.16).

Table 7.17. Factor structure of Endocrine&HRV and Blood Pressure Roots

Left set	**R**
1/Mode HRV, 1/msec	**-0,503**
Baevskiy's Stress Index, ln un	**-0,461**
PSD LFnu band, %	**-0,367**
Age, years	**-0,168**
Sex Index (M=1; F=2)	**0,683**
Triangular Index, units	**0,381**
PSD HF band, msec²	**0,359**
PSD VLF band, msec²	**0,359**
SDNN, msec	**0,331**
Total Power HRV, msec²	**0,309**
Triiodothyronine, nM/L	**0,347**
Calcitonin standardized, Z	**0,345**
Right set	**R1**

BP Diastolic	**-0,983**
BP Systolic	**-0,522**

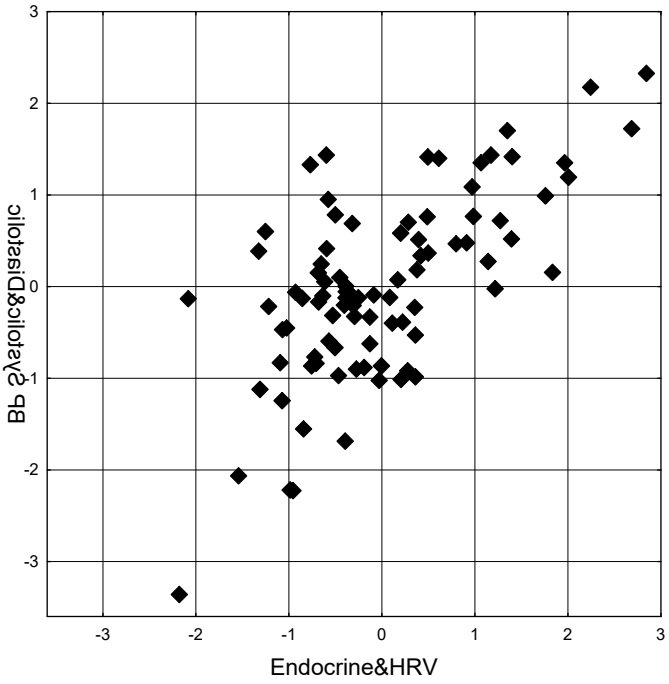

R=0,662; R^2=0,439; $\chi^2_{(24)}$=65; p=10^{-5}; Λ Prime=0,4407

Fig. 7.16. Scatterplot of canonical correlation between Endocrine&HRV variables (X-line) and Blood Pressure Systolic&Diastolic (Y-line)

Immune variables became the next object of analysis of blood pressure regulatory factors (Table 7.18).

Table 7.18. Correlation Matrix for Immune and Blood Pressure Variables

Immune Variables	**BP systolic**	**BP diastolic**
Interleukin-6, ng/L	0,235	0,109
C-Reactive Protein, µg/L	0,272	0,135
IgA Saliva, g/L	-0,119	-0,253
Phagocytosis Index vs St. aur., %	-0,189	-0,249
Microbial Count St. aur., B/Ph	-0,188	-0,139
Phagocytosis Index vs E. coli,%	-0,083	-0,197
Microbial Count E. coli, B/Ph	-0,083	-0,205
Monocytes, %	0,090	0,248
Popovych's Adaptation Index-1	0,205	0,254
Popovych's Adaptation Index-2	0,251	0,170
$CD4^+$ T-helper Lymphocytes, %	-0,167	-0,277
$CD56^+$ NK Lymphocytes, %	0,170	0,312
Entropy of Immunocytogram	0,195	0,245

Two pro-inflammatory factors, as well as the entropy of the immunocytogram, were quite expected to be hypertensive factors in relation to systolic BP. Instead, the presence of both variants of the leukocytary adaptation index in this set was a surprise for us. Despite the insignificant correlation coefficients, the program included in the regression model as hypotensive factors the blood level of T-helpers and the intensity of phagocytosis of Staphylococcus aureus by blood neutrophils. The listed variables, taken together, determine systolic BP level by 32,4% (Table 7.19 and Fig. 7.17).

Table 7.19. Regression Summary for Blood Pressure Systolic
R=0,569; R^2=0,324; Adjusted R^2=0,265; $F_{(7,8)}$=5,5; p=0,00004; SE=16 mmHg

N=88		Beta	St. Err. of Beta	B	St. Err. of B	$t_{(80)}$	p-level
Variables	r		Intercpt	29,8	77,0	0,39	0,699
C-Reactive Protein, µg/L	**0,27**	0,671	0,257	13,46	5,14	2,62	0,011
Popovych's Adaptation Index-2	**0,25**	0,265	0,113	11,77	5,03	2,34	0,022
Interleukin-6, ng/L	**0,24**	-0,298	0,256	-2,132	1,830	-1,16	0,248
Popovych's Adaptation Index-1	0,20	0,237	0,118	7,511	3,745	2,01	0,048
Entropy of Immunocytogram	0,20	0,166	0,106	115,2	73,9	1,56	0,123
CD4⁺ T-helper Lymphocytes, %	-0,17	-0,193	0,108	-0,464	0,261	-1,78	0,079
Microbial Count St. aur., B/Ph	-0,19	-0,170	0,094	-0,387	0,214	-1,81	0,074

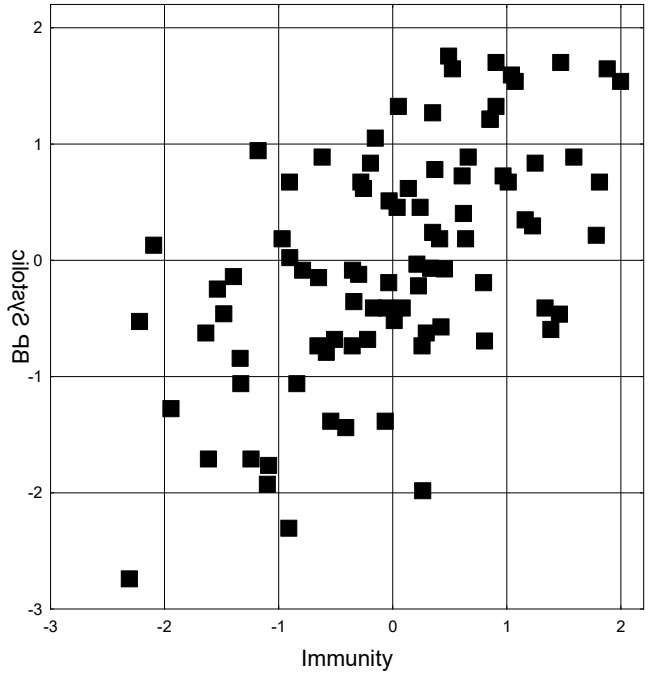

R=0,569; R^2=0,324; $\chi^2_{(7)}$=32; p<10^{-4}; Λ Prime=0,6757

Fig. 7.17. Scatterplot of canonical correlation between Immune variables (X-line) and Blood Pressure Systolic (Y-line)

The factor structure of diastolic BP regulators has two informational variables in common with systolic BP, as well as blood levels of natural killers and monocytes, which are sources of cytokines (probably pro-inflammatory in this situation). Another parameter of the phagocytic function of neutrophils, such as its activity, appeared as a hypotensive factor in the regression model. It is interesting that, in contrast to the previous sets, the immunological determination of diastolic BP was weaker than that of systolic BP (Table 7.20 and Fig. 7.18).

Table 7.20. Regression Summary for Blood Pressure Diastolic
R=0,550; R^2=0,302; Adjusted R^2=0,260; $F_{(5,8)}$=7,1; p<10^{-5}; SE=8,6 mmHg

N=88		Beta	St. Err. of Beta	B	St. Err. of B	$t_{(82)}$	p-level
Variables	r		Intercpt	116	97	1,20	0,235
CD56⁺ NK Lymphocytes, %	**0,31**	0,146	0,111	0,233	0,177	1,32	0,192
Monocytes, %	**0,25**	0,298	0,100	1,426	0,480	2,97	0,004
Popovych's Adaptation Index-1	**0,25**	0,408	0,098	6,989	1,687	4,14	10^{-4}
Entropy of Immunocytogram	**0,24**	0,181	0,103	67,97	38,86	1,75	0,084
Phagocytosis Index vs St. aur., %	**-0,25**	-0,141	0,101	-1,208	0,868	-1,39	0,167

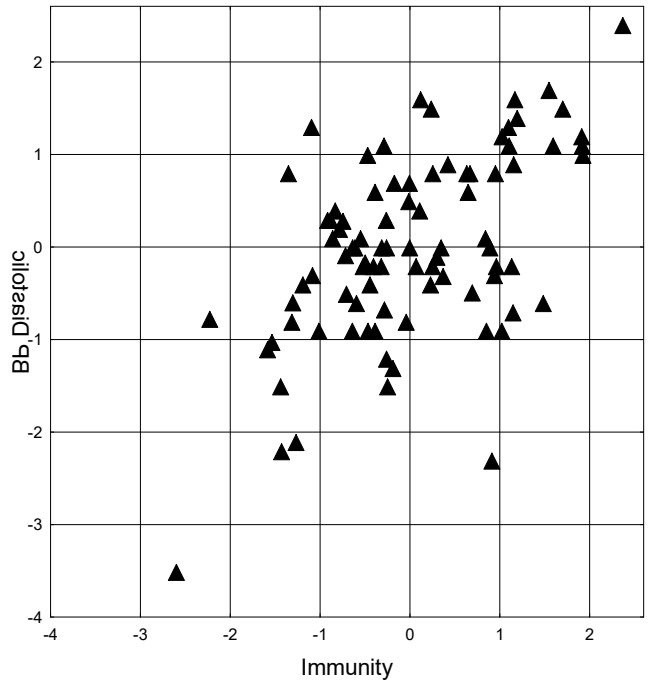

R=0,550; R^2=0,302; $\chi^2_{(5)}$=30; $p<10^{-4}$; Λ Prime=0,6979

Fig. 7.18. Scatterplot of canonical correlation between Immune variables (X-line) and Blood Pressure Diastolic (Y-line)

Canonical analysis proved that natural killers and monocytes as sources of pro-inflammatory cytokines, as well as adaptation index and entropy as carriers of information about the relationship between elements of the leukocytogram and immunocytogram, respectively, are hypertensive factors for both BP parameters.

Instead, hypotensive factors are related to the activity and intensity of phagocytosis by blood neutrophils of *Staphylococcus aureus* as well as T-helpers.

Detailed mechanisms of such effects will be discussed later. Now let's limit ourselves to stating the fact that the listed immune factors determine both BP parameters by 39,5% (Table 7.21 and Fig. 7.19).

Table 7.21. Factor structure of Immune and Blood Pressure Roots

Left set	**R**
$CD56^+$ NK Lymphocytes, %	**-0,437**
Popovych's Adaptation Index-1	**-0,404**
Entropy of Immunocytogram	**-0,388**
Popovych's Adaptation Index-2	**-0,356**
C-Reactive Protein, µg/L	**-0,337**
Monocytes, %	**-0,313**
Interleukin-6, ng/L	**-0,284**
$CD4^+$ T-helper Lymphocytes, %	**0,399**
Phagocytosis Index vs St. aureus, %	**0,389**
Microbial Count Staph. aur., Bac/Ph	**0,278**
Right set	**R1**
BP Diastolic	**-0,937**
BP Systolic	**-0,886**

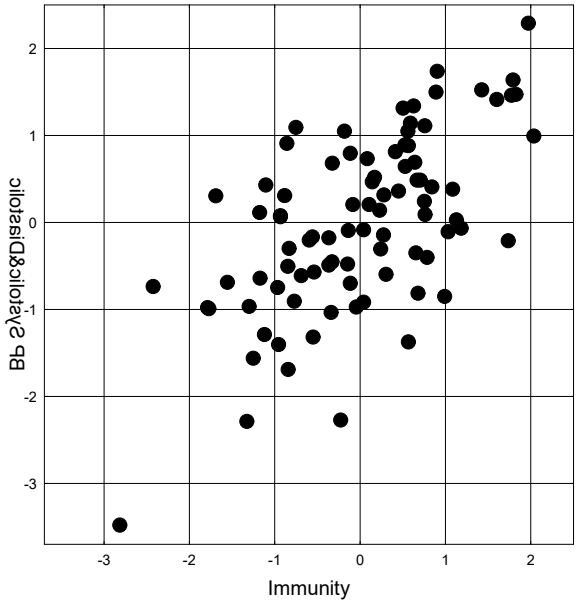

R=0,629; R^2=0,395; $\chi^2_{(20)}$=53; $p<10^{-4}$; Λ Prime=0,5202

Fig. 7.19. Scatterplot of canonical correlation between Immune variables (X-line) and Blood Pressure Systolic&Diastolic (Y-line)

Metabolic parameters made up the last set of variables (Table 7.22).

Table 7.22. Correlation Matrix for Metabolic and Blood Pressure Variables

Metabolic Variables	**BP systolic**	**BP diastolic**
Cholesterol total, mM/L	0,21	0,00
VLD LP Cholesterol, mM/L	0,29	0,16
Dobiásová's & Frohlich's AI	0,19	0,19
Diene conjugates, E^{232}/mL	0,40	0,25
Superoxide dismutase, un/mL	-0,56	-0,41
Catalase, µM/L•h	-0,44	-0,36
Glucose, mM/L	-0,11	-0,23
Phosphate, mM/L	0,19	0,05
Chloride, mM/L	-0,09	-0,25
Sodium, mM/L	-0,09	-0,25
Diuresis, L/24 h	0,11	0,24
Urea Excretion, mM/24 h	0,09	0,21
Uric acid Excretion, mM/24 h	0,25	0,38
Calcium Excretion, mM/24 h	0,09	0,27
Magnesium Excretion, mM/24 h	0,12	0,21
Potassium Excretion, mM/24 h	0,09	0,21
Chloride Excretion, mM/24 h	0,14	0,22
Sodium Excretion, mM/24 h	0,12	0,24
Electrokinetics Index, %	-0,39	-0,19

With regard to systolic BP, the most atherogenic fraction of plasma lipoproteins and uricosuria as well as phosphatemia were quite expected to be the hypertensive factors, while the hypotensive factors were the activity of erythrocyte superoxide dismutase and the electrokinetic index as a marker of a whole range of parameters of the neuro-endocrine-immune complex and metabolism as well as biological age, and more precisely, youth. The listed variables, taken together, determines systolic BP level by 51,3% (Table 7.23 and Fig. 7.20).

Table 7.23. Regression Summary for Blood Pressure Systolic
R=0,716; R^2=0,513; Adjusted R^2=0,483; $F_{(5,8)}$=17,3; $p<10^{-5}$; SE=13 mmHg

N=88		Beta	St. Err. of Beta	B	St. Err. of B	$t_{(82)}$	p-level
Variables	r		Intercpt	143,4	12,4	11,6	10^{-6}
VLD LP Cholesterol, mM/L	**0,29**	0,231	0,079	6,621	2,269	2,92	0,005
Uric acid Excretion, mM/24 h	**0,25**	0,224	0,086	2,763	1,054	2,62	0,010
Phosphate, mM/L	0,19	0,211	0,081	19,446	7,423	2,62	0,010
Electrokinetics Index, %	**-0,39**	-0,272	0,085	-0,418	0,131	-3,19	0,002
Superoxide dismutase, un/mL	**-0,56**	-0,433	0,084	-0,329	0,063	-5,18	10^{-5}

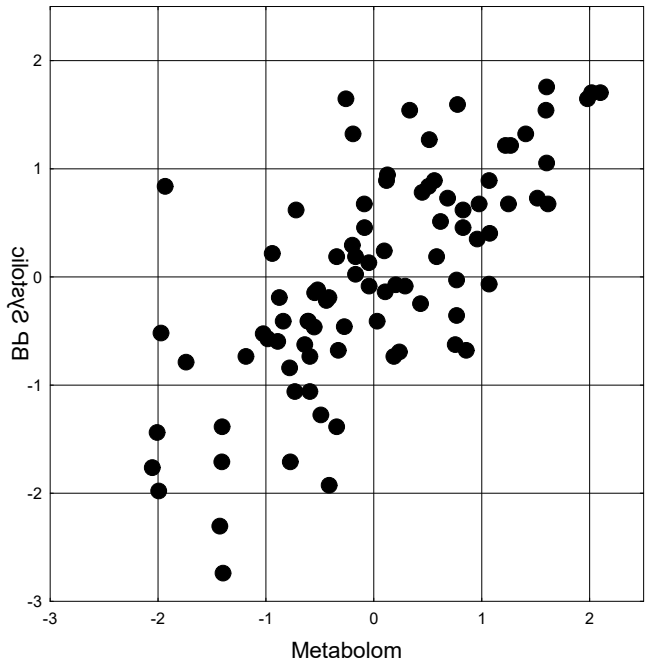

R=0,716; R^2=0,513; $\chi^2_{(5)}$=60; $p<10^{-6}$; Λ Prime=0,4868
Fig. 7.20. Scatterplot of canonical correlation between Metabolic variables (X-line) and Blood Pressure Systolic (Y-line)

Diastolic BP is upregulated, in addition to uricosuria, also by calciuria, natriuria, ureauria as well as plasma atherogenicity. In addition to superoxide dismutase and electrokinetic index, glycemia and natriemia unexpectedly turned out to be downregulators. Despite the expansion of the list of factors, the extent of their determination of diastolic BP is even somewhat smaller than the metabolic determination of systolic BP (Table 7.24 and Fig. 7.21).

Table 7.24. Regression Summary for Blood Pressure Diastolic
R=0,669; R^2=0,448; Adjusted R^2=0,384; $F_{(9,8)}$=7,0; $p<10^{-5}$; SE=7,9 mmHg

N=88		Beta	St. Err. of Beta	B	St. Err. of B	$t_{(78)}$	p-level
Variables	r		Intercpt	126,6	16,6	7,64	10^{-6}
Uric acid Excretion, mM/24 h	**0,38**	0,284	0,133	1,891	0,887	2,13	0,036
Calcium Excretion, mM/24 h	**0,27**	0,267	0,105	0,868	0,342	2,54	0,013
Sodium Excretion, mM/24 h	**0,24**	0,242	0,109	0,027	0,012	2,23	0,029
Urea Excretion, mM/24 h	**0,21**	-0,338	0,156	-0,015	0,007	-2,16	0,034
Dobiásová's & Frohlich's AI	0,19	0,252	0,091	3,569	1,287	2,77	0,007
Electrokinetics Index, %	-0,19	-0,129	0,094	-0,107	0,078	-1,37	0,173
Glucose, mM/L	**-0,23**	-0,140	0,089	-1,577	0,996	-1,58	0,117
Sodium, mM/L	**-0,25**	-0,211	0,090	-0,246	0,106	-2,33	0,022
Superoxide dismutase, un/mL	**-0,41**	-0,298	0,094	-0,123	0,039	-3,18	0,002

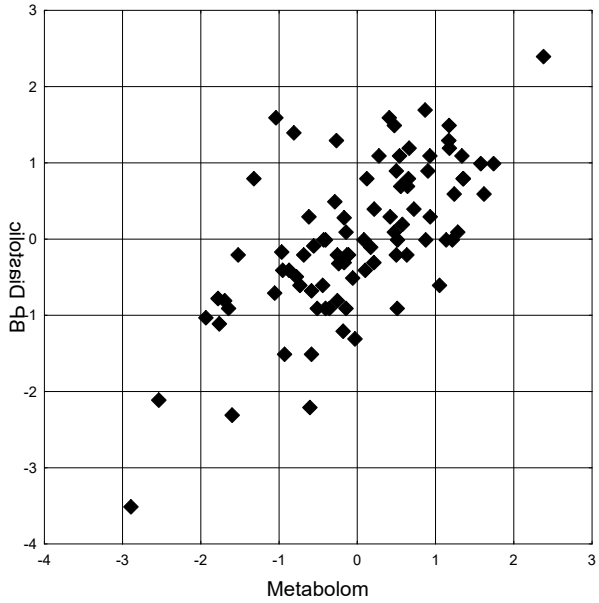

R=0,669; R^2=0,448; $\chi^2_{(9)}$=48; p<10^{-6}; Λ Prime=0,5523

Fig. 7.21. Scatterplot of canonical correlation between Metabolic variables (X-line) and Blood Pressure Diastolic (Y-line)

Combining both regression models in canonical analysis had little effect on the measure of metabolic determination of blood pressure, which was 55,2% (Table 7.25 and Fig. 7.22).

Table 7.25. Factor structure of Metabolic and Blood Pressure Roots

Left set	R
Uric acid Excretion, mM/24 h	-0,408
VLD LP Cholesterol, mM/L	-0,366
Dobiásová's & Frohlich's AI	-0,277
Phosphate, mM/L	-0,223
Sodium Excretion, mM/24 h	-0,214
Calcium Excretion, mM/24 h	-0,192
Urea Excretion, mM/24 h	-0,176
Superoxide dismutase, un/mL	0,750
Electrokinetics Index, %	0,494
Glucose, mM/L	0,199
Sodium, mM/L	0,187
Right set	R1
BP Systolic	-0,979
BP Diastolic	-0,805

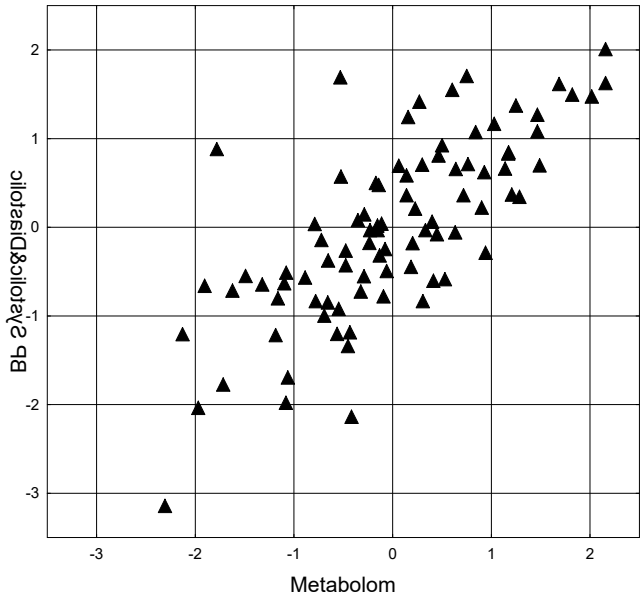

R=0,743; R^2=0,552; $\chi^2_{(22)}$=93; $p<10^{-6}$; Λ Prime=0,3108

Fig. 7.22. Scatterplot of canonical correlation between Metabolic variables (X-line) and Blood Pressure Systolic&Diastolic (Y-line)

A comparative analysis of the coefficients of determination revealed that systolic BP is most subject to the regulatory influence of the metabolome (0,513) and central nervous system (0,490), the immune system has a lesser influence (0,324) and the autonomous nervous&endocrine systems (0,212) have a minimal influence. The metabolome turned out to be the most important regulator of diastolic BP (0,448), while the second position in the hierarchy of influence was occupied by autonomous nervous&endocrine systems (0,429), displacing both central nervous (0,365) and immune (0,302) systems. However, according to the results of the canonical correlation analysis, the central nervous system (0,596) took the leading place, pushing the metabolome (0,552); autonomous nervous&endocrine (0,439) and immune (0,395) systems occupied the following positions in the hierarchy of influence on blood pressure.

If we combine all the mentioned constellations of factors into a single set, which we previously called the *Tensioregulome*, it turns out that the degree of determination of the last systolic BP reaches 0,778 against the average for the four constellations of 0,385; for diastolic BP, the determination reaches 0,721 against 0,386; and for both BP parameters 0,837 versus 0,496, respectively. So, there are reasons to claim that an increase in the number of variables/factors is accompanied by a disproportionate increase in the degree of BP determination by their combination from moderate to high, that is, quantity turns into quality.

And now in more detail about the above. With regard to systolic BP, it was found that among the hypertensive factors included in the Tensioregulome structure, the first two positions are occupied by the age of the patient and the PSD of β-rhythm generating neurons, which are projected onto the O1 locus (Table 7.26). This is followed by markers of inflammation, uricosuria and leukocytary adaptation index as well as PSD of β-rhythm generating neurons, which are projected onto the other four exclusively right-sided loci. The least important hypertensive factors were the variability of β-rhythm, PSD of α-rhythm generating neurons projected on F7 locus and θ-rhythm generating neurons projected on T3 locus as well as Entropy of PSD in T3 locus and of Immunocytogram. Among hypotensive factors, superoxide dismutase leads by a large margin. This is followed by the PSD of δ-rhythm generating neurons projected on four loci and the laterality (rightward shift of symmetry) of α- and β-rhythms. The least important hypotensive factors were the intensity of

phagocytosis of Staphylococcus aureus by blood neutrophils, blood level of T-helper lymphocytes, and female sex. Taken together, the listed variables determine systolic BP by 77,8% (Fig. 7.23), which allows us to estimate its level with an error of 10,0 mmHg.

Table 7.26. Regression Summary for Blood Pressure Systolic
R=0,882; R^2=0,778; Adjusted R^2=0,711; $F_{(20,7)}$=11,7; $p<10^{-5}$; SE=10,0 mmHg

N=88		Beta	St. Err. of Beta	B	St. Err. of B	$t_{(67)}$	p-level
Variables	r		Intercpt	10,9	54,2	0,20	0,841
Age, years	**0,37**	0,234	0,081	0,344	0,120	2,88	0,005
PSD O1-β, %	**0,33**	0,123	0,068	0,281	0,155	1,82	0,074
C-Reactive Protein, µg/L	**0,27**	0,493	0,172	9,884	3,438	2,88	0,005
Interleukin-6, ng/L	**0,24**	-0,291	0,184	-2,077	1,314	-1,58	0,119
Uricosuria, mM/24 h	**0,25**	0,145	0,070	1,786	0,864	2,07	0,043
Popovych's Adaptation Index-2	**0,25**	0,103	0,079	4,562	3,531	1,29	0,201
PSD C4-β, %	**0,25**	-0,291	0,184	-2,077	1,314	-1,58	0,119
PSD T3 Entropy	**0,24**	0,357	0,113	0,501	0,158	3,16	0,002
PSD Fp2-β, %	**0,22**	0,159	0,083	0,210	0,111	1,90	0,061
PSD O2-β, %	**0,21**	0,268	0,080	8,473	2,543	3,33	0,001
PSD F4-β, %	0,20	-0,301	0,114	-0,291	0,110	-2,64	0,010
Deviation β, Hz	**0,21**	0,342	0,066	9,943	1,918	5,18	10^{-5}
PSD T3-θ, %	**0,21**	-0,353	0,073	-0,268	0,056	-4,83	10^{-5}
PSD F7-α, %	0,20	0,219	0,100	0,277	0,126	2,20	0,032
Popovych's Adaptation Index-1	0,20	0,268	0,080	8,473	2,543	3,33	0,001
Entropy of Immunocytogram	0,20	0,109	0,077	75,88	53,43	1,42	0,160
Sex Index (M=1; F=2)	-0,19	-0,187	0,073	-8,259	3,233	-2,55	0,013
CD4⁺ T-helper Ly, %	-0,17	-0,176	0,087	-0,424	0,210	-2,02	0,047
Microb Count Staph. aur., B/Ph	-0,19	0,123	0,068	0,281	0,155	1,82	0,074
Laterality β, %	-0,20	-0,306	0,071	-0,212	0,049	-4,32	10^{-4}
Laterality α, %	**-0,22**	0,248	0,112	0,219	0,098	2,22	0,030
PSD C4-δ, %	-0,20	0,493	0,172	9,884	3,438	2,88	0,005
PSD T5-δ, %	**-0,21**	-0,187	0,073	-8,259	3,233	-2,55	0,013
PSD F3-δ, %	**-0,23**	0,092	0,068	12,79	9,50	1,35	0,183
PSD Fp1-δ, %	**-0,26**	-0,436	0,119	-0,591	0,161	-3,68	10^{-3}
Superoxide Dismutase, un/mL	**-0,56**	-0,353	0,073	-0,268	0,056	-4,83	10^{-5}

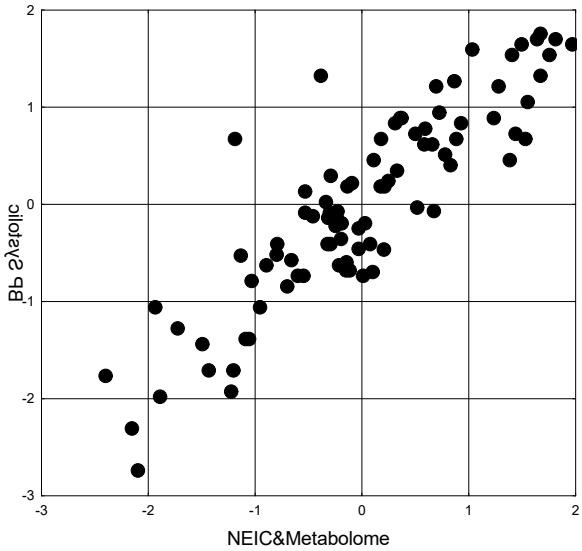

R=0,882; R^2=0,778; $\chi^2_{(20)}$=114; $p<10^{-6}$; Λ Prime=0,2223

Fig. 7.23. Scatterplot of canonical correlation between Tensioregulome (X-line) and Blood Pressure Systolic (Y-line)

With regard to diastolic BP (Table 7.27), it was found that among the hypertensive factors the top position is occupied by the uricosuria. Other significant factors of upregulation were sympathotonic shift of sympatho-vagal balance, circulating catecholamines, calciuria, PSD of β-rhythm generating neurons projected onto the O1 and F8 loci, leukocyte adaptation index, and, to a lesser extent, plasma atherogenicity. The most significant factors of downregulation were female sex and superoxide dismutase, less powerful were vagal tone, calcitonin standardized by sex, the PSD of α-rhythm generating neurons projected onto the O2 locus, and, to a lesser extent, electrokinetics index. Taken together, the listed variables determine diastolic BP by 72,1% (Fig. 7.24), which allows us to estimate its level with an error of 5,8 mmHg.

Table 7.27. Regression Summary for Blood Pressure Diastolic
R=0,849; R^2=0,721; Adjusted R^2=0,663; $F_{(15,7)}$=12,4; $p<10^{-5}$; SE=5,8 mmHg

N=88		Beta	St. Err. of Beta	B	St. Err. of B	$t_{(72)}$	p-level
Variables	r		Intercpt	78,1	14,0	5,56	10^{-6}
Uricosuria, mM/24h	**0,38**	0,189	0,082	1,259	0,547	2,30	0,024
Baevskiy's Stress Index, ln units	**0,32**	0,238	0,134	3,154	1,778	1,77	0,080
1/Mode HRV, 1/msec	**0,29**	-0,242	0,078	-0,017	0,006	-3,11	0,003
Calciuria, mM/24h	**0,27**	0,147	0,071	0,479	0,232	2,06	0,043
PSD O1-β, %	**0,28**	0,125	0,078	0,085	0,053	1,60	0,115
PSD F8-β, μV^2/Hz	**0,22**	0,298	0,071	0,076	0,018	4,18	10^{-4}
Popovych's Adaptation Index-1	**0,25**	0,281	0,071	4,807	1,221	3,94	10^{-4}
Dobiásová's&Frohlich's Ather In	0,19	0,153	0,069	2,163	0,983	2,20	0,031
Electrokinetics Index, %	-0,19	-0,214	0,078	-0,178	0,065	-2,74	0,008
Total Power HRV, $msec^2$	**-0,22**	0,433	0,179	0,0023	0,0009	2,42	0,018
PSD O2-α, μV^2/Hz	**-0,23**	-0,219	0,082	-0,005	0,002	-2,66	0,010
Calcitonin standardized by sex, Z	**-0,24**	-0,233	0,073	-2,717	0,849	-3,20	0,002
PSD HF band, $msec^2$	**-0,25**	-0,142	0,129	-0,0024	0,0022	-1,10	0,277
Superoxide Dismutase, units/mL	**-0,41**	-0,246	0,076	-0,101	0,031	-3,25	0,002
Sex Index (M=1; F=2)	**-0,44**	-0,193	0,082	-4,599	1,952	-2,36	0,021

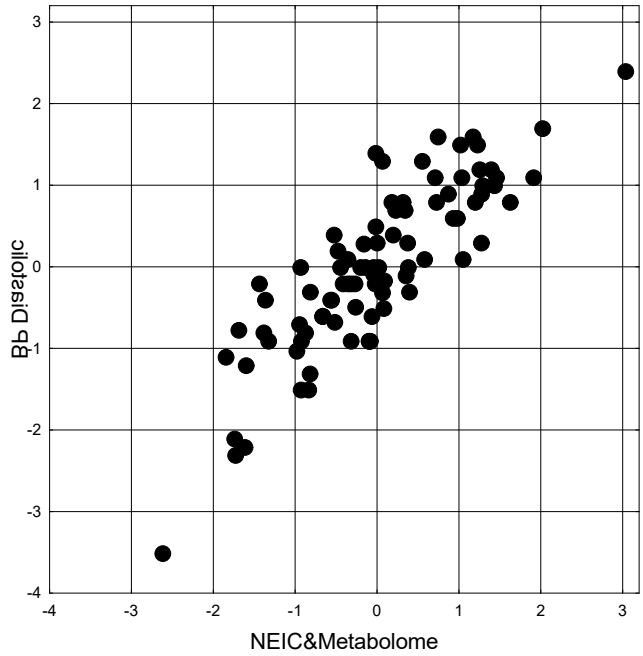

R=0,849; R^2=0,721; $\chi^2_{(16)}$=100; $p<10^{-6}$; Λ Prime=0,2773

Fig. 7.24. Scatterplot of canonical correlation between Tensioregulome (X-line) and Blood Pressure Diastolic (Y-line)

The apotheosis of the above was the analysis of the canonical correlation between Tensioregulome parameters and BP (Table 7.28). The most important hypertensive factors, judging by the factor loadings, were age and electrical activity of β-rhythm generating neurons projecting to the O1 locus. Uricosuria, sympathotonic shift in sympatho-vagal balance, chronic low-intensity inflammation and plasma atherogenicity, as well as information factors reflecting the relationships between elements of the leukocytogram and immunocytogram, and EEG rhythms in the T3 locus had a somewhat weaker upregulating effect on blood pressure. The weakest hypertensive factors were the activity of α-rhythm generating neurons projecting to the F7 locus, calciumuria, and circulating catecholamines. Interestingly, the activity of α-rhythm generating neurons projecting to the O2 locus was a hypotensive factor, but also a weak one. Superoxide dismutase and electrokinetics index as an integral marker of anti-aging were found to be the most powerful hypotensive factors. The factors associated with female sex, calcitonin standardized by sex, electrical activity of δ-rhythm generating neurons projecting to F7 and Fp1 loci, vagal tone, blood level of T-helper lymphocytes, and the intensity of phagocytosis of Staphylococcus aureus by blood neutrophils had a somewhat weaker downregulating effect on blood pressure.

Table 7.28. Factor structure of Tensioregulome and Blood Pressure Roots

Left set	R
Age, years	-0,374
PSD O1-β, %	-0,368
Uricosuria, mM/24 h	-0,331
Baevskiy's Stress Index, ln un	-0,292
C-Reactive Protein, µg/L	-0,278
PSD O2-β, %	-0,270
PSD F4-β, %	-0,262
Popovych's Adaptation Index-2	-0,270
Popovych's Adaptation Index-1	-0,253
Entropy of Immunocytogram	-0,242
Interleukin-6, ng/L	-0,238
Dobiásová's&Frohlich's Ather Ind	-0,225
PSD T3 Entropy	-0,219
PSD F7-α, %	-0,204
Calciuria, mM/24 h	-0,154
Deviation β, Hz	-0,126
PSD F8-β, $\mu V^2/Hz$	-0,110
1/Mode HRV, 1/msec	-0,081
Superoxide Dismutase, un/mL	0,610
Electrokinetics Index, %	0,402
Sex Index (M=1; F=2)	0,298
PSD F7-δ, %	0,264
PSD Fp1-δ, %	0,259
PSD HF band, $msec^2$	0,242
Total Power HRV, $msec^2$	0,235
$CD4^+$ T-helper Lymphocytes, %	0,227
Calcitonin standardized by sex, Z	0,217
PSD C4-δ, %	0,213
Laterality α, %	0,212
Microbial Count Staph. aur., B/Ph	0,205
PSD O2-α, $\mu V^2/Hz$	0,187
Right set	R1
BP Systolic	-0,980
BP Diastolic	-0,802

Taken together, the listed variables as the Tensioregulome determine BP by 83,7% (Fig. 7.25).

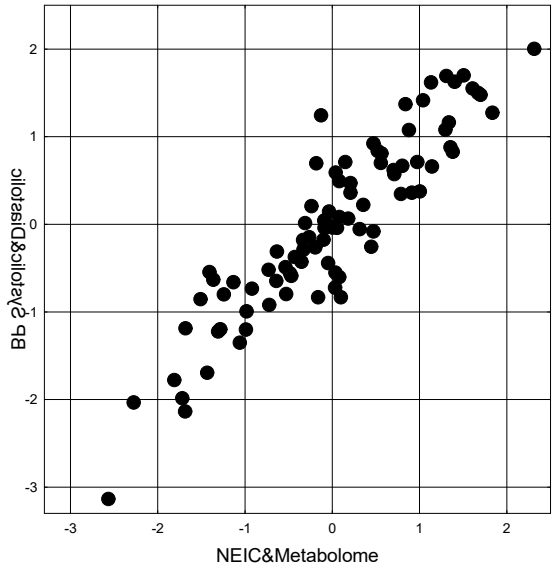

R=0,915; R^2=0,837; $\chi^2_{(62)}$=193; $p<10^{-6}$; Λ Prime=0,0636

Fig. 7.25. Scatterplot of canonical correlation between Tensioregulome (X-line) and Blood Pressure Systolic&Diastolic (Y-line)

After establishing the relationship between Tensioregulome and Blood Pressure, it was time to determine the relationship between changes in these variables caused by balneotherapy. First of all, we note that in contrast to the rather strong relationship between systolic and diastolic blood pressure (Fig. 7.26), the relationship between their ***changes*** is, firstly, weaker, and secondly, ambiguous: in addition to unidirectional changes, there are cases of an increase in diastolic with a decrease in systolic blood pressure and vice versa (Fig. 7.27).

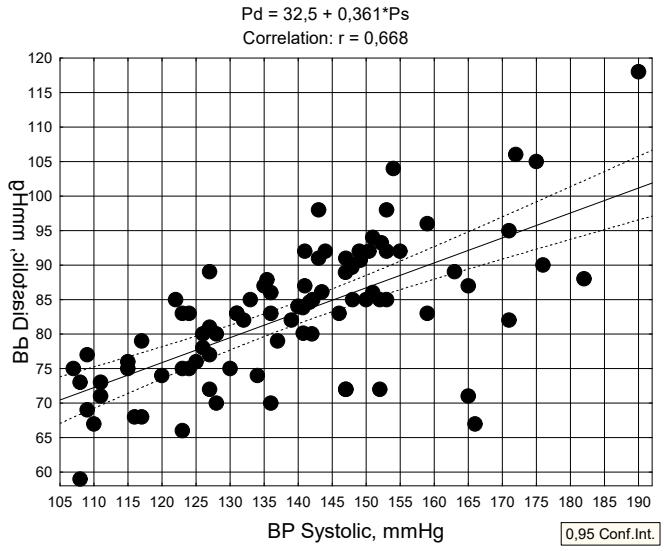

Fig. 7.26. Scatterplot of correlation between Blood Pressure Systolic (X-line) and Diastolic (Y-line)

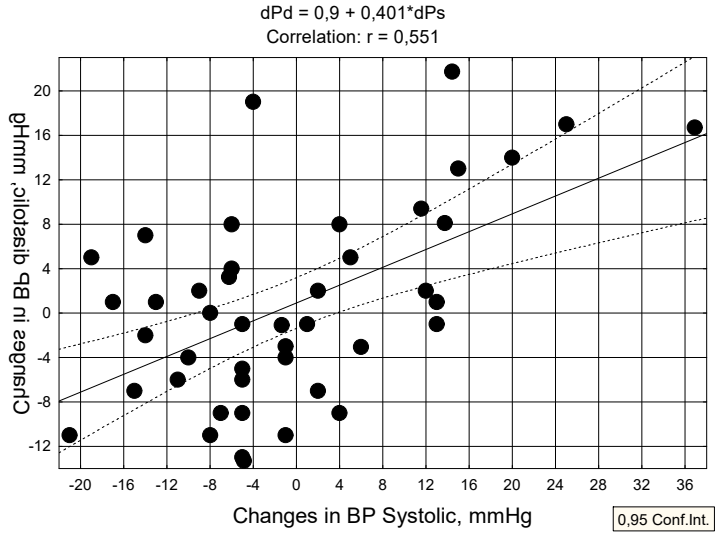

Fig. 7.27. Scatterplot of correlation between changes in Blood Pressure Systolic (X-line) and Diastolic (Y-line)

A first glance at the correlation matrix (Table 7.29) is enough to conclude that there are more or less pronounced unidirectional changes in the electrical activity of CNS neurons and BP. A single negative correlation coefficient reflects an increase in diastolic BP with a leftward shift in α-rhythm symmetry and a decrease in diastolic BP with a rightward shift, respectively.

Table 7.29. Correlation Matrix for changes in EEG and Blood Pressure Variables

EEG Variables	BP systolic	BP diastolic
Laterality α, %	-0,03	-0,31
PSD Fp1-θ, μV²/Hz	0,31	0,08
PSD Fp2-α, μV²/Hz	**0,41**	0,25
PSD F3-β, μV²/Hz	**0,33**	0,20
PSD F4 Entropy	**0,33**	-0,05
PSD F4-α, μV²/Hz	**0,42**	0,24
PSD F8-α, μV²/Hz	**0,45**	**0,34**
PSD F8-θ, μV²/Hz	**0,43**	0,32
PSD T3-θ, %	**0,47**	0,30
PSD T3-α, μV²/Hz	**0,46**	**0,39**
PSD T3-θ, μV²/Hz	**0,48**	**0,45**
PSD T4-α, μV²/Hz	**0,43**	**0,36**
PSD C3-θ, μV²/Hz	**0,37**	0,18
PSD C4-β, μV²/Hz	**0,35**	0,11
PSD C4-α, μV²/Hz	**0,36**	0,28
PSD T5-α, μV²/Hz	**0,34**	**0,40**
PSD T5-θ, μV²/Hz	**0,34**	0,26
PSD P3-α, μV²/Hz	0,23	**0,38**
PSD P3-θ, μV²/Hz	0,32	0,32
PSD P3-δ, μV²/Hz	0,15	**0,39**
PSD O1-θ, μV²/Hz	**0,33**	**0,43**
PSD O1-δ, μV²/Hz	**0,36**	0,15
PSD O2-β, %	0,12	0,31
PSD O2-β, μV²/Hz	0,30	0,23
PSD O2-δ, μV²/Hz	0,30	0,00

After stepwise exclusion, the regression model remained with 6 parameters each of α- and θ-rhythms and 2 parameters each of δ- and β-rhythms, as well as the entropy of PSD in the F4 locus, whose cumulative changes determined changes in systolic BP by 92% (Table 7.30 and Fig. 7.28).

Table 7.30. Regression Summary for changes in Blood Pressure Systolic and EEG
R=0,960; R^2=0,921; Adjusted R^2=0,821; $F_{(19,2)}$=9,2; $p<10^{-5}$; SE=4,6 mmHg

N=35		Beta	St. Err. of Beta	B	St. Err. of B	$t_{(15)}$	p-level
Variables	r		Intercpt	4,316	1,418	3,04	0,008
PSD T3-θ, μV²/Hz	**0,48**	0,647	0,225	0,150	0,052	2,87	0,012
PSD T3-α, μV²/Hz	**0,46**	1,858	0,423	0,132	0,030	4,39	0,001
PSD F8-α, μV²/Hz	**0,45**	-2,465	0,529	-0,119	0,026	-4,66	10^{-3}
PSD F8-θ, μV²/Hz	**0,43**	1,750	0,336	0,289	0,055	5,21	10^{-4}
PSD F4-α, μV²/Hz	**0,42**	-0,618	0,466	-0,055	0,042	-1,33	0,205
PSD Fp2-α, μV²/Hz	**0,41**	0,956	0,483	0,112	0,057	1,98	0,067
PSD C3-θ, μV²/Hz	**0,37**	1,614	0,539	0,118	0,039	3,00	0,009
PSD C4-α, μV²/Hz	**0,36**	0,818	0,181	0,202	0,045	4,52	10^{-3}
PSD O1-δ, μV²/Hz	**0,36**	-1,319	0,445	-0,177	0,060	-2,96	0,010
PSD C4-β, μV²/Hz	**0,35**	2,670	0,432	0,434	0,070	6,18	10^{-4}
PSD T5-α, μV²/Hz	**0,34**	-2,084	0,379	-0,177	0,032	-5,50	10^{-4}
PSD T5-θ, μV²/Hz	**0,34**	-0,628	0,298	-0,047	0,022	-2,11	0,052
PSD O1-θ, μV²/Hz	**0,33**	-0,750	0,284	-0,170	0,065	-2,64	0,019
PSD F3-β, μV²/Hz	**0,33**	-0,801	0,172	-0,275	0,059	-4,67	10^{-3}
PSD F4 Entropy	**0,33**	0,471	0,093	24,13	4,775	5,05	10^{-4}
PSD Fp1-θ, μV²/Hz	0,31	-2,238	0,435	-0,438	0,085	-5,14	10^{-4}
PSD O2-β, μV²/Hz	0,30	1,587	0,337	0,015	0,003	4,71	10^{-3}
PSD O2-δ, μV²/Hz	0,30	0,348	0,154	0,072	0,032	2,26	0,039

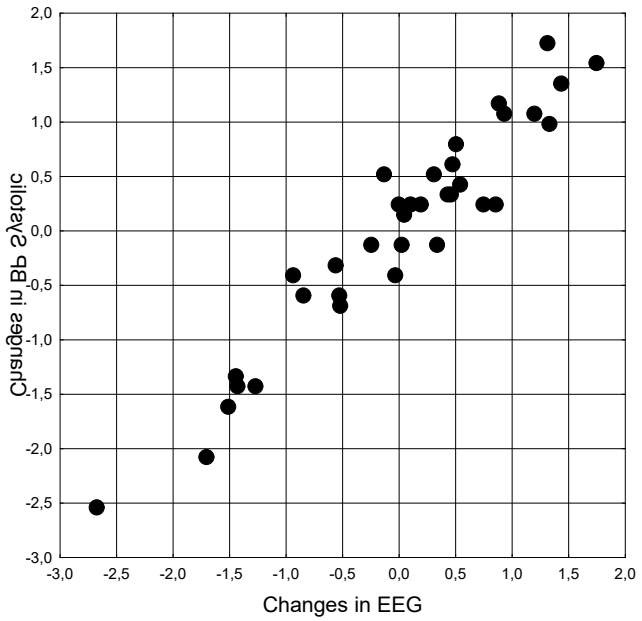

R=0,960; R^2=0,921; $\chi^2_{(19)}$=80; $p<10^{-5}$; Λ Prime=0,0791

Fig. 7.28. Scatterplot of canonical correlation between changes in EEG parameters (X-line) and Blood Pressure Systolic (Y-line)

At the same time, changes in diastolic BP are determined by changes in CNS electrical activity by only 68% (Table 7.31 and Fig. 7.29).

Table 7.31. Regression Summary for changes in Blood Pressure Diastolic and EEG
R=0,823; R^2=0,677; Adjusted R^2=0,543; $F_{(10,2)}$=5,0; p=0,0006; SE=5,5 mmHg

N=35		Beta	St. Err. of Beta	B	St. Err. of B	$t_{(24)}$	p-level
Variables	r		Intercpt	-0,274	1,113	-0,25	0,808
PSD T5-α, μV²/Hz	**0,40**	-0,400	0,291	-0,069	0,051	-1,37	0,183
PSD P3-δ, μV²/Hz	**0,39**	-0,632	0,378	-0,070	0,042	-1,67	0,108
PSD P3-α, μV²/Hz	**0,38**	-0,818	0,379	-0,046	0,021	-2,16	0,041
PSD F8-α, μV²/Hz	**0,34**	0,804	0,371	0,029	0,013	2,17	0,040
PSD F8-θ, μV²/Hz	0,32	0,485	0,301	0,060	0,037	1,61	0,120
PSD P3-θ, μV²/Hz	0,32	0,835	0,226	0,026	0,007	3,70	0,001
PSD O2-β, %	0,31	0,590	0,208	0,013	0,005	2,83	0,009
PSD T3-θ, %	0,30	0,370	0,134	0,629	0,228	2,77	0,011
Laterality α, %	-0,31	-0,583	0,157	-0,125	0,034	-3,72	0,001

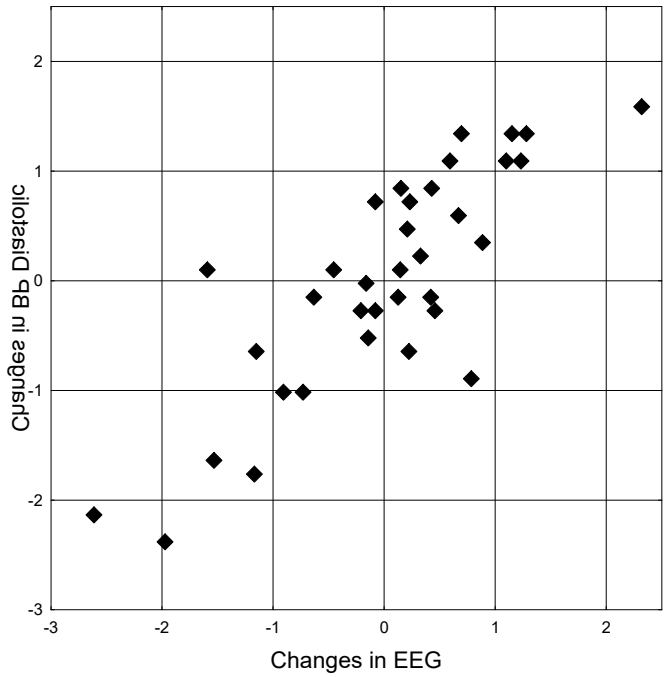

R=0,823; R^2=0,677; $\chi^2_{(10)}$=32; p=0,0005; Λ Prime=0,3226

Fig. 7.29. Scatterplot of canonical correlation between changes in EEG parameters (X-line) and Blood Pressure Diastolic (Y-line)

Canonical correlation analysis shows that balneotherapy-induced changes in BP are upregulated by changes in PSD of θ-rhythm generating neurons projecting, with a single exception, to the left scalp loci, as well as α-, β-, and δ-rhythms generating neurons projecting to both sides of the scalp and along the entire sagittal axis (Table 7.32). The degree of neurogenic determination of both BP parameters is only 2% higher than that of systolic BP (Fig. 7.30).

Table 7.32. Factor structure of changes in EEGs and Blood Pressure Roots

EEG Variables	R
PSD T3-θ, μV²/Hz	**-0,538**
PSD T3-θ, %	**-0,494**
PSD T3-α, μV²/Hz	**-0,512**
PSD F8-α, μV²/Hz	**-0,485**

PSD T4-α, μV²/Hz	**-0,478**
PSD F8-θ, μV²/Hz	**-0,464**
PSD F4-α, μV²/Hz	**-0,438**
PSD Fp2-α, μV²/Hz	**-0,435**
PSD T5-α, μV²/Hz	**-0,401**
PSD O1-θ, μV²/Hz	**-0,400**
PSD C4-α, μV²/Hz	**-0,390**
PSD C3-θ, μV²/Hz	**-0,381**
PSD T5-θ, μV²/Hz	**-0,371**
PSD P3-θ, μV²/Hz	**-0,366**
PSD O1-δ, μV²/Hz	**-0,359**
PSD C4-β, μV²/Hz	**-0,346**
PSD F3-β, μV²/Hz	**-0,345**
PSD O2-β, μV²/Hz	**-0,325**
PSD P3-α, μV²/Hz	**-0,297**
PSD Fp1-θ, μV²/Hz	**-0,296**
PSD F4 Entropy	**-0,290**
PSD O2-δ, μV²/Hz	**-0,269**
PSD P3-δ, μV²/Hz	**-0,229**
PSD O2-β, %	**-0,186**
Laterality α, %	**0,099**
Blood Pressure	**R**
BP Systolic	**-0,978**
BP Diastolic	**-0,605**

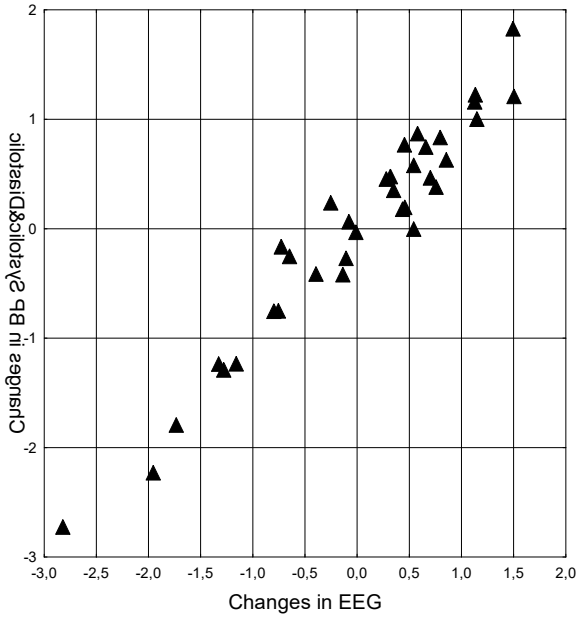

R=0,970; R^2=0,941; $\chi^2_{(50)}$=98; $p<10^{-4}$; Λ Prime=0,0073

Fig. 7.30. Scatterplot of canonical correlation between changes in EEG parameters (X-line) and Blood Pressure Systolic&Diastolic (Y-line)

Contrary to expectations, no significant (module ≥0,29) correlation coefficient was found between changes in BP and HRV and endocrine variables (Table 7.33).

Table 7.33. Correlation Matrix for changes in HRV&Endocrine and Blood Pressure Variables

HRV&Endocrine Variables	**BP systolic**	**BP diastolic**
Baevskiy's Stress Index, ln un	0,23	0,08

PSD ULF band, %	0,19	0,28
Testosterone standardized, Z	0,21	0,24
PSD LFnu band, %	0,17	0,25
PSD ULF band, msec^2	0,00	0,27
PSD LF band, msec^2	0,19	0,19
Parathyroid hormone, pM/L	0,19	0,19
PSD LF band, %	0,11	0,19
LF/HF Ratio	0,04	0,19
PSD HF band, %	-0,10	-0,26
Autonomic Reactivity	-0,15	-0,19

However, taken together, changes in the levels of parathyroid hormone and testosterone standardized by sex and age, as well as 3 HRV parameters, determined changes in systolic BP weakly but statistically significantly (Table 7.34 and Fig. 7.31).

Table 7.34. Regression Summary for changes in Blood Pressure Systolic and HRV&Hormones

R=0,566; R^2=0,320; Adjusted R^2=0,231; $F_{(5,4)}$=3,6; p=0,0095; SE=10,7 mmHg

N=44		Beta	St. Err. of Beta	B	St. Err. of B	$t_{(38)}$	p-level
Variables	r		Intercpt	0,910	2,446	0,37	0,710
Baevskiy's Stress Index, ln units	0,23	0,460	0,153	7,454	2,474	3,01	0,005
Testosterone standardized, Z	0,21	0,266	0,136	3,207	1,637	1,96	0,057
Parathyroid hormone, pM/L	0,19	0,231	0,135	2,363	1,382	1,71	0,095
PSD LF band, msec^2	0,19	0,373	0,151	0,005	0,002	2,47	0,018
PSD ULF band, %	0,19	0,227	0,138	0,466	0,284	1,64	0,109

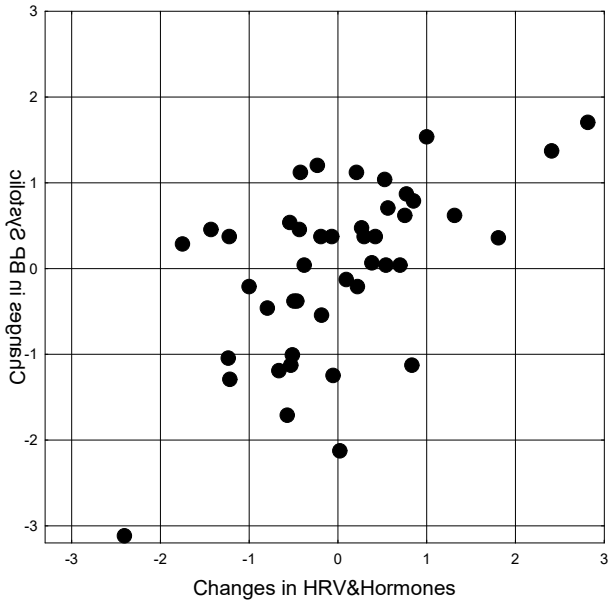

R=0,566; R^2=0,320; $\chi^2_{(5)}$=15; p=0,009; Λ Prime=0,6799

Fig. 7.31. Scatterplot of canonical correlation between changes in HRV&Endocrine parameters (X-line) and Blood Pressure Systolic (Y-line)

A similar situation was noted with regard to the autonomous and hormonal determination of changes in diastolic blood pressure (Table 7.35 and Fig. 7.32).

Table 7.35. Regression Summary for changes in Blood Pressure Diastolic and HRV&Hormones

R=0,547; R^2=0,299; Adjusted R^2=0,207; $F_{(5,4)}$=3,2; p=0,015; SE=7,9 mmHg

N=44		Beta	St. Err. of Beta	B	St. Err. of B	$t_{(38)}$	p-level
Variables	r			Intercpt	2,186	1,17	0,249
PSD ULF band, %	0,28	0,365	0,142	0,546	0,212	2,58	0,014
Testosterone standardized, Z	0,24	0,321	0,139	2,821	1,219	2,31	0,026
PSD LF band, %	0,19	0,197	0,148	0,102	0,076	1,33	0,191
Parathyroid hormone, pM/L	0,19	0,208	0,137	1,549	1,025	1,51	0,139
Autonomic Reactivity	-0,19	-0,237	0,153	-0,728	0,469	-1,55	0,129

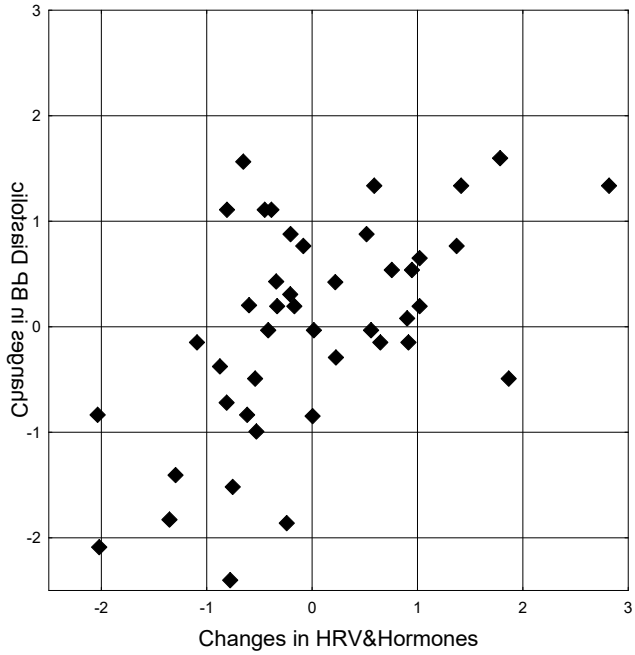

R=0,547; R^2=0,299; $\chi^2_{(5)}$=15; p=0,015; Λ Prime=0,7006

Fig. 7.32. Scatterplot of canonical correlation between changes in HRV&Endocrine parameters (X-line) and Blood Pressure Diastolic (Y-line)

According to the canonical correlation analysis, balneotherapy-induced changes in testosterone, parathyroid hormone and HRV parameters determine changes in BP by 39% (Table 7.36 and Fig. 7.33).

Table 7.36. Factor structure of changes in HRV&Endocrine and Blood Pressure Roots

HRV&Endocrine Variables	**R**
PSD ULF band, %	**-0,421**
Testosterone standardized, Z	**-0,412**
PSD LF band, msec²	**-0,350**
Parathyroid hormone, pM/L	**-0,349**
Baevskiy's Stress Index, ln un	**-0,289**
PSD LF band, %	**-0,268**
Autonomic Reactivity	**0,302**
Blood Pressure	**R**
BP Systolic	**-0,889**
BP Diastolic	**-0,871**

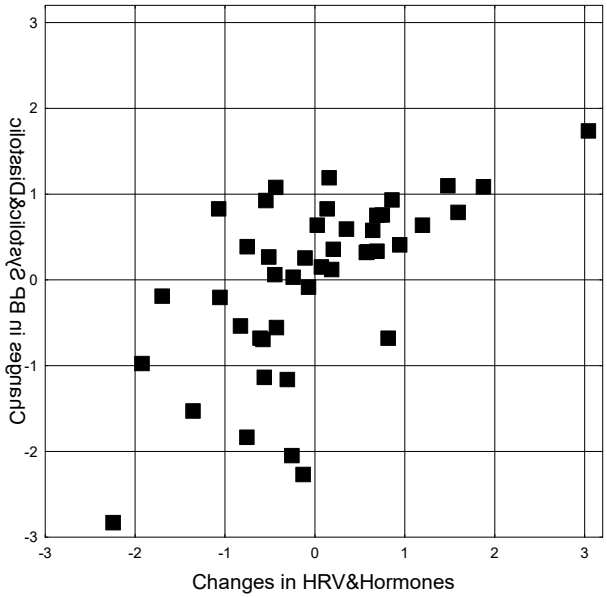

R=0,624; R^2=0,390; $\chi^2_{(14)}$=22; p=0,074; Λ Prime=0,5576

Fig. 7.33. Scatterplot of canonical correlation between changes in HRV&Endocrine parameters (X-line) and Blood Pressure Systolic&Diastolic (Y-line)

Of the immunity parameters whose changes are associated with changes in systolic BP (7.37), only three (7.38) were included in the regression model, which together determine its changes by 32,5% (Fig. 7.34).

Table 7.37. Correlation Matrix for changes in Immune and Blood Pressure Variables

Immune Variables	**BP systolic**	**BP diastolic**
Microbial Count Staph. aureus, B/Ph	**-0,47**	-0,21
Pan Lymphocytes, %	**-0,31**	-0,14
IgG Saliva, g/L	**-0,30**	-0,22
IgA Saliva, g/L	-0,27	**-0,33**
Microbial Count E. coli, B/Ph	-0,22	**-0,37**
IgM Serum, g/L	-0,07	**-0,33**
Bactericidity vs E. coli, 10^9 B/L	0,05	-0,23
Bacteriuria, lg CFU/mL	0,02	**0,32**
$CD56^+$ NK Lymphocytes, %	0,18	0,27
Polymorphonucleary Neutrophils, %	0,26	0,16
IgA Serum, g/L	0,21	0,08

Table 7.38. Regression Summary for changes in Blood Pressure Systolic and Immunity
R=0,570; R^2=0,325; Adjusted R^2=0,274; $F_{(3,4)}$=6,4; p=0,0012; SE=10,4 mmHg

N=44		Beta	St. Err. of Beta	B	St. Err. of B	$t_{(40)}$	p-level
Variables	r		Intercpt	-0,061	1,572	-0,04	0,969
Microbial Count St. aur., B/Ph	**-0,47**	-0,433	0,131	-0,574	0,173	-3,31	0,002
Pan Lymphocytes, %	**-0,31**	-0,274	0,130	-0,522	0,248	-2,11	0,042
IgA Serum, g/L	0,21	0,173	0,131	4,532	3,426	1,32	0,193

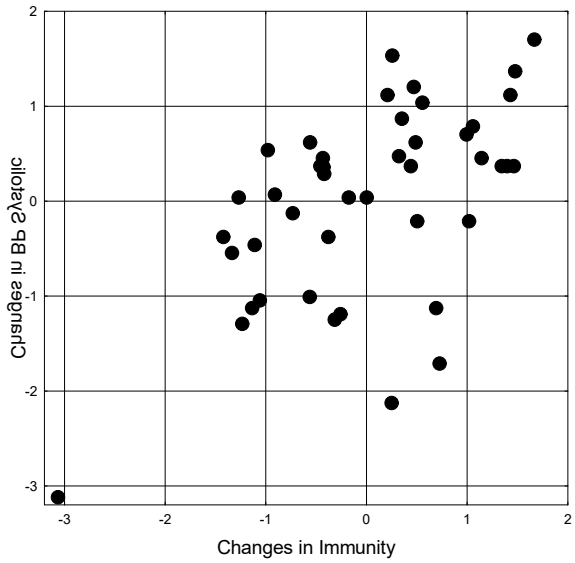

R=0,570; R^2=0,325; $\chi^2_{(3)}$=16; p=0,0012; Λ Prime=0,6753

Fig. 7.34. Scatterplot of canonical correlation between changes in Immune parameters (X-line) and Blood Pressure Systolic (Y-line)

Interestingly, changes in diastolic blood pressure are determined by a completely different constellation of immune parameters, as well as bacteriuria, but to the same extent (Table 7.39 and Fig. 7.35).

Table 7.39. Regression Summary for changes in Blood Pressure Diastolic and Immunity
R=0,556; R^2=0,310; Adjusted R^2=0,239; $F_{(4,4)}$=4,4; p=0,0051; SE=7,7 mmHg

N=44		Beta	St. Err. of Beta	B	St. Err. of B	$t_{(39)}$	p-level
Variables	r			3,026	1,352	2,24	0,031
Bacteriuria, lgCFU/mL	**0,32**	0,608	0,296	4,983	2,425	2,06	0,047
$CD56^+$ NK Lymphocytes, %	0,27	0,303	0,135	0,689	0,307	2,24	0,031
IgM Serum, g/L	**-0,33**	-0,339	0,133	-6,964	2,739	-2,54	0,015
Bactericidity vs E. coli, 10^9 B/L	-0,23	0,340	0,297	0,092	0,080	1,14	0,260

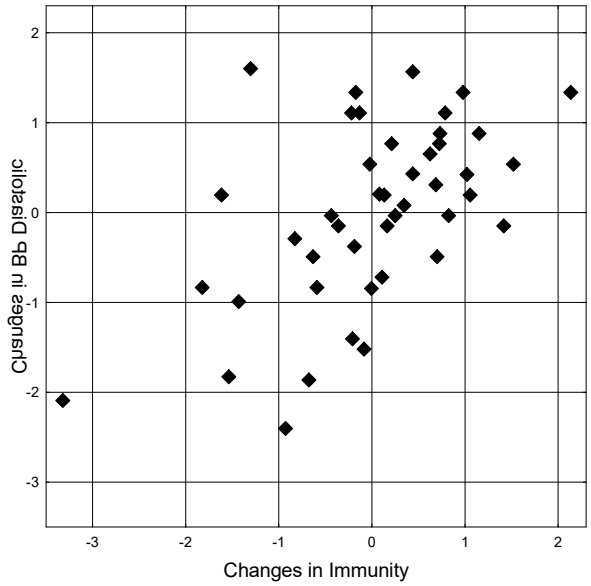

R=0,556; R^2=0,310; $\chi^2_{(4)}$=15; p=0,051; Λ Prime=0,6905

Fig. 7.35. Scatterplot of canonical correlation between changes in Immune parameters (X-line) and Blood Pressure Diastolic (Y-line)

Therefore, as expected, the canonical correlation analysis revealed two pairs of canonical roots (Table 7.40).

The BP-Root of the first pair receives factor loadings from systolic and diastolic BP with opposite signs, and the bacterial-immune root represents variables that are associated with a particular BP parameter (Fig. 7.36).

Instead, BP-Root of the second pair receives factor loadings from systolic and diastolic BP with the same signs, which simplifies the interpretation of the factor structure of the bacterial-immune root. The upregulating effects on BP of bacteriuria, natural killer cells, and IgA, on the one hand, and the downregulating effects of pan lymphocytes, phagocytosing neutrophils, and IgM, on the other hand, are clearly visible (Fig. 7.37).

Table 7.40. Factor structure of changes in Immune and Blood Pressure Roots

Immune Variables	R1	R2
Bacteriuria, lgCFU/mL	-0,551	-0,284
$CD56^+$ NK Lymphocytes, %	-0,195	-0,432
Bactericidity vs E. coli, 10^9 B/L	0,500	0,144
IgM Serum, g/L	0,495	0,358
Microbial Count St. aur., B/Ph	-0,396	0,711
Pan Lymphocytes, %	-0,262	0,462
IgA Serum, g/L	0,210	-0,309
Blood Pressure	R1	R2
BP Systolic	0,401	-0,916
BP Diastolic	-0,544	-0,839

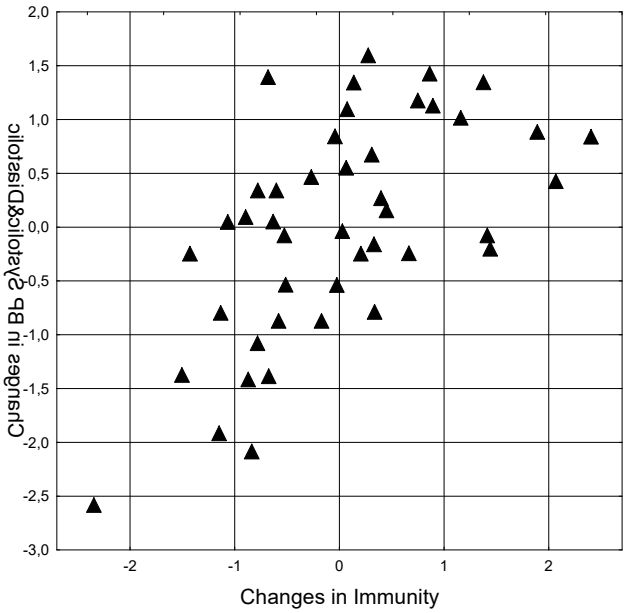

R=0,602; R^2=0,363; $\chi^2_{(14)}$=32; p=0,004; Λ Prime=0,4269

Fig. 7.36. Scatterplot of canonical correlation between changes in Immune parameters (X-line) and Blood Pressure Systolic&Diastolic (Y-line). First pair of Roots

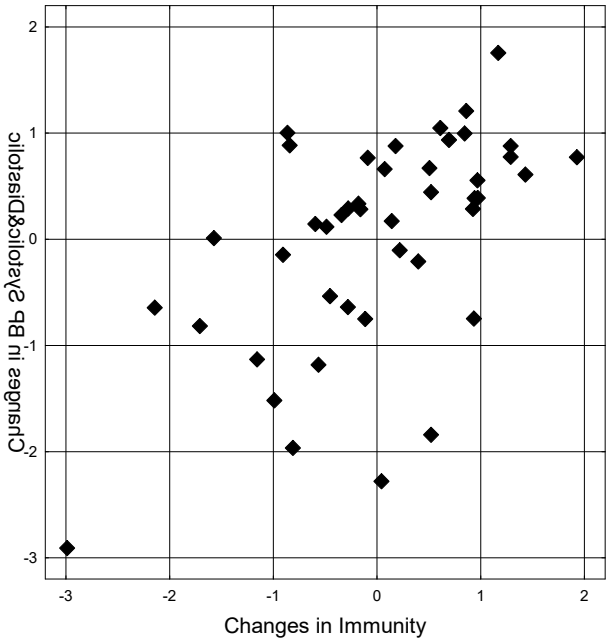

R=0,575; R^2=0,330; $\chi^2_{(6)}$=15; p=0,019; Λ Prime=0,6698

Fig. 7.37. Scatterplot of canonical correlation between changes in Immune parameters (X-line) and Blood Pressure Systolic&Diastolic (Y-line). Second pair of Roots

Quite a few relationships were found between changes in blood pressure and metabolic parameters (Table 7.41).

Table 7.41. Correlation Matrix for Metabolic and Blood Pressure Variables

Metabolic Variables	**BP systolic**	**BP diastolic**
Superoxide dismutase, un/mL	**-0,56**	**-0,50**
Catalase, µM/L•h	**-0,44**	**-0,48**
Glucose, mM/L	-0,03	**-0,21**
Calciemia, mM/L	-0,08	0,19
Phosphatemia, mM/L	-0,07	**0,24**
Sodium Excretion, mM/24 h	0,10	0,20
Uricemia, µM/L	0,18	0,18
Calcium Excretion, mM/24 h	0,21	0,22
VLD LP Cholesterol, mM/L	0,22	-0,08
Magnesiemia, mM/L	**0,38**	0,05
Creatinine Excretion, mM/24 h	**0,26**	**0,24**
Urea Excretion, mM/24 h	**0,28**	**0,25**
Magnesium Excretion, mM/24 h	**0,36**	**0,37**
Uric acid Excretion, mM/24 h	**0,41**	**0,39**
Diuresis, L/24 h	**0,45**	**0,35**
Diene conjugates, E^{232}/mL	**0,64**	**0,43**

The regression model for changes in systolic blood pressure included both antioxidant enzymes as downregulating factors and atherogenic lipoprotein fraction, magnesiemia, magnesiuria, and daily diuresis as upregulating factors, the combined changes of which determined changes in systolic blood pressure by 79% (Table 7.42 and Fig. 7.38).

Table 7.42. Regression Summary for changes in Blood Pressure Systolic and Metabolome

R=0,886; R^2=0,786; Adjusted R^2=0,751; $F_{(6,4)}$=22,6; $p<10^{-5}$; SE=6,1 mmHg

N=44		Beta	St. Err. of Beta	B	St. Err. of B	$t_{(37)}$	p-level
Variables	r		Intercpt	-0,895	1,133	-0,79	0,435
Superoxide dismutase, un/mL	**-0,56**	-0,494	0,108	-0,325	0,071	-4,56	10^{-4}
Catalase, µM/L•h	**-0,44**	-0,235	0,103	-0,059	0,026	-2,28	0,029
VLD LP Cholesterol, mM/L	**0,22**	0,184	0,079	6,330	2,712	2,33	0,025
Magnesiemia, M/L	**0,38**	0,204	0,080	50,93	19,96	2,55	0,015
Magnesiuria, mM/24 h	**0,36**	0,142	0,088	0,857	0,527	1,63	0,112
Diuresis, L/24 h	**0,45**	0,166	0,089	3,566	1,901	1,88	0,069

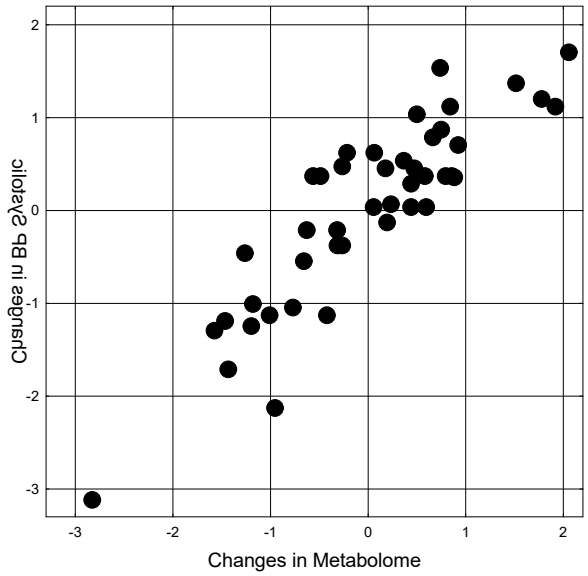

R=0,886; R^2=0,786; $\chi^2_{(6)}$=60; $p<10^{-6}$; Λ Prime=0,2144

Fig. 7.38. Scatterplot of canonical correlation between changes in Metabolic parameters (X-line) and Blood Pressure Systolic (Y-line)

The regression model for changes in diastolic blood pressure included catalase and glucose as downregulating factors, and uricosuria, uricemia, phosphatemia, natriuria, as well as again magnesiuria and daily diuresis as upregulating factors, the combined changes of which determined changes in diastolic blood pressure by 52,5% (Table 7.43 and Fig. 7.39).

Table 7.43. Regression Summary for changes in Blood Pressure Diastolic and Metabolome

R=0,725; R^2=0,525; Adjusted R^2=0,416; $F_{(8,4)}$=4,8; p=0,0005; SE=6,8 mmHg

N=44		Beta	St. Err. of Beta	B	St. Err. of B	$t_{(35)}$	p-level
Variables	r		Intercpt	2,063	1,564	1,32	0,196
Catalase, µM/L•h	**-0,48**	-0,452	0,125	-0,083	0,023	-3,61	0,001
Glucose, mM/L	**-0,21**	-0,173	0,121	-1,379	0,964	-1,43	0,162
Uricemia, µM/L	**0,18**	0,215	0,120	44,69	24,95	1,79	0,082
Sodium Excretion, mM/24 h	**0,20**	0,235	0,136	0,022	0,013	1,72	0,094
Phosphatemia, mM/L	**0,24**	0,244	0,124	11,58	5,868	1,97	0,056
Diuresis, L/24 h	**0,35**	-0,277	0,224	-4,334	3,4934	-1,24	0,223
Magnesium Excretion, mM/24 h	**0,37**	0,239	0,134	1,052	0,591	1,78	0,084
Uric acid Excretion, mM/24 h	**0,39**	0,342	0,197	1,765	1,019	1,73	0,092

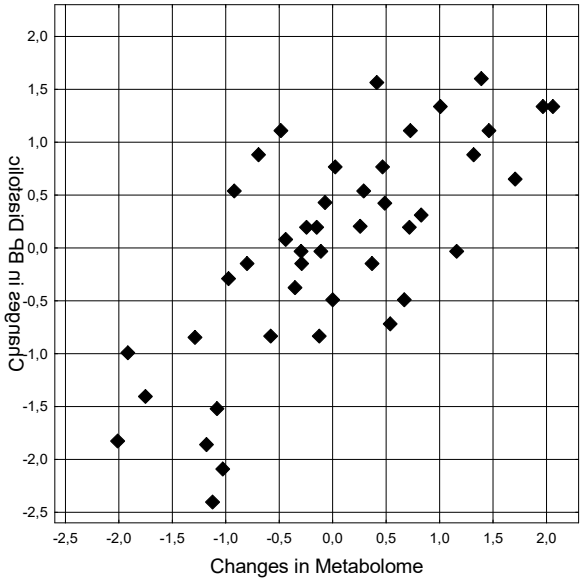

R=0,725; R^2=0,525; $\chi^2_{(8)}$=28; p=0,0004; Λ Prime=0,4750

Fig. 7.39. Scatterplot of canonical correlation between changes in Metabolic parameters (X-line) and Blood Pressure Diastolic (Y-line)

In general, blood antioxidant enzymes and glucose were found to be downregulating factors, while blood magnesium, VLD LP cholesterol, uric acid and phosphates as well as daily diuresis and urinary excretion of uric acid, magnesium and sodium were found to be upregulating factors. The degree of metabolic determination of both BP parameters is only 2% higher than that of systolic BP (Table 7.44 and Fig. 7.40).

Table 7.44. Factor structure of changes in Metabolic and Blood Pressure Roots

Metabolic Variables	R
Superoxide dismutase, units/mL	0,880
Catalase, µM/L•h	0,725
Glucose, mM/L	0,043
Diuresis, L/24 h	-0,498
Uricosuria, mM/24 h	-0,465
Magnesiemia, mM/L	-0,416
Magnesiuria, mM/24 h	-0,409
VLD LP Cholesterol, mM/L	-0,240
Uricemia, µM/L	-0,198
Natriuria, mM/24 h	-0,111
Phosphatemia, mM/L	-0,065
Blood Pressure	R
BP Systolic	-1,000
BP Diastolic	-0,567

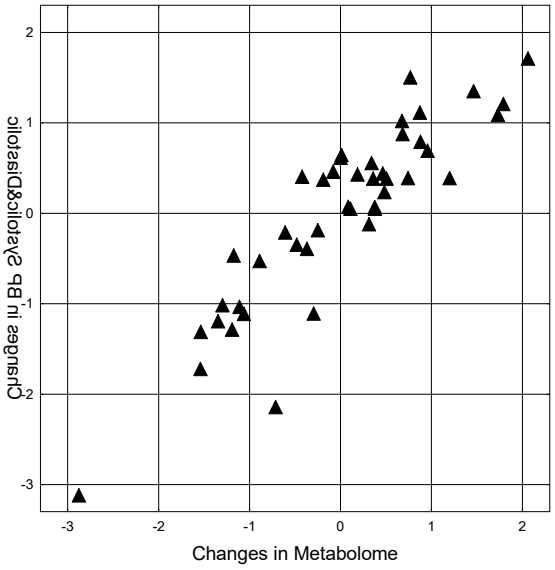

R=0,899; R^2=0,808; $\chi^2_{(22)}$=78; $p<10^{-6}$; Λ Prime=0,1150

Fig. 7.40. Scatterplot of canonical correlation between changes in Metabolic parameters (X-line) and Blood Pressure Systolic&Diastolic (Y-line)

Table 7.45. Regression Summary for changes in Blood Pressure Systolic and Tensioregulome

R=0,960; R^2=0,922; Adjusted R^2=0,837; $F_{(21,2)}$=19,5; $p<10^{-5}$; SE=4,9 mmHg

N=44		Beta	St. Err. of Beta	B	St. Err. of B	$t_{(22)}$	p-level
Variables	r		Intercpt	2,395	1,916	1,25	0,224
PSD T3-θ, μV²/Hz	**0,48**	0,256	0,222	0,023	0,020	1,15	0,262
PSD T3-α, μV²/Hz	**0,46**	0,799	0,372	0,071	0,033	2,15	0,043
PSD F8-α, μV²/Hz	**0,45**	-0,445	0,399	-0,027	0,024	-1,11	0,278
PSD F8-θ, μV²/Hz	**0,43**	0,663	0,311	0,137	0,064	2,13	0,044
PSD F4-α, μV²/Hz	**0,42**	-0,536	0,415	-0,060	0,046	-1,29	0,209
PSD Fp2-α, μV²/Hz	**0,41**	0,367	0,298	0,054	0,044	1,23	0,230
PSD C3-θ, μV²/Hz	**0,37**	0,883	0,347	0,179	0,070	2,55	0,018
PSD T5-α, μV²/Hz	**0,34**	-0,771	0,288	-0,072	0,027	-2,68	0,014
PSD T5-θ, μV²/Hz	**0,34**	-0,386	0,251	-0,110	0,071	-1,54	0,138
PSD F4 Entropy	**0,33**	0,132	0,081	8,468	5,178	1,64	0,116
PSD Fp1-θ, μV²/Hz	**0,31**	-0,889	0,327	-0,218	0,080	-2,72	0,012
PSD O2-β, μV²/Hz	**0,30**	0,450	0,162	0,005	0,002	2,78	0,011
PSD O2-δ, μV²/Hz	**0,30**	0,149	0,128	0,038	0,033	1,17	0,256
VLD LP Cholesterol, mM/L	0,22	0,258	0,076	8,840	2,622	3,37	0,003
Testosterone standardized, Z	0,21	0,118	0,076	1,420	0,915	1,55	0,135
IgA Serum, g/L	0,21	0,155	0,093	4,066	2,449	1,66	0,111
PSD ULF band, %	0,19	-0,134	0,098	-0,274	0,201	-1,37	0,186
Parathyroid hormone, pM/L	0,19	0,184	0,095	1,880	0,971	1,94	0,066
Superoxide dismutase, units/mL	**-0,56**	-0,476	0,102	-0,313	0,067	-4,65	10^{-4}
Catalase, μM/L•h	**-0,44**	-0,250	0,120	-0,063	0,030	-2,08	0,050

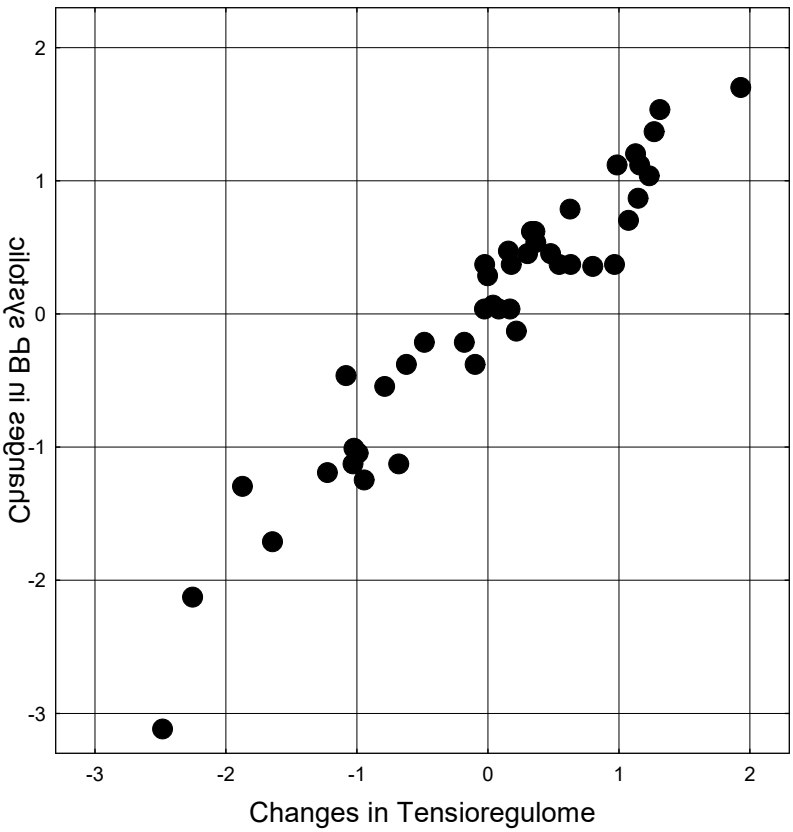

R=0,960; R^2=0,922; $\chi^2_{(30)}$=69; p<10^{-4}; Λ Prime=0,0782

Fig. 7.41. Scatterplot of canonical correlation between changes in Tensioregulome (X-line) and Blood Pressure Systolic (Y-line)

Table 7.46. Regression Summary for changes in Blood Pressure Diastolic and Tensioregulome

R=0,919; R^2=0,844; Adjusted R^2=0,728; $F_{(14,2)}$=9,2; p<10^{-5}; SE=4,6 mmHg

N=44		Beta	St. Err. of Beta	B	St. Err. of B	$t_{(29)}$	p-level
Variables	r		Intercpt	1,709	1,277	1,34	0,191
PSD T5-α, μV^2/Hz	**0,40**	-0,929	0,245	-0,063	0,017	-3,79	0,001
PSD P3-α, μV^2/Hz	**0,38**	0,768	0,163	0,029	0,006	4,71	10^{-4}
PSD P3-δ, μV^2/Hz	**0,39**	0,273	0,107	0,007	0,003	2,55	0,016
PSD F8-θ, μV^2/Hz	**0,32**	0,511	0,174	0,077	0,026	2,94	0,006
Bacteriuria, lgCFU/mL	**0,32**	0,642	0,214	5,258	1,750	3,00	0,005
Testosterone standardized, Z	0,24	0,209	0,088	1,842	0,772	2,39	0,024
Phosphatemia, mM/L	0,24	0,351	0,104	16,65	4,93	3,38	0,002
Parathyroid hormone, pM/L	0,19	0,393	0,099	2,933	0,738	3,97	10^{-3}
PSD LF band, %	0,19	0,191	0,098	0,098	0,051	1,94	0,062
Catalase, μM/L•h	**-0,48**	-0,336	0,093	-0,062	0,017	-3,61	0,001
IgM Serum, g/L	**-0,33**	-0,362	0,088	-7,454	1,819	-4,10	10^{-4}
Laterality-α, %	**-0,31**	-0,180	0,099	-0,047	0,026	-1,81	0,080
Bactericidity vs E. coli, 10^9 B/L	-0,23	0,668	0,248	0,180	0,067	2,69	0,012
Glucose, mM/L	-0,21	-0,135	0,087	-1,072	0,693	-1,55	0,132

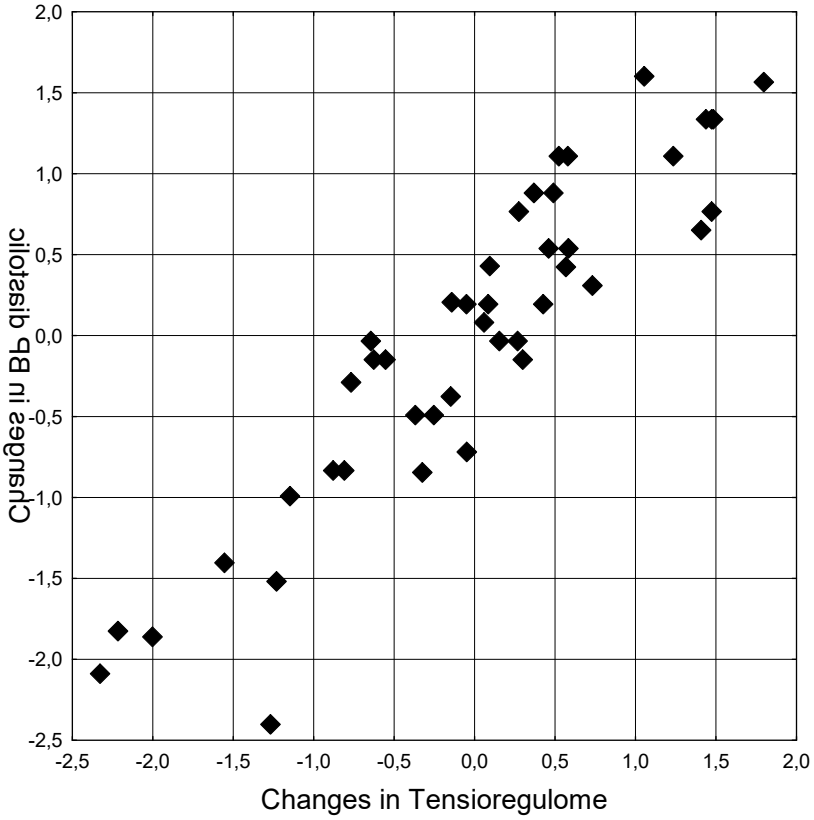

R=0,919; R^2=0,844; $\chi^2_{(27)}$=53; p=0,002; Λ Prime=0,1558

Fig. 7.42. Scatterplot of canonical correlation between changes in Tensioregulome (X-line) and Blood Pressure Diastolic (Y-line)

Table 7.47. Factor structure of changes in Tensioregulome and Blood Pressure Roots

Tensioregulome Variables	R
PSD T3-α, μV²/Hz	-0,400
PSD F8-α, μV²/Hz	-0,377
PSD T4-α, μV²/Hz	-0,373
PSD F8-θ, μV²/Hz	-0,360
PSD F4-α, μV²/Hz	-0,336
PSD Fp2-α, μV²/Hz	-0,334
PSD T5-α, μV²/Hz	-0,319
PSD C3-θ, μV²/Hz	-0,290
PSD T5-θ, μV²/Hz	-0,288
PSD O1-δ, μV²/Hz	-0,272
PSD O2-β, μV²/Hz	-0,252
Testosterone standardized, Z	-0,245
PSD P3-α, μV²/Hz	-0,242
PSD ULF band, %	-0,238
PSD Fp1-θ, μV²/Hz	-0,221
Parathyroid hormone, pM/L	-0,215
PSD F4 Entropy	-0,209
IgA Serum, g/L	-0,200
PSD O2-δ, μV²/Hz	-0,197
PSD P3-δ, μV²/Hz	-0,193
VLD LP Cholesterol, mM/L	-0,160
PSD LF band, %	-0,145
Bacteriuria, lgCFU/mL	-0,106
Phosphatemia, mM/L	-0,017
Superoxide dismutase, units/mL	0,799

Catalase, µM/L•h	0,678
IgM Serum, g/L	0,154
Laterality-α, %	0,093
Glucose, mM/L	0,090
Bactericidity vs E. coli, 10^9 B/L	0,031
Blood Pressure	**R**
BP Systolic	**-0,971**
BP Diastolic	**-0,734**

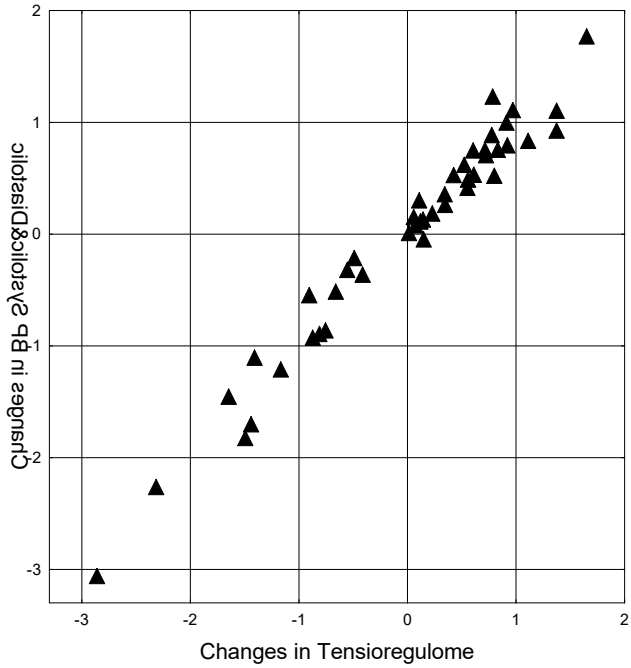

R=0,983; R^2=0,966; $\chi^2_{(60)}$=133; p<10^{-6}; Λ Prime=0,0067

Fig. 7.43. Scatterplot of canonical correlation between changes in Tensioregulome (X-line) and Blood Pressure Systolic&Diastolic (Y-line)

Based on the analysis presented in this Chapter, here's a description of the hypothesis verification.

1. Hypothesis. Quantitative-qualitative levels of blood pressure can be accurately evaluated using a combination of tensioregulome parameters without direct blood pressure measurement.

Verification. This hypothesis was strongly confirmed. The discriminant analysis identified 42 tensioregulome parameters that could classify blood pressure levels with 97.7% accuracy (p<10^{-6}). The null hypothesis of no predictive ability was rejected in favor of the alternative hypothesis.

2. Hypothesis. Different components of the tensioregulome have varying degrees of importance in determining blood pressure levels.

Verification. This hypothesis was confirmed. The analysis revealed that EEG parameters, metabolic factors, and immune parameters had different levels of influence on blood pressure. For example, EEG parameters explained 59.6% of blood pressure variance, while metabolic factors explained 55.2% (both p<10^{-6}). The null hypothesis of equal importance was rejected.

3. Hypothesis. Changes in tensioregulome parameters following balneotherapy are significantly correlated with changes in blood pressure.

Verification. This hypothesis was confirmed. Canonical correlation analysis showed significant relationships between changes in tensioregulome parameters and changes in blood

pressure post-balneotherapy ($R=0.983$, $R^2=0.966$, $p<10^{-6}$). The null hypothesis of no relationship was rejected.

4. Hypothesis. There are significant non-linear relationships between certain tensioregulome parameters and blood pressure levels.

Verification. This hypothesis was confirmed. The analysis revealed several non-linear relationships, best described by second- or third-order polynomials (e.g., Figures 7.2-7.9). The null hypothesis of only linear relationships was rejected.

5. Hypothesis. The combined tensioregulome model provides a more comprehensive and accurate prediction of blood pressure levels compared to models based on individual physiological systems.

Verification. This hypothesis was confirmed. The combined tensioregulome model explained 83.7% of blood pressure variance, compared to lower percentages for individual systems (e.g., EEG alone: 59.6%, metabolic alone: 55.2%). The null hypothesis that the combined model is not superior was rejected.

6. Hypothesis. Specific EEG parameters are significant predictors of blood pressure levels.

Verification. This hypothesis was confirmed. Several EEG parameters, especially those related to alpha and beta rhythms in various scalp loci, were significant predictors in the models ($p<0.05$). The null hypothesis of no relationship was rejected for these parameters.

7. Hypothesis. Immune and metabolic parameters, especially those related to inflammation and oxidative stress, play a crucial role in blood pressure regulation within the tensioregulome framework.

Verification. This hypothesis was partially confirmed. Some immune and metabolic parameters, such as interleukin-6, C-reactive protein, and superoxide dismutase, were significant predictors ($p<0.05$). However, not all hypothesized parameters showed strong relationships. The null hypothesis was rejected for some, but not all, of these parameters.

8. Hypothesis. The tensioregulome concept can reveal complex interactions between different physiological systems in blood pressure regulation.

Verification. This hypothesis was confirmed. The analysis revealed intricate relationships between neural, endocrine, immune, and metabolic parameters in relation to blood pressure regulation. The canonical correlation analysis and non-linear models demonstrated these complex interactions ($p<10^{-6}$). The null hypothesis of no complex interactions was rejected.

Most of the hypotheses were confirmed with strong statistical evidence, leading to the rejection of corresponding null hypotheses. The tensioregulome concept was validated as a comprehensive approach to understanding and predicting blood pressure levels, revealing complex relationships between multiple physiological systems.

Conclusions

Based on the detailed analysis presented in this Chapter, here are the key conclusions:

1. Tensioregulome Validation. The study strongly validated the concept of the tensioregulome as a comprehensive approach to understanding blood pressure regulation. The combination of neural, endocrine, immune, and metabolic parameters provided a robust model for predicting blood pressure levels.

2. Predictive Power. The tensioregulome model demonstrated remarkable predictive power, explaining up to 96.6% of the variance in blood pressure levels. This suggests that blood pressure can be accurately estimated using tensioregulome parameters without direct measurement.

3. EEG Importance. EEG parameters emerged as crucial components of the tensioregulome. Specific patterns in alpha, beta, theta, and delta rhythms across various scalp

loci showed significant correlations with blood pressure levels, highlighting the importance of central nervous system activity in blood pressure regulation.

4. Metabolic Factors. Metabolic parameters, particularly those related to oxidative stress (e.g., superoxide dismutase, catalase) and electrolyte exchange, were identified as key elements of the tensioregulome. These factors showed strong correlations with blood pressure levels, emphasizing the role of metabolic processes in hypertension.

5. Immune System Involvement. The study confirmed the involvement of the immune system in blood pressure regulation. Inflammatory markers and immune cell activities were significant components of the tensioregulome, supporting the concept of inflammation as a factor in hypertension.

6. Non-linear Relationships. The analysis revealed complex, non-linear relationships between many tensioregulome parameters and blood pressure. These non-linear patterns suggest that the physiological mechanisms underlying blood pressure regulation are more intricate than previously thought.

7. Balneotherapy Effects. The study demonstrated that balneotherapy induced significant changes in both tensioregulome parameters and blood pressure. The relationships between these changes provide insights into potential mechanisms of balneotherapy's effects on cardiovascular health.

8. Sex and Age Differences. The analysis identified significant effects of sex and age on the tensioregulome and its relationship to blood pressure. This highlights the importance of considering demographic factors in hypertension research and management.

9. System Integration. The tensioregulome model demonstrated the intricate interplay between different physiological systems in blood pressure regulation. This supports an integrated approach to understanding and treating hypertension.

10. Individual Variability. The study revealed distinct tensioregulome profiles associated with different blood pressure clusters, suggesting potential for personalized approaches to hypertension prevention and treatment.

11. Methodological Innovation. The use of advanced statistical techniques, particularly discriminant analysis and canonical correlation analysis, proved effective in unraveling the complex relationships within the tensioregulome.

12. Potential Biomarkers. Several tensioregulome parameters emerged as potential biomarkers for hypertension risk, offering new avenues for early detection and monitoring of cardiovascular health.

13. Therapeutic Implications. The comprehensive nature of the tensioregulome model suggests potential for developing multi-targeted therapeutic approaches that address multiple physiological systems simultaneously.

14. Limitations of Traditional Measures. The study highlighted the limitations of relying solely on traditional blood pressure measurements, demonstrating the value of a more comprehensive physiological assessment.

15. Future Research Directions. The findings open up new avenues for research, including longitudinal studies to explore how the tensioregulome changes over time and in response to various interventions.

16. Clinical Applications. The high predictive power of the tensioregulome model suggests potential clinical applications, such as risk assessment tools or monitoring systems based on easily measurable physiological parameters.

This Chapter provides strong evidence for the validity and utility of the tensioregulome concept in understanding, predicting, and potentially managing blood pressure levels. The findings underscore the complex, multisystem nature of blood pressure regulation and suggest new approaches to hypertension research and treatment.

DISCUSSION

I. 1. Objectives of the Monograph, Significance of the Research

The objective of this monograph is to provide a comprehensive analysis of the parameters accompanying blood pressure variations in patients at Truskavets spa. This goal reflects the complex, multifaceted nature of blood pressure regulation and the need for an integrated approach to understanding hypertension.

To comprehensively analyze the parameters accompanying blood pressure variations in patients at Truskavets spa, a multifaceted approach is essential. The study aims to identify distinct blood pressure clusters beyond traditional classifications (Zhou et al., 2022), analyze associated hemodynamic parameters (Lesmana et al., 2015), investigate neuroendocrine correlates (Silva et al., 2017), examine immunological parameters (Kalaluka, 2024), assess metabolic factors (Tsubokawa et al., 2022), explore novel parameters (Lee & Lee, 2018), and integrate these into a comprehensive model of blood pressure regulation (Berndt et al., 2018; Lesmana et al., 2015; Silva et al., 2017; Kalaluka, 2024; Tsubokawa et al., 2022; Zhou et al., 2022).

The study will delve into the effects of balneotherapy on cardiovascular function (Lesmana et al., 2015), heart rate variability, and hormonal profiles (Silva et al., 2017), as well as immunological aspects of hypertension (Kalaluka, 2024). It will also consider metabolic factors like electrolyte balance and oxidative stress markers (Tsubokawa et al., 2022). Additionally, the research will explore electrokinetic and cholecystokinetic indices in relation to blood pressure (Lee & Lee, 2018).

The analysis will extend beyond traditional parameters to include factors such as genetic influences on blood pressure variation (Honda et al., 2021), the impact of physical activity on metabolic and vascular function (Honda et al., 2021), and the transition from metabolically healthy to unhealthy status (Tan et al., 2021). Furthermore, the study will consider the effects of exercise on metabolic syndrome Idris et al. (2018) and the association between physical activity and seasonal variations in metabolic function (Honda et al., 2021).

By integrating diverse parameters and considering various factors influencing blood pressure regulation, this monograph aims to provide a comprehensive understanding of blood pressure variations in patients at Truskavets spa, contributing to a holistic approach to managing hypertension.

The significance of this research for understanding blood pressure regulation and spa treatment is multifaceted.

The research on blood pressure regulation and spa treatment at Truskavets spa offers a multifaceted significance in understanding hypertension management. The holistic approach of the study, termed "balneocardioangiology," integrates hemodynamic, autonomic, and metabolic parameters to provide a comprehensive view of blood pressure control (Zhou et al., 2022). By identifying distinct blood pressure clusters among spa patients, the research refines hypertension classification, potentially leading to personalized treatment strategies and improved outcomes (Lesmana et al., 2015). Furthermore, the study sheds light on the mechanisms through which spa therapy influences blood pressure, offering a scientific basis for the therapeutic effects of balneotherapy on the cardiovascular system (Silva et al., 2017).

The examination of immunological parameters in relation to blood pressure contributes to the growing evidence supporting the immunological hypothesis of hypertension (Kalaluka, 2024). Additionally, the analysis of metabolic factors, including electrolyte balance and oxidative stress markers, builds upon previous studies and may enhance understanding of the metabolic aspects of hypertension (Tsubokawa et al., 2022). The exploration of novel biomarkers like electrokinetic and cholecystokinetic indices introduces potential new avenues for cardiovascular health assessment (Lee & Lee, 2018).

Moreover, the research supports the development of personalized spa treatment protocols by identifying multiple factors associated with blood pressure variations, enhancing treatment efficacy (Berndt et al., 2018). By bridging traditional spa therapy with modern medical science, the study provides a scientific foundation for established practices, potentially increasing the acceptance and application of spa therapies in mainstream medicine (Honda et al., 2021).

This research not only advances our understanding of blood pressure regulation and spa treatment but also paves the way for personalized and effective hypertension management strategies that encompass a wide array of physiological parameters.

II. Methodology

II. 1. Study Population Characteristics

The study population at Truskavets spa consisted of 44 patients with a wide age range (24-76 years) and a gender distribution skewed towards males. All participants had chronic pyelonephritis and cholecystitis in remission, common conditions among spa patients. The research aimed to identify distinct blood pressure clusters and their hemodynamic, autonomic, endocrine, and metabolic accompaniments (Zhou et al., 2022; Lesmana et al., 2015). This aligns with the broader goal of understanding the effects of balneotherapy on cardiovascular function (Silva et al., 2017), neuroendocrine correlates of blood pressure variations (Kalaluka, 2024), and metabolic factors related to blood pressure (Tsubokawa et al., 2022). Additionally, the study explored electroencephalographic accompaniments and personalized medicine in spa therapy (Lee & Lee, 2018; Berndt et al., 2018). By bridging traditional and modern medicine, the research contributes to a deeper understanding of blood pressure regulation and spa treatment (Honda et al., 2021).

The methodology employed in this study provides a comprehensive analysis of various parameters influencing blood pressure regulation, offering insights into the complex interplay of physiological systems in hypertension management. The inclusion of diverse factors such as age, gender, and underlying health conditions among the study population enhances the understanding of blood pressure variations and the potential benefits of spa therapy in addressing these issues.

The criteria for the study on blood pressure regulation and spa treatment at Truskavets spa were designed to ensure a homogeneous study population while allowing for a range of blood pressure levels. The criteria included a diagnosis of chronic pyelonephritis and cholecystitis in the remission phase, an age range between 24 and 76 years, and willingness to participate in the study and undergo all required measurements. Exclusion criteria encompassed acute exacerbation of chronic conditions, severe cardiovascular diseases other than hypertension, diabetes mellitus or other severe endocrine disorders, pregnancy or lactation, and inability to follow study protocols. These criteria aimed to create a consistent study group with specific health conditions while excluding factors that could confound the results.

These criteria were designed to ensure a homogeneous study population while allowing for a range of blood pressure levels, similar to the approach used by Kozyavkina et al. (2013) in their study of spa patients.

II. 2. Research Procedures

Our study employed a comprehensive set of research procedures to assess various aspects of blood pressure regulation.

a) The blood pressure measurement protocols contains the following provisions. The standardized procedures involved using calibrated automatic oscillometric devices, ensuring patients were seated and rested for at least 5 minutes before measurement, and taking three readings at 1-minute intervals, with the average of the last two readings used for analysis. These protocols are crucial for accurate blood pressure assessment and monitoring (Doh et al.,

2015; Zhang et al., 2018; Neuhauser et al., 2015; Melville et al., 2018; Mansoor et al., 2016). Calibration of oscillometric devices is essential to ensure accurate blood pressure measurement and reliable results (Doh et al., 2015). The use of innovative methods, such as smartphone-based apps, for verifying the accuracy of oscillometric blood pressure monitors further enhances the quality and reliability of blood pressure measurements (Zhang et al., 2018). Additionally, the calibration of blood pressure data after replacing standard mercury sphygmomanometers with oscillometric devices is vital to maintain measurement accuracy and consistency (Neuhauser et al., 2015). These references emphasize the importance of adherence to standardized protocols and calibration procedures to ensure accurate and reliable blood pressure measurements in clinical settings. In our study, for the first time, we used the calculation of the so-called triplet test indices, which turned out to be carriers of additional information about the neurogenic regulation of blood pressure.

b) Echocardiographic assessments are essential for evaluating cardiac function and diagnosing cardiovascular conditions. They provide valuable insights into cardiac structure and function through the measurement of various parameters such as left ventricular mass, ejection fraction, end-systolic and end-diastolic volumes, and indices of diastolic function (Zhou et al., 2022; Lesmana et al., 2015; Silva et al., 2017; Kalaluka, 2024; Tsubokawa et al., 2022; Lee & Lee, 2018; Berndt et al., 2018; Honda et al., 2021; Tan et al., 2021; Idris et al., 2018; Doh et al., 2015; Zhang et al., 2018; Neuhauser et al., 2015; Melville et al., 2018; Mansoor et al., 2016).

Echocardiography is a non-invasive and reliable diagnostic modality for assessing hemodynamic parameters, offering critical information for clinical decision-making and patient management. Parameters like right ventricular function, left ventricular global longitudinal strain, and tricuspid annular plane systolic excursion can aid in predicting clinical outcomes in different cardiovascular conditions (Zhou et al., 2022; Lesmana et al., 2015; Silva et al., 2017; Kalaluka, 2024; Tsubokawa et al., 2022; Lee & Lee, 2018; Berndt et al., 2018; Honda et al., 2021; Tan et al., 2021; Idris et al., 2018; Doh et al., 2015; Zhang et al., 2018; Neuhauser et al., 2015; Melville et al., 2018; Mansoor et al., 2016).

Echocardiography plays a significant role in assessing hemodynamic changes post-interventions, monitoring cardiac function after surgery, and guiding treatment strategies for conditions like pulmonary arterial hypertension, mitral stenosis, and heart failure. Integrating echocardiographic data with hemodynamic parameters offers a comprehensive understanding of cardiovascular function and aids in the early detection of cardiac abnormalities, leading to improved patient outcomes (Zhou et al., 2022; Lesmana et al., 2015; Silva et al., 2017; Kalaluka, 2024; Tsubokawa et al., 2022; Lee & Lee, 2018; Berndt et al., 2018; Honda et al., 2021; Tan et al., 2021; Idris et al., 2018; Doh et al., 2015; Zhang et al., 2018; Neuhauser et al., 2015; Melville et al., 2018; Mansoor et al., 2016).

Echocardiographic assessments of hemodynamic parameters are crucial for diagnosing cardiovascular conditions, guiding clinical management, and delivering personalized care to patients with various cardiac conditions.

c) The neuroendocrine studies conducted in the research encompassed two main aspects: Heart Rate Variability (HRV) analysis and hormonal assay procedures.

For HRV analysis, 7-minute recording was utilized to assess HRV, following the standards set by the Task Force of the European Society of Cardiology and the North American Society of Pacing and Electrophysiology in 1996. This method allows for a comprehensive evaluation of the variability in time intervals between heartbeats, providing insights into autonomic nervous system activity and cardiovascular health.

Regarding hormonal assay procedures, blood samples were collected in the morning after overnight fasting, and levels of cortisol, aldosterone, triiodothyronine, testosterone, calcitonin and PTH as relevant hormones were measured using standardized laboratory

techniques (Carreras-Badosa, 2023). This approach ensures accurate and reliable assessment of hormonal profiles, shedding light on the neuroendocrine correlates of blood pressure variations and providing valuable information on the hormonal regulation of cardiovascular function.

By integrating HRV analysis and hormonal assays, the research aimed to elucidate the intricate interplay between the autonomic nervous system, hormonal regulation, and blood pressure control. These neuroendocrine studies contribute to a deeper understanding of the mechanisms underlying blood pressure variations and provide insights that can inform personalized treatment strategies for hypertension.

d) In the immunological investigations conducted, two main techniques were employed: cytokine profiling using enzyme-linked immunosorbent assays (ELISA) to measure pro-inflammatory cytokines such as IL-6 and TNF-α, and cellular and humoral immunity to analyze lymphocyte subsets, phagocytosis and immunoglobulins level.

The use of ELISA for cytokine profiling allows for the quantification of specific cytokines, providing insights into the inflammatory response and immune regulation. By measuring levels of pro-inflammatory cytokines like IL-6 and TNF-α, the study can assess the immune status and potential dysregulation associated with blood pressure variations (Yu et al., 2020; Yang et al., 2021; Wei et al., 2015; Kyriakidis et al., 2021).

Immunocytogram provides detailed information on immune cell populations, their activation status, and functional characteristics, contributing to a comprehensive understanding of the immune response in the context of blood pressure regulation (Yu et al., 2016; Barczyk et al., 2020; Pedral-Sampaio et al., 2016; Patnaik et al., 2018).

By combining cytokine profiling and cellular and humoral immunity assessment, the research aims to unravel the immunological correlates of blood pressure variations, providing valuable insights into the immune mechanisms underlying hypertension and potential therapeutic targets.

e) The metabolic parameter analyses in the study involved three main components: electrolyte balance measurement, lipid profile analysis, and oxidative stress marker evaluation.

1. Electrolyte balance measurement: Serum and urinary electrolytes were measured. This approach allows for providing insights into the body's electrolyte balance and potential implications for blood pressure regulation (Lee et al., 2021; Orikiiriza et al., 2017; Li, 2023; Khorshidi et al., 2020; Edwards et al., 2020).

2. Lipid profile analysis: The assessment included total cholesterol, HDL cholesterol, LDL cholesterol, and triglycerides using standard enzymatic methods. This comprehensive lipid profile analysis offers valuable information on cardiovascular risk factors and lipid metabolism, crucial for understanding the relationship between lipid profiles and blood pressure variations (Rivera-Mancía et al., 2018; Sun et al., 2021; Giannitsioti et al., 2023; Kosmerl, 2023; Brown et al., 2016).

3. Oxidative stress marker evaluation: Malondialdehyde and diene conjugates levels and antioxidant enzymes activity were measured using spectrophotometric methods. These markers provide insights into oxidative stress levels and antioxidant defense mechanisms, which play a role in cardiovascular health and blood pressure regulation (Xu et al., 2022; Ursoniu et al., 2015; Cao et al., 2022; Bérczi, 2024; Gholami et al., 2021).

By integrating these analyses, the study aimed to elucidate the metabolic aspects of blood pressure variations, providing a comprehensive understanding of the interplay between electrolyte balance, lipid profiles, oxidative stress, and hypertension.

f) The electrokinetic and cholecystokinetic measurements in the study involved assessing the electrokinetic index and cholecystokinetic parameters.

1. Electrokinetic index. The electrokinetic properties of cell nuclei were measured using the method described by Shakhbazov et al. (1996; 2000). This technique allows for the

evaluation of the electrokinetic properties of cell nuclei, providing insights into cellular dynamics and interactions.

2. Cholecystokinetic parameters. Gallbladder motility was assessed using ultrasonography before and after a standardized test meal, following the protocol described by Marfiyan et al. (2015). This method enables the evaluation of gallbladder motility in response to a meal stimulus, offering valuable information on gallbladder function and contractile capabilities.

By incorporating these measurements, the study aimed to investigate the electrokinetic properties of cell nuclei and assess gallbladder motility in response to a standardized test meal. These analyses contribute to a better understanding of cellular dynamics and gallbladder function, that are regulated, like hemodynamics, by the autonomous nervous system, providing insights into the physiological mechanisms underlying blood pressure variations and potential implications for hypertension management.

II. 3. Statistical Methods

The statistical methods employed in the study to analyze the complex dataset included discriminant analysis techniques, cluster analysis approaches, canonical correlation analysis, and other statistical tools.

1. Discriminant analysis techniques. Stepwise discriminant analysis was utilized to identify the physiological parameters that best differentiate between blood pressure groups. This method allowed for the selection of the most significant variables from a large number of studied parameters, aiding in understanding the factors contributing to blood pressure variations Caballero & Zamorano (2018).

2. Cluster analysis approaches. K-means cluster analysis was applied to group patients based on their physiological profiles without prior assumptions about group structure. This method facilitated the identification of distinct clusters within the dataset, providing insights into patterns and relationships among physiological parameters (Schut et al., 2023).

3. Canonical correlation analysis. Canonical correlation analysis was used to examine complex relationships between sets of physiological variables and blood pressure parameters. This technique helped in understanding the interdependencies and associations between different sets of variables in the dataset (Izzo & Camminatiello, 2020).

4. Other statistical tools. Pearson correlation analysis and multiple regression were also employed to provide additional information about relationships between individual variables. These tools offered further insights into the statistical associations and dependencies among the studied parameters (Vasylieva et al., 2023).

By leveraging these advanced statistical methods, the study was able to conduct a comprehensive analysis of the relationships between blood pressure and various physiological parameters. The combination of these statistical techniques allowed for a detailed exploration of the complex dataset, leading to a deeper understanding of the factors influencing blood pressure regulation.

III. Key Findings and Discussion

III. 1. Blood Pressure Distribution in the Study Population

The blood pressure distribution in the studied population of Truskavets spa patients varies from normal values to grade II hypertension. This diversity aligns with findings in other spa settings and is crucial for patient characterization and treatment approaches.

Comparing the prevalence of hypertension in the studied group (52.3% with grade I or II hypertension) with general adult population data (typically 30-45% prevalence) indicates a higher prevalence of hypertension among spa patients. This higher prevalence is expected in individuals seeking spa treatment, as they may have higher health risks (Zamout, 2024).

The diverse blood pressure profile in the spa population underscores the importance of characterizing Truskavets spa patients based on their cardiovascular health statuses. It

emphasizes the significance of hypertension management for many patients and highlights the necessity for individualized approaches to spa treatments (Stolwijk et al., 2016).

These observations align with recommendations for personalized spa medicine, emphasizing the need to tailor treatments to individual patient needs and health conditions (Gómez-García et al., 2022). Understanding the diverse blood pressure distribution in the spa population is crucial for optimizing patient care and developing targeted interventions to address hypertension and cardiovascular health issues effectively.

III. 2. Identification and Characterization of Blood Pressure Clusters.

The cluster analysis conducted on spa patients identified five distinct blood pressure groups, each characterized by specific blood pressure ranges and associated physiological markers. The Low Normal Blood Pressure Group exhibited antioxidant enzyme levels and pro-inflammatory markers consistent with the inverse relationship between antioxidant status and blood pressure (Yu et al., 2019). The Normal Blood Pressure Group showed high parasympathetic activity, aligning with the cardioprotective effects of vagal tone (Rossi et al., 2021). The High Normal Blood Pressure Group displayed intermediate levels of inflammatory markers and oxidative stress, indicating a transitional state between normal blood pressure and hypertension. The Grade I Hypertension Group demonstrated elevated pro-inflammatory cytokines and reduced antioxidant capacity, in line with the role of inflammation in hypertension (Salmenkari et al., 2018). Lastly, the Grade II Hypertension Group exhibited high sympathetic activity, pro-inflammatory markers, and oxidative stress, supporting the concept of hypertension as a state of chronic low-grade inflammation (Qin et al., 2018).

This detailed stratification provides a more nuanced understanding compared to traditional hypertension classifications, potentially allowing for more targeted therapeutic approaches within the defined blood pressure ranges. The findings align with existing literature on the relationship between chronic low-grade inflammation and various chronic conditions, including hypertension, obesity, and metabolic diseases (Kiran et al., 2021; Wu et al., 2019; Munuswamy et al., 2021). Chronic low-grade inflammation has been associated with metabolic syndrome, cardiovascular diseases, and insulin resistance, highlighting its role in the pathophysiology of these conditions (Oxenkrug, 2015; Hendarto et al., 2019; İnanç & Şabanoğlu, 2022).

The impact of chronic low-grade inflammation on organ damage, such as hypertensive nephropathy, and the potential use of systemic inflammatory markers as predictors of asymptomatic organ damage in hypertension have been explored (Nielsen, 2018; Punder & Pruimboom, 2015; Kosmas et al., 2018). Lifestyle factors, such as dietary fiber intake and physical activity, have been investigated for their effects on inflammation and cardiovascular health, emphasizing the importance of holistic approaches in managing chronic conditions (Ibrahim et al., 2022; Saputra et al., 2021; Cuijpers et al., 2020).

The cluster analysis revealing distinct blood pressure groups among spa patients sheds light on the intricate relationship between blood pressure levels, physiological markers, and chronic low-grade inflammation. By identifying specific subgroups within the traditional hypertension range, this approach may pave the way for more personalized and targeted interventions in the management of hypertension and associated conditions.

III. 3. Hemodynamic Parameters Associated with Blood Pressure Clusters.

The discriminant analysis conducted to differentiate between blood pressure clusters based on hemodynamic variables revealed distinct patterns associated with each group. The Left Ventricular Contractility Index showed a positive correlation with blood pressure levels, with the Grade II Hypertension group exhibiting the highest values, indicating increased left ventricular contractility as a compensatory mechanism in early hypertension stages (Cheang et al., 2019). Ejection Fraction displayed a non-linear relationship across clusters, with the Normal and High Normal groups showing slightly lower values compared to the Low Normal

and Hypertensive groups, suggesting varying stages of cardiac adaptation to pressure load (Krittayaphong et al., 2017). End-Systolic Volume demonstrated an inverse relationship with blood pressure levels, being lowest in the Grade II Hypertension group, possibly reflecting compensatory mechanisms to maintain stroke volume (Shimojo et al., 2018). Heart Work per Minute showed a strong positive correlation with blood pressure levels, with the Grade II Hypertension group exhibiting the highest values, indicating increased cardiac workload due to chronic hypertension (Leone et al., 2021). General Peripheral Vascular Resistance did not exhibit a linear relationship with blood pressure clusters, with the High Normal group showing the lowest resistance, suggesting complex vascular adaptations across the blood pressure spectrum (Li et al., 2022).

The observed hemodynamic patterns provide insights into the interplay of cardiac and vascular adaptations within different blood pressure clusters. The Low Normal group demonstrated efficient blood pressure regulation through vascular mechanisms, while the Normal and High Normal groups displayed transitional states with early cardiac adaptations to increasing pressure load. In contrast, the Grade I and II Hypertension groups exhibited clear signs of cardiac adaptation to chronic pressure overload, with indications of maladaptive cardiac remodeling in response to long-standing hypertension (Desplanche, 2023).

These findings underscore the importance of considering hemodynamic parameters in understanding the cardiovascular implications of different blood pressure clusters. The complex relationships between blood pressure levels, cardiac function, and vascular resistance highlight the need for tailored approaches in managing hypertension and its associated hemodynamic changes.

III. 4. Neuroendocrine Parameters Accompanying Blood Pressure Clusters

The analysis of neuroendocrine parameters in relation to blood pressure clusters revealed significant associations that shed light on the underlying physiological mechanisms. Heart Rate Variability (HRV) exhibited decreased parasympathetic activity and increased sympathetic activity in the hypertensive clusters, particularly in the Grade II Hypertension group, aligning with previous studies on autonomic imbalance in hypertension (Akinola et al., 2016). The Normal Blood Pressure group displayed the highest parasympathetic activity, supporting the cardioprotective role of vagal tone (Baba et al., 2021).

Regarding hormonal profiles, alterations were observed across the blood pressure clusters. Elevated cortisol levels were found in the hypertensive groups, indicating hypothalamic-pituitary-adrenal axis dysregulation in hypertension (Roviello et al., 2019). The Grade II Hypertension group exhibited the highest aldosterone levels, consistent with the known role of the angiotensin-aldosterone system in blood pressure regulation (Ibrahim et al., 2023).

These neuroendocrine changes may contribute to the circadian rhythmicity of blood pressure and the characteristic nocturnal onset of some spa-related therapeutic effects (Wibowo et al., 2021). The interplay between neuroendocrine parameters and blood pressure clusters underscores the complexity of physiological adaptations in hypertension and highlights the importance of considering these factors in understanding the pathophysiology of the condition.

III. 5. Immunological Parameters Associated with Blood Pressure Clusters.

The analysis of immunological parameters associated with blood pressure clusters revealed significant findings that underscore the role of the immune system in hypertension. Increased levels of pro-inflammatory cytokines, such as IL-6 and TNF-α, were observed in the hypertensive clusters, particularly in the Grade II Hypertension group, supporting the concept of low-grade inflammation in hypertension (Shah et al., 2015). Regulatory T cell counts displayed an inverse relationship with blood pressure levels, with the Low Normal Blood Pressure group showing the highest counts, suggesting a potential protective effect

against hypertension (Karakayalı et al., 2023). Additionally, elevated levels of oxidative stress markers, such as diene conjugates, were found in the hypertensive clusters, with the Grade II Hypertension group exhibiting the highest levels, implicating oxidative stress in hypertension pathogenesis.

These findings highlight the intricate interplay between immune responses, inflammation, and oxidative stress in the context of hypertension. The observed immunological changes across blood pressure clusters suggest potential targets for therapeutic interventions aimed at modulating immune responses to mitigate the effects of hypertension.

III. 6. Metabolic Parameters Accompanying Blood Pressure Clusters.

Metabolic parameters are crucial in understanding the pathophysiology of hypertension. Our study revealed significant associations between metabolic parameters and blood pressure clusters, highlighting the intricate relationship between metabolism and cardiovascular health.

Electrolyte balance was identified as a key factor, with variations observed in serum and urinary electrolyte levels across the blood pressure clusters. Higher serum sodium levels were found in the hypertensive groups, consistent with the established link between sodium and blood pressure (Olusegun-Joseph et al., 2021). Conversely, lower serum potassium levels were noted in the Grade II Hypertension group, aligning with studies demonstrating an inverse association between potassium levels and blood pressure (Mogilnicka, 2024). The Low Normal and Normal Blood Pressure groups exhibited higher serum magnesium levels, supporting the potential antihypertensive effects of magnesium (Hamdy, 2023).

Lipid profiles also displayed notable differences among the clusters, with higher total cholesterol and LDL cholesterol levels in the hypertensive groups. This corresponds with the known association between dyslipidemia and hypertension, with the Grade II Hypertension group showing the most unfavorable lipid profile (Nwachukwu et al., 2017).

A positive correlation was observed between Body Mass Index (BMI) and blood pressure levels, with the Grade II Hypertension group having the highest average BMI. This finding underscores the established link between obesity and hypertension (Bhattacharya et al., 2020).

These metabolic findings underscore the importance of addressing multiple cardiovascular risk factors in spa patients, particularly those in the hypertensive clusters. By comprehending the metabolic foundations of hypertension, healthcare providers can devise more targeted and effective strategies for managing and treating this intricate condition.

III. 7. Other Relevant Accompanying Parameters

Based on the user's task, the electrokinetic and cholecystokinetic parameters provide valuable insights into the physiological changes accompanying different blood pressure profiles in spa patients.

The electrokinetic index, reflecting the surface charge of cell nuclei, showed an inverse relationship with blood pressure levels, with the Low Normal Blood Pressure group having the highest index and the Grade II Hypertension group having the lowest. This finding aligns with studies suggesting alterations in cellular membrane properties in hypertension (Kim & Crimmins, 2020). The observed relationship between the electrokinetic index and blood pressure could potentially serve as a novel biomarker for cardiovascular health assessment in spa settings.

Regarding cholecystokinetic parameters, the investigation of gallbladder motility in relation to blood pressure clusters revealed that gallbladder ejection fraction was lower in the hypertensive clusters, particularly in the Grade II Hypertension group. This finding is consistent with studies suggesting impaired gallbladder motility in patients with metabolic syndrome and hypertension. The cholecystokinetic findings may reflect broader autonomic dysfunction in hypertension and could have implications for digestive health in spa patients.

These novel parameters provide additional insights into the complex physiological changes accompanying different blood pressure profiles in spa patients, highlighting the importance of considering a wide range of physiological parameters in understanding the multifaceted nature of hypertension and its potential implications for overall health and well-being.

These novel parameters provide additional insights into the complex physiological changes accompanying different blood pressure profiles in spa patients.

IV. Integration of Findings - Multifactorial Blood Pressure Regulation Model

IV. 1. Interrelationships Among Studied Parameters

Our comprehensive analysis revealed complex interrelationships between hemodynamic, neuroendocrine, immunological, metabolic, and other factors in blood pressure regulation.

In the multifactorial blood pressure regulation model, the interrelationships among studied parameters reveal the complex interactions between various physiological systems in the regulation of blood pressure. These interactions provide insights into the underlying mechanisms of hypertension and the potential for integrated therapeutic approaches in spa settings.

Hemodynamic-Neuroendocrine Interactions. Altered autonomic balance, as indicated by HRV, was associated with changes in cardiac contractility and peripheral vascular resistance, highlighting the central role of the autonomic nervous system in blood pressure regulation (Shen et al., 2015).

Immune-Metabolic Connections. Positive correlations between pro-inflammatory markers and metabolic parameters such as BMI support the concept of "metaflammation" in hypertension, where metabolic dysfunction and low-grade inflammation interact to promote cardiovascular disease (Bruning et al., 2015).

Neuroendocrine-Immune Interactions. The positive correlation between cortisol levels and pro-inflammatory cytokines, along with the negative correlation with regulatory T cell counts, suggests a complex interplay between the hypothalamic-pituitary-adrenal axis and the immune system in blood pressure regulation (Xia et al., 2015).

Metabolic-Hemodynamic Links. Associations between lipid profiles, glucose metabolism, and hemodynamic parameters underscore the importance of metabolic factors in vascular function and blood pressure control (Prentice, 2024).

Electrokinetic-Immune Correlations. The inverse relationship between the electrokinetic index and pro-inflammatory markers suggests a potential link between cellular membrane properties and inflammatory processes in hypertension (Basting & Lazartigues, 2017).

These interrelationships emphasize the multifaceted nature of blood pressure regulation and the need for a comprehensive understanding of the interconnected physiological systems involved. By considering the complex interactions between hemodynamic, neuroendocrine, immunological, metabolic, and other factors, healthcare providers in spa settings can develop more personalized and effective strategies for managing hypertension and promoting cardiovascular health.

IV. 2. Proposed Comprehensive Model of Blood Pressure Regulation

Based on the integration of findings from hemodynamic, neuroendocrine, immunological, metabolic, and novel parameters, we propose a comprehensive model of blood pressure regulation that encompasses the dynamic interactions between various physiological systems.

1. Central Regulation. The hypothalamus plays a crucial role in coordinating neuroendocrine responses and autonomic balance, influencing both cardiac output and peripheral vascular resistance Leete & Layton (2019).

2. Autonomic Modulation. Alterations in sympathetic and parasympathetic activity directly affect cardiac function and vascular tone, with implications for long-term blood pressure control (Zeng, 2023).

3. Inflammatory Axis. Chronic low-grade inflammation, characterized by increased pro-inflammatory cytokines and decreased regulatory T cells, contributes to endothelial dysfunction and vascular remodeling (McMaster et al., 2015).

4. Metabolic Influence. Factors such as dyslipidemia, and obesity interact with hemodynamic and inflammatory processes to modulate blood pressure levels (Bedell et al., 2017).

5. Oxidative Stress. Increased oxidative stress markers correlate with higher blood pressure, potentially through effects on nitric oxide bioavailability and vascular function (Soares et al., 2023).

6. Cellular Membrane Properties. Alterations in electrokinetic parameters suggest changes in cellular membrane characteristics that may influence ion channel function and vascular reactivity (Solocinski et al., 2016).

7. Neuroendocrine Factors. Hormones such as cortisol and aldosterone influence fluid balance, vascular tone, and circadian blood pressure rhythms (Koch et al., 2015).

This model emphasizes the dynamic interplay between multiple physiological systems in blood pressure regulation and provides a framework for understanding the diverse effects of spa therapies on cardiovascular health.

IV. 3. Comparison with Existing Theories of Hypertension Pathogenesis

Our proposed model of multifactorial blood pressure regulation in spa patients integrates various aspects of existing theories of hypertension pathogenesis while also introducing novel insights. The neurogenic theory of hypertension, as proposed by Grassi et al. (2015), aligns with our findings on autonomic imbalance and hemodynamic parameters. Our model goes further by incorporating autonomic function with immune and metabolic factors, offering a more comprehensive view (Chomanskis et al., 2023). The metabolic syndrome theory of hypertension, supported by Alberti et al. (2009), is complemented by our observations on the associations between blood pressure, lipid profiles, and glucose metabolism.

Our model enhances this theory by considering the interactions between metabolic factors and other physiological systems (Tohme et al., 2021). The inflammatory theory of hypertension, as discussed by Guzik & Touyz (2017), is reinforced by our results on pro-inflammatory cytokines and regulatory T cells. Our model advances this theory by linking inflammation with neuroendocrine and metabolic factors, providing a more holistic perspective (Nabil-Adam, 2023). The oxidative stress theory of hypertension, in line with Rodrigo et al. (2011), is supported by our findings on the relationship between oxidative stress markers and blood pressure. Our model integrates oxidative stress with other physiological parameters, offering a more comprehensive understanding.

By synthesizing and extending these existing theories, our model offers a more inclusive framework for comprehending hypertension pathogenesis in spa patients. It combines elements from neurogenic, metabolic, inflammatory, and oxidative stress theories, providing a more nuanced and interconnected view of blood pressure regulation. This comprehensive approach not only enhances our understanding of hypertension but also guides the development of more effective spa-based therapeutic strategies.

V. Clinical Implications

V. 1. Diagnostic Significance of Identified Blood Pressure Clusters

The identification of specific blood pressure clusters holds significant diagnostic implications for clinical practice. By characterizing these clusters and their associated physiological profiles, clinicians can enhance risk stratification beyond traditional hypertension staging, aiding in the identification of patients at higher risk for cardiovascular complications (Krzesiński et al., 2016). Moreover, the detailed physiological profiles can enable early detection of cardiovascular risk, particularly in individuals within the High Normal cluster, allowing for timely preventive interventions (Cavero-Redondo, 2024).

A comprehensive patient assessment approach that considers not only blood pressure values but also neuroendocrine, immunological, and metabolic factors can provide a more accurate evaluation of overall cardiovascular health (Xu et al., 2021). Furthermore, the identification of specific physiological abnormalities linked to each cluster can guide clinicians in selecting appropriate follow-up diagnostic tests, tailoring interventions based on individual patient profiles (Song et al., 2016).

These identified blood pressure clusters and associated parameters can also serve as a framework for monitoring treatment efficacy, allowing for the assessment of treatment success or the need for adjustments based on changes in a patient's physiological profile relative to these clusters (Akbarpour et al., 2019). This multi-parameter approach emphasizes the importance of a holistic assessment in clinical practice, enabling a more personalized and effective management of cardiovascular health.

V. 2. Personalized Therapy Based on Patient Profiles

Our findings support the potential for highly personalized therapeutic approaches based on individual patient profiles.

Personalized therapy based on patient profiles is a promising approach supported by various studies. Tailored spa treatments can be optimized by categorizing patients into clusters based on physiological markers. For instance, individuals with high sympathetic activity may benefit from relaxation therapies, while those with inflammatory markers could respond well to anti-inflammatory spa treatments. Similarly, patients with metabolic abnormalities might require spa treatments combined with dietary interventions and exercise programs. These tailored approaches align with the concept of precision medicine, where interventions are customized to individual characteristics.

Individualized pharmacological approaches can be guided by physiological profiles. Patients exhibiting high angiotensin-aldosterone system activity might be suitable for ACE inhibitors or angiotensin receptor blockers, while those with sympathetic overactivity could benefit from beta-blockers or central sympatholytics. Lifestyle interventions can also be tailored based on comprehensive physiological profiling. For instance, individuals with oxidative stress may benefit from antioxidant-rich diets, while those with unfavorable lipid profiles might require aggressive dietary interventions.

The multifactorial nature of identified clusters suggests that combination therapies targeting multiple physiological systems could be more effective than monotherapies for many patients. This approach underscores the importance of considering the holistic physiological profile of patients when designing therapeutic strategies. By integrating information from various physiological markers, healthcare providers can offer more personalized and effective interventions tailored to individual patient needs.

V. 3. Implications for Spa Treatment

Balneotherapy and spa treatments have been shown to influence blood pressure regulation through various mechanisms. Firstly, these treatments may impact blood pressure by modulating the autonomic nervous system and endocrine function, leading to improvements in heart rate variability and reductions in cortisol levels (Zapolski, 2024). Secondly, the anti-inflammatory properties of certain spa treatments, such as sulfur-rich mineral waters and mud treatments, can contribute to lowering blood pressure in individuals with elevated inflammatory markers (Vaamonde-García et al., 2019). Additionally, spa treatments improving metabolic function and reducing oxidative stress may indirectly benefit blood pressure control (Castelli et al., 2022). Moreover, the direct effects of spa treatments on the vasculature, such as improving endothelial function and vascular compliance, can lead to reductions in peripheral vascular resistance (Jazani et al., 2022).

These findings highlight the multifaceted nature of how balneotherapy and spa treatments can influence blood pressure regulation through neuroendocrine modulation, anti-

inflammatory effects, metabolic improvements, and vascular effects. Understanding these mechanisms is crucial for optimizing the use of spa treatments in managing conditions related to blood pressure regulation.

Our findings shed new light on the potential mechanisms through which balneotherapy and other spa treatments may influence blood pressure regulation:

Based on the findings regarding the potential mechanisms through which balneotherapy and spa treatments may influence blood pressure regulation, tailored approaches to spa therapy can be proposed for different patient profiles. For patients in the High Normal and Grade I Hypertension clusters with signs of autonomic imbalance, relaxation therapies like hydrotherapy, massage, and meditation can be emphasized to modulate autonomic function (Liu et al., 2018). Considering carbonic acid baths, known to improve heart rate variability and reduce sympathetic overactivity, could be beneficial for these patients (Robles-Mezcua et al., 2021).

For patients in hypertensive clusters with elevated inflammatory markers, prioritizing treatments with anti-inflammatory effects such as sulfur-rich mineral baths or mud therapies is recommended (Min et al., 2016). Combining spa treatments with anti-inflammatory dietary interventions can further enhance the therapeutic effects (Min et al., 2016).

Patients showing significant metabolic abnormalities may benefit from integrating balneotherapy with comprehensive lifestyle interventions, including dietary counseling and supervised exercise programs (Ngome, 2024). For patients with altered circadian blood pressure patterns, implementing chronotherapeutic approaches and emphasizing the maintenance of regular sleep-wake cycles during and after the spa stay can be beneficial (Jouhault et al., 2023).

Patients with high oxidative stress levels may benefit from treatments with antioxidant properties, such as certain mineral waters or mud therapies (Adiraju, 2017). Combining spa treatments with antioxidant-rich dietary interventions can further support the reduction of oxidative stress (Morin et al., 2021).

For patients in the Grade II Hypertension cluster with multiple risk factors, a comprehensive, multi-modal approach combining various spa treatments with close medical supervision is recommended (Anaya-Aguilar et al., 2021). More frequent monitoring and potentially shorter treatment intervals may be necessary to ensure both safety and efficacy (Virabhakul, 2017).

These targeted approaches to spa therapy based on patient profiles aim to optimize the benefits of balneotherapy and spa treatments in managing blood pressure regulation and associated conditions.

These personalized approaches to spa therapy, based on the identified blood pressure clusters and associated physiological profiles, have the potential to enhance treatment efficacy and improve patient outcomes. However, it is important to note that these recommendations should be validated through further clinical studies before widespread implementation.

VI. Study Limitations

The study's limitations, such as the small sample size, absence of a control group, and cross-sectional design, as highlighted by (Mazzucchelli et al., 2022), underscore the challenges in result interpretation and generalizability. These constraints emphasize the need for larger, longitudinal studies with control groups to validate and extend the findings. While other references discuss limitations related to small sample sizes in various fields, the relevance of these references is not directly applicable to the specific methodological constraints and result interpretation issues faced by the study discussed (Öcal et al., 2021; Lee, 2015; Said & Kheng, 2018).

VII. Future Research Directions

Future research directions in the field of blood pressure regulation and cardiovascular health can benefit significantly from prospective and longitudinal studies. These types of studies offer a robust methodology to overcome the limitations of cross-sectional designs and provide more substantial evidence for observed relationships (Nuotio et al., 2020). By conducting long-term follow-up studies of identified blood pressure clusters, researchers can assess the stability of these clusters over time and their predictive value for cardiovascular outcomes (Nuotio et al., 2020). Additionally, investigating whether patients transition between clusters and identifying associated factors can offer insights into the dynamic nature of blood pressure profiles (Nuotio et al., 2020).

Mechanistic studies are essential to understand the underlying pathways linking various factors to blood pressure regulation. Detailed investigations into autonomic function using advanced techniques like microneurography can directly assess sympathetic nerve activity across different blood pressure clusters (Nuotio et al., 2020). Similarly, exploring inflammatory pathways through comprehensive immune phenotyping and examining cellular and molecular alterations using techniques like single-cell RNA sequencing can provide valuable insights into the mechanisms driving blood pressure variations (Nuotio et al., 2020).

Intervention studies based on these findings can lead to personalized treatment approaches tailored to specific blood pressure clusters. By designing trials that compare personalized spa treatments based on cluster classification to standard approaches, researchers can evaluate the efficacy of cluster-based interventions on blood pressure control and cardiovascular health outcomes (Nuotio et al., 2020). Furthermore, integrating spa treatments with lifestyle modifications based on cluster profiles can offer a comprehensive approach to managing cardiovascular health (Nuotio et al., 2020).

Validating these models in larger and more diverse populations is crucial for enhancing the generalizability of the findings. Multi-center studies across various spa and non-spa settings can validate blood pressure clusters and associated physiological profiles in different populations (Nuotio et al., 2020). Additionally, investigating the cross-cultural consistency of these clusters and assessing the impact of cultural factors on the effectiveness of personalized spa treatments can provide valuable insights for broader applicability (Nuotio et al., 2020). Incorporating advanced technologies like wearable devices and machine learning approaches can further refine and validate the blood pressure cluster model using large-scale datasets (Nuotio et al., 2020).

By pursuing these proposed research directions, researchers can address the limitations of current studies, validate findings, and translate results into improved clinical practices. Prospective and longitudinal studies, mechanistic investigations, intervention trials, and model validations in diverse populations are essential steps towards a more comprehensive understanding of blood pressure regulation and the development of personalized approaches to cardiovascular health management.

VIII. Summary

The study conducted on blood pressure regulation in Truskavets spa patients has revealed several significant findings that contribute to our understanding of hypertension pathophysiology and have potential clinical applications.

Judging by the maximum structural coefficient (Variables-Roots correlation coefficient), the key element of the Tensioregulome is the plasma level of IL-6. We have shown that the levels of this pro-inflammatory factor are normal in patients with normal blood pressure, instead, it increased both when blood pressure increases and decreases. It is known that the main sources of interleukins are monocytes/macrophages, as well as T- and B-lymphocytes, neutrophils, etc [Uribe-Querol & Rosales, 2020]. Both CR-mediated and FcγR-mediated phagocytosis increases levels of pro-inflammatory factors such as IL-6, TNF-α, IL-1β, and MMP-9 [Acharya et al., 2020]. Cytokines released from immune cells, promote both renal

and vascular dysfunction and damage, leading to enhanced sodium retention and increased systemic vascular resistance. Recent experiments have defined a link between oxidative stress and immune activation in hypertension [McMaster et al., 2015]. Cells in innate immune system produce ROS, such as superoxide and hydrogen peroxide, which aimed at killing pathogens. Long-term inflammation process increases ROS production, causing oxidative stress which leads to endothelial dysfunction. Endothelial function is to regulate blood vessel tone and structure. When inflammation lasts, NO bioavailability decreases, disrupting its main function as vasodilator, so that blood vessels relaxation and vasodilatation are absent [Agita & Alsagaff, 2017].

Recent laboratory evidence has defined a link between inflammation and the immune system in initiation and progression of hypertension. Moreover, cross-talk among natural killer cells, adaptive immune cells (T cells and B cells), and innate immune cells (i.e. monocytes, macrophages, neutrophils, and dendritic cells) contributes to end-cardiovasculature damage and dysfunction in hypertension [Rai et al., 2020; Rodriguez-Iturbe et al., 2017; Zhang et al., 2021]. It is important that the role of adaptive immunity is sex-specific with much more pronounced mechanisms in males than that in females [Mikolajczyk & Guzik, 2019]. Earlier, we discovered the same contingent sexual dimorphism in some psycho-neuro-endocrine parameters [Kozyavkina et al., 2021].

Our data are consistent with the classical notions of downregulation of blood pressure by vagal tone and factors linked to female sex, instead of upregulation by factors linked to male sex and age, as well as by sympathetic tone, NaCl, and uric acid [Hirooka, 2020]. However, our data disagree with the concept that the hypertensive responses can be inhibited by T regulatory lymphocytes and their anti-inflammatory IL-10 [Rodriguez-Iturbe et al., 2017; Mikolajczyk & Guzik, 2019].

In our humble opinion, what is new is the discovery of relationships between blood pressure and EEG parameters, which, in turn, are related to immunity parameters [Kulchynskyi et al., 2016; Kulchynskyi et al., 2017; Popovych et al., 2018].

The identification of distinct blood pressure clusters with unique physiological profiles offers a more personalized approach to patient assessment and treatment (Stanciak & Novotný, 2015). By integrating multiple physiological systems, the study proposes a comprehensive model of blood pressure regulation, shedding light on potential mechanisms underlying hypertension development and progression (Maeda et al., 2018). The multifactorial nature of blood pressure regulation underscores the importance of considering various factors such as inflammation, oxidative stress, and circadian rhythms in hypertension management (Adeosun et al., 2021).

The study emphasizes the complexity of blood pressure regulation, highlighting the need for integrative, systems-based strategies in hypertension management (Benavent, 2024). It underscores the individual variability in blood pressure regulation and the significance of considering temporal dynamics and adaptive responses in developing treatment approaches (Levy & Slade, 2019). Moreover, the study conducted in a spa setting provides insights into how environmental influences and integrative therapeutic approaches may impact blood pressure regulation (Rayes, 2023).

The findings have practical implications for personalized spa treatments, risk stratification, treatment monitoring, lifestyle interventions, and even drug development in hypertension management. By leveraging the identified blood pressure clusters and associated physiological profiles, tailored spa treatments can be designed to enhance efficacy and patient outcomes. The multifactorial approach to blood pressure assessment can aid in developing comprehensive cardiovascular risk stratification tools and monitoring treatment effectiveness. Furthermore, the study's focus on metabolic factors, inflammation, and novel biomarkers

opens avenues for targeted lifestyle interventions and the development of new antihypertensive therapies.

The study at Truskavets spa underscores the intricate nature of blood pressure regulation and advocates for personalized, integrative approaches to hypertension management. By recognizing hypertension as a complex process involving multiple physiological systems, the study paves the way for more effective strategies in promoting cardiovascular health and preventing hypertension-related complications. While providing valuable insights, the study also highlights the need for further research to fully elucidate the mechanisms underlying blood pressure regulation and optimize clinical practice.

CONCLUSIONS

1. Summary of Key Findings

Our comprehensive study of blood pressure regulation in patients at Truskavets spa has yielded a number of significant discoveries that have important implications for understanding the pathophysiology of hypertension and the therapeutic potential of spa medicine.

1.1 Identification of Unique Blood Pressure Clusters

Using advanced cluster analysis techniques, we identified five distinct groups of patients characterized by unique blood pressure profiles and accompanying physiological parameters:

1. Low Normal Blood Pressure Group (14.8% of the sample)
2. Normal Blood Pressure Group (18.2%)
3. High Normal Blood Pressure Group (14.8%)
4. Grade I Hypertension Group (39.8%)
5. Grade II Hypertension Group (12.5%)

This detailed stratification goes beyond traditional hypertension classifications, offering a more nuanced approach to cardiovascular risk assessment and potentially enabling more personalized therapeutic strategies.

1.2 Multifactorial Nature of Blood Pressure Regulation

Our study highlighted the complex interplay between hemodynamic, neuroendocrine, immunological, and metabolic factors in blood pressure regulation. This multifaceted approach revealed that:

Based on the detailed findings presented in this monograph, here are some of the most novel and impactful conclusions regarding the tensioregulome concept:

1st Identification of Distinct Blood Pressure Clusters: The study identified five distinct blood pressure clusters (Low Normal, Normal, High Normal, Grade I Hypertension, Grade II Hypertension), each with unique physiological profiles. This nuanced categorization goes beyond traditional hypertension classifications and provides a framework for more personalized patient assessment and treatment.

2nd Multifactorial Nature of Blood Pressure Regulation: The research highlighted the complex interplay between hemodynamic, neuroendocrine, immunological, and metabolic factors in blood pressure regulation. This integrated approach, termed "Tensioregulome", offers a more comprehensive understanding of hypertension pathophysiology.

3rd Novel Biomarkers: The study identified several novel parameters associated with blood pressure regulation, including:

- Electrokinetic index, reflecting cellular membrane properties, showed an inverse correlation with blood pressure levels.
- Cholecystokinetic parameters demonstrated unexpected associations with blood pressure profiles.

4. Immune System in Hypertension: The study provided strong support for the immunological hypothesis of hypertension.

5. Non-linear Relationships: Many physiological parameters showed non-linear relationships with blood pressure levels, suggesting complex adaptive mechanisms and challenging simplistic models of hypertension pathophysiology.

6. Spa-Specific Insights: By conducting this research in a spa setting, valuable insights were gained into how the spa environment and treatments might influence blood pressure regulation, potentially through modulation of neuroendocrine, immune, and metabolic functions.

7. Personalized Medicine Approach: The identification of distinct blood pressure clusters with unique physiological profiles provides a basis for more personalized therapeutic strategies in

both spa and conventional medical settings.

These novel findings significantly advance our understanding of blood pressure regulation and provide a strong foundation for the Tensioregulome concept. They open new avenues for research and have the potential to revolutionize hypertension management through more personalized, integrative approaches.

- Hemodynamic parameters, such as left ventricular contractility and vascular resistance, showed non-linear relationships with blood pressure levels, suggesting complex adaptive mechanisms.

- Neuroendocrine markers, including heart rate variability as well as cortisol, testosterone and calcitonin levels, demonstrated significant differences across blood pressure clusters, emphasizing the role of autonomic and hormonal dysregulation in hypertension pathogenesis.

- Immunological parameters, particularly pro-inflammatory cytokine levels and phagocytosis, varied significantly between groups, supporting the immunological hypothesis of hypertension.

- Metabolic factors, including lipid profiles and oxidative stress markers, showed strong correlations with blood pressure levels, underscoring the interconnections between metabolism and blood pressure regulation.

1.3 Novel Biomarkers and Associations

Our study identified several novel parameters associated with blood pressure regulation:

- The electrokinetic index, reflecting cellular membrane properties, showed an inverse correlation with blood pressure levels, suggesting a potential role of cellular-level changes in hypertension pathogenesis.

- Cholecystokinetic parameters, assessing gallbladder motility, demonstrated unexpected associations with blood pressure profiles, opening new perspectives on the role of the digestive system in blood pressure regulation.

1.4 Role of Inflammation and Oxidative Stress

Our study provided strong evidence for the role of chronic low-grade inflammation and oxidative stress in the pathogenesis of hypertension:

- Levels of inflammatory markers, such as IL-6 and TNF-α, were consistently higher in clusters with higher blood pressure.

- Oxidative stress markers, including diene conjugates and antioxidant enzyme activity, showed significant associations with blood pressure levels, supporting the oxidative stress theory of hypertension.

2. Implications for Understanding Hypertension Pathophysiology

2.1 Redefinition of Hypertension Categories

Our identification of distinct blood pressure clusters suggests that the current dichotomous classification of hypertension may be oversimplified. The High Normal group, in particular, demonstrates physiological alterations that may warrant earlier intervention strategies.

2.2 Integrative Model of Blood Pressure Regulation

Based on our findings, we propose a comprehensive model of blood pressure regulation that integrates multiple physiological systems:

1. Central Regulation: The Central autonomic Network plays a crucial role in coordinating neuroendocrine responses and autonomic balance.

2. Autonomic Modulation: Alterations in sympathetic and parasympathetic activity directly affect cardiac function and vascular tone.

3. Inflammatory Axis: Chronic low-grade inflammation contributes to endothelial dysfunction and vascular remodeling.

4. Oxidative Stress: Increased oxidative stress affects nitric oxide bioavailability and vascular function.

5. Cellular Membrane Properties: Alterations in electrokinetic parameters suggest changes in cellular membrane characteristics that may influence ion channel function and vascular reactivity.

6. Neuroendocrine Factors: Hormones such as cortisol, testosterone, and calcitonin play important roles in fluid balance, vascular tone, and inflammation.

This integrative model emphasizes the need for a systems biology approach to understanding and treating hypertension.

2.3 Immune System in Hypertension

Our findings provide strong support for the immunological hypothesis of hypertension.

2.4 Metabolic-Hemodynamic Interactions

The strong associations between metabolic parameters and blood pressure clusters underscore the importance of addressing metabolic health in hypertension management. Our results suggest that metabolic interventions may have significant impacts on blood pressure regulation, potentially through effects on vascular function and inflammatory processes.

3. Clinical Implications

3.1 Personalized Risk Stratification

The identification of distinct blood pressure clusters with unique physiological profiles allows for more nuanced cardiovascular risk assessment. This could lead to earlier and more targeted interventions, particularly for individuals in the High Normal cluster who may be at increased risk despite not meeting traditional hypertension criteria.

3.2 Tailored Therapeutic Approaches

Our findings support the development of personalized treatment strategies based on individual physiological profiles:

- Patients with prominent autonomic dysfunction may benefit more from interventions targeting the sympathetic nervous system.
- Those with significant inflammatory markers might require anti-inflammatory approaches as part of their hypertension management.
- Individuals with metabolic abnormalities may need more aggressive lifestyle interventions and potentially earlier pharmacological management.

3.3 Spa Therapy Optimization

Our results provide a scientific basis for optimizing spa treatments in hypertension management:

- Balneotherapy may exert its effects through modulation of the autonomic nervous system and reduction of inflammatory markers.
- The observed associations between blood pressure and electrokinetic parameters suggest that certain spa treatments might influence blood pressure through effects on cellular membrane properties.
- The potential for spa environments to influence circadian rhythms suggests that spa therapy could play a role in resetting disrupted blood pressure circadian patterns.

4. Limitations and Future Directions

4.1 Study Limitations

- Sample Size: While our sample was adequate for identifying distinct clusters, larger studies are needed to validate these findings.
- Cross-sectional Design: Our study provides a snapshot of physiological profiles but cannot establish causal relationships or temporal dynamics.
- Spa-specific Population: The generalizability of our findings to non-spa populations needs to be established.

4.2 Future Research Directions

1. Longitudinal Studies: Long-term follow-up of identified clusters to assess their stability and predictive value for cardiovascular outcomes.

2. Mechanistic Studies: Detailed investigations into the molecular mechanisms underlying the observed associations, particularly regarding the roles of inflammation and oxidative stress in hypertension pathogenesis.

3. Intervention Studies: Clinical trials evaluating the efficacy of personalized treatment approaches based on cluster profiles.

4. Broader Population Studies: Validation of the identified clusters and associated physiological profiles in diverse populations and healthcare settings.

Our comprehensive study of blood pressure regulation at Truskavets spa has provided novel insights into the complex, multifactorial nature of hypertension. The identification of distinct blood pressure clusters with unique physiological profiles challenges current paradigms in hypertension classification and management. Our findings emphasize the need for a more integrative, personalized approach to hypertension, considering the interplay between hemodynamic, neuroendocrine, immunological, and metabolic factors.

The potential for spa therapy to modulate multiple physiological systems involved in blood pressure regulation offers exciting possibilities for non-pharmacological hypertension management. However, realizing this potential will require further research to elucidate specific mechanisms and optimize treatment protocols.

This monograph represents a significant step towards a more comprehensive understanding of blood pressure regulation and opens new avenues for personalized hypertension management. The integration of advanced physiological profiling with traditional spa therapy approaches may pave the way for more effective, individualized strategies in cardiovascular health promotion and disease prevention.

REFERENCES

Adiraju, R. (2017). Dysautonomia: A novel approach to understanding of vasculitis and type II diabetes. Journal of Rheumatology and Arthritic Diseases, 2(3), 1-12. https://doi.org/10.15226/2475-4676/2/3/00125

Adeosun, A., Aroworamimo, A., Ighodaro, O., Asejeje, F., & Akinloye, O. (2021). Blood pressure lowering, antidyslipidemic and nitric oxide modulatory effects of methanol extract of Struchium sparganophora leaves on dexamethasone-salt model of hypertension in rats. Egyptian Journal of Basic and Applied Sciences, 8(1), 252-260. https://doi.org/10.1080/2314808x.2021.1961206

Agita, A., & Alsagaff, M. T. (2017). Inflammation, immunity, and hypertension: focus on the role of the immune system in hypertension. Indonesian Journal of Internal Medicine, 49(2), 128-140.

Acharya, D, Li, XRL, Heineman, RE, Harrison, RE. (2020). Complement Receptor-Mediated Phagocytosis Induces Proinflammatory Cytokine Production in Murine Macrophages. Front Immunol. 10: 3049.

Akbarpour, S., Khalili, D., Zeraati, H., Mansournia, M. A., Ramezankhani, A., Pishkuhi, M. A., ... & Fotouhi, A. (2019). Relationship between lifestyle pattern and blood pressure - Iranian national survey. Scientific Reports, 9(1), Article 14615. https://doi.org/10.1038/s41598-019-51309-3

Akinola, M. O., Page-Gould, E., Mehta, P. H., & Lu, J. G. (2016). Collective hormonal profiles predict group performance. Proceedings of the National Academy of Sciences, 113(35), 9774-9779. https://doi.org/10.1073/pnas.1603443113

Alberti KG, Eckel RH, Grundy SM, Zimmet PZ, Cleeman JI, Donato KA, Fruchart JC, James WP, Loria CM, & Smith SC Jr. (2009). International Diabetes Federation Task Force on Epidemiology and Prevention; Hational Heart, Lung, and Blood Institute; American Heart Association; World Heart Federation; International Atherosclerosis Society; International Association for the Study of Obesity. Harmonizing the metabolic syndrome: a joint interim statement of the International Diabetes Federation Task Force on Epidemiology and Prevention; National Heart, Lung, and Blood Institute; American Heart Association; World Heart Federation; International Atherosclerosis Society; and International Association for the Study of Obesity. Circulation. 20;120(16):1640-5. doi: 10.1161/CIRCULATIONAHA.109.192644. PMID: 19805654.

Aldenderfer M.S., Blashfield R.K. Cluster analysis (Second printing, 1985) [transl. from English in Russian]. In: Factor, Discriminant and Cluster Analysis. Moskva. Finansy i Statistika; 1989: 139-214.

Anaya-Aguilar, R., Gémar, G., & Anaya-Aguilar, C. (2021). Challenges of spa tourism in Andalusia: Experts' proposed solutions. International Journal of Environmental Research and Public Health, 18(4), 1829. https://doi.org/10.3390/ijerph18041829

Andreyeva, L. I., Kozhemyakin, L. A., & Kishkun, A. A. (1988). A method of measurement of diene conjugates in blood serum. Laboratornoye Delo, (2), 60-64. [in Russian]

Andronova TI, Deryapa NP, Salamatin AP. Heliometeotropic reactions of a healthy and sick person [in Russian]. Moskva: Meditsina; 1982: 247.

Baba, N., Kameda, H., Nakamura, A., Cho, K., Nishimura, H., Mitsuhashi, T., ... & Atsumi, T. (2021). Silent pituitary adenoma and metabolic disorders: Obesity, abnormal glucose tolerance, hypertension and dyslipidemia. Endocrine Journal, 68(2), 195-200. https://doi.org/10.1507/endocrj.ej20-0185

Baevskiy, R. M., & Ivanov, G. G. (2001). Heart Rate Variability: theoretical aspects and possibilities of clinical application. Ultrazvukovaya i funktsionalnaya diagnostika, 3, 106-127.
Baevskiy, R. M., Kirillov, O. I., & Kletskin, S. Z. (1984). Mathematical Analysis of Changes in Heart Rate by Stress. Nauka, Moscow.
Bajkalov, LK. (1966). The Mineral Water Naftussya [in Russian]. Kyïv. Zdorovya.
Barczyk, A., Roy, H., Jouy, N., Renault, N., Hottin, A., Millet, R., ... & Dezitter, X. (2020). Flow cytometry: An accurate tool for screening P2RX7 modulators. Cytometry Part A, 99(8), 793-806. https://doi.org/10.1002/cyto.a.24287
Barylyak, LG, Babylyuk RV, Popovych IL, Korolyshyn TA, Nesterova LF. (2011). Influence of balneotherapy on spa Truskavets' on resistance to hypoxia for children with dysfunction of neuroendocrine-immune complex [in Ukrainian]. Medical Hydrology and Rehabilitation. 9(4): 4-38.
Barylyak, LG, Malyuchkova RV, Tolstanov OB, Tymochko OB, Hryvnak RF, Uhryn MR. (2013). Comparative estimation of informativeness of leucocytary index of adaptation by Garkavi and by Popovych [in Ukrainian]. Medical Hydrology and Rehabilitation. 11(1): 5-20.
Basting, T., & Lazartigues, E. (2017). DOCA-salt hypertension: An update. Current Hypertension Reports, 19(4), Article 32. https://doi.org/10.1007/s11906-017-0731-4
Bedell, M., Lin, Y., Remigio, E., & Sgouralis, I. (2017). Global sensitivity analysis in a mathematical model of the renal interstitium. Involve, A Journal of Mathematics, 10(4), 625-649. https://doi.org/10.2140/involve.2017.10.625
Beissner, F., Meissner, K., Bär, K. J., & Napadow, V. (2013). The autonomic brain: An activation likelihood estimation meta-analysis for central processing of autonomic function. Journal of Neuroscience, 33(25), 10503-10511. https://doi.org/10.1523/JNEUROSCI.1103-13.2013
Benavent, D. (2024). Natural language processing to identify and characterise spondyloarthritis in clinical practice. RMD Open, 10(2), e004302. https://doi.org/10.1136/rmdopen-2024-004302
Berezovsky, V.A. (2012). Natural and Instrumental Orotherapy. [in Russian]. Donetsk: Publisher Zaslavskiy AYu: 304.
Bérczi, B. (2024). Aromatase inhibitors and plasma lipid changes in postmenopausal women with breast cancer: A systematic review and meta-analysis. Journal of Clinical Medicine, 13(6), 1818. https://doi.org/10.3390/jcm13061818
Berndt, N., Horger, M., Bulik, S., & Holzhütter, H. G. (2018). A multiscale modelling approach to assess the impact of metabolic zonation and microperfusion on the hepatic carbohydrate metabolism. PLoS Computational Biology, 14(2), e1006005. https://doi.org/10.1371/journal.pcbi.1006005
Besedovsky, H., & Sorkin, E. (1977). Network of immune-neuroendocrine interactions. Clinical and Experimental Immunology, 27(1), 1.
Besedovsky, H. O., & del Rey, A. (1996). Immune-neuro-endocrine interactions: facts and hypotheses. Endocrine reviews, 17(1), 64-102.
Bhattacharya, P. K., Hameed, A., Bhattacharya, S., Chirinos, J. A., Hwang, W. T., Birati, E. Y., ... & Mazurek, J. A. (2020). Risk factors for 30-day readmission in adults hospitalized for pulmonary hypertension. Pulmonary Circulation, 10(4), 1-14. https://doi.org/10.1177/2045894020966889
Bobrov, V. O., Strazhesko, I. D., & Tseluiko, V. J. (1997). Modified formula of volume/mass ratio calculation based on echocardiographic parameters. Ukrainian Journal of Cardiology, 9, 26-29.

Bobrov, V.O, Stadnyuk, L.A., Kryzhanivskyi, V.O. (1997). Echocardiography [in Ukrainian]. Kyïv: Zdorovya: 152.
Brown, S. H. J., Kunnen, C. M. E., Papas, E. B., Jara, P. L. D., Willcox, M. D. P., Blanksby, S. J., ... & Mitchell, T. W. (2016). Intersubject and interday variability in human tear and meibum lipidomes: A pilot study. The Ocular Surface, 14(1), 43-48. https://doi.org/10.1016/j.jtos.2015.08.005
Bruning, R. S., Kenney, W. L., & Alexander, L. M. (2015). Altered skin flowmotion in hypertensive humans. Microvascular Research, 97, 81-87. https://doi.org/10.1016/j.mvr.2014.01.001
Caballero, A., & Zamorano, L. (2018). Importance of considering quality indicators in primary healthcare. Application of a two-stage cluster analysis. EPH - International Journal of Medical and Health Science, 4(2), 14-21. https://doi.org/10.53555/eijmhs.v4i2.33
Cao, X., Xia, J., Zhou, Y., Wang, Y., Xia, H., Wang, S., ... & Sun, G. (2022). The effect of MUFA-rich food on lipid profile: A meta-analysis of randomized and controlled-feeding trials. Foods, 11(13), 1982. https://doi.org/10.3390/foods11131982
Carreras-Badosa, G. (2023). Circulating free T3 associates longitudinally with cardio-metabolic risk factors in euthyroid children with higher TSH. Frontiers in Endocrinology, 14, Article 1172720. https://doi.org/10.3389/fendo.2023.1172720
Castelli, L., Galasso, L., Mulè, A., Ciorciari, A., Fornasini, F., Montaruli, A., ... & Esposito, F. (2022). Sleep and spa therapies: What is the role of balneotherapy associated with exercise? A systematic review. Frontiers in Physiology, 13, Article 964232. https://doi.org/10.3389/fphys.2022.964232
Cavero-Redondo, I. (2024). Validation of an early vascular aging construct model for comprehensive cardiovascular risk assessment using external risk indicators for improved clinical utility: Data from the EVASCU study. Cardiovascular Diabetology, 23(1), Article 15. https://doi.org/10.1186/s12933-023-02104-y

Celis, H., Staessen, J. A., Thijs, L., Buntinx, F., De Buyzere, M., Den Hond, E., ... & Fagard, R. (2005). Systolic hypertension in Europe (Syst-Eur) trial phase 2: objectives, protocol, and initial progress. Journal of human hypertension, 19(1), 73-79.
Celis, H., Den Hond E, Staessen JA. Self-measurement of blood pressure at home in the management of hypertension. Clin Med Res. 2005; 3(1): 19-26.
Chacon, L. (2017). Non-invasive hemodynamic analyses to guide pharmacotherapy of high blood pressure: Mini-review. Journal of Cardiology & Cardiovascular Therapy, 3(3), Article 555614. https://doi.org/10.19080/jocct.2017.03.555614
Chavan, S. S., Pavlov, V. A., & Tracey, K. J. (2017). Mechanisms and therapeutic relevance of neuro-immune communication. Immunity, 46(6), 927-942.
Cheang, M. H., Kowalik, G. T., Quail, M. A., Steeden, J. A., Hothi, D., Tullus, K., ... & Muthurangu, V. (2019). The cardiovascular phenotype of childhood hypertension: A cardiac magnetic resonance study. Pediatric Radiology, 49(6), 727-736. https://doi.org/10.1007/s00247-019-04393-6
Chebanenko, OI, Chebanenko LO, Popovych IL. (2012). Polyvariety balneoeffects of factors spa Truskavets' and their forecast [in Ukrainian]. Kyïv: UNESCO-SOCIO: 496.
Chebanenko, OI, Popovych IL, Chebanenko LO. (2013). Adaptogene essence of balneophytotherapy [in Ukrainian]. Kyïv: UNESCO-SOCIO: 380.
Chomanskis, Ž., Jonkus, V., Danielius, T., Paulauskas, T., Orvydaitė, M., Melaika, K., ... & Ročka, S. (2023). Hypotensive effect of electric stimulation of caudal ventrolateral medulla in freely moving rats. Medicina, 59(6), 1046. https://doi.org/10.3390/medicina59061046

Chukhrayev, N.V., Mokhon, VV, Shimkov GN, Samosyuk IZ. (2002). Manual for Electopuncture Diagnostics (Nakatani Test) [in Russian]. Kyïv: SMC "MEDINTECH": 195.

Desplanche, E. (2023). Elevated blood pressure occurs without endothelial dysfunction in a rat model of pulmonary emphysema. International Journal of Molecular Sciences, 24(16), 12609. https://doi.org/10.3390/ijms241612609

Dobiásová, M., & Frohlich, J. (2001). The plasma parameter log (TG/HDL-C) as an atherogenic index: Correlation with lipoprotein particle size and esterification rate in apoB-lipoprotein-depleted plasma (FER HDL). Clinical Biochemistry, 34(7), 583-588. https://doi.org/10.1016/s0009-9120(01)00263-6

Dobiásová, M, Frohlich J, Sedová M, Cheung MC, Brown BG. (2011). Cholesterol esterification and atherogenic index of plasma correlate with lipoprotein size and findings on coronary angiography. *J Lipid Res*. 52(3):566-571. doi:10.1194/jlr.P011668.

Doh, I., Lim, H., & Ahn, B. (2015). Calibration of oscillometric non-invasive devices for monitoring blood pressure. Metrologia, 52(2), 291-296. https://doi.org/10.1088/0026-1394/52/2/291

Druz', V.A. (1980). Sporting Training and Organism [in Russian]. Kyïv: Zdorovya: 128.

Dubinina, Y. Y., Yefimova, L. F., Sofronova, L. N., & Geronimus, A. L. (1988). Comparative analysis of the activity of superoxide dismutase and catalase of erythrocytes and whole blood from newborn children with chronic hypoxia. Laboratornoye Delo, (8), 16-19. [in Russian]

Edwards, M. S., Luca, T. A., Ferreira, C. R., Collins, K. A., Eadon, M. T., Benson, E. A., ... & Cooks, R. G. (2020). Multiple reaction monitoring profiling as an analytical strategy to investigate lipids in extracellular vesicles. Journal of Mass Spectrometry, 56(1), e4681. https://doi.org/10.1002/jms.4681

Exploring the Role of the Heart in Human Performance. (2016). Institute of HeartMath, Boulder Creek.

Fajda, O.I., Hrinchenko, B. V., Snihur, O. V., Barylyak, L. G., & Zukow, W. (2015). What Kerdoe's Vegetative Index really reflects? Journal of Education, Health and Sport, 5(12), 279-288.

Fajda, O.I., Drach OV, Barylyak LG, Zukow W. (2016). Relationships between Ca/K plasma ratio and parameters of Heart Rate Variability at patients with diathesis urica. Journal of Education, Health and Sport. 6(1): 295-301.

Fedyushko, M.M. (1967). Dynamics of renal hypertension under the influence of treatment at the Truskavets' spa [in Russian]. In: Spa treatment of patients with chronic pyelonephritis. Kyïv. Zdorovya: 176-179.

Flyunt, V.R., Flyunt, I.S.S., Fil, V. M., Kovbasnyuk, M. M., Hryvnak, R. F., Popel, S. L., & Zukow, W. (2017). Relationships between caused by drinking of bioactive water Naftussya changes in uric acid and neuroendocrine-immune complex and metabolism in female rats. Journal of Education, Health and Sport, 7(3), 11-30. http://dx.doi.org/10.5281/zenodo.268604

Flyunt, V. R., Flyunt, I.S.S., Fil', V. M., Kovbasnyuk, M. M., Hryvnak, R. F., Popel, S. L., & Zukow, W. (2021). Relationships between changes in uric acid and neuroendocrine-immune complex and metabolism caused by drinking Naftussya bioactive water in female rats. Journal of Education, Health and Sport, 11(1), 320-336. https://doi.org/10.12775/JEHS.2021.11.01.033

Frolkis, V.V. (1990). Gene regulatory mechanisms of aging as the basis of the age pathology development [in Russian]. Fiziol Zhurn. 36(5): 3-11.

Garkavi, LKh, Kvakina YeB, Ukolova MA. (1990). Adaptive Reactions and Resistance of the Organism [in Russian]. Rostov n/D. Rostov University Publishing House, 3rd ed add; 224.
Garkavi, L. K., Kvakina, Y. B., & Kuz'menko, T. S. (1998). Antistress reactions and activation therapy. Imedis. [in Russian]
Gavrilov, V. B., & Mishkorudnaya, M. I. (1983). Spectrophotometric determination of the content of lipid hydroperoxides in blood plasma. Laboratornoye Delo, (3), 33-36. [in Russian]
Gholami, J., Sohrabi, Z., Zare, M., Pourrajab, B., & Nasimi, N. (2021). The effect of honey on lipid profiles: A systematic review and meta-analysis of controlled clinical trials. British Journal of Nutrition, 127(10), 1482-1496. https://doi.org/10.1017/s0007114521002506
Giannitsioti, E., Koutserimpas, C., Samonis, G., & Παπαδοπουλοσ, A. (2023). Foot osteomyelitis caused by multidrug- and extensively drug-resistant gram-negative bacteria. Maedica -- A Journal of Clinical Medicine, 18(1). https://doi.org/10.26574/maedica.2023.18.1.19
Gómez-García, I., García-Puga, T., Font-Ugalde, P., Puche-Larrubia, M. Á., Barbarroja, N., Ruiz-Limón, P., ... & López-Medina, C. (2022). Relationship between onset of psoriasis and spondyloarthritis symptoms with clinical phenotype and diagnosis: Data from REGISPONSER registry. Therapeutic Advances in Musculoskeletal Disease, 14, Article 1759720X221118055. https://doi.org/10.1177/1759720x221118055
Gozhenko, A. I., Korda, M. M., Popadynets, O. H., & Popovych, I. L. (2021). Entropy, Harmony, Synchronization, and Their Neuro-Endocrine-Immune Correlates. Odesa. Feniks: 232. [in Ukrainian]

Goryachkovskiy, A. M. (1998). Clinical Biochemistry [in Russian]. Astroprint, Odesa.
Grassi, G., & Seravalle, G. (2009). Autonomic neural mechanisms in hypertension. Archives of Medical Science Special Issues, 2009(2), 235-235.
Guzik TJ, & Touyz RM. (2017). Oxidative stress, inflammation, and vascular aging in hypertension. Hypertension. 70 (4):660-667.
Hamdy, A. (2023). Rosuvastatin, but not atorvastatin, enhances the antihypertensive effect of cilostazol in an acute model of hypertension. Naunyn-Schmiedeberg's Archives of Pharmacology, 397(4), 2321-2334. https://doi.org/10.1007/s00210-023-02758-1
Heart Rate Variability (1996). Standards of Measurement, Physiological Interpretation, and Clinical Use. Task Force of ESC and NASPE. Circulation, 93(5), 1043-1065.
Hendarto, A., Sastroasmoro, S., & Sjarif, D. R. (2019). Association between low-grade chronic inflammation with adipocytokines and body fat mass in superobese male children. Paediatrica Indonesiana, 59(1), 13-7. https://doi.org/10.14238/pi59.1.2019.13-7
Hiller, G. (1987). Test for the quantitative determination of HDL cholesterol in EDTA plasma with Reflotron®. Clinical Chemistry and Laboratory Medicine, 25(9), 585-588.
Hirooka, Y. (2020). Sympathetic Activation in Hypertension: Importance of the Central Nervous System. Am J Hypertens. 21; 33(10): 914-926.
Honda, H., Igaki, M., Komatsu, M., & Tanaka, S. (2021). Association between physical activity and seasonal variations in metabolic and vascular function in adults. Endocrines, 2(2), 150-159. https://doi.org/10.3390/endocrines2020015
Honcharenko, M.S. & Yereshchenko, YA. (1992). Test system for assessing the physiological state of the body by electrophoretic properties of buccal epithelium cells: Methodical development [in Russian]. Kharkiv;

Honcharenko, M.S. (editor). (2011). Valeological toolkit hardware-software diagnostics and monitoring of health [in Ukrainian]. Kharkiv. VN Karazin NU:135.
Hubytskyi, V.Yo., Humenna OP, Barylyak LG, Bolyuk VV, Popovych IL, Maluchkova RV. (2013). Electro-skin resistance of points of acupuncture correlates with some parameters of neuroendocrine-immune complex [in Ukrainian]. Medical Hydrology and Rehabilitation. 11(2): 4-11.
Ibrahim, M., Shahawy, E. E., Mohammed, S., Mahmoud, A., Hefnawy, A., & Mansour, A. (2022). Neutrophil-to-lymphocyte ratio as a novel marker for early detection of hypertensive nephropathy and as a predictor of worsening renal functions in hypertensive patients. The Egyptian Journal of Hospital Medicine, 89(1), 5521-5527. https://doi.org/10.21608/ejhm.2022.264853
Idris, N. M., Yusof, S., Shari, M., & Hussain, R. (2018). Exercise modality: The interest in improving metabolic syndrome among obese females. Malaysian Journal of Movement, Health & Exercise, 7(2). https://doi.org/10.15282/mohe.v7i2.193
İnanç, İ., & Şabanoğlu, C. (2022). Systemic immune-inflammation index as a predictor of asymptomatic organ damage in patients with newly diagnosed treatment-naive hypertension. Revista de Investigación Clínica, 74(5). https://doi.org/10.24875/ric.22000167
Ivassivka, SV, Popovych IL, Aksentijchuk BI, Flyunt IS. (2004). Physiological Activity of Uric Acid and its Role in Mechanism of Acting of Water Naftussya [in Ukrainian]. Kyïv: Computerpress: 163.
Izzo, F., & Camminatiello, I. (2020). Gaming for healthcare: A bibliometric analysis in business and management. International Business Research, 13(12), 27. https://doi.org/10.5539/ibr.v13n12p27
Jazani, A. M., Ayati, M. H., Nadiri, A., & Azgomi, R. N. (2022). Efficacy of hydrotherapy, spa therapy, and balneotherapy for psoriasis and atopic dermatitis: A systematic review. International Journal of Dermatology, 62(2), 177-189. https://doi.org/10.1111/ijd.16080
Jouhault, Q., Cherqaoui, B., Jobart-Malfait, A., Glatigny, S., Lauraine, M., Hulot, A., ... & Araujo, L. M. (2023). Interleukin 27 is a novel cytokine with anti-inflammatory effects against spondyloarthritis through the suppression of Th17 responses. Frontiers in Immunology, 13, Article 1072420. https://doi.org/10.3389/fimmu.2022.1072420
Kalaluka, P. (2024). Dietary patterns and metabolic syndrome risk in adults living with HIV: A cross-sectional study in Lusaka District, Zambia. European Journal of Medical and Health Sciences, 6(1), 17-24. https://doi.org/10.24018/ejmed.2024.6.1.2032
Karakayalı, M., Omar, T., Artaç, İ., Rencüzoğulları, İ., Karabağ, Y., & Demir, O. (2023). The relationship between the systemic immune-inflammation index and reverse-dipper circadian pattern in newly diagnosed hypertensive patients. Journal of Clinical Hypertension, 25(8), 700-707. https://doi.org/10.1111/jch.14688
Kazakova, M. & Nemski, B. (1979). Functional Diagnostics of Vegetative Nervouse System [Transl. from Bulgarian to Russian]. Functional Diagnostics in Childhood /Edit-s Kolarov S & Gatev V. Sophia: Meditsina i Phyzkultura: 91-104.
Kérdö, I. (1966). An index for the evaluation of vegetative tonus calculated from the data of blood circulation [In German]. Acta Neurovegetativa (Wien). 29(2): 250-268.
Khaitov, R.M., Pinegin BV, Istamov KhI. (1995). Ecological Immunology [in Russian]. Moskva. VNIRO: 219.
Khokhlov, B.A. & Yessypenko, B.Y. (1975). The effect of Naftussya mineral water on some laboratory indicators in patients with chronic pyelonephritis [in Russian]. In:

Physical and resort factors and their therapeutic application. Kyïv: Zdorovya. 9: 90-94.
Khramov YuA, Veber VP. Vegetative maintenance and hemodynamics in hypertensive disease [in Russian]. Novosibirsk: Nauka; 1985: 129.
Khorshidi, M., Zarezadeh, M., Moghaddam, O. M., Emami, M. R., Kord-Varkaneh, H., Mousavi, S. M., ... & Aryaeian, N. (2020). Effect of evening primrose oil supplementation on lipid profile: A systematic review and meta-analysis of randomized clinical trials. Phytotherapy Research, 34(10), 2628-2638. https://doi.org/10.1002/ptr.6716
Kim, J. K., & Crimmins, E. M. (2020). Blood pressure and mortality: Joint effect of blood pressure measures. Journal of Clinical Cardiology and Cardiovascular Therapy, 2(1). https://doi.org/10.31546/2633-7916.1009
Kiran, S., Kumar, V., Murphy, E. A., Enos, R. T., & Singh, U. P. (2021). High fat diet-induced CD8+ T cells in adipose tissue mediate macrophages to sustain low-grade chronic inflammation. Frontiers in Immunology, 12, Article 680944. https://doi.org/10.3389/fimmu.2021.680944
Klecka, W.R. (1989). Discriminant Analysis [trans. from English in Russian] (Seventh Printing, 1986). In: Factor, Discriminant and Cluster Analysis. Moskva. Finansy i Statistika: 78-138.
Klimov, A.N. & Nikulcheva, N.G. (1995). *Lipids, Lipoproteides and Atherosclerosis* [in Russian]. St-Pb:Piter Pres:304.
Klimov, A. N., Nikulcheva, N. G., Shatilina, L. M., Kuzmin, A. A., Pleskov, V. M., & Andreyenkov, V. G. (1995). Lipoprotein-lipid relationships in blood plasma in the diagnostics of atherosclerosis: A method of discrete screening of risk factors for atherosclerosis and its therapy orientation. Kardiologiya, 35(7), 47-51. [in Russian]

Koch, E., Staab, J., Fuest, M., Witt, K., Voss, A., & Plange, N. (2015). Blood pressure and heart rate variability to detect vascular dysregulation in glaucoma. Journal of Ophthalmology, 2015, 1-9. https://doi.org/10.1155/2015/798958
Korkushko, O.V., Pysaruk AV, Shatylo VB. (2009). Importance of Heart Rate Variability Analysis in Cardiology: Age Aspects [in Russian]. Circulation and Hemostase. 1-2: 127-139.
Korolyuk, M. A., Ivanova, L. I., Mayorova, I. G., & Tokarev, V. E. (1988). A method of determining catalase activity. Laboratornoye Delo, (1), 16-19. [in Russian]
Kostyuk, P.G., Popovych IL, Ivassivka SV (Eds). (2006). Chornobyl', adaptive defensive systems and rehabilitation [in Ukrainian]. Kyïv: Computerpress: 348.
Kotelnikov, S.A., Nozdrachov AD, Odynak MM et al. (2002). Heart Rate Variability: Notions about Mechanisms [in Russian]. Fiziologiya cheloveka. 28(1): 130-140.
Kosmas, C. E., Silverio, D., Tsomidou, C., Salcedo, M. F., Montan, P. D., & Guzman, E. (2018). The impact of insulin resistance and chronic kidney disease on inflammation and cardiovascular disease. Clinical Medicine Insights: Endocrinology and Diabetes, 11, Article 1179551418792257. https://doi.org/10.1177/1179551418792257
Kosmerl, E. (2023). Food matrix impacts bioaccessibility and assimilation of acid whey-derived milk fat globule membrane lipids in Caco-2 cells. Frontiers in Nutrition, 10, Article 1177152. https://doi.org/10.3389/fnut.2023.1177152
Kozyavkina, N.V., Kozyavkina OV, Vovchyna YV, Popovych IL. (2019). Neurogenic mechanism of the influence of balneotherapy on arterial pressure. In: Proceedings of the XX Congress of the Ukrainian Physiological Society named after P.G. Kostyuk. Fiziol Zhurn. 65(3,Sup): 54-54.

Kozyavkina, N.V., Kozyavkina OV, Vovchyna YV. (2019). Balneotherapy influences on arterial pressure by neurogenic mechanism. In: Rehabilitation Medicine and Health-Resort Institutions Development. Proceedings of the 19th International Applied Research Conference (Kyïv, 11-12 December 2019). Edited by O. Gozhenko and W. Zukow. Toruń, Kyïv: 41-42.

Kozyavkina, N.V., Voronych-Semchenko NM, Vovchyna YV, Zukow W, Popovych IL. (2020). Quantitative and qualitative blood pressure clusters in patients of Truskavets' spa and their hemodynamic accompaniment. Journal of Education, Health and Sport. 10(6): 445-454.

Kozyavkina, N. V., Voronych-Semchenko, N. M., Vovchyna, Y. V., Zukow, W., & Popovych, I. L. (2020). Autonomic and endocrine accompaniments of quantitative-qualitative blood pressure clusters in patients of Truskavets' spa. Journal of Education, Health and Sport, 10(7), 465-477.

Kozyavkina, N. V., Vovchyna, Y. V., Voronych-Semchenko, N. M., Zukow, W., & Popovych, I. L. (2021). Electroencephalographic accompaniment of quantitative-qualitative blood pressure clusters in patients of Truskavets' spa. Journal of Education, Health and Sport, 11(10), 435-444.

Kozyavkina, N. V., Voronych-Semchenko, N. M., Vovchyna, Y. V., Zukow, W., Gozhenko, O. A., & Popovych, I. L. (2021). Variety of blood pressure reactions in patients of Truskavets' spa and their hemodynamic, autonomic and hormonal accompaniments. Balneo and PRM Research Journal, 12(3), A17.

Kozyavkina, N. V., Voronych-Semchenko, N. M., Vovchyna, Y. V., Zukow, W., & Popovych, I. L. (2022). Metabolic accompaniment of quantitative-qualitative blood pressure clusters in patients of Truskavets' spa. Journal of Education, Health and Sport, 12(2), 377-386.

Kozyavkina, N. V., Popovych, I. L., Popovych, D. V., Zukow, W., & Bombushkar, I. S. (2021). Sexual dimorphism in some psycho-neuro-endocrine parameters in humans. Journal of Education, Health and Sport, 11(5), 370-391.

Kozyavkina, N. V., Vovchyna, Y. V., Voronych-Semchenko, N. M., Zukow, W., Popovych, D. V., & Popovych, I. L. (2022). Immune accompaniment of quantitative-qualitative blood pressure clusters in patients of Truskavets' spa. Journal of Education, Health and Sport, 12(3), 320-329.

Kozyavkina, N.V., Popovych IL, Vovchyna YV, Voronych-Semchenko NM, Zukow W, Popovych DV. (2022). Evaluation of quantitative-qualitative levels of blood pressure by Tensioregulome. Journal of Education, Health and Sport. 12(8): 1216-1236.

Kozyavkina, O.V. & Barylyak, L.G. (2008). Ambivalent vegetotropic effects of bioactive water Naftussya and opportunity of their forecasting in rats. Medical Hydrology and Rehabilitation. 6(3):123-127.

Kozyavkina, O.V. (2011). Vegetotropic effects of bioactive water Naftussya at children with dysfunction of neuro-endocrine-immune complex, those endocrine-immune accompaniment and opportunity of their forecasting [in Ukrainian]. Medical Hydrology and Rehabilitation. 9(2):24-39.

Kozyavkina, O.V., Popovych, I.L., Zukow, W. (2013). Immediate vegetotropic effects of bioactive water Naftussya and their neuro-endocrine-immune accompaniment in healthy men. Journal of Health Sciences. 3(5): 391-408.

Kozyavkina, O. V., Kozyavkina, N. V., Gozhenko, O. A., Gozhenko, A. I., Barylyak, L. G., & Popovych, I. L. (2015). Bioactive Water Naftussya and Neuroendocrine-immune Complex. Kyiv: UNESCO-SOCIO:349.

Krittayaphong, R., Rangsin, R., Thinkhamrop, B., Hurst, C., Rattanamongkolgul, S., Sripaiboonkij, N., ... & Wangworatrakul, W. (2017). Prevalence of chronic kidney disease associated with cardiac and vascular complications in hypertensive patients: A multicenter, nation-wide study in Thailand. BMC Nephrology, 18(1), Article 115. https://doi.org/10.1186/s12882-017-0528-3

Krzesiński, P., Stańczyk, A., Gielerak, G., Piotrowicz, K., Banak, M., & Wójcik, A. (2016). The diagnostic value of supine blood pressure in hypertension. Archives of Medical Science, 2, 310-318. https://doi.org/10.5114/aoms.2016.59256

Kulchinskyi, A. B., Kovbasnyuk, M. M., Korolyshyn, T. A., Kyjenko, V. M., Zukow, W., & Popovych, I. L. (2016). Neuro-immune relationships at patients with chronic pyelonephritis and cholecystitis. Communication 2. Correlations between parameters EEG, HRV and Phagocytosis. Journal of Education, Health and Sport, 6(10), 377-401.

Kulchynskyi, A.B., Gozhenko AI, Zukow W, Popovych IL. (2017). Neuro-immune relationships at patients with chronic pyelonephritis and cholecystitis. Communication 3. Correlations between parameters EEG, HRV and Immunogram. Journal of Education, Health and Sport. 7(3): 53-71.

Kyrylenko, I.G., Korolyshyn TA, Zukow W, Barylyak LG, Popovych IL. (2016). Electrokinetic index of buccal epithelium correlated with some functional and metabolic parameters. In: IX International Symposium "Actual Problems of Biophysical Medicine" (Kyïv, May12-15, 2016). Kyïv. Bohomolets' Institute of Physiology: 50-51.

Kyrylenko, I.G., Fajda OI, Drach OV, Popel SL, Popel RL, Zukow W. (2016). Relationships between electrokinetic index of buccal epithelium and some functional and metabolic parameters at men with chronic pyelonephrite. Journal of Education, Health and Sport. 6(1): 302-314.

Kyrylenko, I.G. (2018). Changes in electrokinetic index of buccal epithelium correlated with changes in some parameters of EEG, HRV, hemodynamics and metabolism. Experimental and Clinical Physiology and Biochemistry. 2(82): 5-14.

Kyrylenko, I.G., Flyunt I-SS, Fil' VM, Zukow W, Popovych IL. (2018). Changes in electrokinetic index of buccal epithelium correlated with changes in some parameters of immunity and fecal microbiocenosis. Journal of Education, Health and Sport. 8(10): 168-170.

Kyrylenko, I.G., Fediaieva SI, Miesoiedova V, Popadynets' OO, Żukow X. (2022). Vegetative, metabolic and immune accompaniments of changes in the electrokinetic index of the buccal epithelium under the influence of therapeutic factors. Journal of Education, Health and Sport. 12(1): 344-354.

Kyriakidis, K., Vartholomatos, E., & Markopoulos, G. (2021). Evaluation of antiplatelet activity of phenolic compounds by flow cytometry. European Journal of Medical and Health Sciences, 3(1), 165-170. https://doi.org/10.24018/ejmed.2021.3.1.703

Lapovets, L. E., & Lutsyk, B. D. (2002). Handbook of laboratory immunology. LSMU, L'viv.

Lee, C. (2015). Medical technology and related interventions on maternal-fetal attachment: A literature review. International Journal of Nursing & Clinical Practices, 2(1), Article 144. https://doi.org/10.15344/2394-4978/2015/144

Lee, C., Li, R., Zhu, L., Tribble, G., Zheng, W., Ferguson, B., ... & Van Dyke, T. E. (2021). Subgingival microbiome and specialized pro-resolving lipid mediator pathway profiles are correlated in periodontal inflammation. Frontiers in Immunology, 12, Article 691216. https://doi.org/10.3389/fimmu.2021.691216

Lee, H., & Lee, H. (2018). The effects of circuit training on the indexes of sarcopenia and the risk factors of metabolic syndrome in aged obese women. Journal of Exercise Rehabilitation, 14(4), 666-670. https://doi.org/10.12965/jer.1836232.116

Leete, J., & Layton, A. T. (2019). Sex-specific long-term blood pressure regulation: Modeling and analysis. Computers in Biology and Medicine, 104, 139-148. https://doi.org/10.1016/j.compbiomed.2018.11.002

Leone, D., Airale, L., Bernardi, S., Mingrone, G., Astarita, A., Cesareo, M., ... & Milan, A. (2021). Prognostic role of the ascending aorta dilatation in patients with arterial hypertension. Journal of Hypertension, 39(6), 1163-1169. https://doi.org/10.1097/hjh.0000000000002752

Lesmana, C. R., Pakasi, L. S., Inggriani, S., Aidawati, M. L., & Lesmana, L. A. (2015). Prevalence of non-alcoholic fatty pancreas disease (NAFPD) and its risk factors among adult medical check-up patients in a private hospital: A large cross sectional study. BMC Gastroenterology, 15(1), Article 174. https://doi.org/10.1186/s12876-015-0404-1

Levy, B. R., & Slade, M. D. (2019). Positive views of aging reduce risk of developing later-life obesity. Preventive Medicine Reports, 13, 196-198. https://doi.org/10.1016/j.pmedr.2018.12.012

Li, Y. (2023). Widely targeted metabolomic profiling combined with transcriptome analysis provides new insights into lipid biosynthesis in seed kernels of Pinus koraiensis. International Journal of Molecular Sciences, 24(16), 12887. https://doi.org/10.3390/ijms241612887

Li, Y., Haseler, E., McNally, R., Sinha, M., & Chowienczyk, P. (2022). A meta-analysis of the haemodynamics of primary hypertension in children and adults. Journal of Hypertension, 41(2), 212-219. https://doi.org/10.1097/hjh.0000000000003326

Lin, H.J., Wang TD, Yu-Chih Chen M, et al. (2020). 2020 Consensus Statement of the Taiwan Hypertension Society and the Taiwan Society of Cardiology on Home Blood Pressure Monitoring for the Management of Arterial Hypertension. Acta Cardiol Sin. 36(6): 537-561.

Liu, Z., Ge, Y., Xu, F., Xu, Y., Liu, Y., Xia, F., ... & Chen, J. D. (2018). Preventive effects of transcutaneous electrical acustimulation on ischemic stroke-induced constipation mediated via the autonomic pathway. American Journal of Physiology-Gastrointestinal and Liver Physiology, 315(2), G293-G301. https://doi.org/10.1152/ajpgi.00049.2018

Lukovych, Yu.S., Ohorodnyk IO, Popel SL, Krayevyi VO. (2012). Relationships between blood pressure and heart rate variability parameters and the effect on them of balneotherapy at Truskavets' spa [in Ukrainian]. Medical Hydrology and Rehabilitation. 10(4): 154-159.

Maeda Y, Konishi M, Kiba T, Sakuraba Y, Sawaki N, Kurai T, Ueda Y, Sakakibara H, Yanagisawa S. (2018). A NIGT1-centred transcriptional cascade regulates nitrate signalling and incorporates phosphorus starvation signals in Arabidopsis. Nat Commun. 10;9(1):1376. doi: 10.1038/s41467-018-03832-6. PMID: 29636481; PMCID: PMC5893545.

Maydannyk, V.H. (1994). Anatomical and physiological features of organs and systems of the child's body [in Ukrainian]. In: Medicine of childhood (Editor: Moshchych, PS). Vol I. Kyïv. Zdorovya: 187-238.

Makarenko, Y. V. (1988). A comprehensive determination of the activity of superoxide dismutase and glutathione reductase in red blood cells in patients with chronic liver disease. Laboratornoye Delo, (11), 48-50. [in Russian]

Mansoor, K., Shahnawaz, S., Rasool, M., Chaudhry, H., Ahuja, G., & Shahnawaz, S. (2016). Automated versus manual blood pressure measurement: A randomized crossover trial in the emergency department of a tertiary care hospital in Karachi, Pakistan: Are third world countries ready for the change?. Open Access Macedonian Journal of Medical Sciences, 4(3), 404-409. https://doi.org/10.3889/oamjms.2016.076

Marfiyan, O.M., Korolyshyn TA, Barylyak LG, Kovbasnyuk MM, Yavors'kyi OV, Zukow W, Popovych IL. (2015). Neuroendocrine-immune and metabolic accompaniments of cholecystokinetic effects of balneotherapy on spa Truskavets'. Journal of Education, Health and Sport. 5(5): 21-30.

Marfiyan, O.M., & Zukow, W. (2015). Relationships between parameters of gall-bladder motility and neuroendocrine-immune complex and metabolism in men with chronic cholecystitis and pyelonephritis. Journal of Education, Health and Sport. 5(12): 434-449.

Matusik, P. S., Matusik, P. T., & Stein, P. K. (2023). Heart rate variability in patients with hypertension and its relationship to target organ damage: A systematic review. Frontiers in Neuroscience, 17, Article 1142818. https://doi.org/10.3389/fnins.2023.1142818

Mazzucchelli, R., Almodóvar, R., Turrado-Crespí, P., Crespí-Villarías, N., Pérez-Fernández, E., García-Zamora, E., ... & Vadillo, J. (2022). Trends in orthopaedic surgery for spondyloarthritis: Outcomes from a national hospitalised patient registry (MBDS) over a 17-year period (1999--2015). Trend-ESPA study. RMD Open, 8(1), e002107. https://doi.org/10.1136/rmdopen-2021-002107

McMaster, W. G., Kirabo, A., Madhur, M. S., & Harrison, D. G. (2015). Inflammation, immunity, and hypertensive end-organ damage. Circulation research, 116(6), 1022-1033.

Melville, S., Teskey, R., Philip, S., Simpson, J., Lutchmedial, S., & Brunt, K. M. (2018). A comparison and calibration of a wrist-worn blood pressure monitor for patient management: Assessing the reliability of innovative blood pressure devices. Journal of Medical Internet Research, 20(4), e111. https://doi.org/10.2196/jmir.8009

Mikolajczyk, T. P., & Guzik, T. J. (2019). Adaptive immunity in hypertension. Current hypertension reports, 21(9), 1-12.

Min, H. K., Kim, J. K., Lee, S. Y., Kim, M. K., Lee, S. H., Kwok, S. K., ... & Park, S. H. (2016). Rebamipide prevents peripheral arthritis and intestinal inflammation by reciprocally regulating Th17/Treg cell imbalance in mice with curdlan-induced spondyloarthritis. Journal of Translational Medicine, 14(1), Article 190. https://doi.org/10.1186/s12967-016-0942-5

Mogilnicka, I. (2024). Hypertensive rats show increased renal excretion and decreased tissue concentrations of glycine betaine, a protective osmolyte with diuretic properties. PLoS One, 19(1), e0294926. https://doi.org/10.1371/journal.pone.0294926

Morin, M., Hellgren, K., Lindström, U., & Frisell, T. (2021). Is family history a predictor of response to tumour necrosis factor inhibitors in spondyloarthritis? A Swedish nationwide cohort study. Scandinavian Journal of Rheumatology, 51(1), 10-20. https://doi.org/10.1080/03009742.2021.1887928

Munuswamy, R., Brandt, J., Burtin, C., Derave, W., Aumann, J., Spruit, M., ... & Michiels, L. (2021). Monomeric CRP is elevated in patients with COPD compared to non-COPD control persons. Journal of Inflammation Research, 14, 4503-4507. https://doi.org/10.2147/jir.s320659

Nabil-Adam, A. (2023). Modulation of MAPK/NF-κB pathway and NLRP3 inflammasome by secondary metabolites from red algae: A mechanistic study. ACS Omega, 8(41), 37971-37990. https://doi.org/10.1021/acsomega.3c03480

Nance, D. M., & Sanders, V. M. (2007). Autonomic innervation and regulation of the immune system (1987--2007). Brain, behavior, and immunity, 21(6), 736-745.
Neuhauser, H. K., Ellert, U., Thamm, M., & Adler, C. (2015). Calibration of blood pressure data after replacement of the standard mercury sphygmomanometer by an oscillometric device and concurrent change of cuffs. Blood Pressure Monitoring, 20(1), 39-42. https://doi.org/10.1097/mbp.0000000000000081
Newberg, A. B., Alavi, A., Baime, M., Pourdehnad, M., Santanna, J., & d'Aquili, E. (2001). The measurement of regional cerebral blood flow during the complex cognitive task of meditation: a preliminary SPECT study. Psychiatry Research: Neuroimaging, 106(2), 113-122.
Ngome, C. (2024). Comparative analysis of participatory forest management in Kenya: Embaringo and Gathiuru Community Forest Associations. Asia-Pacific Journal of Convergent Research Interchange, 10(1), 227-245. https://doi.org/10.47116/apjcri.2024.01.19
Nielsen, F. H. (2018). Magnesium deficiency and increased inflammation: Current perspectives. Journal of Inflammation Research, 11, 25-34. https://doi.org/10.2147/jir.s136742
Nuotio, J., Suvila, K., Cheng, S., Langén, V., & Niiranen, T. (2020). Longitudinal blood pressure patterns and cardiovascular disease risk. Annals of Medicine, 52(3-4), 43-54. https://doi.org/10.1080/07853890.2020.1733648
Nwachukwu, D. C., Eze, A. A., Nwachukwu, N. Z., Aneke, E., Agu, P. C., Azubike, N., ... & Okoye, O. (2017). Monotherapy with amlodipine or hydrochlorothiazide in patients with mild to moderate hypertension: Comparison of their efficacy and effects on electrolytes. Malawi Medical Journal, 29(2), 108. https://doi.org/10.4314/mmj.v29i2.6

Öcal, A., Xiao, L., & Park, J. (2021). Reasoning in social media: Insights from Reddit "Change My View" submissions. Online Information Review, 45(7), 1208-1226. https://doi.org/10.1108/oir-08-2020-0330
Olusegun-Joseph, A., Okunowo, B., Akintunde, A., & Karaye, K. (2021). Prevalence and pattern of electrolyte imbalance in hypertensives admitted in Nigerian teaching hospitals. International Cardiovascular Forum Journal, 21, Article 11. https://doi.org/10.17987/icfj.v21i0.741
Oxenkrug, G. (2015). Increased plasma levels of xanthurenic and kynurenic acids in type 2 diabetes. Molecular Neurobiology, 52(2), 805-810. https://doi.org/10.1007/s12035-015-9232-0
Parati, G., Stergiou GS, Asmar R, Bilo G, de Leeuw P, Imai Y; Kario K. et al on behalf of the ESH Working Group on Blood Pressure Monitoring. European Society of Hypertension guidelines for blood pressure monitoring at home: a summary report of the Second International Consensus Conference on Home Blood Pressure Monitoring. (2008). J Hypertension. 26(8): 1505-1526.
Pat. 2007113, RF. 1994. Device for evaluating the electrokinetic properties of buccal epithelium cells.
Pat. 28113, Ukraine, NSI A61V10/00. Method of rapid testing efficiency rehabilitation of health. Shakhbazov VG, Kolupaeva TV, Shuvalov IM et al. 2000; Bul №5.
Patnaik, S. K., Kumar, P., Bamal, M., Patel, S., Yadav, M. P., Kumar, V., ... & Kanitkar, M. (2018). Cardiovascular outcomes of Nephrotic syndrome in childhood (CVONS) study: A protocol for prospective cohort study. BMC Nephrology, 19(1), Article 349. https://doi.org/10.1186/s12882-018-0878-5
Pavlov, V. A., Chavan, S. S., & Tracey, K. J. (2018). Molecular and functional neuroscience in immunity. Annual review of immunology, 36, 783-812.

Pedral-Sampaio, G., Alves, J. S., Schriefer, A., Magalhães, A., Meyer, R., Glesby, M. J., ... & Carvalho, L. P. (2016). Detection of IgG anti-Leishmania antigen by flow cytometry as a diagnostic test for cutaneous leishmaniasis. PLoS One, 11(9), e0162793. https://doi.org/10.1371/journal.pone.0162793

Popovych, I.L., Ruzhylo SV, Ivassivka SV, Aksentiychuk BI (editors). (2005). Balneocardioangiology [in Ukrainian]. Kyïv. Computerpress:229.

Popovych, I.L. (2011). Stresslimiting adaptogene mechanism of biological and curative activity of water Naftussya [in Ukrainian]. Kyïv: Computerpress:300.

Popovych, I. L., Lukovych, Y. S., Korolyshyn, T. A., Barylyak, L. G., Kovalska, L. B., & Zukow, W. (2013). Relationship between the parameters heart rate variability and background EEG activity in healthy men. Journal of Health Sciences, 3(4), 217-240.

Popovych, I. L., Kozyavkina, O. V., Kozyavkina, N. V., Korolyshyn, T. A., Lukovych, Yu. S., & Barylyak, L. G. (2014). Correlation between indices of the heart rate variability and parameters of ongoing EEG in patients suffering from chronic renal pathology. Neurophysiology, 46(2), 139-148.

Popovych, I.L., Kul'chyns'kyi AB**,** Gozhenko AI, Zukow W, Kovbasnyuk MM, Korolyshyn TA**.** (2018). Interrelations between changes in parameters of HRV, EEG and phagocytosis at patients with chronic pyelonephritis and cholecystitis. Journal of Education, Health and Sport. 8(2): 135-156.

Popovych, I.L., Gozhenko AI, Korda MM, Klishch IM, Popovych DV, Zukow W (editors). (2022). Mineral Waters, Metabolism, Neuro-Endocrine-Immune Complex. Odesa. Feniks: 252.

Popovych, I. L., Kozyavkina, N. V., Barylyak, L. G., Vovchyna, Y. V., Voronych-Semchenko, N. M., Zukow, W., & Tsymbryla, V. V. (2022). Variants of changes in blood pressure during its three consecutive registrations. Journal of Education, Health and Sport, 12(4), 365-375.

Popovych, I.L., Kozyavkina NV, Vovchyna YV, Voronych-Semchenko NM, Zukow W, Popovych DV. (2022). Tensioregulome as an accompaniment of quantitative-qualitative blood pressure clusters. Journal of Education, Health and Sport. 12(6): 418-436.

Prentice, D. (2024). A case report on multiple sclerosis associated with atrial fibrillation and neurogenic hypertension: Area postrema syndrome?. Cureus, 16(2), e55860. https://doi.org/10.7759/cureus.55860

Punder, K., & Pruimboom, L. (2015). Stress induces endotoxemia and low-grade inflammation by increasing barrier permeability. Frontiers in Immunology, 6, Article 223. https://doi.org/10.3389/fimmu.2015.00223

Qin, T., Ang, T. F. A., DeCarli, C., Auerbach, S., Devine, S., Stein, T. D., ... & Qiu, W. Q. (2018). Association of chronic low-grade inflammation with risk of Alzheimer disease in ApoE4 carriers. JAMA Network Open, 1(6), e183597. https://doi.org/10.1001/jamanetworkopen.2018.3597

Rai, A., Narisawa M, Li P, Piao L, Li Y, Yang G, Cheng XW. (2020). Adaptive immune disorders in hypertension and heart failure: focusing on T-cell subset activation and clinical implications. J Hypertension. 38(10): 1878-1889.

Rayes, H. (2023). The impact of spondyloarthritis on health-related quality of life and healthcare resource utilization in Saudi Arabia: A narrative review and directions for future research. Open Access Rheumatology: Research and Reviews, 15, 161-171. https://doi.org/10.2147/oarrr.s414530

Rivera-Mancía, S., Jiménez-Osorio, A. S., Medina-Campos, O. N., Colin-Ramírez, E., Vallejo, M., Alcántara-Gaspar, A., ... & Pedraza-Chaverrí, J. (2018). Activity of antioxidant enzymes and their association with lipid profile in Mexican people without

cardiovascular disease: An analysis of interactions. International Journal of Environmental Research and Public Health, 15(12), 2687. https://doi.org/10.3390/ijerph15122687

Robles-Mezcua, A., Villaescusa-Catalan, J., Melero-Tejedor, J., & García-Pinilla, J. M. (2021). A new approach to the treatment of advanced heart failure: A case report. European Heart Journal - Case Reports, 5(2), ytaa541. https://doi.org/10.1093/ehjcr/ytaa541

Rodrigo, R., González, J. & Paoletto, F. (2011). The role of oxidative stress in the pathophysiology of hypertension. Hypertens Res 34, 431–440 https://doi.org/10.1038/hr.2010.264

Rodríguez-Iturbe, B., Pons, H., & Johnson, R. J. (2017). Role of the immune system in hypertension. Physiological reviews, 97(3): 1127-1164.

Rossi, J., Barbalho, S. M., Araújo, R. L., Bechara, M. D., Sloan, K. P., & Sloan, L. A. (2021). Metabolic syndrome and cardiovascular diseases: Going beyond traditional risk factors. Diabetes/Metabolism Research and Reviews, 38(3), e3502. https://doi.org/10.1002/dmrr.3502

Roviello, G., Michelet, M., D'Angelo, A., Nobili, S., & Mini, E. (2019). Role of novel hormonal therapies in the management of non-metastatic castration-resistant prostate cancer: A literature-based meta-analysis of randomized trials. Clinical & Translational Oncology, 22(7), 1033-1039. https://doi.org/10.1007/s12094-019-02228-2

Ruzhylo, S.V., Tserkovnyuk AV, Popopvych IL. (2003). Actotropic Effects of Balneotherapeutic Complex of Truskavets spa [in Ukrainian]. Kyïv: Computerpress: 131.

Ruzhylo, S.V., Fihura OA, Zukow W, Popovych IL. (2015). Immediate neurotropic effects of Ukrainian phytocomposition. Journal of Education, Health and Sport. 5(4): 415-427.

Said, Z., & Kheng, G. L. (2018). A review on mindfulness and nursing stress among nurses. Analitika, 10(1), 31. https://doi.org/10.31289/analitika.v10i1.1589

Sagawa, K. (1981). The end-systolic pressure-volume relation of the ventricle: definition modifications and clinical use. Circulation. 63(6): 1223-1227.

Samosyuk, I.Z., Lysenyuk VP, Lymans'kyi YuP, Povzhytkov AN, Bojchuk RR, Antonchenko VYa. (1994). Nontraditional Methods of Diagnostics and Therapy (Methods by Foll, Nakatani, Akabane. Homeopaty and Reflexotherapy) [in Russian]. Kyïv: Zdorovya:240.

Salmenkari, H., Holappa, M., Siltari, A., Korpela, R., & Vapaatalo, H. (2018). Local intestinal ACE-like activity and corticosterone production in hypertensive and aging rats. Pharmacology & Pharmacy, 9(01), 27-37. https://doi.org/10.4236/pp.2018.91003

Schiller, N. B., & Osipov, M. A. (1993). Clinical Echocardiography [in Russian]. Mir, Moscow.

Schut, A., Bruin, L., Rooij, B., Lidington, E., Timbergen, M., Graaf, W., ... & Husson, O. (2023). Physical symptom burden in patients with desmoid-type fibromatosis and its impact on health-related quality of life and healthcare use. Cancer Medicine, 12(12), 13661-13674. https://doi.org/10.1002/cam4.5985

Secomb, T. W. (2016). Hemodynamics. Comprehensive Physiology, 6(2), 975-1003. https://doi.org/10.1002/cphy.c150038

Shah, K. H., Shi, P., Giani, J. F., Janjulia, T., Bernstein, E. A., Li, Y., ... & Shen, X. Z. (2015). Myeloid suppressor cells accumulate and regulate blood pressure in hypertension. Circulation Research, 117(10), 858-869. https://doi.org/10.1161/circresaha.115.306539

Shakhbazov, V.G., Kolupaeva TV, Nabokov AL. (1986). New method for determining biological age of man [in Russian]. Lab delo. 7: 404-407.

Shakhbazova, L.V., Mosiy HYe, Tkachuk SP, Shakhbazov OB. (2005). Dynamics of the daily profile of blood pressure and heart rate variability in patients with essential hypertension under the influence of treatment at the Truskavets' spa [in Ukrainian]. Medical Hydrology and Rehabilitation. 3(4): 44-47.

Shakhbazova, L.V., Mosiy HYe, Shakhbazov OB, Pavelko OM. (2006). Features of the course and correction of arterial hypertension in patients with concomitant autonomic dysfunction in the Truskavets' spa [in Ukrainian]. Medical Hydrology and Rehabilitation. 4(3): 65-68.

Shannon, C.E. (1948) A Mathematical Theory of Communication. Bell System Technical Journal. 27:379-423 and 623-656.

Sheiko, V.I., Makarenko MV, Ivanyura IO. (2007). Condition of higher nervous activity and immune system after vilosen administration [in Ukrainian]. Fiziol Zhurn. 53(2): 65-69.

Shkorbatov, Y.G., Kolupaeva TV, Shakhbazov VG, Pustovoyt PA. (1995). About communication electrokinetic properties of nuclei cells of human with physiological parameters [in Russian]. Fiziologiya cheloveka. 21(2):25-27.

Shen, X. Z., Li, Y., Li, L., Shah, K. H., Bernstein, K. E., Lyden, P., & Shi, P. (2015). Microglia participate in neurogenic regulation of hypertension. Hypertension, 66(2), 309-316. https://doi.org/10.1161/hypertensionaha.115.05333

Shimojo, G., Dias, D., Malfitano, C., Sanches, Í., Llesuy, S., Ulloa, L., ... & De Angelis, K. (2018). Combined aerobic and resistance exercise training improve hypertension associated with menopause. Frontiers in Physiology, 9, Article 1471. https://doi.org/10.3389/fphys.2018.01471

Silva, C. M. S., Cândido, A. P. C., Pala, D., Barbosa, P. F. C., Machado-Coelho, G. L. L., Oliveira, F. L. P., ... & Freitas, R. N. (2017). Clustered cardiovascular risk factors are associated with inflammatory markers in adolescents. Annals of Nutrition and Metabolism, 70(4), 259-267. https://doi.org/10.1159/000458767

Soares, A. A., Contreras, J. E., Mironova, E., Archer, C. R., Stockand, J. D., & El-Aziz, T. M. A. (2023). P2Y2 receptor decreases blood pressure by inhibiting ENaC. JCI Insight, 8(14), e167704. https://doi.org/10.1172/jci.insight.167704

Solocinski, K., Holzworth, M., Wen, X., Cheng, K. Y., Lynch, I. J., Cain, B. D., ... & Gumz, M. L. (2016). Desoxycorticosterone pivalate-salt treatment leads to non-dipping hypertension in Per1 knockout mice. Acta Physiologica, 220(1), 72-82. https://doi.org/10.1111/apha.12804

Song, X., Li, G., Qiao, A., & Chen, Z. (2016). Association of simultaneously measured four-limb blood pressures with cardiovascular function: A cross-sectional study. Biomedical Engineering Online, 15(2), Article 147. https://doi.org/10.1186/s12938-016-0266-y

Stanciak, J., & Novotný, J. (2015). The quality of life of the patients with rheumatoid arthritis before and after balneotherapy. Journal of Health Science, 3(5), 275-280. https://doi.org/10.17265/2328-7136/2015.05.005

Stolwijk, C., van Onna, M., Boonen, A., & van Tubergen, A. (2016). Global prevalence of spondyloarthritis: A systematic review and meta-regression analysis. Arthritis Care & Research, 68(9), 1320-1331. https://doi.org/10.1002/acr.22831

Sun, R., Wu, T., Guo, H., Xu, J., Chen, J., Tao, N., ... & Zhong, J. (2021). Lipid profile migration during the tilapia muscle steaming process revealed by a transactional analysis between MS data and lipidomics data. NPJ Science of Food, 5(1), Article 15. https://doi.org/10.1038/s41538-021-00115-1

Tan, T., Zhou, Y., Wu, Y., Fan, Z., Xu, R., & Gao, X. (2021). Transition from metabolically healthy to unhealthy status associated with risk of carotid artery plaque in Chinese adults. BMC Cardiovascular Disorders, 21(1), Article 534. https://doi.org/10.1186/s12872-021-02279-w

Thayer, J. F., & Sternberg, E. M. (2010). Neural aspects of immunomodulation: focus on the vagus nerve. Brain, behavior, and immunity, 24(8), 1223-1228.

Tiselius, H. G., Almgård, L. E., Larsson, L., & Sörbo, B. (1978). A biochemical basis for grouping of patients with urolithiasis. *European Urology*, *4*(4), 241-249. https://doi.org/10.1159/000473965

Tohme, S., Vancheswaran, A., Mobbs, K., Kydd, J., & Lakhi, N. (2021). Predictable risk factors of upper-extremity deep venous thrombosis in a Level I trauma center. International Journal of General Medicine, 14, 2637-2644. https://doi.org/10.2147/ijgm.s311669

Tracey, K. J. (2007). Physiology and immunology of the cholinergic antiinflammatory pathway. The Journal of clinical investigation, 117(2), 289-296.

Tsubokawa, M., Nishimura, M., Tamada, Y., & Nakaji, S. (2022). Factors associated with reduced heart rate variability in the general Japanese population: The Iwaki cross-sectional research study. Healthcare, 10(5), 793. https://doi.org/10.3390/healthcare10050793

Uchakin, P. N., Uchakina, O. N., Tobin, B. V., & Ershov, F. I. (2007). Neuroendocrine Immunomodulation. Vestnik Ross AMN, 9, 26-32.

Uribe-Querol, E., & Rosales, C. (2020). Phagocytosis: Our Current Understanding of a Universal Biological Process. Front Immunol. 11: 1066.

Ursoniu, S., Sahebkar, A., Şerban, C., & Banach, M. (2015). Systematic review/meta-analysis lipid profile and glucose changes after supplementation with astaxanthin: A systematic review and meta-analysis of randomized controlled trials. Archives of Medical Science, 2, 253-266. https://doi.org/10.5114/aoms.2015.50960

Ushakov, I.B., YA Kukushkin, Bogomolov AV. (2008). Physiology of labor and reliability activity of human [in Russian]. Moskwa: Nauka:317.

Vaamonde-García, C., Vela-Anero, Á., Hermida-Gómez, T., Fernández-Burguera, E., Filgueira-Fernández, P., Goyanes, N., ... & Meijide-Faílde, R. (2019). Effect of balneotherapy in sulfurous water on an in vivo murine model of osteoarthritis. International Journal of Biometeorology, 64(3), 307-318. https://doi.org/10.1007/s00484-019-01807-w

Vadziuk, S.N., Volkova NM, Mykula MM, Tserkovniuk RG. (1998). The influence of weather on the psychophysiological state of a healthy person [in Ukrainian]. Ternopil. Dzhura: 144.

Vasylieva, T., Gavurová, B., Доценко, T., Bilan, S., Strzelec, M., & Khouri, S. (2023). The behavioral and social dimension of the public health system of European countries: Descriptive, canonical, and factor analysis. International Journal of Environmental Research and Public Health, 20(5), 4419. https://doi.org/10.3390/ijerph20054419

Vignali DA, Collison LW, Workman CJ. (2008). How regulatory T cells work. Nat Rev Immunol. 8(7): 523-532.

Vinogradova, T. S. (1986). The instrumental methods in the study of the cardiovascular system [in Russian]. Medicine, Moscow.

Virabhakul, V. (2017). How do spa-goers make decisions when faced with a choice conflict? Discrete choice experiments for day spas in Thailand. New Trends and Issues Proceedings on Humanities and Social Sciences, 4(1), 596-612. https://doi.org/10.18844/prosoc.v4i1.2306

Vistak, H.I., & Popovych, I.L. (2011). Vegetotropic effects of bioactive water Naftussya and their endocrine and immune support in female rats. Medical Hydrology and Rehabilitation, 9(2), 40-58.

Vistak, H.I., Kozyavkina OV, Popovych IL, Zukow W. (2013). Vegetotropic effects of bioactive water Naftussya spa Truskavets' and their thyroide, metabolic and haemodynamic accompaniments at the women. Journal of Health Sciences. 3(10):557-582.

Vovchyna, Yu.V., Lukovych YuR, Matiyishyn GYo, Hryvnak RF, Tymochko OO, Andrusiv OV, Burkovska MM. (2013). Hemodynamic variants term effects of bioactive water Naftussya on blood pressure, their electrolyte accompaniment and the ability to forecast [in Ukrainian]. Medical Hydrology and Rehabilitation. 11(3):50-59.

Vovchyna, Yu. V., & Zukow, W. (2014). The influence of balneotherapy on spa Truskavets' on arterial pressure and its regulation at children. Journal of Health Sciences, 4(10), 151-160.

Vovchyna, Yu. V., Voronych, N. M., Zukow, W., & Popovych, I. L. (2016). Relationships between normal or borderline blood pressure and some neural, endocrine, metabolic and biophysic parameters in women and men. Journal of Education, Health and Sport, 6(2), 163-182.

Wei, C., Jenks, S., & Sanz, I. (2015). Polychromatic flow cytometry in evaluating rheumatic disease patients. Arthritis Research & Therapy, 17(1), Article 46. https://doi.org/10.1186/s13075-015-0561-1

Whelton, P. K., Carey, R. M., Aronow, W. S., Casey, D. E., Collins, K. J., Himmelfarb, C. D., ... & Wright, J. T. (2018). 2017 ACC/AHA/AAPA/ABC/ACPM/AGS/APhA/ASH/ASPC/NMA/PCNA guideline for the prevention, detection, evaluation, and management of high blood pressure in adults: a report of the American College of Cardiology/American Heart Association Task Force on Clinical Practice Guidelines. Journal of the American College of Cardiology, 71(19), e127-e248.

Wibowo, A., Hastuti, P., & Susanti, V. (2021). Polymorphism of thyroid hormones receptor, angiotensin-converting enzyme, and high blood pressure in childbearing age women with hyperthyroidism. Open Access Macedonian Journal of Medical Sciences, 9(A), 387-392. https://doi.org/10.3889/oamjms.2021.6193

Wilder, J.F. (1967). Stimulus and response: the low of initial value. Bristol: J Wright & Sons Ltd.:352.

Xia, H., Sriramula, S., Chhabra, K. H., & Lazartigues, E. (2015). Brain ACE2 overexpression reduces DOCA-salt hypertension independently of endoplasmic reticulum stress. American Journal of Physiology-Regulatory, Integrative and Comparative Physiology, 308(5), R370-R378. https://doi.org/10.1152/ajpregu.00366.2014

Xu, S., Chen, X., Sheng, C., Cheng, Y., Wang, H., Yu, W., ... & Wang, J. (2021). Comparison of the mean of the first two blood pressure readings with the overall mean of three readings on a single occasion. Journal of Hypertension, 40(4), 699-703. https://doi.org/10.1097/hjh.0000000000003065

Xu, Y., Wu, H., & Lü, X. (2022). Influence of continuous positive airway pressure on lipid profiles of obstructive sleep apnea: A systematic review and meta-analysis. Medicine, 101(42), e31258. https://doi.org/10.1097/md.0000000000031258

Yang, F., Zhang, F., Yang, L., Li, H., & Zhou, Y. (2021). Establishment of the reference intervals of whole blood neutrophil phagocytosis by flow cytometry. Journal of Clinical Laboratory Analysis, 35(8), e23884. https://doi.org/10.1002/jcla.23884

Yang, Y., Li, J., Zhou, Z., Wu, S., Zhao, J., Jia, W., ... & Cheng, R. (2023). Gut microbiota perturbation in early life could influence pediatric blood pressure regulation in a

sex-dependent manner in juvenile rats. Nutrients, 15(12), 2661. https://doi.org/10.3390/nu15122661

Yessypenko, B. Y. (1981). Physiological effect of Naftussya mineral water. Zdorov'ya, Kyïv.

Yu, J., Tan, L., Wu, Q., Rao, Y., Ao, J., Yang, W., ... & Chen, J. (2020). Multiple myeloma with CD138 changed from positive to negative: A case report. Cytometry Part B: Clinical Cytometry, 100(2), 249-253. https://doi.org/10.1002/cyto.b.21869

Yu, P., Ren, H., Tao, H., He, C., Wan, J., & Su, H. (2019). Metabolomics study of the anti-inflammatory effects of endogenous omega-3 polyunsaturated fatty acids. RSC Advances, 9(71), 41903-41912. https://doi.org/10.1039/c9ra08356a

Zamout, P. (2024). The prevalence of chronic obstructive pulmonary disease in patients with spondyloarthritis compared to the general population in the southernmost region of Sweden: A case--control study. Clinical and Experimental Medicine, 24(1), 103-110. https://doi.org/10.1007/s10238-024-01335-x

Zapolski, T. (2024). The influence of balneotherapy using salty sulfide--hydrogen sulfide water on selected markers of the cardiovascular system: A prospective study. Journal of Clinical Medicine, 13(12), 3526. https://doi.org/10.3390/jcm13123526

Zeng, Z. (2023). Gut microbiome and metabolome in aneurysm rat with hypertension after ginsenoside Rb1 treatment. Frontiers in Pharmacology, 14, Article 1287711. https://doi.org/10.3389/fphar.2023.1287711

Zhang, R. M., McNerney, K. P., Riek, A. E., & Bernal-Mizrachi, C. (2021). Immunity and hypertension. Acta Physiologica, 231(1), e13487.

Zhang, Z., Xi, W., Wang, B., Chu, G., & Wang, F. (2018). A convenient method to verify the accuracy of oscillometric blood pressure monitors by the auscultatory method: A smartphone-based app. Journal of Clinical Hypertension, 21(2), 173-180. https://doi.org/10.1111/jch.13460

Zhou, T., Yang, H., Wang, H., Luo, N., Xia, Y., & Jiang, X. (2022). Association between ACAT1 rs1044925 and increased hypertension risk in Tongdao Dong. Medicine, 101(49), e32196. https://doi.org/10.1097/md.0000000000032196

Horbachevs'kyi National Medical University, Ternopil', Ukraine
National Medical University, Ivano-Frankivs'k, Ukraine
Kozyavkin International Rehabilitation Clinic, Truskavets', Ukraine
Nicolaus Copernicus University, Torun, Poland
Bohomolets' Institute of Physiology National Academy of Sciences, Kyïv, Ukraine

Nataliya V. Kozyavkina
Yuliya V. Vovchyna
Nataliya M. Voronych-Semchenko
Walery Zukow
Igor L. Popovych

196

TENSIOREGULOME CONCEPT.
Quantitative-qualitative blood pressure clusters of patients at Truskavets' spa and their accompaniments

TERNOPIL'
UKRMEDKNYHA
2024

Authors

Nataliya V. Kozyavkina, MD, PhD; Horbachevs'kyi National Medical University, Ternopil'; Kozyavkin International Rehabilitation Clinic
nataliakozyavkina72@gmail.com; clinic@kozyavkin.com

Yuliya V. Vovchyna, MD; Ivano-Frankivs'k National Medical University

Nataliya M. Voronych-Semchenko, MD, DS, Prof.; Ivano-Frankivs'k National Medical University

Walery Zukow, MD, DS; Nicolaus Copernicus University, Torun, Poland
w.zukow@wp.pl

Igor L. Popovych, MD, PhD, Senior Res. fel.; Bohomolets' Institute of Physiology; Kozyavkin International Rehabilitation Clinic; i.popovych@biph.kiev.ua; i.l.popovych@gmail.com

We dedicate the monograph to memory of Volodymyr Illich Kozyavkin (1947-2022) with gratitude for the support of the Truskavetsian Scientific School of Balneology

Our comprehensive study of blood pressure regulation at Truskavets spa has provided novel insights into the complex, multifactorial nature of hypertension. The identification of distinct blood pressure clusters with unique physiological profiles challenges current paradigms in hypertension classification and management. Our findings emphasize the need for a more integrative, personalized approach to hypertension, considering the interplay between hemodynamic, neuroendocrine, immunological, and metabolic factors.

The potential for spa therapy to modulate multiple physiological systems involved in blood pressure regulation offers exciting possibilities for non-pharmacological hypertension management. However, realizing this potential will require further research to elucidate specific mechanisms and optimize treatment protocols.

This monograph represents a significant step towards a more comprehensive understanding of blood pressure regulation and opens new avenues for personalized hypertension management. The integration of advanced physiological profiling with traditional spa therapy approaches may pave the way for more effective, individualized strategies in cardiovascular health promotion and disease prevention.

Recommended for publication by the Academic Council
of Horbachevs'kyi National Medical University
(protocol No. 9 dated 25/06/2024)

Reviewers:

Vastyanov Ruslan S., MD, DS, Prof., head of the department of general and clinical pathophysiology named after VV Podvysotskyi of the National Medical University, Odesa, Ukraine

Regeda Mykhaylo S., MD, DS, Prof., head of the department of pathophysiology of the Danylo Halyts'kyi National Medical University, L'viv, Ukraine

Kozyavkina NV, Vovchyna YV, Voronych-Semchenko NM, Zukow W, & Popovych IL. Tensioregulome Concept. Quantitative-qualitative Blood Pressure Clusters of Patients at Truskavets' Spa and Their Accompaniments. Ternopil': Ukrmedknyha; 2024: 258.
ISBN 978-1-4452-7212-2 DOI http://dx.doi.org/10.5281/zenodo.12664757

The monograph highlights the results of priority clinical-physiological studies of the state of blood pressure in patients of Truskavets' spa and its hemodynamics, neuro-endocrine, immune, metabolic, and biophysics accompaniments. The authors put forward the concept of ***Tensioregulome*** as a constellation of factors that determines the level of blood pressure and its changes under the influence of balneotherapy. For physiologists, cardiologists, endocrinologists, immunologists, biophysicists, medical rehabilitation specialists.

ISBN 978-1-4452-7212-2

DOI http://dx.doi.org/10.5281/zenodo.12664757

© Horbachevs'kyi National Medical University, Ternopil', 2024
© Ivano-Frankivs'k National Medical University, 2024
© Kozyavkin International Rehabilitation Clinic, Truskavets', 2024
© Nicolaus Copernicus University, Torun, 2024
© Bohomolets' Institute of Physiology, Kyïv, 2024
© Authors

ISBN 978-1-4452-7212-2
DOI http://dx.doi.org/10.5281/zenodo.12664757